

BULGARIAN CHEMICAL COMMUNICATIONS

2021 Volume 53 / Special Issue A

Dedicated to the National Research Programme BioActiveMed and the Centre of Competence "Clean & Circle" in the frame of the Scientific Conference "Ecological Products for Health", October 04-08, 2020; Velingrad, Bulgaria

*Journal of the Chemical Institutes
of the Bulgarian Academy of Sciences
and of the Union of Chemists in Bulgaria*

National Research Programme “Innovative Low-Toxic Bioactive Systems for Precision Medicine (BioActiveMed)”



The **National Research Programme “Innovative Low-Toxic Bioactive Systems for Precision Medicine (BioActiveMed)”** was approved by DCM №658/14.09.2018 and is performed on the basis of a signed agreement Grant DO1-217/30.11.2018 between Ministry of Education and Science and Bulgarian Academy of Sciences (BAS). A prerequisite for the implementation of the NRP BioActiveMed is the fact that Bulgaria, with its unique climatic and ecological factors, offers an amazing variety of plant and animal species. Isolated extracts contain a series of bioactive compounds that resembles combined therapy with several synthetic compounds. It is well known that extracts from natural products are less toxic than synthetic and are better tolerated by the human body. Therefore, the proposed in the Programme approach is one of the key to overcoming multiple drug resistance.

The Programme is focused on the development of new low toxic bioactive substances and systems containing extracts of natural sources (of plant or animal origin) from Bulgaria for the prevention and support of the therapy of certain diseases. The first step is the isolation and purification of bioactive substances of plant and animal origin, their appropriate incorporation in suitable innovative systems and development of new methodologies for their characterization and determination of quality and applicability as new products in personalized and preventative medicine. One of the planned long-term applications is the implementation of new innovative healthy and safe food supplements and cosmetics with a preventive potential for personalized medicine.

The research has been carried out with the participation of leading scientists with proven

scientific capacity, as well as with the active participation of young scientists and PhD students from the Consortium formed. The leading organization is the Bulgarian Academy of Sciences and the following scientific organizations (seven scientific units from the BAS) and higher education organizations with the highest capacity in the field of the Programme are Partners: Institute of Organic Chemistry with Center of Phytochemistry (Partner 1), Institute of Molecular Biology (Partner 2), Institute of Microbiology (Partner 3), Institute of Neurobiology (Partner 4), Institute of Experimental Morphology, Pathology and Anthropology with Museum (Partner 5), Institute of Polymers (Partner 6), Institute of Information and Communication Technologies (Partner 7), Medical University – Sofia (Partner 8), Sofia University “St. Kliment Ohridski” (Partner 9), Medical University – Plovdiv (Partner 10), Plovdiv University “Paisii Hilendarski” (Partner 11) and National Sports Academy “Vasil Levski” (Partner 12).

The research activities are divided in the following **8 work packages (WPs)**:

Work package 1 (WP 1). Preparation of novel bioactive substances/systems containing extracts of natural sources (of plant or animal origin) from Bulgaria.

WP Leader Prof. DSc Pavlina Dolashka

The aim of the WP 1 is to isolate and purify bioactive substances (BASs) of plant or animal origin and to incorporate them into appropriate innovative systems. Isolated individual BASs or obtained innovative systems will be used for preparation of innovative products for potential applicability to improve human health. It is also envisaged to characterize in details the structure and properties of the BASs in order to explain their mechanism of action. The following Bulgarian plant and animal species will be studied:



Ginkgo biloba seeds



Tamus communis L.



Betonica bulgarica



Salvia



Nepeta nuda



Thymus



Gentiana



Helix aspersa



Rapana venosa

Work package 2 (WP 2). Investigation of the anti-infective potential of the obtained low-toxic bioactive BASs/systems.

WP Leader Prof. Dr. Svetlozara Petkova

The purpose of the WP 2 is to evaluate the antifungal activity of the obtained low-toxic bioactive BASs/systems containing extracts of Bulgarian natural sources (of plant or animal origin) on fungal strains, as well as their antiparasitic and antiviral activity. The antifungal potential and determination of the inhibition dose will be carried out against *Aspergillus*, *Mucor*, *Penicillium*, *Cladosporium*, *Fusarium*, *Alternaria*, *Botrytis sp.* Studies will also be provided on an *in vivo* parasitic model of *Trichinella*, as well as on a model of sleeping sickness (*African trypanosomiasis*). In addition, the first and second types of Human Herpes Virus will be used as viral models.

Work package 3 (WP 3). Investigation of the obtained low-toxic bioactive BASs/systems on bacterial in vitro systems.

WP Leader Prof. DSc. Hristo Najdenski, DVM, Corr. Member of BAS

WP3 will study the antibacterial activity of the obtained bioactive BASs/systems containing extracts of natural sources (of plant or animal origin) against Gram(+) and Gram(-) bacteria, which are high-risk pathogens and have developed multiple drug resistance. The use of the following microorganisms is envisaged, according to the ISO 20776-1:2006: *Staphylococcus aureus* ATCC 29213, *Enterococcus faecalis* ATCC 29212, *Pseudomonas aeruginosa* ATCC 27853,

Escherichia coli ATCC 35218, *S. aureus* NBIMCC 3359, *S. aureus* ATCC 3865 P, *S. aureus* NBIMCC 8327, *S. epidermidis* NBIMCC 1093, *B. cereus* ATCC 9634 and *Candida albicans* SAIMC 562I.

Work package 4 (WP 4). In vitro and in vivo study of the effectiveness of the obtained low-toxic bioactive BASs/systems against neurodegenerative diseases.

WP Leader Prof. Dr. Lyubka Tancheva

This WP aims to study *in vitro* neurotoxicity of the obtained BASs/systems and *in vitro* activity onto models of Alzheimer's disease (AD) and Parkinson's disease (PD), as well. *In vivo* efficacy of the obtained innovative BASs/systems on the impaired cognitive and motor functions of experimental animals with an experimental model of AD and PD will also be studied.

Work package 5 (WP 5). Study of the antitumor activity of the obtained low-toxic bioactive BASs/systems.

WP Leader Prof. Dr. Iva Ugrinova

The studies in this WP are focused on *in vitro* study of the antineoplastic activity of the isolated extracts and obtained BASs/systems in models of malignant diseases. Several cancer models will be used – three lung cell lines MRC-5, A549 and H1299, three lines of breast cancer MCF-10A, MCF-7 and MDA-MB-231, and two lines of cervical cancer HeLa and Wish. Malignant-transformed skin T-cell lymphoma cell lines will also be used (CTCL) – MJ (ATCC № CRL-8294) and HuT-78 (ATCC № TIB-161TM, ECACC № 88041901), as well as bladder cancer cells T-24

(DSMZ № ACC 376), SW-1710 (DSMZ № ACC 426) и CAL-29 (DSMZ № ACC 515).

Work package 6 (WP 6). Modeling, prognosis and modulation of the therapeutic effect of BASs through a theoretical, computational and experimental methods and techniques.

WP Leader Prof. Dr. Nevena Ilieva-Litova

This WP aims to identify potential biotherapists in peptide mixtures of natural origin as a basis for alternative approaches for treatment of the infectious diseases caused by multidrug-resistant bacterial strains and in immunocompromised patients. An *in silico* studies of the behavior in solution of isolated peptides in mono- and multi-peptide compositions will also be performed.

Work package 7 (WP 7). Study of the applicability of the obtained low-toxic bioactive BASs/systems in the biopharmaceutical industry.

WP Leader Prof. DSc. Spiro Konstantinov, MD

The work package is focused on study of the applicability of the obtained low-toxic bioactive BASs/systems as food supplements or cosmetics in terms of genotoxicity, carcinogenicity, mutagenicity and teratogenicity, as well as the development of innovative systems for the supply

of low-toxic extracts/BASs, ensuring optimal bioavailability after oral or local administration.

Work package 8 (WP 8). Development of innovative food supplements and cosmetics for local application with preventive potential for personalized medicine.

WP Leader Prof. Dr. Stoyan Shishkov

This package aims to develop end products as innovative food supplements and cosmetics for local application with preventive potential. The main object of the WP is to select the most effective BASs/systems for incorporation in food supplements or cosmetics.

More information can be found on the web page of the Programme: www.bioactivemed-nrp.com.

Prof. PhD Olya Stoilova

Bulgarian Academy of Sciences, 1040 Sofia, 15th November 1, str.; E-mail: olya.stoilova@cu.bas.bg

Innovative and Applied Potential of Center of Competence "Clean technologies for Sustainable Environment – Water, Waste, Energy for Circle Economy"



European Union

European Regional
Development Fund



Project BG05M2OP001-1.002-0019: „Clean technologies for sustainable environment – water, waste, energy for circular economy“ (Clean&Circle) for creation and development of a Centre of Competence

Leading organization: Sofia University "St. Kliment Ohridski"

Partners

- University of Architecture, Civil Engineering and Geodesy;
- University of Forestry - Sofia;
- "Prof. Dr. Assen Zlatarov" University - Bourgas;
- Institute of Physical Chemistry "Academician Rostislav Kaishev" - Bulgarian Academy of Sciences;
- Institute of Organic Chemistry with Center for Phytochemistry - Bulgarian Academy of Sciences;
- Institute of Microbiology "Stefan Angelov" - Bulgarian Academy of Sciences;
- "Cleantech Bulgaria" Foundation.

Associate Partners

- Sofia Municipality
- Sofia Waste Treatment Plant;
- "Sofiyska Voda" AD,
- Interplast BG Ltd.,
- Energy Agency - Plovdiv,
- University of Modena, Italy

Project budget: The total cost of the project is BGN 23 667 925.86, of which BGN 20 117 736.97 European and BGN 3 550 188.89, national co-financing.

Term of implementation: 30 March 2018 - 30 November 2023.

Project aim: Building effective infrastructure and research capacity to develop innovations in the circular economy focusing on water, energy and waste management.

Brief project description: Three vertical and four horizontal modules lay the foundation of the Centre of Competence. The vertical modules are "Water", "Solid Waste" and "Transfer". The "Water" and "Solid Waste" modules will cover two main aspects: "Monitoring, Evaluation and Identification of Problems" and "Clean Technologies" – development of clean Technologies. In both modules, the horizontal priorities will include activities relating to the circular economy and achievement of energy and resource efficiency through:

1. Innovations through efficient operation of the water and waste treatment facilities and of the water supply and sewerage networks;

2. Increasing the share of the renewable and alternative energy sources by producing biogas, bioethanol, biodiesel, hydrogen, hydro power, combined with sediment bioremediation technologies and solving of crucial environmental problems;

3. Recovery of resources such as phosphorus, precious and rare metals, bioremediation of sludge, soils and sediments that have accumulated toxic pollutants;

4. Obtaining alternative resources - zeolite from ashes, slags, cake, new construction and composite materials from waste, RDF fuel, high quality bioreactors from composting plants, microbiological detoxification preparations, etc.

All activities in the CoC will be integrated into an electronic cloud for the exchange and rapid use of information, as well as for its structuring in dedicated electronic cards.

The innovation activity based on excellence in research and technology is an important priority. Real-time control of processes is planned through automated chemical, physical, technological, microbiological, and molecular methods. Sensors and biosensors will be developed to control and manage water treatment processes.

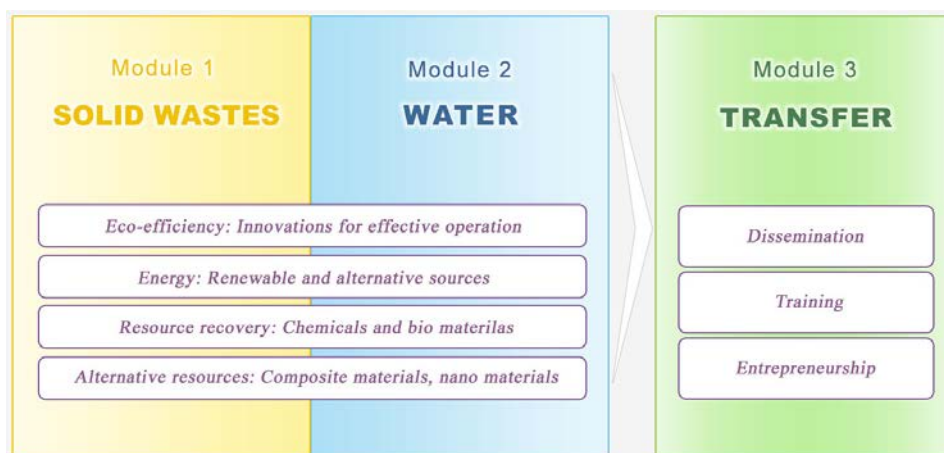


Fig. 1. Clean & Circle CoC Concept: The center will consist of three vertical modules that are connected in an information technology cloud - water, solid waste and transfer. Horizontal upgrading activities will be: eco-efficiency, energy, resource recovery and alternative resources.

The CoC will conduct top-level research to develop products, services and clean technologies with high resource and energy efficiency, and significant economic, social and environmental added value.

A key focus is placed on the vertical module "Transfer". It foresees activities related to training, dissemination of results, technology transfer and technological entrepreneurship. Large-scale actions for joint master's, doctoral and post-doctoral programmes are planned, where the training and qualification of specialists will be distinguished by the two types of interdisciplinary important for the EU Road map, respectively, between natural sciences and technical sciences for the purpose of creating holistic and operational clean technologies, and training for technology entrepreneurs, development of their soft skills and ability to reach the end of the technological process following the economic models of implementation and commercialization through start-ups and spin-offs creation.

As a result of the deployment of this module, Clean & Circle CoC will attract specialists with diverse key competences and qualifications, capable of team-working and achieving synergy.

A separate programme has been developed for implementation of each of the vertical and horizontal priorities, and the elements of these programs will be coordinated by the CoC's governing bodies and personally by the Project coordinator.

The project includes an investment part to build and equip the Centre of Competence, and

renovation activities to improve the working conditions in existing laboratories. Within the project framework, 2 laboratory complexes with 11 laboratories and 1 accelerator for technological entrepreneurship and transfer with two laboratories will be built. They will facilitate the completion of the R&D tasks and activities planned.

Expected outcomes

1. Expected results of the R&D programme of the CoC:

- Analyzed and evaluated potential for energy efficiency of residential and industrial water supply systems;
- Suggested methods of reducing energy consumption in the operation of local water supply systems;
- Increased energy capacity of sludge in existing sewerage systems;
- Suggested alternative technology schemes where the aim is not only to purify the waste water but also to obtain products of high calorific value;
- Implemented methods for ultrasound substrates treatment and presented algorithms to increase the yield of biogas by about 25% and methane in biogas;
- Developed, automated, verified, commercialized and implemented system for control of the methanogenesis process based on fluorescence techniques;
- Developed fuel and electrolysis cells to produce hydrogen from waste water

Established optimal technological regimes and technical solutions for application of microbiological fuel cells in the treatment of wastewater and sludge;

- Established a new approach for non-reactive purification of heavily contaminated with heavy metals (copper) and nitrates fluids;
- Pilot testing of the technology for treatment of real waste water and stabilization of unnecessary active sludge in order to obtain a cheap and an energy-efficient alternative for treatment of domestic and industrial waste water;
- The obtained innovative results will be presented at international conferences and will be published in international journals with an impact factor;
- Young specialists will be trained in the course of all project developments. These are masters and PhD students working on their master's thesis and dissertation papers;
- New specialized educational products will be introduced - modules of the disciplines taught at the partnering universities.

2. Developed new products for the economy

- "Solid Waste": glass-crystalline and ceramic materials; geopolymer materials; zeolites, pilot installations for: hydrothermal synthesis and treatment of materials, composites on silicate basis; database and maps of major enterprises, sources of waste products and links to enterprises that use the waste products as raw materials;
- "Water": Pilot installations of: household and industrial wastewater treatment technologies, bioremediation technologies; technology for purification of natural resources and waste products by plasma technologies; new highly selective methods for molecular indication of detoxification processes, anaerobic biodegradation processes, denitrification, nitrification and processes for biological elimination of phosphorus; microbiological preparations for purification with a prescription for use; development of strategies for control of technological processes, of receiving water basins or of technologically affected water basins with hydropower; biosensors; combustion and electrolytic cells to produce hydrogen from waste water; a high-selective indicator method for managing biogas production; map and data base for ranking of sources of pollution of the water

basins with trivial and dangerous pollutants; manuals with verified mechanisms and algorithms to accelerate the water purification processes;

- Applications for the circular economy: Innovation in clean technologies for optimizing biogas and RDF production at the enterprises; increasing the efficiency of construction waste recovery; developing strategies for environmental risk assessment and management in enterprises and wastewater treatment plants; estimation of biodegradability of plasmids; toxicity assessment; evaluation of resources, waste, new materials and technological processes by chemical, physico-chemical, technological, microbiological, enzymatic and molecular-biological indicators, and expert data evaluation.

Strategic programme for development of the Centre's R&D and innovations

The Strategic programme for development of the Centre's R&D and innovations involves development of approaches and technologies for recovery of natural resources in the course of the disposal of waste and wastewater - recovery of phosphorus and other chemical elements, of bio-products, and obtaining of valuable products (microbiological and augmentation preparations) from wastes.

New construction materials will be developed from construction waste and residues from waste disposal technologies. Green zeolites, valuable material for water and air purification and concentration and extraction of new valuable chemical elements present in water as a pollutant will be generated from waste ashes from heat plants and incinerators. Adsorbents and catalysts, mesopores and nanocomposites, useful for effective water treatment, will be produced from agricultural waste. The valuable for agriculture - compost and bio-fertilizers enriched with macro- and microelements will be obtained.

Innovative approaches and technologies for efficient use of energy in water cycles will be developed. Special innovations will be implemented and tested in energy production technologies from the biomass of excess active sludge, biomass from algal technologies in water treatment plants, and biomass of plant and food waste.

Technologies will be developed to convert composite waste, non-recyclable construction waste

into RDF fuel. Technologies to produce hydrogen from pollutants in wastewater based on fuel and electrolysis cells will be developed.

All these innovative approaches and future technologies are the steps towards the introduction of resource and energy efficiency in the water and solid waste sectors, towards the restoration of biological and technical resources, and sustainable development of the economy, environment and society. They will lead to an increase in the competitiveness of the Bulgarian economy. A large part of the technologies envisaged are technologically advanced TRL-3, TRL-4. This means that technologies can go to pilot studies, scaling and verifying, and commercializing.

The new products from waste and wastewater with a high potential for inclusion in the circular economy are: valuable chemical elements, biosurfactants, microbiological preparations, bioreactors enriched with macro- and trace elements recovered from waste, microbiological preparations, valuable materials for industry and purification technologies, construction materials, renewable energy from waste, etc.

Technologies for obtaining such products will be sought, developed, described, verified, scaled, and implemented. These technologies will be patented as national and international patents, while the shortest possible ways for their dissemination will be pursued and they will be implemented through commercialization based on spin-off and start-up small businesses or through innovative business models included in the large companies - associated partners of the CoC (through scaling and technology transfer).

The innovative products and the above-mentioned technologies will lead to economic development nationwide at a macroeconomic level as they will tackle key economic issues, such as recovery of construction waste, waste from thermal power plants and other industrial waste, as well as plant food waste, through scientific and innovative approaches.

From each waste a substantial product or raw material for other production will be obtained, which will lead to high economic efficiency on the one hand and to high environmental and social added value on the other. The opportunity for fast commercialisation and the introduction of products and technologies to the market will lead to an increase in the competitiveness of the Bulgarian economy in the field of clean technologies.

Each created technology will be accompanied by a business plan and the most effective and

efficient channels for its economic and technological dissemination and realization will be selected.

Research, technology, training and business innovations will serve as a powerful driver for introduction of the key elements of the circular economy linked to resource and energy efficiency in the "water" and "waste" sectors. The distance between the scientific achievements, real technologies and business will be shortened and gradually eliminated. The ultimate goal of the sought-after scientific and technological innovations is to turn any waste into a substantial raw material or energy with its maximum value, i.e. in each new element the technological, economic, environmental and social potential will be sought and evaluated.

The implementation of the above-mentioned innovation chain of the circular economy will involve students - bachelors and masters, PhDs, postgraduates, young researchers. They will be trained according to the dual system of "learning by doing" and "qualification in the course of the scientific and technological innovations", which in turn will ensure the sustainability of the CoC and will enable the financial investment to start playing off.

Research infrastructure development plan

The project „Clean technologies for sustainable environment – waters, waste, energy for circular economy“ (Clean&Circle) for creation and development of a Centre of Competence plans to build a distributed research infrastructure, according to the needs and tasks the partners will perform and the expected results of the project. The new research infrastructure will be built up in three stages, as follows:

Stage I: Construction of a new building for the needs of the Centre of Competence, with an acceleration of technology entrepreneurship, putting it into operation and substantial renovation of existing laboratories.

Expected results:

1. A new building of the CoC constructed and put into operation.

A new 4-storey building with an underground floor, rectangular in plan, with a corridor system, with a uniform distribution of the floors within a property, provided for the needs of the Centre of Competence with a decision of the Academic Council of Sofia University of 21.12.2016.

Stage II. Equipment and commissioning of the laboratory complexes and the accelerator for technological entrepreneurship of the CoC.

Expected results:

- Equipped specialized laboratory complex in the scientific area "waters";
- Equipped specialized laboratory complex in the scientific area "solid waste";
- The technology entrepreneurship accelerator equipped with a prototyping laboratory;
- Equipped common premises of the new CoC building;
- New laboratory complexes put into operation.

Stage III. Creation of CoC's common information system to integrate large amounts of data, to implement data analysis and forecasting methods, and to link applications, data and services with stakeholders in order to achieve competitive advantage.

Expected results:

Established common information system of the CoC with the capability to integrate large amounts of data, application of data analysis and prognostic methods, and liaison with stakeholders, as well as training of the partners and their customers to use the technology cloud.

The project envisages the first and third stages to be implemented in parallel and the second stage will start depending on the readiness to substantially modernize the scientific infrastructure of each partner.

Work packages to carry out the envisaged research activities of the project

Work Package 1: Water: Indication, monitoring and control

The objective is to assess the potential benefits or damages to preserving and improving the ecological status of the water intakes following application of the circular economy principles in the water sector, and in particular after increasing the amount of re-used water.

Work Package 2: Water: Clean technologies

The goal is to develop new or to improve existing water treatment and purification technologies prior to reuse. The technology upgrade will consist of exploring technologies consistent with the principles of sustainable development with inclusion of new materials and processes, innovative means of water treatment and purification. They will provide higher quality than the conventional water treatment technologies.

To this end, the research program includes development of technologies for complete water treatment, including pollutants, the removal of which is unresolved so far. It is envisaged to explore completely new purification technologies based on newly synthesized adsorbents and materials based on nanostructures from waste products of agriculture and industry. All technologies developed under laboratory or pilot conditions will be subject to the principles of the circular economy.

Work Package 3: Solid Waste: Identification, monitoring and innovative control and characterization methods

The envisaged tasks and activities of the work package fall entirely within the ISSS priorities for solid waste management and recovery. The characteristics for assessing their useful properties are outlined for the purpose of processing the accumulated industrial waste into new raw materials, materials and articles, and introduction of new environmentally friendly technologies - little and/or waste-free, according to the principles of the circular economy and resource efficiency. Qualitative characteristics leading to serious environmental problems are identified. The possibilities of risk assessment, methods for prevention, reduction and elimination of dangerous phenomena and products are explored.

Work package 4: Solid waste: Disposal and recovery technologies

The work programme envisages studies for production of materials and products through processing of the accumulated industrial and municipal waste from 5 large groups of solid waste: industrial waste (mainly from the metallurgical and extractive industries), construction (concrete, ceramics, glass, gypsum, plasters, heat-insulating mineral-fiber materials), ash waste from power plants, biomass from food waste and plants, and biodegradable municipal waste.

Work Package 5: Application of the circular economy in the "Water" and "Solid Waste" sectors

The aim of this work package is to develop research and technology approaches for resource recovery and efficient use of energy in the "Water" and "Solid waste" sectors. On the basis of this objective, the following tasks are formulated for implementation: 1/ Recovery of resources (chemical elements/ phosphorus), gypsum,

biosurfits, microbiological preparations from waters, sludge and solid waste; 2/ Efficient use of energy (renewable and alternative energy sources).

Time frame for carrying out research activities

The long-term joint work of the project partners creates preconditions for starting the research work from the first working month of the project. Preparatory R&D activities are foreseen until the purchase and commissioning of the equipment and construction/renovation of the necessary infrastructure, as well as simultaneous implementation of the activities of the individual modules. The construction of the research structure, including the construction of the new building, will take place in the first 32 project months (the third project year). During this time, the building of the scientific capacity and the envisaged technology development will take place at the existing and renovated premises of the project partners.

Specific practical objectives and tasks to be addressed by the research planned

- Preservation and improvement of the ecological status of the water intake;
- Need to create new or improve existing water treatment and purification technologies before reuse;
- Processing of accumulated industrial waste into new raw materials, materials and products and introduction of new environmentally friendly technologies - little and/or waste-free;

- Processing of accumulated industrial and household waste;
- Need to recover resources;
- Need for efficient use of energy and renewable and alternative energy sources.

Expected benefits of project implementation

The expected benefits of the project implementation will manifest in and will have impact on the following areas of industry, economy and society: energy and energetics, environment, closed water supply cycles, health and food, physical sciences and engineering, social innovation and e-Infrastructures.

Indirectly but with great influence, the benefits will affect the development of tourism in all its aspects - marine, rural, ecological, cultural, as well as the healthy lifestyles – i.e. prolonging the working capacity of the population.

Prof. Dsc. Dr. Yana Topalova

Faculty of Biology, Sofia University "St. Kliment Ohridski" Dragan Tzankov bld. 8, 1164 Sofia, Bulgaria; E-mail: yanatop@abv.bg



Assessment of the toxicity and antiproliferative activity of hemocyanins from *Helix lucorum*, *Helix aspersa* and *Rapana venosa*

I. Yankova¹, E. Ivanova¹, K. Todorova¹, A. Georgieva¹, V. Dilcheva¹, I. Vladov¹, S. Petkova¹, R. Toshkova¹, L. Velkova², P. Dolashka², I. Iliev^{1*}

¹ Institute of Experimental Morphology, Pathology and Anthropology with Museum, Bulgarian Academy of Sciences, Sofia 1113, Bulgaria

² Institute of Organic Chemistry with Centre of Phytochemistry, Bulgarian Academy of Sciences, Acad. G. Bonchev Str. Bl. 9, 1113 Sofia, Bulgaria

Received January 27, 2021; Revised February 17, 2021

Hemocyanins (Hcs) are respiratory, oxygen-carrying metalloproteins that are freely dissolved in the hemolymph of many molluscs and arthropods. The interest in hemocyanins has grown significantly since it was found that they can be successfully used in immunotherapy of neoplastic diseases as non-specific or active stimulators of the immune system. The present study aims to assess the cytotoxicity, *in vivo* toxicity and antiproliferative activity of hemocyanins isolated from marine snail *Rapana venosa* (RvH), garden snails *Helix lucorum* (HIH) and *Helix aspersa* (HaH). For *in vitro* safety testing, 3T3 Neutral Red Uptake (NRU) test was used. The experiments for antiproliferative activity of the hemocyanins were performed by MTT assay on a panel of cell lines - a model of breast cancer. The *in vivo* toxicological assessment was performed by regular clinical examinations of hemocyanin-treated laboratory mice and histopathological analysis of hematoxylin/eosin stained preparations of parenchymal organs. The evaluation of the *in vitro* cytotoxicity showed that the tested hemocyanins does not induce toxic effects in nontumorigenic epithelial cell lines. In contrast, significant reduction of the viability of human breast carcinoma cell lines was found after treatment with high concentrations of hemocyanins. The *in vivo* experiments showed no signs of organ and systemic toxicity in the hemocyanin-treated animals. The presented data indicate that Hcs show a potential for development of novel anticancer therapeutics due to their beneficial properties, biosafety and lack of toxicity or side effects.

Key words: hemocyanins (Hcs); cytotoxicity; antitumor activity; *in vivo* biosafety testing

INTRODUCTION

Breast cancer is the most common malignant diseases among women in Europe, accounting for more than 12% of the total number of new cases of cancer diagnosed in 2018 [1]. The frequency of newly diagnosed cases of breast cancer in Bulgaria is about 4 061 per year, 30% of which are fatal [2]. Despite the great advances of the modern medicine in the diagnosis and treatment of cancer, the number of cases has been growing every year, which is why breast cancer is the leading cause of death in women worldwide [3]. Due to the increasingly common multidrug resistance to cancer chemotherapy [4], it is necessary to search for new alternatives to the standard antineoplastic drugs. One such good alternative is the usage of hemocyanins. They are copper-containing respiratory glycoproteins with complex quaternary structure, localized in the hemolymph of some invertebrates belonging to the Mollusca and Arthropoda phyla [5, 6]. Hemocyanins have found an application as carrier proteins and adjuvants in

antibody production and as non-specific immunostimulants in bladder cancer therapy [7, 8]. Among the hemocyanins, the Keyhole Limpet Hemocyanin (KLH), isolated from the marine snail *Megatura crenulata* has been most extensively studied and applied in immunotherapy [9, 10]. However, the restricted geographical distribution of *M. crenulata* does not allow the extraction of high quantities of Hcs.

As an alternative of KLH, we propose hemocyanins isolated from *H. aspersa*, *H. lucorum* and *R. venosa*, which are widespread throughout the world, including in Bulgaria. The structure and chemical composition of these hemocyanins have been studied in detail and described by Bulgarian research team [11-13]. The presence of a variety of carbohydrate components in hemocyanins can lead to a direct interaction with receptors on the surface of cancer cells. As a result, apoptosis or necrosis can be induced [14]. In addition, the carbohydrate components can induce antitumor immunity [15].

The aim of the present study was to determine the cytotoxicity and antiproliferative activity of HaH, HIH, and RvHI in permanent cell lines and to evaluate their biosafety *in vivo*.

* To whom all correspondence should be sent:

E-mail: taparsky@abv.bg

EXPERIMENTAL

Isolation of native hemocyanins from garden snails Helix aspersa and Helix lucorum and subunit RvH from marine snail Rapana venosa

The hemolymph from garden snails *Helix aspersa* and *Helix lucorum*, and marine snail *Rapana venosa* was collected after cutting the foot muscles. The rough particles and hemocytes were removed after filtration and centrifugation at 10,000 rpm (at 4 °C) for 20 min. It is known that hemolymph of these snails contained above 90% hemocyanin as a major protein with molecular mass around 9000 kDa. Therefore the crude hemolymph extract was subject to ultrafiltration on membrane 100 kDa (Millipore Ultrafiltration Membrane Filters) and the fraction above 100 kDa containing predominantly native hemocyanin was put to ultracentrifuge at 22,000 rpm (rotor Kontron-Hermle A8.24, centrifuge CENTRIKON) at 4 °C for 3 h, as a result the total hemocyanins were obtained as sediment. After removal of the supernatant, the precipitated total hemocyanins HaH and HIH were solubilized in 50 mM Tris buffer (pH 7.5) containing 20 mM CaCl₂ and further purified by gel filtration [16].

The native RvH was obtained also after ultracentrifugation at 22,000 rpm (at 4 °C) for 180 min and was purified by gel filtration. After dissociation of native RvH and purified on an ion-exchange chromatography, two subunit RvHI and RvHII (with molecular masses 420 kDa and 400 kDa, respectively) were obtained [16].

All the hemocyanins were filtered through a bacterial filter with a pore size of 0.2 µm (Corning®; Incorporated Life Sciences, St. Lowell, MA, USA) under sterile conditions.

Cell cultures

Two human mammary carcinoma cell lines MCF-7 and MDA-MB-231 were used as models for breast cancer. The MCF-7 cell line has some characteristics of differentiated mammary epithelium including expression of estrogen and progesterone receptors (ER⁺, PR⁺ and Her-2⁻) [17, 18]. The MDA-MB-231 is a highly aggressive, invasive and poorly differentiated triple-negative (ER⁻, PR⁻ and Her-2⁻) breast cancer [19]. The cell lines BALB/c 3T3 (mouse embryonic fibroblasts) and MCF-10A (human breast epithelial cell line) were used as models for healthy tissue. Cells were cultured in Dulbecco Modified Eagle's medium (DMEM) supplemented with 10% (v/v) fetal

bovine serum (Gibco, Austria), 100 U/ml penicillin and 0.1 mg/ml streptomycin (Lonza, Belgium) in an incubator at 37 °C, 5% CO₂ and 95% humidity. Plastic flasks 25 cm² (Greiner, Germany), were used to grow the cells. The cells were kept in exponential phase of growth and after processing with trypsin-EDTA (FlowLab, Australia).

BALB/c 3T3 NRU cytotoxicity test

Neutral Red Uptake test (NRU-assay) is a colorimetric method for assessment of cell viability *in vitro* [20]. This method is based on the ability of living cells to include the Neutral Red dye in their lysosomes. BALB/c 3T3 cells were plated at a density of 1×10⁴ cells in 100 µl culture medium in each well of 96-well flat-bottomed microplates and allowed to adhere for 24 h before treatment with hemocyanins, dissolved in PBS and further diluted in culture medium. A wide concentration range was applied (from 7.5 to 1000 µg/ml) and the cells were incubated for additional 24 h. After treatment with Neutral Red medium for 3 h, washing and application of Ethanol/Acetic acid solution (NR Desorb), the absorption was measured on a TECAN microplate reader at wavelength 540 nm.

In vitro antiproliferative activity

The antiproliferative/antitumor activity testing was performed on MCF-10A, MCF-7 and MDA-MB-231 cell lines by MTT-dye reduction assay [21]. The assay is based on the metabolism of the tetrazolium salt MTT to formazan by mitochondrial reductases. The cells were plated at a density of 1×10³ cells in 100 µl in each well of 96-well microplates and allowed to adhere for 24 h. The cells were then treated with hemocyanins applied at a concentration range from 7.5 to 1000 µg/ml for 72 h. The formazan absorption was registered using a microplate reader at λ=540 nm. For assessment of the antiproliferative activities, the IC₅₀ values were calculated using non-linear regression analysis (GraphPad Prism4 Software). The statistical analysis included application of One-way ANOVA followed by Bonferroni's post hoc test. p<0.05 was accepted as the lowest level of statistical significance. All results are presented as mean ± SD.

In vivo testing for toxic and pathological effects

In vivo studies were performed on 16 white laboratory mice with body weight about 25-30 g in order to test the biosafety of hemocyanins and to

exclude any toxicity or adverse pathological effects. The experimental animals were divided into four groups—one control and three experimental groups. The control animals were injected three times subcutaneously with saline solution. The animals from the experimental groups were injected three times subcutaneously as follows: the first group with the hemocyanin HaH, the second group with HIH and the third with RvHI at a dose of 1 mg/kg bw. All procedures were consistent with the recommendations for in vivo animal studies in accordance with the requirements of Regulation № 20/ 01.11.2012 regarding laboratory animals and animal welfare and European legislation.

Histological examination

Materials from livers, kidneys, spleen, lungs and heart were fixed in 10% buffered formalin (pH 7) (Alkaloid AD, Skopje), dehydrated, embedded in paraffin (Emmonya, Biotech Ltd, Bulgaria), sliced into 5-10 μm , dewaxed in xylene (Alkaloid AD, Skopje) and stained with Mayer's Hematoxylin (Emmonya, Biotech Ltd, Bulgaria) and Eosin (Bio optica, Milano, Italy) according to routine histological techniques. Investigations were performed on a microscope Leica DM 5000B, Germany and micrographs were taken.

RESULTS

In vitro effects of hemocyanins on the cell viability and proliferation

The Hcs were studied for cytotoxicity by standard method (3T3 NRU-test). The BALB/c 3T3 cells were incubated with the test compounds (total native hemocyanins HaH and HIH and structural subunit RvHI) at concentrations ranging from of 7.5 to 1000 $\mu\text{g/ml}$ for 24 h, after which the cytotoxicity expressed as a percentage of the negative control was determined. The obtained results are shown in Fig. 1, A). The tested Hcs were non-toxic (the cytotoxicity values determined for all hemocyanin concentrations tested do not show a significant difference compared to the negative control), so CC_{50} values can not be determined at the applied concentration range.

Cell viability testing was performed by standard MTT dye reduction assay. Normal human mammary epithelial cells (MCF-10A) were incubated with the test hemocyanins at concentrations ranging from 7.5 to 1000 $\mu\text{g/ml}$ for 72 h. The cell viability expressed as a percentage of the negative control was determined. The dose-

response curves are shown in Fig. 1, B). HaH induced a slight reduction of the viability of MCF-10A cells. At the highest concentration studied, the cell viability was decreased by only 6%. The other two hemocyanins (HIH and RvHI) showed a significant increase in the cell viability of about 12 and 8%, respectively, compared to the negative control.

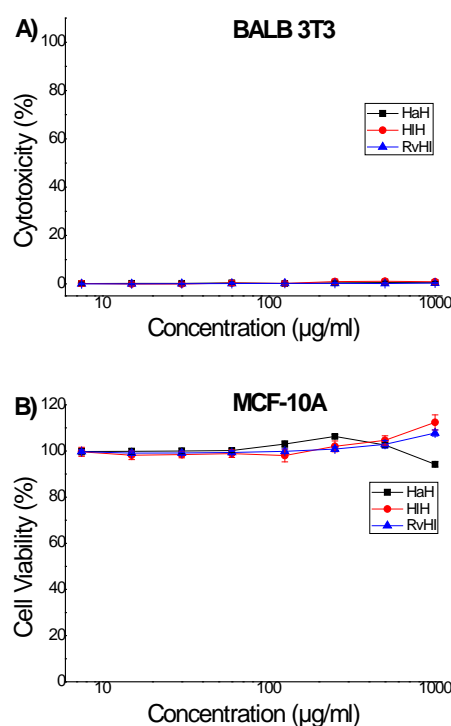


Fig. 1. *In vitro* cytotoxic (A) and proliferative (B) activity of hemocyanins (HaH, HIH and RvHI).

In vivo toxicological investigations

All animals from the experimental groups showed good general condition and appetite throughout the test period. Livers, spleen, lungs, kidneys and heart of the hemocyanin-treated experimental mice did not show any histopathological signs of toxicity at the doses used (Fig. 2). LD_{05} was not reached and the concentrations were assessed in the region of LD_0 . In the spleen of the treated mice, no pathological changes were observed. The histoarchitecture was normal with preserved white and red pulp ratio. Myeloid and erythroid hyperplasia with megakaryocytes was also found, evidential of extramedullary hematopoiesis, which is commonly observed in rodents, especially mice, as a normal component of the pulp of the spleen (Fig. 2, B).

Megakaryocytes are more common in young than in adult animals, but in certain circumstances,

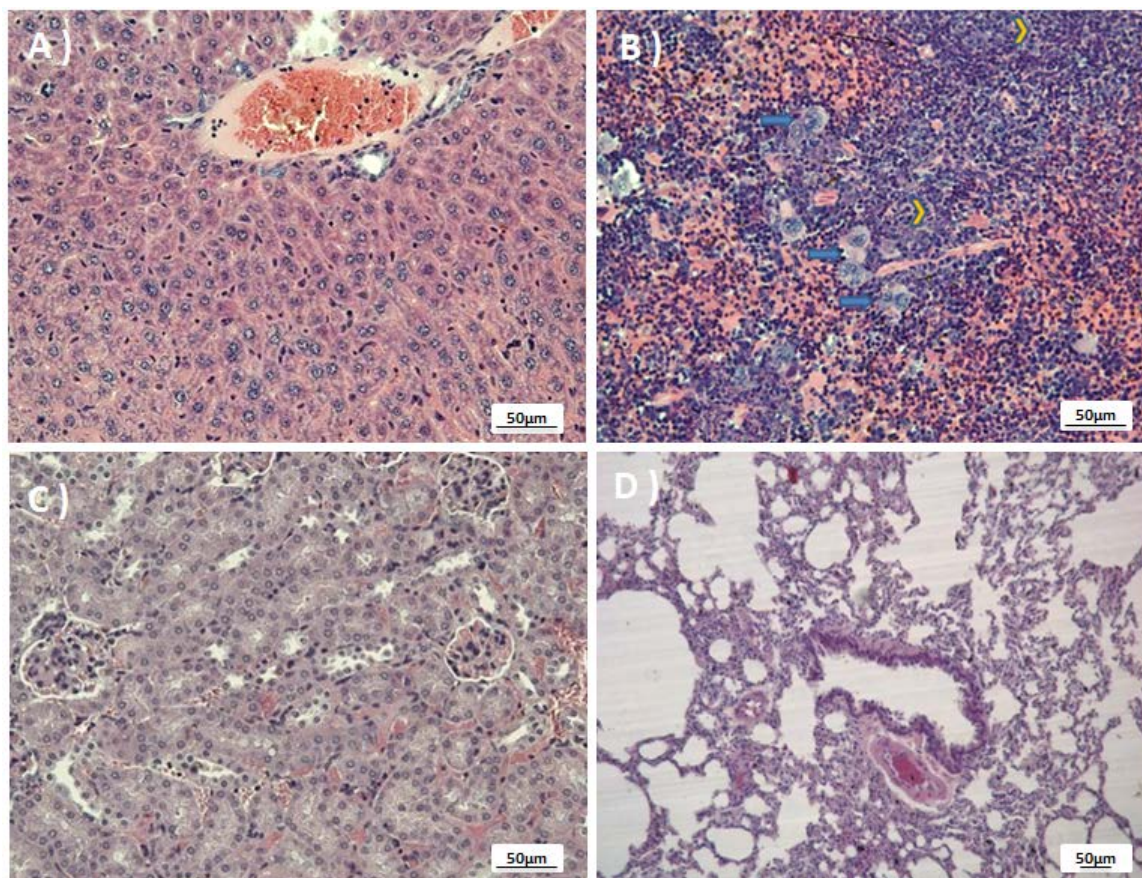


Fig. 2. *In vivo* toxicity screening and organ pathology. Animals were injected three times subcutaneously with 1mg/kg bw HaH. A) livers, B) spleen, C) kidneys and D) lungs. In the spleen, two small germinal centers (yellow arrows) with a thin marginal zone (black arrow) adjacent to the red pulp were observed. White to red pulp ratio were maintained. Myeloid and erythroid hyperplasia with megakaryocytes (blue arrows). Livers, kidneys and lung showed normal morphology.

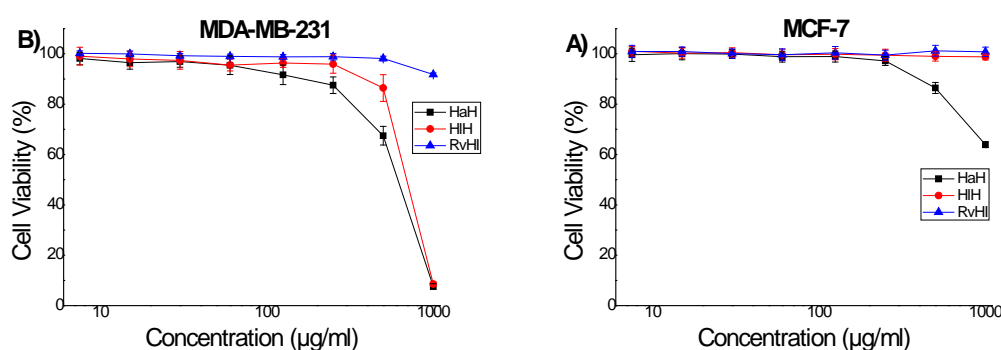


Fig. 3. Cell viability of breast carcinoma cells treated with hemocyanins (HaH, HIH and RvHI) for 72 h. A) MCF-7 and B) MDA-MB-231.

different external agents may provoke their increase. The obtained results showed that hemocyanins – HaH-total, HIH-total and subunit RvHI applied three times at a dose of 1 mg/kg bw did not cause any pathohistological changes indicative of toxic damage to the parenchymal organs. The degree of hyperplasia in the spleen was within the normal range and was similar to those

observed in the controls. Lungs, kidneys, heart and livers also showed normal morphology.

Antitumor activity

The *in vitro* antitumor activity of the hemocyanins was determined by MTT dye reduction assay on two cancer cell lines MCF-7 and MDA-MB-231 (Fig. 3). In the MCF-7 cell line, the

hemocyanins showed similar activity to those found in MCF-10A cells (Fig. 3, A). Low antitumor activity of HaH-total (36% decrease of the cell viability) was observed at the highest concentration studied (1000 µg/ml). For the other tested hemocyanins (HIH-total and subunit RvHI), no difference was observed compared to the negative control.

In the MDA-MB-231 cell line, the hemocyanins (HaH and HIH) showed a weak antitumor effect (Fig. 3, B), with IC₅₀ values 644 ± 24 and 732 ± 19 µg/ml, respectively. No significant decrease of cell viability in the carcinoma cells treated with subunit RvHI was observed.

DISCUSSION

Molluscan Hcs are oligomeric glycoproteins with complex dodecameric quaternary structures and heterogeneous glycosylation patterns, primarily consisting of *N*-glycans, which contribute to their structural stability and immunomodulatory properties in mammals [22]. Hemocyanins from different molluscan species have been considered for use in diverse biomedical and clinical applications.

Gastropod Hcs including tested hemocyanins are glycoproteins with a high carbohydrate content of about 9% (w/w) that may contain unusual monosaccharides, such as a methylated hexoses (for example, *O*-methyl-D-mannose and *O*-methyl-D-galactose), β(1,2)-linked xylose, α(1,3)-linked fucose, α(1,6)-linked fucose or hexuronic acid [22]. The glycan moieties play diverse roles in biological systems that make them relevant for use as biotherapeutics.

The tested hemocyanins differ significantly in their structural organization, molecular weight, carbohydrate structure and monosaccharide composition. The native *R. venosa* hemocyanin (RvH), like KLH, is composed of two polypeptide structural subunits RvHI and RvHII with molecular weight 420 and 400 kDa, respectively [23]. Total hemocyanins from garden snails *H. aspersa* and *H. lucorum* (HaH-total; HIH-total) are with molecular weight about 9MDa and consist of three structural subunits – two α- and one βc-isoforms [24]. Each of them ranging from 350 to 450 kDa, includes eight globular folded domains known as functional units (FUs) with molecular masses of about 47-65 kDa. Native HIH and HaH as well as subunit RvHI exhibit a predominant dodecameric structure as revealed by electron microscopy [23-25].

One of the main characteristics of the hemocyanins from snails *R. venosa*, *H. aspersa* and

H. lucorum are their carbohydrate structures. Recent structural studies of the two isoforms of RvH demonstrate the presence mainly of high mannose, complex and hybrid-type glycan structures as well as unusual *N*-glycan structures with an internal fucose residue (β1-2) binding GalNAc and hexuronic acid [22]. The presence of mono- and bi-antenna *N*-linked glycan structures from complex and high mannose type were established in hemocyanins from *H. lucorum* and *H. pomatia* [26, 27]. Most of them contain variously methylated glycan structures of 3-*O*-methyl-D-mannose and 3-*O*-methyl-D-galactose as well as core modification - mainly with β1-2-linked xylose to β-mannose and/or α1-6-fucosylation of GlcNAc residue (the Asn-bound GlcNAc). The methylated structures are heterogeneous in terms of involved monosaccharides and position of methylation. Most of the analyzed glycans of β-HIH contain mainly a terminal and/or inner MeHex residue, in some cases even up to four such residues are present [26]. The chemical composition of hemocyanins (copper ions, oligosaccharide and amino acid sequences) determines their low toxicity [28]. In practice, hemocyanins toxicity has been studied on different cell lines under *in vitro* conditions, mainly in experiments to determine antiviral activity [29, 30]. Therefore, only cell lines suitable for the replication of the respective viruses were used, but not suitable for the determination of cytotoxicity, which would give us correct information about possible toxicity and pathological effects under *in vivo* conditions. In this study, we examined the cytotoxicity of total hemocyanins HaH and HIH, and subunit RvHI on the BALB/c 3T3 cell line by the NRU-test. This method has been approved for the determination of cytotoxicity by the ICCVAM (Interagency Coordinating Committee on the Validation of Alternative Methods) that coordinates U.S. federal government evaluation of new, revised, and alternative test methods [31]. The results obtained by this *in vitro* method show that the tested hemocyanins are non-toxic even at the highest concentrations used (1000 µg/ml). In addition, through this *in vitro* method, we predicted the absence of toxicity at *in vivo* conditions, which we proved by toxicological experiments and histological analyses. The results of *in vivo* experiments showed that the livers, spleen, lungs, kidneys and heart of the hemocyanin-treated mice remained intact and no histopathological signs of toxicity were observed at the doses used. Moreover, in experiments to determine cell viability of the

normal epithelial cell line (MCF-10A), we found that HIH and RvHI even increase cell proliferation. MCF-10A is a reliable model for normal human mammary epithelial cells, with functional cellular mechanisms of apoptosis and cell proliferation. As a result, they are very sensitive to external influences. The observed increase of the proliferative activity of treated cells is evidence of the regenerative properties of hemocyanins known from the traditional medicine [32]. This is the reason why hemocyanins are widely used in cosmetics and medicine. Most biological studies related to hemocyanins focus on their immunological properties. Due to the strong activation of humoral immunity, they are used as adjuvants and molecular carriers of weakly immunogenic antigens, such as tumor antigens [33]. Therefore, there is great interest in the research related to the use of hemocyanins in the immunotherapy of neoplastic diseases. In addition, there is evidence of successful treatment of bladder cancer by direct application of hemocyanins to the affected tissue. Moreover, *in vitro* experiments were performed to determine the antitumor activity of hemocyanins on tumor cell lines (647-V, T-24 and CAL-29) -models of bladder cancer [34]. All these literature data show the presence of structural and chemical features of the hemocyanin molecule that may directly affect the proliferation and viability of cancer cells. Therefore, we performed *in vitro* experiments to determine the antitumor activity of the studied hemocyanins on the cell lines MCF-7 and MDA-MB-231, which are models of hormone-dependent and hormone-independent breast cancer, respectively. The results showed that the MCF-7 cell line was not sensitive to the studied hemocyanins, while the triple-negative cell line MDA-MB-231 showed a significant growth inhibition after treatment with high concentrations of HaH and HIH. Since it is known that MDA-MB-231 cell line has a very high proliferative potential and metabolic activity, it is likely that the observed antitumor effect is due to an interaction between the hemocyanins and the cytoplasmic membrane that decrease its permeability and block the transmembrane transport of metabolites, thus leading to reduced vitality and cell death.

We hypothesize that the difference in the antitumor activity of the investigated hemocyanins is most likely due to the difference in their specific carbohydrate moieties, which are located on the surface of the didecimeric structures [22]. The observed higher antitumor activity of HIH and HaH

compared to RvHI is probably due to the high content of methylated *N*-glycans as well as β 1-2-linked xylose to β -mannose in inner core in these Hcs. It is known that the glycans carrying a xylose residue linked to the inner core are often found in plants and demonstrate a high immunogenicity for mammalian species [35].

CONCLUSION

The results obtained and the subsequent analysis showed that the tested hemocyanins were not cytotoxic and did not cause pathological changes in the treated experimental animals. The increased viability of the normal cells and the observed growth inhibitory effect in mammary carcinoma cells with high proliferative potential indicate the possibility of application of hemocyanins in the field of regenerative medicine and cosmetics, as well as in adjunctive therapy of neoplasms with high proliferative index.

Acknowledgements: *The work was financially supported by the Ministry of Education and Science of the Republic of Bulgaria, National Scientific Program "Innovative Low-Toxic and Biologically Active Means for Precision Medicine" – BioActiveMed, grant number № 01-358/17.12.2020.*

REFERENCES

1. Eurostat, Cancer statistics – Specific cancers, online data codes: hthh_cd_aro and hthh_cd_asdr2.
2. World Health Organization, International Agency for Research on Cancer, The Global Cancer Observatory, 2020, <https://gco.iarc.fr/today/data/factsheets/populations/100-bulgaria-fact-sheets.pdf>.
3. N. Azamjah, Y. Soltan-Zadeh, F. Zayeri, *Asian Pac. J. Cancer Prev.*, **20**, 2015 (2019).
4. N. Patel, M. Rothenberg, *Invest. New Drugs*, **12**, 1 (1994).
5. S. Kato, T. Matsui, C. Gatsogiannis, Y. Tanaka, *Biophys. Rev.*, **10**, 191 (2018).
6. H. Bak, B. Neuteboom, P. Jekel, N. Soeter, J. Vereijken, J. Beintema, *FEBS Lett.*, **204**, 141 (1986).
7. D. Mora, M. Salman, A. Myrick, J. Rhyhan, L. Miller, E. Saetre, D. Eckery, *Fish Shellfish Immun.*, **71**, 255 (2017).
8. D. Lamm, J. DeHaven, D. Riggs, C. Delgra, R. Burrell, *Urol. Res.*, **21**, 33 (1993).
9. J. Harris, J. Markl, *Micron*, **30**, 597 (1999).
10. A. Kantele, M. Häkkinen, J. Zivny, C. Elson, J. Mestecky, J. Kantele, *J. Immunol. Res.*, 614383 (2011).

11. L. Velkova, P. Dolashka, A. Dolashki, W. Voelter, B. Atanasov, *BBA-Proteins Proteom.*, **1804**, 2177 (2010).
12. P. Dolashka, F. Zal, A. Dolashki, L. Molin, P. Traldi, B. Salvato, *J. Mass Spectrom.*, **47**, 940 (2012).
13. L. Velkova, P. Dolashka, J. Van Beeumen, B. Devreese, *Carbohydr. Res.*, **449**, 1 (2017).
14. D. Green, F. Llambi, *Cold Spring Harb, Perspect. Biol.*, **7**, a006080 (2015).
15. M. Palacios, R. Tampe, M. Campo, T. Zhong, M. López, F. Salazar-Onfray, M. Becker, *Eur. J. Med. Chem.*, **150**, 74 (2018).
16. A. Georgieva, K. Todorova, I. Iliev, V. Dilcheva, I. Vladov, S. Petkova, R. Toshkova, L. Velkova, A. Dolashki, P. Dolashka. *Biomedicines*. **8**, 194 (2020).
17. E. Sweeney, R. Mcdaniel, P. Maximov P. Fan, V. Craig, *Horm. Mol. Biol. Clin. Investig.*, **9**, 143 (2013).
18. M. Gunduz, E. Gunduz, F. Shirazi, *InTech*, 85 (2011).
19. K. Chavez, S. Garimella, S. Lipkowitz, *Breast Dis.*, **32**, 35 (2010).
20. E. Borenfreund, J. Puerner, *Toxicol. Lett.*, **24**, 119 (1985).
21. T. Mosmann, *J. Immunol. Methods*, **65**, 55 (1983).
22. P. Dolashka, A. Daskalova, A. Dolashki, W. Voelter, *Biomolecules*, **10**, 1470 (2020).
23. P. Dolashka-Angelova, H. Schwarz, A. Dolashki, S. Stevanovic, M. Fecker, M. Saeed, W. Voelter, *Biochim. Biophys. Acta*, **1646**, 77 (2003).
24. L. Velkova, I. Dimitrov, H. Schwarz, S. Stevanovic, W. Voelter, B. Salvato, P. Dolashka-Angelova, *Comp. Biochem. Physiol.*, **157**, 16 (2010).
25. A. Dolashki, L. Velkova, W. Voelter, P. Dolashka, Z. *Naturforsch. C*, **74**, 113 (2019).
26. L. Velkova, P. Dolashka, J. Van Beeumen, B. Devreese, *Carbohydr. Res.*, **449**, 1 (2017).
27. J. Van Kuik, H. Van Halbeek, J. Kamerling, J. Vliegthart, *Eur. J. Biochem.*, **159**, 297e301 (1986).
28. M. Del Campo, S. Arancibia, E. Nova, F. Salazar, A. Gonzalez, *Rev. Med. Chil.*, **139**, 236 (2011).
29. P. Dolashka, N. Nesterova, S. Zagorodnya, A. Dolashki, G. Baranova, A. Golovan, W. Volter, *Global J. Pharmacol.*, **8**, 206 (2014).
30. N. Zanjani, M. Miranda-Saksena, P. Valtchev, R. Diefenbach, L. Hueston, E. Diefenbach, F. Sairi, V. Gomes, V. Cunningham, A. Dehghani, *Antimicrob. Agents Chemother.* **60**, 1003 (2016).
31. ICCVAM-Recommended Test Method Protocol, Appendix C1: BALB/c 3T3 NRU cytotoxicity test method, NIH Publication No. 07-4519 (2006).
32. B. Bonnemain, *Altern. Med.*, **2**, 25 (2005).
33. A. Kantele, M. Häkkinen, J. Zivny, C. Elson, J. Mestecky, J. Kantele, *J. Immunol. Res.*, **2011**, 614383 (2011).
34. O. Antonova, L. Yossifova, R. Staneva, S. Stevanovic, P. Dolashka, D. Toncheva, *JBUON*, **20**, 180, (2015).
35. M. Gutternigg, K. Ahrer, H. Grabher-Meier, S. Burgmayr, E. Staudacher. *Eur. J. Biochem.*, **271**, 1348e1356 (2004).

Antibacterial activity of bioactive fractions from mucus and hemolymph of different snails species and crab

M. Aleksova¹, L. Velkova², P. Dolashka², G. Radeva^{1*}

¹ Roumen Tsanev Institute of Molecular Biology, Bulgarian Academy of Sciences, Acad.G. Bonchev Str. Bl. 21, 1113 Sofia, Bulgaria

² Institute of Organic Chemistry with Centre of Phytochemistry, Bulgarian Academy of Sciences, Acad. G. Bonchev Str. Bl. 9, 1113 Sofia, Bulgaria

Received January 28, 2021; Revised March 04, 2021

This study aims to evaluate the antibacterial activity of six samples contained biologically active fractions isolated from various molluscs species (garden and marine snails) and one representative of the arthropods (*Carcinus aestuarii*, also known as Mediterranean green crab). The minimum inhibitory concentration (MIC) values for *Escherichia coli* and *Brevindomonas diminuta* were in ranges of 145-682.5 µg/ml and 290-431.5 µg/ml, respectively. The dissociated hemocyanin from *Carcinus aestuarii* (CaH) showed the strongest MIC (145-290 µg/ml) and effective concentrations (EC₅₀ values 75.46-112.2 µg/ml) against all Gram-negative bacterial strains. Two of the tested samples – protein fraction from *Helix aspersa* mucus with Mw above 20 kDa and peptide fraction from *Helix lucorum* hemolymph with Mw below 10 kDa, demonstrated selective antibacterial activity against *E. coli* or *B. diminuta*, respectively. The results in this study showed that the bioactive fractions isolated from mucus and hemolymph of different snail species and isoforms of *C. aestuarii* hemocyanin could be considered as new natural antibacterial agents with potential biomedical application. Further studies are needed to confirm the antibacterial activity with a wider range of bacterial strains.

Key words: antibacterial activity; *Helix aspersa*; *Helix lucorum*; *Rapana venosa*; *Carcinus aestuarii*; minimum inhibitory concentration

INTRODUCTION

Increasing antimicrobial resistance to conventional antibiotics has become a global health threat in the last few decades. Bacteria and other microbes develop mutations that protect them against antibiotics and other antimicrobial drugs, meaning that infections will become more difficult, even impossible to treat. The 700,000 or more deaths that antimicrobial resistance now causes every year could grow to 10 million by 2050. New antibacterial agents are urgently needed – for example, to treat carbapenem-resistant gram-negative bacterial infections as identified in the World Health Organization (WHO) priority pathogen list. It is worth noting that for *E. coli*, *K. pneumonia* and other representatives of the family *Enterobacteriaceae*, the proportion of bacteria resistant to commonly used specified antibacterial drugs exceeded 50% in many WHO regions [1].

Antimicrobial peptides are important in the first line of the host defence system of many animal species [2]. Their value in the innate immunity lies in their ability to function without either high

specificity or memory. In recent years, it has been widely recognized that many organisms use antimicrobial peptides (AMPs) as part of their host defence system against the invasion of microorganisms [3, 4]. Glycoprotein “hemocyanin” and antimicrobial peptides from the hemolymph and mucus are important component of the innate immunity [5]. The hemolymph from snail contains bioactive compounds as glycans, peptides, glycopeptides, and proteins. Many of them have been discovered in recent years [6]. One of them is a hemocyanin, an oxygen-transport glycoprotein found in the hemolymph of both mollusc and arthropod [7]. Moreover, the mucus of land snails is a rich source of peptides and proteins with broad-spectrum antibacterial activity. The following compounds are known to have activity against a large spectrum of microorganisms including bacteria, filamentous fungi, viruses, protozoan and metazoan parasites [8, 9].

Phyla Mollusca and Arthropoda constitute a large reservoir for pharmacologically active compounds. Mucus from *H. aspersa* and hemolymph from *H. lucorum* and *R. venosa*, as well hemocyanin from *C. aestuarii* are a complex mixture of bioactive components with promising application in treatment of pathogenic bacteria [9-

* To whom all correspondence should be sent:
E-mail: gradeva@bio21.bas.bg

12]. Dolashki *et al.* (2020) found that three peptide fractions from garden snail *Cornu aspersum* (also recognised as *Helix aspersa*), those with Mw <3 kDa, Mw 3–5 kDa and Mw 5–10 kDa, have antibacterial activity against the Gram+ bacterial strain *Brevibacillus laterosporus*, and compounds with Mw 10–30 kDa revealed a very high inhibition effect against *E. coli* [10]. Researches indicated that the mucus fraction with Mw between 30 and 100 kDa from the common brown snail *H. aspersa* had a strong antibacterial effect against several strains of *Pseudomonas aeruginosa* and a weak effect against *Staphylococcus aureus* [13]. Mucus from the African giant land snail *Achatina fulica* also inhibited the growth of *S. aureus*, but the broad spectrum of activity reported by other workers was not observed [13].

Furthermore, it has been reported that several peptides from the hemolymph of the garden snails *H. lucorum* and *H. aspersa* exhibit a broad spectrum of antimicrobial activity against *S. aureus*, *Staphylococcus epidermidis*, *E. coli*, *Helicobacter pylori* and *Propionibacterium acnes* [5, 12].

The present study aimed to evaluate the antibacterial activity of six fractions isolated from mucus and hemolymph of three snail species - *Helix aspersa*, *Helix lucorum*, *Rapana venosa* and a crab species *Carcinus aestuarii* against Gram-negative bacteria for potential biomedical application.

EXPERIMENTAL

Sample collection and preparation of extracts

In this study, six samples were prepared and tested, as shown in Table 1.

S1 contained *C. aestuarii* hemocyanin (CaH), dissociated in subunits (isoforms) with molecular mass ~75 kDa. The native CaH was obtained from hemolymph of Mediterranean crab *C. aestuarii* as described [14]. The native protein was dissociated into its subunits, by dialysis for 24 h against 100 mM sodium bicarbonate buffer, pH 9.5, containing 20 mM EDTA and 1 M urea. Before the antimicrobial assay, the dissociation buffer was replaced with 50 mM Tris-HCl buffer, pH 7.6.

The mucus was collected from garden snails *H. aspersa* grown in Bulgarian farms using patented technology, as described [10]. Fractions S2 and S3 were obtained by separation of the purified mucus extract by ultrafiltration on polyethersulfone

membrane filters with pore size 20 kDa and 2 kDa (Microdyn Nadir™ from STERLITECH Corporation, MWCO 20 kDa Goleta, CA, USA; Sartorius Stedim Biotech, 2 kDa, Göttingen, Germany).

Table 1. List of fractions isolated from mucus and hemolymph of different snail species and hemolymph of crab *C. aestuarii*.

Sample	Purified fractions and compound mixtures (µg/ml)	Source
S1	Dissociated hemocyanin (CaH) (9 290)	<i>Carcinus aestuarii</i>
S2	Fraction from mucus with Mw above 20 kDa (2 730)	<i>Helix aspersa</i>
S3	Fraction from mucus with Mw 2-20 kDa (775.1)	<i>Helix aspersa</i>
S4	Fraction from hemolymph with Mw below 10 kDa (1 726)	<i>Helix lucorum</i>
S5	Fraction from hemolymph with Mw 10-50 kDa (1 305)	<i>Rapana venosa</i>
S6	Hydrolysate of hemocyanin subunit βc – HaH with Mw below 30 kDa	<i>Helix aspersa</i>

The hemolymph from garden snails *H. lucorum* and marine snail *R. venosa* were obtained as described previously in [15, 6]. Fractions S4 and S5 were obtained after ultrafiltration of *H. lucorum* hemolymph and respectively *R. venosa*, using membrane filters from 10 kDa, 50 kDa and 100 kDa NMW (EMD Millipore Corporation, regenerated cellulose, Billerica, MA, USA).

S6 was obtained after proteolytic hydrolysis of structural subunit βc of *H. aspersa* hemocyanin (βc – HaH). The subunit βc – HaH (Mw ~400 kDa) was obtained after dissociation of native hemocyanin HaH as described [16]. After trypsin digestion of βc–HaH (ratio 1:200, trypsin:hemocyanin), at temperature 37°C for 8 hours, the proteolytic mixture was subjected to membrane ultrafiltration by Amicon® Ultra-15 centrifugal tube with 30 kDa membrane. So, the S6 contains peptides and polypeptides from βc – HaH with MW below 30 kDa.

Antibacterial activity assay

Bacterial strains

Gram-negative strains *E. coli* DSM 1607, *E. coli* DSM 1116 and *B. diminuta* DSM 1635 were obtained from DSMZ-German Collection of Microorganisms and Cell Cultures GmbH and used for the antibacterial screening. Strains were selected according to the list for antibiotic susceptibility

testing. Bacterial strains were subcultured in 10 ml nutrient broth for 24 h at 37 °C (*E. coli* DSM 1607, *E. coli* DSM 1116) and for 24 h at 28 °C (*B. diminuta* DSM 1635) and kept frozen at –80 °C in broth media supplemented with 25% (v/v) glycerol as a stock culture. Before the antimicrobial assays, they were inoculated into the nutrient broth and were incubated at 37 °C (*E. coli* DSM 1607, *E. coli* DSM 1116) and at 28 °C (*B. diminuta* DSM 1635) for 24 h.

Microdilution assay

Minimum inhibitory concentrations (MIC) was determined by using the broth microdilution method according to Clinical Laboratory and Standards (CLSI) guidelines [17]. Briefly, the bacterial suspension cultured to the logarithmic phase was diluted to 0.5 McFarland Standard (approximately 1.5×10^8 CFU/mL) and then diluted 150 times to 1×10^6 CFU/mL using nutrient fractions. A 50 μ l volume of serial twofold dilutions of BACs with nutrient broth was dispensed in 96-well microtiter plates. Subsequently, an equal volume of adjusted inoculum (1×10^6 CFU/mL) was added to each well of the Microtiter plates up to a final volume of 100 μ L. The nutrient media with bacterial culture without bioactive fractions was used as a negative control, and in the positive control bioactive fractions were replaced by aminoglycoside antibiotics gentamicin (GEN) – (stock solution 40 mg/ml) and tobramycin (TOBR) (stock solution 40 mg/ml). The growth was observed and the optical density was read at 600 nm spectrophotometrically (Varioskan™ LUX multimode microplate reader, Thermo Fisher Scientific) for the development of turbidity. After incubation for 24 h at 37 °C, MIC was defined as the lowest concentration of the bioactive fractions that prevents visible growth of a microorganism. Effective concentration of each sample was determined that reduced the growth of the tested bacteria by 50% (EC₅₀). The growth of bacteria was expressed as a percentage of the highest optical density observed in the inoculum. EC₅₀ was determined using dose response curve in GraphPad Prism 9 statistics software.

RESULTS AND DISCUSSION

Six different fractions were isolated and purified from garden snails *H. aspersa* and *H. lucorum*, marine snail *R. venosa* and marine crab *C. aestuarii*, according to Table 1. Two fractions from mucus of garden snail *H. aspersa* (with Mw above

20 kDa and with Mw 2-20 kDa, respectively) and two fractions from hemolymph of *H. lucorum* (Mw below 10 kDa) and *R. venosa* (Mw 10-50 kDa) were analysed by MALDI-TOF/MS/MS (date not shown). MALDI-MS analyzes prove the presence of peptides rich in important amino acids such as glycine, proline, tryptophan, etc., which are characteristic of peptides with antibacterial activity against Gram-positive and Gram-negative bacteria.

The pharmacological potential of natural products has great attention due to the bioactivity nature of those products and several medicines prepared mainly from plant or animal origin are used by people. Recently, the marine and arthropodan organisms attract the attention of researchers due to the presence of pharmacologically active drugs. Several bioactive compounds have been isolated and characterized and some of them are active substances in the drugs [18, 19, 10, 15].

Even though molluscs are widely used for various studies in research institutions, the antibacterial nature of the substances is not well characterized. Therefore, from representatives of molluscs and arthropods were isolated fractions that were tested for antibacterial activity against three strains of Gram-negative bacteria (*E. coli* DSM 1607, *E. coli* DSM 1116 and *B. diminuta* DSM 1635). We have purified several fractions with bioactive compounds from Arthropods: hemolymph of crab *C. aestuarii* - dissociated hemocyanin CaH (S1), from Molluscs: mucus from *H. aspersa* with Mw above 20 kDa (S2), mucus from *H. aspersa* with Mw 2-20 kDa (S3); hemolymph from *H. lucorum* with Mw below 10 kDa (S4), hemolymph from *R. venosa* with Mw 10-50 kDa (S5) and hydrolysate of *H. aspersa* hemocyanin - subunit β – HaH with Mw below 30 kDa (S6).

Mucus peptides with an MW below 5 kDa include many important amino acids such as glycine, proline and tryptophan. They were determined by MALDI-MS analyzes (data not shown). These amino acids are associated with established antibacterial activity in many peptides.

The tested concentrations of the above-mentioned fractions for antibacterial screening are shown in Table 2.

The values of minimum inhibitory concentration (MIC) of all fractions isolated from crab and snail species are presented on Fig. 1. S1 had strong antibacterial activity on all of the tested microorganisms (*E. coli* DSM 1607, *E. coli* DSM 1116, *B. diminuta* DSM 1635).

Table 2. Range of tested concentrations ($\mu\text{g/ml}$) of the bioactive fractions for antibacterial activity.

Sample	<i>E. coli</i> DSM 1607	<i>E. coli</i> DSM 1116	<i>B. diminuta</i> DSM 1635
S1	4645-18.14	4645-18.14	4 645- 18.14
S2	1365-170.625	1365-170.625	1365-170.625
S3	385-48.438	Not tested	385-48.438
S4	863-107.875	863-107.875	863-53.9
S5	652.5-81.563	652.5-81.563	652.5-81.563
S6	600-37.5	600-37.5	600-37.5

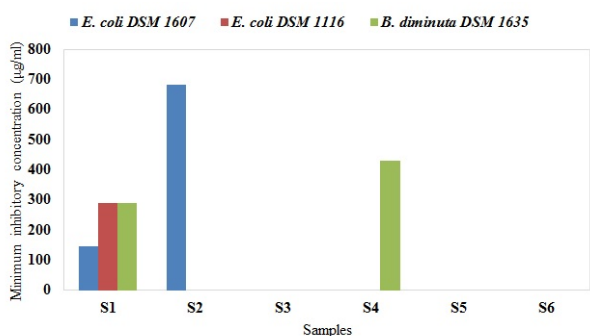


Fig. 1. Minimum inhibitory concentration (MIC) of the samples against the tested bacterial strains.

S1 exhibited strongest antibacterial activity against *E. coli* DSM 1607 (MIC - 145 $\mu\text{g/ml}$) and MIC value 290 $\mu\text{g/ml}$ for *E. coli* DSM 1116 and *B. diminuta* DSM 1635, respectively. The antibacterial activity of S2 was recorded only against *E. coli* DSM 1607, (MIC - 682.5 $\mu\text{g/ml}$), whereas of S4 only against *B. diminuta*, (MIC - 431.5 $\mu\text{g/ml}$). S3, S5 and S6 did not present any antibacterial activity against the Gram negative bacterial strains, even at the highest concentration tested. To compare the effectiveness of the six samples, we used positive controls with aminoglycoside antibiotics gentamycin and tobramycin. Gentamycin showed a MIC value 2 $\mu\text{g/ml}$ against *E. coli* DSM 1116, 0.06 $\mu\text{g/ml}$ against *E. coli* DSM 1607, and 8 $\mu\text{g/ml}$ against *B. diminuta* DSM 1635. Tobramycin showed equal activity against *E. coli* DSM 1116, higher MIC value against *E. coli* DSM 1607 (0.125 $\mu\text{g/ml}$), and no activity against *B. diminuta* DSM 1635.

The MIC and EC_{50} values of the active samples S1, S2 and S4 are compared on Fig. 2.

The EC_{50} value was used to estimate the least concentration of the compound that is required to produce 50% of maximum effect and the higher the potency. Among the all active fractions against the tested bacterial strains, the value of EC_{50} was lowest for S1 (75.46 $\mu\text{g/ml}$) against *E. coli* DSM 1607. Therefore, S1 showed the highest efficacy

among the tested substances against *E. coli* DSM 1607 (Fig. 2). The EC_{50} values of the fractions S2 (442.1 $\mu\text{g/ml}$) and S4 (279.9 $\mu\text{g/ml}$) displayed low to moderate effect against *E. coli* DSM 1607 and *B. diminuta* DSM 1635, respectively (Fig. 2).

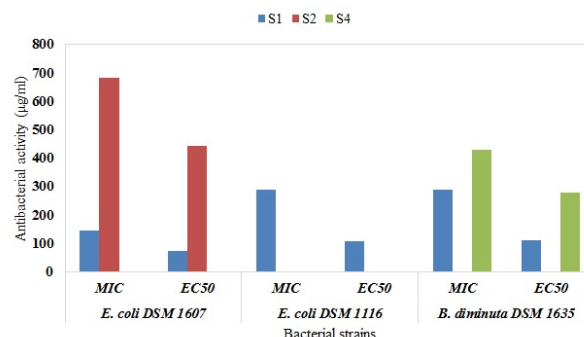


Fig. 2. The MIC and effective concentrations (EC_{50}) values of the active samples S1, S2 and S4.

Among the six tested fractions, the hemocyanin (S1) from crab *C. aestuarii* showed strong antibacterial activity against the selected Gram negative bacterial strains even at very low concentration. It was demonstrated that the grade of hemocyanin glycosylation plays an important role in its functional antibacterial properties [12, 14, 20]. Recent studies suggest that an important modification of hemocyanin, which enables it to function as a molecule involved in the immune process is its glycosylation [21-23]. Moreover, the glycosylation of hemocyanin subunits has been reported to be important for its antiviral effects [21-23] and various anti-tumour properties [24, 25]. Kizheva et al. (2019) demonstrated that native hemocyanin from the crab *Eriphia verrucosa* had no antimicrobial activity unlike its glycosylated structural subunits [12]. The authors found the strongest antibacterial activity of the structural subunits with highest carbohydrate content against *E. coli* and *Bacillus subtilis*. The hemocyanin of the crab *Carcinus aestuarii* contains a carbohydrate moiety that represents 1.6% of protein mass [14, 20]. Dolashka-Angelova et al. (2001) found that the subunit referred to as Ca2 of *C. aestuarii* hemocyanin is with highly carbohydrate content (6.3%) and contains O- and one N-linked carbohydrate chains [20]. Therefore, in this study, we tested dissociated into its subunits *C. aestuarii* hemocyanin to determine its antibacterial activity.

CONCLUSION

Our results indicate the presence of different natural antibacterial substances in the studied various molluscs species and one representative of

the arthropods. Among the six tested samples in this study, the hemocyanin (S1) of the crab *C. aestuarii* demonstrated strong antibacterial activity against tested bacteria even at very low concentration. This sample containing dissociated subunits of CaH showed considerable antimicrobial activity, which could probably add to the arsenal of antibiotics as candidates with low resistance rates. It is notable from the results that S1 showed different range of MIC values against two strains of *E. coli*. S1 showed the highest effectiveness against *E. coli* DSM 1607 according to the observed EC₅₀ values. The results of this study clearly elucidate the antibacterial potential of the active fractions. Further research with a wider range of bacterial strains is needed for the support their potential biomedical application.

Acknowledgements: This research was funded by the Bulgarian Ministry of Education and Science through the National Scientific Program “Innovative Low-Toxic Biologically Active Means for Precision Medicine” BioActiveMed, grant number DOI-217/30.11.2018, by the Project VS.076.18N (FWO) and by the Bulgarian Science Fund (Grant KP-06-OPR 03-10/2018).

REFERENCES

- World Health Organization. Global Priority List of Antibiotic-Resistant Bacteria to Guide Research, Discovery, and Development of New Antibiotics. 2017. Available online: <http://www.who.int/medicines/publications/global-priority-list-antibiotic-resistant-bacteria> (accessed on 17 April 2019).
- H. G. Boman, *Annu. Rev. Immunol.*, **13**, 61 (1995).
- H. G. Boman, *Cell*, **65**, 205 (1991).
- M. Zasloff, *Nature*, **415**, 389 (2002).
- P. Dolashka, A. Dolashki, L. Velkova, S. Stevanovic, L. Molin, P. Traldi, R. Velikova, W. Voelter, *J. BioSci. Biotechnol.*, SE/ONLINE 147 (2015).
- P. Dolashka-Angelova, H. Schwarz, A. Dolashki, S. Stevanovic, M. Fecker, M. Saeed, W. Voelter, *Biochim. Biophys. Acta*, **1646**, 77 (2003).
- C. J. Coates, J. Nairn, *Dev. Comp. Immunol.*, **45**, 43 (2014).
- L. Zhang, R. L. Gallo, *Curr. Biol.*, **26**, R14 (2016).
- P. Dolashka, V. Moshtanska, V. Borisova, A. Dolashki, S. Stevanovic, T. Dimanov, W. Voelter, *Peptides*, **32**, 1477 (2011).
- A. Dolashki, L. Velkova, E. Daskalova, N. Zheleva, Y. Topalova, V. Atanasov, W. Voelter, P. Dolashka, *Biomedicines*, **8**, 315 (2020).
- P. Dolashka, A. Dolashki, W. Voelter, J. Van Beeumen, S. Stevanovic, *Int. J. Curr. Microbiol. App. Sci.*, **4**, 1061 (2015).
- Y. K. Kizheva, I. K. Rasheva, M. N. Petrova, A. V. Milosheva-Ivanova, L. G. Velkova, P. A. Dolashka, A. Dolashki, P. K. Hristova, *Biotechnol. Biotechnol. Equip.*, **33**, 873 (2019).
- S. Pitt, M. A. Graham, C. G. Dedi, P. M. Taylor-Harris, A. Gunn, *Br. J. Biomed. Sci.*, **72**, 174 (2015).
- P. Dolashka-Angelova, A. Dolashki, S. N. Savvides, R. Hristova, J. Van Beeumen, W. Voelter, B. Devreese, U. Weser, P. Di Muro, B. Salvato, S. Stevanovic, *J. Biochem.*, **138**, 303 (2005).
- A. Alexandrova, L. Petrov, L. Velkova, A. Dolashki, E. Tsvetanova, A. Georgieva, P. Dolashka, *J. Pharm. Pharmacogn. Res.*, **9**, 143 (2021).
- O. Antonova, P. Dolashka, D. Toncheva, H.G. Rammensee, M. Floetenmeyer, S. Stevanovic, *Z. Naturforsch. C J. Biosci.*, **69**, 325 (2014).
- CLSI, Methods for dilution antimicrobial susceptibility tests for bacteria that grow aerobically, 11th ed. CLSI M07, Wayne PA, Clinical and Laboratory Standards Institute (2018).
- I. Rizvi, D. R. Riggs, B. J. Jackson, D. W. McFadden, *Am. J. Surg.*, **194**, 628 (2007).
- A. Georgieva, K. Todorova, I. Iliev, V. Dilcheva, I. Vladov, S. Petkova, R. Toshkova, L. Velkova, A. Dolashki, P. Dolashka, *Biomedicine*, **8**, 194 (2020).
- P. Dolashka-Angelova, M. Beltramini, A. Dolashki, B. Salvato, R. Hristova, W. Voelter, *Arch. Biochem. Biophys.*, **389**, 153 (2001).
- P. Dolashka-Angelova, B. Lieb, L. Velkova, N. Heilen, K. Sandra, L. Nikolaeva-Glomb, A. Dolashki, A. S. Galabov, J. Van Beeumen, S. Stevanovic, W. Voelter, B. Devreese, *Bioconjug. Chem.*, **20**, 1315 (2009).
- L. Velkova, D. Todorov, I. Dimitrov, S. Shishkov, J. Van Beeumen, P. Dolashka-Angelova, *Biotech. Biotech. Equip.*, **23**, 606 (2009).
- P. Dolashka, L. Velkova, S. Shishkov, K. Kostova, A. Dolashki, I. Dimitrov, B. Atanasov, B. Devreese, W. Voelter, J. Van Beeumen, *Carbohydr. Res.*, **345**, 2361 (2010).
- S. Arancibia, C. Espinoza, F. Salazar, M. Del Campo, R. Tampe, T. Y. Zhong, P. De Ioannes, B. Moltedo, J. Ferreira, E. Lavellee, A. Manubes, A. Ioannes, M. Becker, *PLoS One*, **9**, e87240 (2014).
- W. M. Salama, M. M. Mona, *J. Cancer Biomed. Res.*, **1**, 28 (2018).

FISH investigation of the bacterial groups anammox and *Azoarcus-Thauera* at treatment of landfill leachate

M. Belouhova^{1*}, N. Dinova¹, I. Yotinov¹, S. Lincheva², I. Schneider¹, Y. Topalova¹

¹ Biological faculty, Sofia University "St. Kliment Ohridski", Dragan Tsankov blvd., 8, Sofia, Bulgaria

² Municipal Enterprise for Waste Treatment, Locality Sadinata, Yana, Bulgaria

Received January 28, 2021; Revised February 26, 2021

The landfill leachate is heavily polluted wastewater produced in the landfills. The management of the purification of the leachate is especially challenging and that is why new approaches and indicators are needed. The quantity, localization, interaction, clustering of the key microbial groups, responsible for the critical transformation processes can be used as indication leading to better performance of the technology. This study is focused on two bacterial groups (Anammox and *Azoarcus-Thauera* cluster) which have potential to serve as indicators for the landfill leachate treatment. Their quantity and activity were studied by FISH during lab-scale treatment of leachate from the Municipal Enterprise for Waste Treatment (MEWT), Sofia, Bulgaria. Two activated sludges (AS) were used – one from the MEWT and another from the WWTP (wastewater treatment plant) of Sofia. The obtained results showed that 74% of the COD was eliminated when leachate was diluted 50 and 25 times and 31% - when undiluted leachate was used. At the end of the process (21 day) the *Azoarcus-Thauera* group formed large aggregations in the AS from MEWT. They were 17.50% of the bacteria there while in the AS from the WWTP of Sofia they represented only 2.61%. The quantity of the anammox bacteria remained almost unchanged during the process and was 10.75% of the community from MEWT which eliminated 98 mg/L more ammonium ions at the end of the process and 6% from the community from the WWTP of Sofia. The two studied groups gave more complex information about the processes in the AS related to the elimination of the nitrogen and carbon containing pollutants. They could be used for better management of the biological processes during landfill leachate treatment.

Key words: landfill leachate; anammox, *Azoarcus-Thauera*; activated sludge; fluorescence in-situ hybridization

INTRODUCTION

According to Eurostat the waste generation in EU is approx. 2.50 billion of tons per year, which makes 5 tons per person. In the same time in Bulgaria 7 times more solid waste is generated per capita. Not only this but the percentage of the waste that is landfilled is 75% (while in the EU is 26%) [1]. In the same time every EU member has to comply with the stringent environmental EU legislation. This highlights that the landfills management and the efficient treatment of the leachate that is generated from them is of big importance for maintaining good environmental health in all EU and especially in Bulgaria.

The landfill leachate is the liquid that is drained through the landfill. Because of this it is contaminated with extremely high concentrations of the pollutants. The landfill leachate is usually collected and is treated in dedicated wastewater treatment plants (WWTP). As Wang *et al.* [2] mentions, this liquid contains a hundred times more pollutants than the domestic wastewater. The main categories of the pollutants in the leachate are

dissolved organic matter, inorganic macro components, heavy metals and organic xenobiotics [3]. According to different studies the COD (chemical oxygen demand) varies from 500 mgO₂/L [4, 5] up to 70 000 mgO₂/L [6] or even more. The BOD/COD ratio varies from 0.4-0.6 to less than 0.03 [7-9]. One of the most challenging pollutants in the landfill leachate is the ammonium nitrogen. Its concentration ranges from 50 mg/L up to 2200 mg/L and for the most of the landfills it is approx. 300-500 mg/L [9, 10]. The presented characteristics of the landfill leachate (the extremely high COD and NH₄⁺ concentration) show that the two main problems in achievement of a highly efficient purification are: 1/ elimination of the xenobiotics (measured as COD) and 2/ elimination of the nitrogen (entering the WWTPs as ammonium nitrogen). The processes in the WWTPs (wastewater treatment plants) receiving landfill leachate are usually based on activated sludge treatment [11, 12]. This type of treatment is based on the biodegradation activity of the bacteria in the sludge. Many bacterial groups are known to possess capabilities for xenobiotics elimination (*Pseudomonas*, *Acinetobacter* [13, 14], *Bacillus* [15-17], *Alcaligenes* [18-20] and some of them are

* To whom all correspondence should be sent:

E-mail: mihaela.kirilova@uni-sofia.bg

verified as an indicators for the rate and efficiency of the xenobiotics detoxification [21-23]. The connection between the rate of the specific transformation process and the microbial group that accomplishes them have been proved and application of this connection for managerial tool has been demonstrated. Recently due to the sequencing and fluorescent *in-situ* hybridization (FISH) analyses of the complex communities of the activated sludges many other bacterial groups gain attention [24]. An example of this are the bacteria from the genera *Azoarcus* [25, 26] and *Thauera* [27]. They are of interest when high content of nitrogen pollutants is present in the wastewater because they are critically important in the denitrification processes [28, 29].

In parallel the bacterial group that is put on the focus when high concentrations of ammonia are present in a wastewater – the anammox bacteria [30] They are able to perform anaerobic ammonium oxidation (Anammox) and are of special interest when landfill leachate is treated. The reason for this is that not only they eliminate the ammonium ions, but also they do this in anaerobic conditions without using organic carbon sources (since they are autotrophs) [12]. In the anammox process the ammonia is oxidized by nitrite (as an electron acceptor) to nitrogen gas. This happens in the absence of oxygen [31]. The use of anammox bioreactors is considered to be an improved biotechnology for elimination of the high ammonia concentrations in the landfill leachate [32].

The high ammonia concentrations in the landfill leachate and the complex, and very often not so efficient, process of its removal simultaneously with the presence of xenobiotics, poses a serious challenge to the managing biotechnologists. In the field there is a need for more information on the processes of carbon and nitrogen elimination, and also – of new indicators reflecting the new data gathered in different studies. This provoked the investigation of the two bacterial groups discussed above (the *Azoarcus-Thauera* cluster and the anammox bacteria) as innovative indicators for management of the landfill leachate treatment in a solid waste treatment plant.

MATERIALS AND METHODS

Work hypothesis

The work hypothesis of the study was based on the information for the probable key role of the bacteria from the groups of *Azoarcus-Thauera* cluster and anammox in the landfill leachate

treatment. This is prerequisite for their use as indicators for the elimination of the nitrogen containing pollutants though the anammox pathway and through the ordinary denitrification process (but one coupled with the elimination of the xenobiotics). For exploring the potential of *Azoarcus-Thauera* cluster and anammox the characteristics of their populations in activated sludges treating landfill leachate should be studied. For this purpose, a model process of stepwise increase of the leachate concentration would be suitable for obtaining information about the connection between efficiency of the target transformation processes / anammox and denitrification/and the changes in the number, activity and spatial distribution of the key bacteria.

Materials

The landfill leachate used in the experiments was taken from the Municipal enterprise for waste treatment in Sofia, Bulgaria. The landfill was functioning from 2012. The leachate from it is collected in 600 m³ reservoirs. After that it is treated in WWTP with biological treatment in 4 SBRs (each 200 m³) with 12 hours cycles. The WWTP purifies 20K m³ of leachate per year. The samples of leachate for the laboratory experiments was taken from the influent chamber in the WWTP in the MEWT.

In the present study two activated sludges were used. The one was from the Municipal enterprise for waste treatment (MEWT) taken from SBR in the phase “denitrification”. This microbial community has been treating the landfill leachate in the full-scale bioreactors and it is well acclimated to it.

The other activated sludge was taken from the WWTP of Sofia from the denitrifying zone of an aeration tank. This AS was adapted to the purification of municipal wastewater of Sofia Town, that contaminated preliminary with trivial pollutants /easily biodegradable/ and xenobiotics in low concentrations /COD – 280 – 300 mgO₂/L/. The community wasn't adapted towards biodegradation of the heavily polluted landfill leachate.

Two identical lab-scale SBR bioreactors were constructed. Their working volume was 4 L. Their reaction stage was in aerobic regime and the complete cycle was performed for 48 h. Each cycle had the following phases: filling with landfill leachate, reaction (mixing of the AS and the leachate) by aeration, settling, decantation of the

treated wastewater. The activated sludge was added in the bioreactor to reach a final concentration of 3 g/L. In the first bioreactor the activated sludge from MEWT was used, in the second the activated sludge from the WWTP of Sofia Town was added. The purpose was to compare flexibility of adaptation potential of the two different activated sludge as well as to analyze the adaptive changes in the microbial structure and function for elimination of the pollutants in the leachate.

Microscopical analysis of the two activated sludges showed that the one from MEWT contains smaller flocs, less filamentous microorganisms and significantly more free-swimming bacteria (Fig. 1). In the activated sludge from the WWTP of Sofia Town the flocs were larger in size, denser and a normal quantity of the filamentous microorganisms was found.

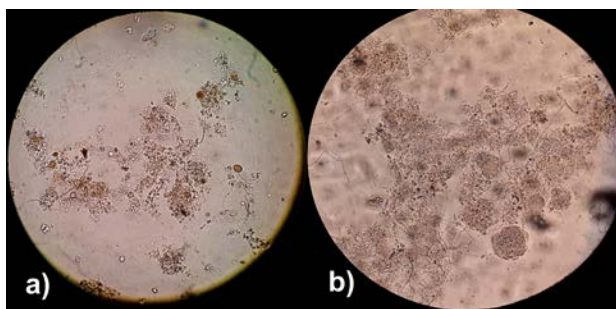


Fig. 1. Microscopic images of control samples of activated sludge from MEWT (a) and from WWTP (b) (400X).

Methods

The model treatment was performed for 21 days. During 1-7 day the landfill leachate was diluted 50 times with distilled water. After 7 days the concentration of the pollutants in the bioreactors was increased with the addition of portion of leachate diluted 25 times. At the period 14-21 day the portion of landfill leachate was added without dilution. Also, to make the process closer to the real one in the MEWT, glycerol was added as it was in the full-scale treatment. Its concentration was taken as BOD₅ and the compound was added up to the BOD₅:COD ratio equal to 1:3.

The technological parameters monitored in the model landfill leachate treatment were: 1/ COD (potassium dichromate method), performed according Eaton *et al.* [33]; 2/ concentrations of the ammonium ions according BDS ISO 7150/1 standard; 3/ concentrations of the nitrate ions according to BDS ISO 7890-3 standard; 4/ concentrations of the nitrite ions according BDS EN 26777.

The efficiency of the COD removal was calculated according the following formula:

$$\text{Eff (\%)} = ((\text{COD}_{\text{Influent}} - \text{COD}_{\text{Effluent}}) / \text{COD}_{\text{Influent}}) * 100$$

Two microbial groups were studied – the aerobic heterotrophs cultured on Nutrient agar and the denitrifying bacteria cultured on Giltay medium [34]. The microorganisms were incubated for 48 h at 30 °C in presence of oxygen for the aerobic heterotrophs and for 7 days in oxygen free atmosphere in anaerobic jars for the denitrifiers.

The fluorescence *in-situ* hybridization was performed according Nielsen *et al.* [35]. The samples were preserved in paraformaldehyde according to the protocol of Amann *et al.* [36]. They were pretreated with 1M HCl in order to loosen the structure of the extracellular matrix in the flocs of the activated sludge. In the study two bacterial groups related to the nitrogen and xenobiotics elimination were examined. The *Azoarcus-Thauera* cluster was monitored during the model process by FISH with the oligonucleotide probe AT1458 (5'- GAA TCT CAC CGT GGT AAG CGC -3') [37, 38]. For the anammox bacteria the probe Amx820 (5'- AAA ACC CCT CTA CTT AGT GCC C -3') was applied [38, 39]. The domain *Bacteria* was investigated with EUBmix, consisting of three probes - EUB338 (5'-GCT GCC TCC CGT AGG AGT-3'), EUB338-II (5'-GCA GCC ACC CGT AGG TGT-3'), EUB338-III (5'-GCT GCC ACC CGT AGG TGT-3') [38, 40].

The fluorescence images were taken with epifluorescent microscope Leica DM6 B. Digital image analysis was performed on the images obtained from FISH in order to estimate the quantity of the bacteria from the *Azoarcus-Thauera* cluster and the anammox group [41].

RESULTS AND DISCUSSION

During the model process information about the main technological and microbiological parameters was gathered. The initial COD for the process in two bioreactors was 1445.036 mgO₂/L. After the initial adaptation period during the first day, registered in the two biological systems the COD was lowered with 8.2 times for the activated sludge from MEWT and 10.3 times for the activated sludge from WWTP of Sofia (Fig. 2). After that the COD of the effluent from the two bioreactors remained relatively low during 1-14 day (e.g., when the concentration of the landfill leachate was lowered with 50 and 25 times). The mean value of the parameter was 384.87 mgO₂/L which is 26% of

the COD of the influent. This shows that in the two model bioreactors, treating leachate, the elimination of the carbon containing pollutants was 74%. The registered effect was due to the adaptation of the microbial community to the biodegradation first of the leachate diluted 50 times, after that to the one diluted 25 times.

At the final period (15-21 day) landfill leachate without dilution was supplied in the wastewater

treatment systems. The COD of the influent was approx. 3800 mgO₂/L. The high concentration of the pollutants inhibited the biodegradation purification process and its efficiency was only 27.63% for the reactor with activated sludge (AS) from MEWT and 33.87% for the one with AS from the WWTP of Sofia.

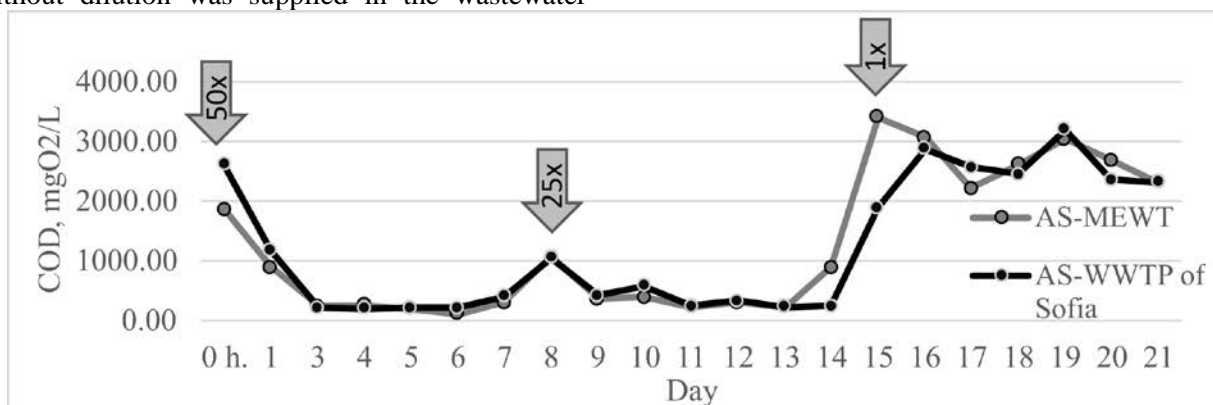


Fig. 2. COD of the effluent from the reactor with activated sludge from the Municipal Enterprise for Waste treatment (AS-MEWT) and with activated sludge from the WWTP of Sofia (AS- WWTP of Sofia). The increase of the landfill leachate concentration was indicated with arrows.

Table 1. Concentrations of the three of the nitrogen ions in the effluent from the two model bioreactors (AS-MEWT – activated sludge from the Municipal Enterprise for Waste treatment; AS-WWTP of Sofia – activated sludge from the WWTP of Sofia).

Day	AS-MEWT			AS-WWTP of Sofia		
	NH ₄ ⁺ (mg/L)	NO ₂ ⁻ (mg/L)	NO ₃ ⁻ (mg/L)	NH ₄ ⁺ (mg/L)	NO ₂ ⁻ (mg/L)	NO ₃ ⁻ (mg/L)
2	20.06	0.02	452.08	4.37	0.04	0.77
4	4.03	0.01	225.43	3.75	2.89	38.48
7	2.84	0.03	154.39	2.11	4.53	155.70
9	9.26	0.01	78.84	3.26	0.66	10.52
11	3.05	0.01	162.04	3.72	0.52	193.08
14	5.87	0.02	235.33	10.32	11.47	236.42
16	493.12	1.80	20.38	374.80	0.34	18.00
18	632.10	0.79	23.20	649.15	0.71	23.64
21	573.20	0.97	4.39	670.85	0.45	4.90
Mean value	193.73	0.41	150.68	191.37	2.40	75.72

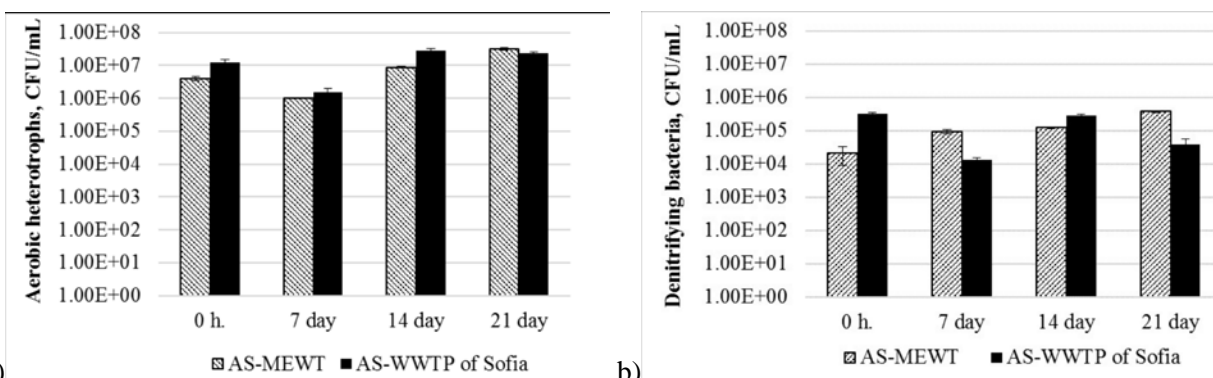


Fig. 3. Two key groups of bacteria for the landfill leachate treatment – a) the aerobic heterotrophs and b) the denitrifying bacteria.

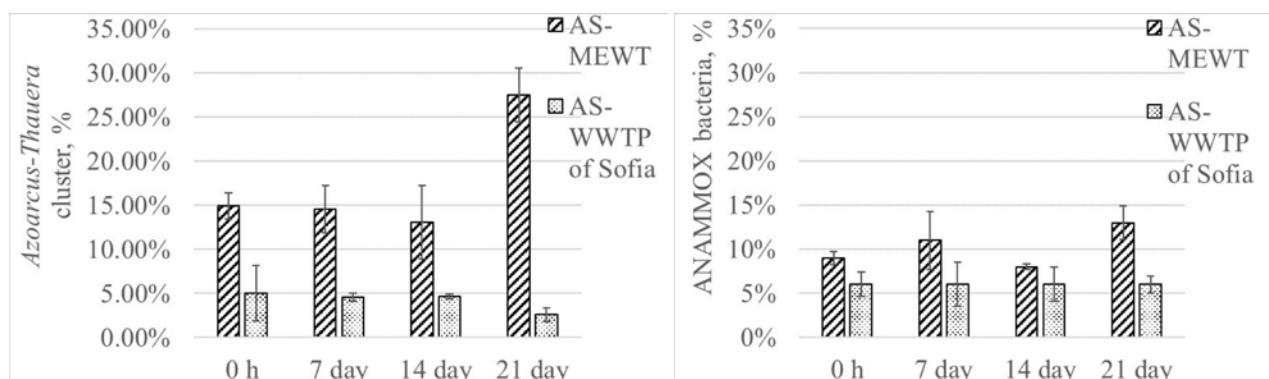


Fig. 4. Digital image analysis of the FISH pictures taken on samples from the activated sludge from MEWT (AS-MEWT) and from WWTP of Sofia (AS-WWTP of Sofia) during the model experiment.

An analysis of the key nitrogen ions was performed (Table 1). The concentrations of the ammonium ions showed that almost all of them were eliminated up to the 14th day. The concentration of the remaining ammonium ions in the effluent treated by the AS from MEWT was 7.52 mg/L and for the one treated by the AS from the WWTP of Sofia was just 4.59 mg/L. During the period 9th -21st day the undiluted landfill leachate raised the concentrations up to 670.85 mg/L. In the leachate this concentration was 207.42 mg/L. This result demonstrated the inhibition of the nitrogen transformation activity of the ASs as well as some destructive changes in the biological AS-structure.

The concentrations of the nitrites were low, as it is normal for this form of the nitrogen in landfill leachate (Table 1). The concentration of the nitrates varied significantly – from 4.39 mg/L up to 452.08 mg/L for the bioreactor with AS from MEWT and from 0.77 mg/L up to 236.42 mg/L for the bioreactor with AS from the WWTP of Sofia. Their concentration was low at 21st day. This is related to the inefficient nitrification resulting in low level of generation of nitrates. Also, the data presented in the Table 1 showed that the mean concentration of the nitrates in the system with activated sludge from the WWTP of Sofia is two times lower than the one in the bioreactor with AS from MEWT. During the period of low toxicity (1st -7th day), the activated sludge from the WWTP of Sofia eliminated 4.4 times more nitrates. This result demonstrated the difference in the two denitrifying communities. The standard microbiological analyses (Fig. 3) showed that the denitrifying bacteria in the AS from WWTP of Sofia in the beginning of the model landfill leachate treatment were 15 times more than the same bacteria in the other community. Most probably the easily biodegradable pollutants in the domestic wastewater (treated in the WWTP of Sofia) favored their development. On the 14th day (at x25 dilution

of the landfill leachate) the number of the denitrifying bacteria was considerably higher compared to the previous control point (7th day) – up to 21 times more (Fig. 3). At this sampling points the FISH analysis showed decrease in the *Azoarcus-Thauera* cluster and the anammox bacteria (Fig. 4). During that period of time the accumulation of the nitrates was considerable. These effects were probably related to the inhibition of the mentioned groups key for elimination of the nitrogen.

At the end of the treatment the FISH analysis of the domain *Bacteria* demonstrated significant quantity of the suspended bacterial cells, especially in the activated sludge from MEWT (as shown on Fig. 5). The result corresponded to the cultivation analyses – in the same samples the highest value for the aerobic heterotrophs was registered (3.15×10^7 CFU/mL), indicating that in the bioreactors there are microorganisms which are capable of successful development in the unfavorable environment. They could be further managed to increase the biodegradation efficiency.

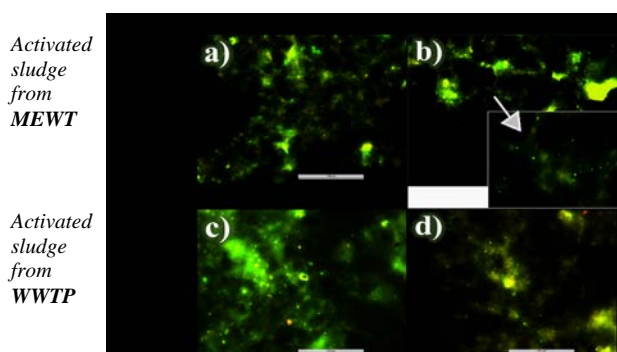


Fig. 5. Fluorescent images from FISH for the domain *Bacteria* (probe EUBmix) in the activated sludge from MEWT in the beginning (a) 0 h.) and the end of the experiment (b) 21st day) and from WWTP of Sofia in the beginning (c) 0 h.) and the end of the experiment (d) 21st day). The pictures are taken with 400x magnification; the marker indicates 100 μm.

The FISH analysis at the end of the biodegradation process showed that the bacteria from the *Azoarcus-Thauera* cluster formed large aggregations in the flocs of the activated sludge from MEWT (Fig. 6). They were 17.50% of the bacteria in that community compared to the only 4.22% in the sludge from the WWTP of Sofia (Fig. 4). Another interesting feature of the *Azoarcus-Thauera* group was that in the MEWT derived sludge they increased their abundance with 12.60%. This data is supported by the analyses of the denitrifying bacteria (Fig. 3). This is probably related to the fact that these bacteria had have previous adaptation to the landfill leachate. Also, they possess capabilities for biodegradation of xenobiotics which were present in high concentrations in that period of time (Fig. 2). In the activated sludge from WWTP of Sofia significantly lower quantity of the *Azoarcus-Thauera* cluster was found (Fig. 6). The result corresponds to the lack of previous adaptation to the pollutants. It is related also to the initial low quantity which hinder the development of stable population in that community.

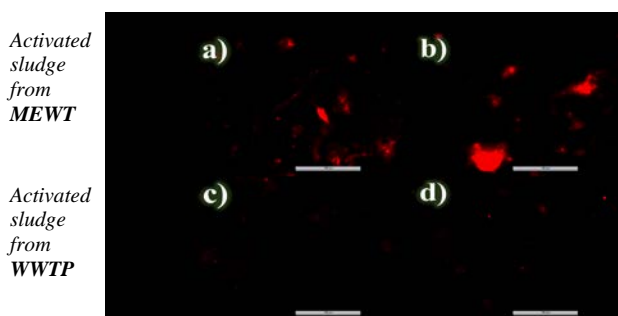


Fig. 6. Fluorescent images from FISH for *Azoarcus-Thauera* cluster in the activated sludge from MEWT in the beginning (a) 0 h.) and the end of the experiment (b) 21st day) and from WWTP of Sofia in the beginning (c) 0 h.) and the end of the experiment (d) 21st day). The pictures are taken with 400x magnification, the marker indicates 100 μ m.

The obtained results from the experiments showed that the group of *Azoarcus-Thauera* were good indicator for the processes in the activated sludge degrading landfill leachate but only when already adapted community was used.

The results from the FISH analysis for the anammox bacteria showed that the quantity of the target microorganisms didn't changed significantly during the process despite the large fluctuations of the main carbon and nitrogen related parameters of the treatment process (Fig. 2 and Table 1). This was probably due to the fact that they are autotrophs and thus independent from the organic carbon. The

anammox bacteria were found in dense area in the flocs which probably had protective effect against the toxic and aerated environment (Fig. 7). In the activated sludge from WWTP of Sofia the studied microorganisms had more disperse distribution. They were presented in lower quantities (6% of the community) compared the MEWT activated sludge (10.25%). On the other hand, the higher number of the anammox bacteria in the sludge from MEWT probably contributed to the lowering of the concentrations of the nitrites in the bioreactor with that community (Table 1).

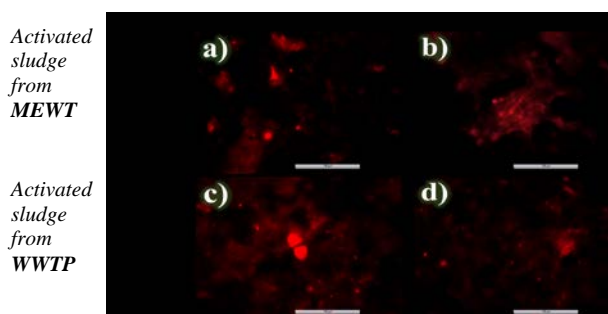


Fig. 7. Fluorescent images from FISH for the anammox bacteria in the activated sludge from MEWT in the beginning (a) 0 h.) and the end of the experiment (b) 21st day) and from WWTP of Sofia in the beginning (c) 0 h.) and the end of the experiment (d) 21st day). The pictures are taken with 400x magnification, the marker indicates 100 μ m.

Another effect that could be related to the presence of more anammox in the bioreactor with activated sludge from MEWT was the better performance of that reactor for elimination of the ammonium ions and the nitrite ions (needed for the anammox process) on 14th and 21st day (the time period of higher loading with pollutants). At the end of the model process the bioreactor with more anammox bacteria eliminated 14.55% more of the ammonium ions or 98 mg/L. In the same time the concentrations of nitrates in the two systems were approximately the same (Table 1) eliminating the possibility of nitrogen removal by nitrification/denitrification mechanisms. Thus, the ammonium ions were probably transformed by the anammox process.

The discussed effects that could be related to anammox showed that the abundance of the corresponding bacteria, studied with FISH could be used as indication for the elimination of the nitrogen pollutants by means of the anammox pathway.

The results discussed in this study correspond to the results from other studies. For example, *Azoarcus-Thauera* cluster was found to be 15-20%

of activated sludge treating landfill leachate [42]. In the activated sludge from MEWT they were between 13.11% and 27.48%. The microorganisms from this group are obviously important in the landfill leachate treatment and they are often found as one of the main groups in microbial communities treating such type of wastewater [43, 44]. However, as demonstrated in this research, they represent much smaller part of the bacteria in activated sludges in the WWTPs treating domestic wastewater (sometimes even less than 1%) [45]. In the present study *Azoarcus-Thauera* cluster represented 4% (mean value) in the activated sludge from the WWTP of Sofia city.

There isn't much data published on the quantity of the anammox bacteria determined with FISH in activated sludges treating landfill leachate in common bioreactors (such as SBRs). It is well known that these bacteria constitute the largest part of the community (more than 50%) in dedicated anammox bioreactors for landfill leachate [46]. In a typical bioreactor for landfill leachate, they represent much smaller part of the community. In our experiments we found them to be up to 12.97%. Other authors reported that the share of anammox bacteria treating landfill leachate is approximately 20% [47, 48].

This study is focused on the exploration of the potential of two unusual bacterial groups for biological control of the landfill leachate treatment. However, among the heterotrophic bacteria, which are the major group of organisms in the activated sludge, there are many other microorganisms which are important in the pollutants elimination. The most important of them, as being able to participate in both the xenobiotics biodegradation and the denitrification, are the bacteria in the genus *Pseudomonas*. In our previous studies their key role in the detoxification of different pollutants had been demonstrated [49-51]. Details related to the importance of their spatial arrangement and the unculturable part of the group had been elucidated [49, 51].

The investigation of the role of the different bacterial groups in the model landfill leachate treatment continues. Special attention will be paid to the g. *Pseudomonas* by using cultivation and cultivation-independent techniques.

The obtained results demonstrated the correspondence between: 1/ the technological processes in the model bioreactors, the dynamics of the key parameters of the treatment (the COD and the concentration of key nitrogen ions) and 2/ the amount of the two bacterial groups which are

important in the biological landfill leachate treatment. Currently the biological processes in the WWTP purifying such waters are usually controlled by using the traditional parameters (COD, BOD₅, concentrations of the main nitrogen and phosphorus forms, number of the culturable bacteria). This strategy often gives wrong results because the metabolic biodegradation processes of the landfill leachate purification differ significantly from a conventional wastewater treatment process as combination, as critical concentrations of the pollutants, as key microbial groups. Thus, new indicators will be useful for proper management of treatment processes. The experiments described in the article demonstrated that the *Azoarcus-Thauera* group and the anammox bacteria could be used for better estimation of the xenobiotic's elimination and the extent of the anammox process established in a given WWTP in a landfill for domestic solid waste. The future investigation will be focused on the elucidation of the level of correlation of the quantity of *Azoarcus-Thauera* with the rate and efficiency of the leachate treatment.

CONCLUSION

In the presented study the potential of two unconventional bacterial groups as indicators of nitrogen elimination in landfill leachate was explored. The performed experiments were based on model treatment processes with two activated sludges – one from MEWT and one from WWTP of Sofia. The obtained results showed that the *Azoarcus-Thauera* cluster increased significantly their abundance in the sludge from MEWT when high concentration of pollutants was applied. The cultivation analyses, the data for COD and NO₃⁻ demonstrated that the fluctuations of these bacteria were probably more related to the biodegradation of the xenobiotic compounds in the leachate than the elimination of nitrates. The results for the anammox bacteria demonstrated that they are perspective for estimation of the contribution of the anammox process to the total nitrogen elimination.

Acknowledgements: This investigation has been supported financially by Operational Program 'Science and education for smart growth', co-financed by the European Union through the European structural and investment funds, project BG05M2OP001-1.002-0019: 'Clean Technologies for Sustainable Environment - Waters, Waste, Energy for a Circular Economy' and by project PT019-DG-56-22/22.05.19 "Gradual adaptation of activated sludge towards biodegradation of leachate from Sofia Waste Treatment Plant" funded by Municipal enterprise for waste treatment.

REFERENCES

1. <https://ec.europa.eu/eurostat>.
2. K. Wang, L. Li, F. Tan, D. Wu, *Archaea*, **2018**, 1 (2018).
3. D. Baderna, F. Caloni, E. Benfenati, *Environ. Int.*, **122**, 21 (2019).
4. T. Hoilijoki, *Water Res.*, **34**, 5, 1435 (2000).
5. D. Trebouet, J. P. Schlumpf, P. Jaouen, J. P. Maleriat, F. Quemeneur, *Environ. Technol.*, **20**, 587 (1999).
6. A. A. Tatsi, A. I. Zouboulis, K. A. Matis, P. Samaras, *Chemosphere*, **53**, 737 (2003).
7. I. M.-C. Lo, *Environ. Int.*, **22**, 433 (1996).
8. S. Renou, J. G. Givaudan, S. Poulain, F. Dirassouyan, P. Moulin, *J. Hazard. Mater.*, **150**, 468 (2008).
9. E. Mohammad-pajooh, D. Weichgrebe, G. Cuff, *J. Environ. Manage.*, **187**, 354 (2017).
10. H. Luo, Y. Zeng, Y. Cheng, D. He, X. Pan, *Sci. Total Environ.*, **703**, 135468 (2020).
11. Y. Peng, *Arab. J. Chem.*, **10**, S2567 (2017).
12. L. Miao, G. Yang, T. Tao, Y. Peng, *J. Environ. Manage.*, **235**, 178 (2019).
13. Y. Topalova, Biological control and management of wastewater treatment, Pensoft, Sofia, 2009.
14. J. R. van der Meer, in: *Pseudomonas*, J.-L. Ramos, R. C. Levesque (eds), vol. 6, Springer US, Boston, MA, 2006, p. 189.
15. K. K. Bhatt, M. K. Lily, G. Joshi, K. Dangwal, *Turkish J. Biochem.*, **43**, 693 (2018).
16. D. Velupillaimani, A. Muthaiyan, *Environ. Sustain.*, **2**, 381 (2019).
17. A. Paz, J. Carballo, M. J. Pérez, J. M. Domínguez, *Chemosphere*, **181**, 168 (2017).
18. R. E. Duran, E. Duran Roberto, V. Mandez, L. Rodraguez-Castro, B. Barra-Sanhueza, F. Salva-Serra, E. R. B. Moore, E. Castro-Nallar, M. Seeger, *Front. Microbiol.*, **10**, 528 (2019).
19. S. Verma, R. Bhargava, V. Pruthi, *Int. Biodeterior. Biodegradation*, **57**, 207 (2006).
20. A. Chowdhury, S. Pradhan, M. Saha, N. Sanyal, *Indian J. Microbiol.*, **48**, 114 (2008).
21. I. Yotinov, Y. Todorova, I. Schneider, E. Daskalova, Y. Topalova, *J. Nanosci. Nanotechnol.*, **16**, 7696 (2016).
22. Y. Topalova, R. Dimkov, I. Ivanov, S. Sergieva, R. Arsov, *Biotechnol. Biotechnol. Equip.*, **12**, 91, (1998).
23. M. Grekova-Vasileva, Y. Topalova, *Biotechnol. Biotechnol. Equip.*, **23**, 1136 (2009).
24. D. Zhang, R. Vahala, Y. Wang, B. F. Smets, *Int. Biodeterior. Biodegradation*, **113**, 88 (2016).
25. J. A. Valderrama, V. Shingler, M. Carmona, E. Díaz, *J. Biol. Chem.*, **289**, 1892 (2014).
26. B. Blázquez, M. Carmona, E. Díaz, *Front. Microbiol.*, **9**, 1 (2018).
27. Y. Shinoda, Y. Sakai, H. Uenishi, Y. Uchihashi, A. Hiraishi, H. Yukawa, H. Yurimoto, N. Kato, *Appl. Environ. Microbiol.*, **70**, 1385 (2004).
28. Y. N. Li, A. W. Porter, A. Mumford, X. H. Zhao, L. Y. Young, *J. Appl. Microbiol.*, **112**, 269 (2012).
29. H. Anders, A. Kaetzke, P. Kampfer, W. Ludwig, G. Fuchs, *Int. J. Syst. Evol. Microbiol.*, **45**, 327 (1995).
30. K. J. Gijis, *Nat. Rev. Microbiol.*, **6**, 320 (2008).
31. Y. Kimura, K. Isaka, F. Kazama, *Bioresour. Technol.*, **102**, 4390 (2011).
32. M. Azari, U. Walter, V. Rekers, J.-D. Gu, M. Denecke, *Chemosphere*, **174**, 117 (2017).
33. A. D. Eaton, L. S. Clesceri, E. W. Rice, A. E. Greenberg, Standard Methods for the Examination of Water and Wastewater, vol. 21, APHA-AWWA-WEF, Washington, D.C., 2005.
34. S. I. Kuznetsov and G. A. Dubinina, Methods for investigation of waters microorganisms, Acad. Sc. USSR Moskow, 1989.
35. P. H. Nielsen, H. Daims, H. Lemmer, I. Arslan-Alaton, T. Olmez-Hanci, FISH Handbook for Biological Wastewater Treatment: Identification and Quantification of Microorganisms in Activated Sludge and Biofilms by FISH. IWA Publishing, London, 2009.
36. R. Amann, W. Ludwig, K.-H. Schleifer, *Microbiol. Rev.*, **59**, 143 (1995).
37. R. Rabus, H. Wilkes, A. Schramm, G. Harms, A. Behrends, R. Amann, F. Widdel, *Environ. Microbiol.*, **1**, 145 (1999).
38. A. Loy, F. Maixner, M. Wagner, M. Horn, *Nucleic Acids Res.*, **35**, D800 (2007).
39. M. Schmid, S. Schmitz-Esser, M. Jetten, M. Wagner, *Environ. Microbiol.*, **3**, 450 (2001).
40. H. Daims, A. Brühl, R. Amann, K.-H. Schleifer, M. Wagner, *Syst. Appl. Microbiol.*, **22**, 434 (1999).
41. H. Daims, S. Lücker, M. Wagner, *Environ. Microbiol.*, **8**, 200 (2006).
42. M. Wang, G. Cao, N. Feng, Y. Pan, *Chin. J. Chem. Eng.*, **28**, 3109 (2020).
43. A. Isabel Díaz, P. Oulego, A. Laca, J. Manuel González, M. Díaz, *CLEAN—Soil Air Water*, **47**, 1900156 (2019).
44. C. Etchebehere, M.I. Errazquin, P. Dabert, L. Muxí, *FEMS Microbiol Ecol*, **40**, 106 (2002).
45. M. Zielińska, P. Rusanowska, J. Jarzabek, J. L. Nielsen, *Environ. Technol.*, **34**, 2367 (2016).
46. M. Azari, W. Uwe, R. Volker, G. Ji-Dong, D. Martin, *Chemosphere*, **174**, 126 (2017).
47. A. Banach-Wiśniewska, M. Tomaszewski, G. Cema, A. Ziemińska-Buczyńska, *Chemosphere*, **238**, 124597 (2020).
48. F. Dai, M.C. De Prá, M.B. Vanotti, K.R. Gilmore, W.E. Cumbie, *J. Environ. Manag.*, **232**, 951, (2019).
49. Y. Topalova, R. Dimkov, D. Kozuharov, I. Ribarova, I. Ivanov, M. Nunes, C. Cheng, *Journal Biotechnol. Biotechnol. Equip.*, N1 **17**, 52 (2003).
50. Y. Topalova, R. Dimkov, I. Ivanov, S. Sergieva, R. Arsov, *Biotechnol. Biotechnol. Equip.*, **12**, 95 (1998).
51. M. Belouhova, I. Schneider, St. Chakarov, I. Ivanova, Y. Topalova, *Biotechnol. Biotechnol. Equip.*, **28**, 642 (2014).

Natural medicine: an evaluation of the *in vitro* cytotoxic effect of several Bulgarian fungal species on two panels of cancer cell lines

A. Dushkov, M. Petrova, J. Todorova, A. Gospodinov, I. Ugrinova*

Institute of Molecular Biology, Bulgarian Academy of Sciences, 1113, Sofia, Bulgaria

Received January 14, 2021; Revised March 01, 2021

The medicinal potential of Bulgaria's wild-growing fungi has, until recently, largely gone unexplored by the native scientific community. While many of the region's mushrooms have long been prized by residents as a valuable food source, they have generally not been thought of as having the medicinal value of certain herbs, for example. However, the growing body of scientific literature confirming the diverse beneficial effects of many Asian mushrooms (long held in high regard by ancient medicinal traditions of their respective regions), as well as the somewhat surprising discovery that some of these same mushrooms can be found in Bulgaria, has sparked our interest in exploring the effects they may have on different types of cancer, with the goal of either complementing existing treatments or, perhaps, uncovering new treatments based on compounds isolated from fungal extracts. We have prepared different ethanol and water extracts from the mushrooms *Trametes versicolor*, *Lenzites betulina*, *Fomes fomentarius*, *Fomitopsis betulina* and *Amanita muscaria* and have examined the primary cytotoxic effect of these crude extracts on a panel of human skin and lung cancer cells *in vitro*, with the goal of establishing their IC₅₀ values via MTT (3-(4,5-Dimethylthiazol-2-yl)-2,5-diphenyltetrazolium bromide) assay, comparing them, and gaining perspective for future research. Our results show that all extracts exhibit varying degrees of cytotoxicity even at low concentrations, warranting further inquiries into their anti-tumor potential.

Key words: fungi; cancer; cytotoxicity; replication; natural medicine

INTRODUCTION

Historically, different civilizations' attitudes toward mushrooms in general have been very dissimilar. As Gordon and Valentina Pavlovna Wasson point out [1], there is a clear dichotomy between civilizations that readily accept mushrooms as a food source and even medicine (termed 'mycophilic') and those that disregard them or outright reject them as such ('mycophobic'). A good example of a mycophilic civilization is ancient China, where mentions of mushrooms can be found in some of the oldest known medicinal texts, such as the *Huangdi Neijing*. China is also the home of some of the first known mushroom cultivation attempts – the fungus *Auricularia auricula-judae* is known to have first been grown intentionally in China around the year 600 A.D [2]. In comparison, after the Roman Age, many Western European civilizations have either not paid much attention to mushrooms in general, or regarded them as unnatural and dangerous due to their proclivity for growing on dead and rotting matter, their sudden appearance after rainfall as compared to the slow-growing plants (even appearing in circles, whose common name 'fairy rings' reflects their supposed supernatural origin in

the Western European mind), and their curious shapes, colors and odors. Bulgaria is, in some ways, no exception to this – while some of the local mushrooms have been well regarded as delicious edibles, evidence for their medicinal use is scarce. However, the times are changing, and with the growing availability of information accumulated on the medicinal properties of staple Asian mushrooms, the scientific community is gaining an interest in exploring the beneficial effects of their consumption and the mechanisms of action of their active compounds. The realization that some of the best medicinal fungi from Asia – the well-known *Trametes versicolor* (kawaratake, 雲芝 *yun zhi*), *Ganoderma lucidum* (reishi), *Grifola frondosa* (maitake), and *Inonotus obliquus* (chaga), for example – can be found in Bulgaria's forests, has prompted us to take active interest in examining the effects of several local species on cancerous cells *in vitro*.

The species of mushroom we studied in this work – all wood-growing fungi, except for *Amanita muscaria* - have each been indicated to contain compounds that exhibit some kind of anti-cancer activity via various mechanisms. *Trametes versicolor*, or 'turkey's tail', contains a compound known as polysaccharide K, or Krestin (PSK), a protein-bound polysaccharide used as an adjuvant

* To whom all correspondence should be sent:
E-mail: ugryiva@gmail.com

immunotherapeutic in Japan for more than three decades [3] that exhibits both immunopotentiating antitumor effects [4] and an ability to directly induce apoptosis in cell cultures *in vitro* [5]. A water extract derived from *Lenzites betulina* has been shown to have mild anti-tumor activity against the highly malignant murine tumor cell line Sarcoma 180 [6], while petroleum ether and ethyl acetate extracts from the fungus have exhibited a high degree of toxicity towards HeLa (human cervix epitheloid) and SMMC-7721 (human hepatoma) tumor cell lines compared to the positive control – quercetin [7]. An ethanol extract derived from *Fomes fomentarius*, a fungus curiously found (alongside *Fomitopsis betulina*) in the possession of ‘the Iceman’ Ötzi, a 5000 year old mummy [8], has been discovered to induce apoptosis in MDA-MB-231 breast cancer cells via AKT targeting [9], while the ‘water-extractable’ polysaccharide MFKF-AP1 β isolated from *F. fomentarius* fruiting bodies has shown a growth-inhibiting and apoptosis-inducing (via single strand DNA breakage) effect in human lung carcinoma A549 cells [10]. A pentacyclic triterpene known as betulinic acid, a compound found in the bark of white birch trees (*Betula pendula*) and the fruiting bodies of *Fomitopsis betulina* [11] (also known in literature as *Piptoporus betulinus*), a fungus which grows almost exclusively on them, has been demonstrated to be a ‘melanoma-specific cytotoxic agent’, effectively inhibiting tumor growth in athymic (nude) mice injected with human malignant melanoma MEL-2 and MEL-1 cells by inducing apoptosis via cell cycle arrest in the G0/G1 phase and generation of 50-kbp DNA fragments [12]. Finally, the iconic mushroom *Amanita muscaria* became a subject of interest after Vladimir Vazharov, author of the book ‘Medicinal Fungi in Bulgaria’ (2016, second ed., Biana, Sofia), personally brought to our attention the use of ethanol extracts of its fruiting bodies as an adjuvant therapy in the treatment of different cancers by many people in Russia and Japan, as well as recovered patients whose development he has observed himself; a study by Yoshida *et. al.* reports the presence of the β -(1-6)-branched (1-3)- β -D-glucans lentinan and schizophyllan in the fruiting bodies, which, despite not showing direct cytotoxicity against tumor cells, are thought to ‘prime’ the immune response to tumors and have been shown to have the effect of increasing the ratio of macrophages in murine peritoneal exudate cells by more than 50% when administered to mice [13].

In this study, we performed an evaluation of the primary cytotoxicity of crude extracts – ethanol, water, and a 1:1 mixture of the two – from the fruiting bodies of the fungi on human skin and lung cancer cell panels, with a non-cancerous lung fibroblast cell line used as a point of comparison. The IC₅₀ values for the different extracts, taking into account the species of mushroom and the type of extraction method used, were established and compared. The wood-growing fungi (all the species in the study except *A. muscaria*) were tested on the skin cancer cell lines, while *A. muscaria* was tested on the lung cancer cell lines.

EXPERIMENTAL

Fungi

All the fungal fruiting bodies used in this study, with the exception of *A. muscaria*, were collected by our team in the Vitosha mountain nature reserve near Sofia, Bulgaria. The fruiting bodies were dried out completely at 65 °C before being crushed thoroughly for extraction.

Extraction methods

All the extracts used were prepared in our laboratory, with the exception of the *A. muscaria* ethanol and ethanol/DMSO extracts, which were kindly provided to us by Vladimir Vazharov. Two types of extract were prepared for each wood fungus species using water and ethanol.

The water extraction was carried out by placing 5 grams of dried, crushed fruiting bodies in 50mL tubes before pouring boiling water inside (30mL for *T. versicolor*, 45mL for all other mushrooms except *A. muscaria*) and leaving them to soak at 80 °C for 24 hours. After that, the tubes were centrifuged at 6000 rpm for 10 minutes and the supernatant of each tube was removed and filtered separately through four layers of gauze in order to remove all residual pieces of the fruiting bodies. The leftover biomaterial from each mushroom was thereafter placed in the same respective gauze used for that species and the remaining liquid was pressed out thoroughly and collected with the rest of the respective extract. The extracts were again centrifuged under the above mentioned conditions, after which the supernatant was collected and ran through filters with a pore diameter of 0.45 μ m to ensure sterility.

The ethanol extraction was performed by placing 5 grams of dried, crushed fruiting bodies in 50mL tubes, then adding 96% ethanol (20mL for *T.*

versicolor, 45mL for all other mushrooms except *A. muscaria*). After soaking for 24h with occasional stirring, the extracts were subjected to the same centrifugation and filtering steps (using gauze and 0.45 µm filters) as the water extracts.

In the experiment, both the activities of the pure water and ethanol extracts, as well as the activity of a 1:1 mixture of the two (with the exception of *A. muscaria*), were evaluated.

The *A.muscaria* extracts were prepared by Vladimir Vazharov. The ethanol extract was prepared by filling a 500 mL glass bottle with dried mushroom caps, torn into small pieces, and pouring a 50% water-ethanol mixture inside until all the caps were covered completely, then leaving them to soak at room temperature and away from light for 18 days. When the time was up, the liquid was poured out (the caps were once again pressed in gauze to collect the entire quantity). The extract was then ran through a funnel with a cotton filled tube in order to filter out residual biomaterials, and finally filtered through a 0.45 µm filter. The ethanol/DMSO extract was prepared in an identical way with added DMSO for a final concentration of 5%.

Cell lines

The cell lines used in this study include a panel of lung cells - the healthy lung fibroblasts MRC-5, the human non-small cell lung carcinoma cell line H1299 and the adenocarcinomic human alveolar basal epithelial cell line A549 – a panel of skin cancer cells, consisting of the human epithelial malignant melanoma cell lines A375 and A375 KRAS and the human melanoma cell lines Hs 895 and Hs 895.T. – and the epithelial human breast cancer cell line MDA-MB231. H1299 cells were grown in RPMI 1640 medium, A549 – in F-12K medium; A375, A375 KRAS, Hs 895 and Hs 895.T were grown in DMEM medium; MRC-5 were grown in MEM medium, while MDA-MB231 cells were grown in Leibovitz's L-15 medium. All media was purchased from Thermo Fischer Scientific. We added fetal bovine serum (FBS) (final concentration in the media - 10%) and penicillin/streptomycin (Thermo Fischer Scientific) to all media. The cells were grown in an incubator under conditions of 37 °C and 5% CO₂.

Cytotoxicity test (MTT assay)

In order to evaluate the extracts' cytotoxicity, we performed an MTT cytotoxicity assay. This

method is based on the addition of the yellow tetrazoleum salt MTT (3-(4,5-Dimethylthiazol-2-yl)-2,5-diphenyltetrazolium bromide) to the growth medium and its biotransformation by the cells to a violet formazan. Viable cells contain NAD(P)H-dependent oxidoreductase enzymes, which reduce MTT to formazan. This changes the color of the cell media with MTT to varying shades of violet; the darker the solution, the greater the number of viable, metabolically active cells.

The cells from all cell lines were seeded in 96-well plates (100 µL/well) at a density of 1×10^5 cells per milliliter and, after 24h of incubation at 37 °C, were treated with different concentrations of extract added to the medium. As a positive control, in the plates used to test the ethanol extracts, additional wells were treated only with EtOH or a 1:1 EtOH-water mixture with the same concentrations as those that would be present in the wells with the extract. After letting the cells grow in the presence of the extract (the time of treatment being 72h for all fungi), we removed the medium with extract from the wells and replaced it with a phenol-free medium with added MTT (Invitrogen) (final concentration of 0.5 mg/mL). After keeping the cells in our incubator for 2.5 more hours, the medium was removed from the wells and DMSO aliquots of 100 µL were added into each well as a solvent for the formazan crystals that had formed. The cellular viability was measured on a multifunctional microplate reader Varioscan Lux. GraphPad Prism 6 software was used to establish the IC₅₀ values of each extract on each cell line for each of the amounts of time of treatment and to generate graphs.

In the plates, the amount of medium used per well for incubation and treatment was 100 µL. For all fungi except *A. muscaria*, the amounts of extract used, both water and ethanol, were 10, 5, 2.5, 1.25 and 0.625 µL per 100 µL of medium (the same values can also be thought of as percentage of extract per well), with three-well repeats for each amount. In the case of the *A.muscaria* extract, the final concentration of EtOH in the wells after extract addition was used to define the amount of extract in that well, i.e. we treated the extract as a 50% ethanol solution and represented the extract concentrations in the wells as the final diluted ethanol content of each well after extract addition (a 1% *A.muscaria* extract concentration shown on the graphs represents a 1% EtOH content in that well). For *A. muscaria*, we used concentrations of 1%, 0.9%, 0.8%, 0.7%, 0.6%, 0.5%, 0.4% and 0.3%, with four-well repeats for each of them.

RESULTS AND DISCUSSION

Our primary experiments were focused on setting up a framework within which to compare the different extraction methods' efficacy, taking into account the species of fungus which they were applied to, in producing an extract capable of inducing a cytotoxic response in our cell cultures. To that end, we carried out an MTT assay, which allowed us to establish the half-effective lethal dose (IC₅₀) for many of the extracts against the two cell line panels. The cells from all tested cell lines were treated with water and ethanol extracts from wood-growing fungi for 72h. The results, shown in Table 1 as IC₅₀ values given in amount of μL of extract per 100 μL of medium (or % of extract per well), indicate a varied response to the different extracts' presence, depending on the solvent used for extraction (and thus the compounds present in the extract) and the type of cell line involved.

All the extracts displayed varying degrees of primary cytotoxic activity when applied to the wells, albeit with varying degrees of success among the different cell lines. A comparison of the IC₅₀ values of the wood-growing fungi (excluding *A. muscaria*) yields the conclusion that out of these species, the extracts derived from *F. betulina* have the overall highest cytotoxic effect when applied directly to the cancer cells, likely due to the presence of betulinic acid, which is soluble in ethanol. This is consistent with the IC₅₀ values of all the *F. betulina* extracts – the ethanol extract's value is noticeably lower as compared to the water and water/ethanol extracts from the same species. Betulinic acid dissolves even more readily in DMSO, which could be considered for addition to the solvent during the extraction process in order to increase the quantity of the compound in the extract, although its toxicity to cells must be taken into account if it is to be used. The *F. fomentarius* ethanol extract displayed by far the least activity

against Hs 895.T cells among all the cell lines treated with it, and a noticeably higher activity against another two of the cell lines, one of which was the MDA-MB-231 breast cancer cells, confirming previous studies describing the ethanol extract's apoptosis-inducing effects [9], and the other - the A375 malignant melanoma cells; the extract's similar IC₅₀ values for the two cell lines (the value for A375 being slightly lower) raise the question of whether or not the cytotoxic effect against A375 cells is due to AKT signaling, as in the case of the MDA-MB-231 cells [9]. The water *F. fomentarius* extract had significantly higher IC₅₀ values than the ethanol one against in all the cell lines, suggesting either that perhaps more time is needed for extraction of a sufficient quantity of the polysaccharide MFKF-AP1 β needed to observe an effect similar to that described for the A549 lung cancer cell line [10], or that the compound's amount is sufficient but does not have the same apoptosis-inducing effect on these skin and breast cancer cell lines as on the A549 cells. We note that the *F. fomentarius* water extract's effect on the A375 cells was significantly more noticeable than on the MDA-MB-231 and Hs 895.T cells. The *T. versicolor* extracts, both water and ethanol, were toxic to the A375 melanoma cells to a greater extent than to the other cell lines treated with them, showing only slightly less cytotoxicity than *F. betulina* against this particular cell line. Although PSK is known to be soluble in hot water and insoluble in a variety of organic solvents [14], the ethanol extract had a lower IC₅₀ value, which might indicate that optimization of the extraction process is needed. The data for *Lenzites betulina* shows that overall it was the least toxic of all the species examined, which might indicate the absence of ethanol soluble directly cytotoxic compounds in its fruiting bodies, despite evidence for cytotoxic activity when using petroleum ether and ethyl

Table 1. IC₅₀ values of extracts from wood-growing fungi, represented in μL of extract per 100 μL of growth medium (same as percentage of extract per well). NT – Not Tested.

Cells/ Species	<i>Trametes versicolor</i>			<i>Lenzites betulina</i>			<i>Fomes fomentarius</i>			<i>Fomitopsis betulina</i>			Positive control	
	H ₂ O	EtOH	H ₂ O+ EtOH	H ₂ O	EtOH	H ₂ O+ EtOH	H ₂ O	EtOH	H ₂ O+ EtOH	H ₂ O	EtOH	H ₂ O+ EtOH	EtOH	H ₂ O+ EtOH
A375	2.4	1.22	1.7	3.8	1.7	2.6	4.9	1.9	3.2	1.8	0.84	1.4	1.5	2
A375 KRAS	NT	NT	3.3	NT	NT	5	NT	NT	5	NT	NT	NT	NT	4.1
Hs 895	NT	NT	1.6	NT	NT	2.6	NT	NT	3.8	NT	NT	NT	NT	2.3
Hs 895.T	9.9	7.2	8.4	15.8	8	9.2	12.7	8.5	9.4	4.8	6.6	7.8	7.9	8.8
MDA- MB231	5.2	2.7	4.8	6.2	3.8	5.6	9.6	3.2	5.4	NT	NT	NT	3	5.2

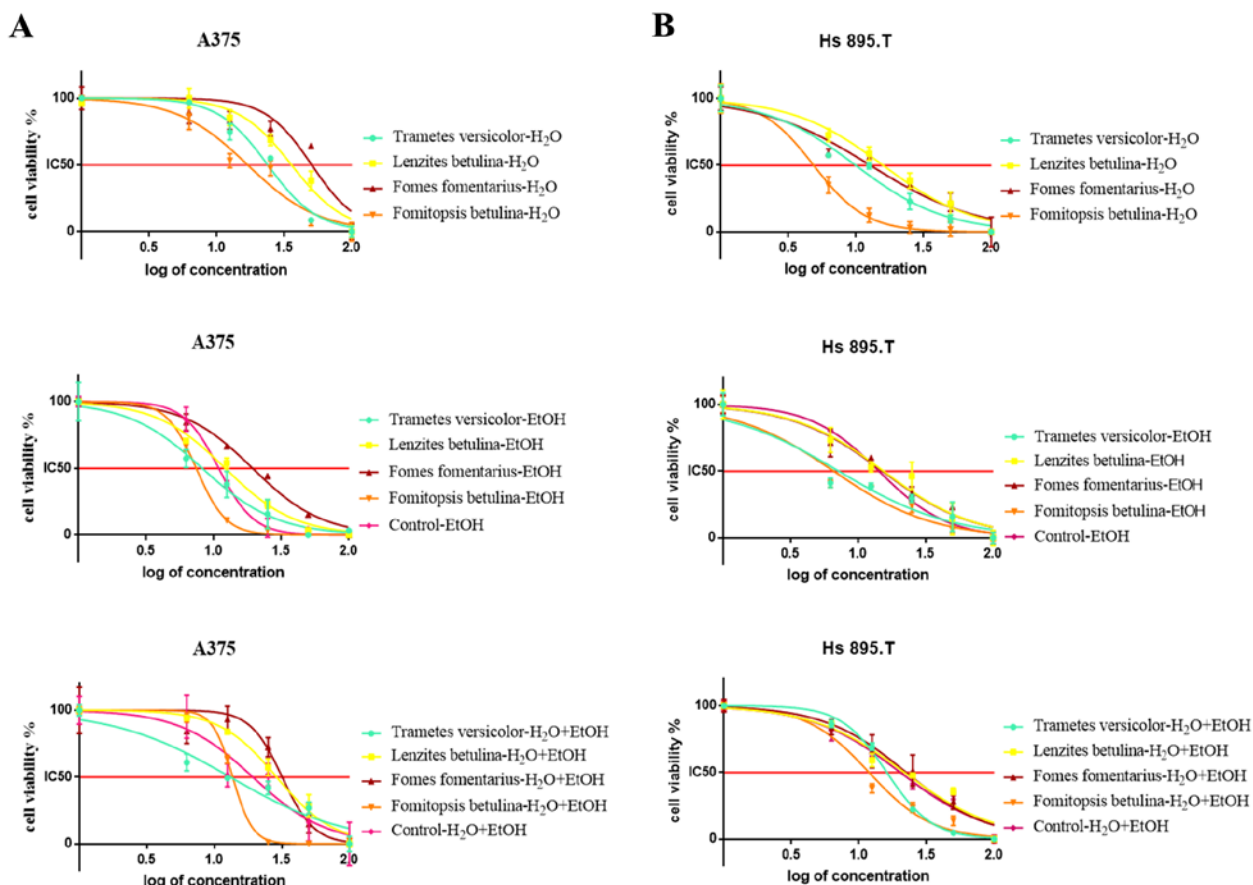


Fig. 1. Graphs representing the changes in cell viability for the cell line A375 (A) and the cell line Hs 895.T (B), treated with increasing fungal extract concentrations for 72h.

acetate when performing the extraction [7]. None of the instances of a water/ethanol mixture used for treatment had the lowest IC_{50} as compared to the pure water and ethanol extract values for the respective species, suggesting that these species contain no compounds that exhibit a synergistic effect while being soluble in different solvents.

Our results were quantified using GraphPad Prism software. The resulting graphs illustrate the changes in cell viability brought on with increasing extract concentrations. We used the graphs for the A375 and Hs895.T cell lines (Fig. 1, concentrations shown in logarithmic scale along the X axis and cell viability shown in % along the Y axis) to represent the different tendencies in cytotoxic action when treating with different extracts. The graphs present the results shown in Table 1, indicating the *F. betulina* ethanol extract as the most effective in inducing drops in viability; however, the *T. versicolor* ethanol extract is almost as effective as the *F. betulina* one. The water/ethanol 1:1 mixtures have overall been more effective than the water extract, yet less effective than the ethanol one, suggesting that the compounds present in the ethanol extract have a

primary role in the observed cytotoxicity induced by the water/ethanol mixture.

Fig. 2 illustrates the observed effect after 72h of treatment of A375 cells with the various *F. betulina* extracts in concentrations close to the IC_{50} value as compared to untreated (negative control) cells. In every case, the treated cells are in a noticeably less viable state than the controls. The figure also illustrates the effect of ethanol and 1:1 ethanol-water mixture addition (with the same concentrations as those that would be present in the wells treated with the respective extract) to the cell medium; the ethanol-water mixture has a mild cytotoxic effect, while treatment with pure ethanol has a slightly more pronounced effect, yet both of them are visibly less effective than the fungal extracts containing the same ethanol concentrations. The state of the cells is consistent with the experimental data pictured on the graphs in Fig.1.

As noted in a study by Faulstich *et al* [15], *A. muscaria*'s toxicity is relatively low compared to other *Amanita* species, such as *A. phalloides*, due to its' significantly lower amatoxin content; because of this, we wanted to examine the cytotoxicity of its

fruiting bodies. To that effect, we ran a cytotoxicity assay using MTT in order to establish the primary cytotoxic effect of the extract on lung cells, both cancerous (H1299, A549) and non-cancerous (MRC-5). The results, presented as graphs where the X axis denotes a logarithmic increase in

concentration and the Y axis denotes the percentage of viable cells (Fig. 3), show the definitive cytotoxic effect of the *A. muscaria* ethanol extract's presence in the medium even in extremely minute (<1%) quantities.

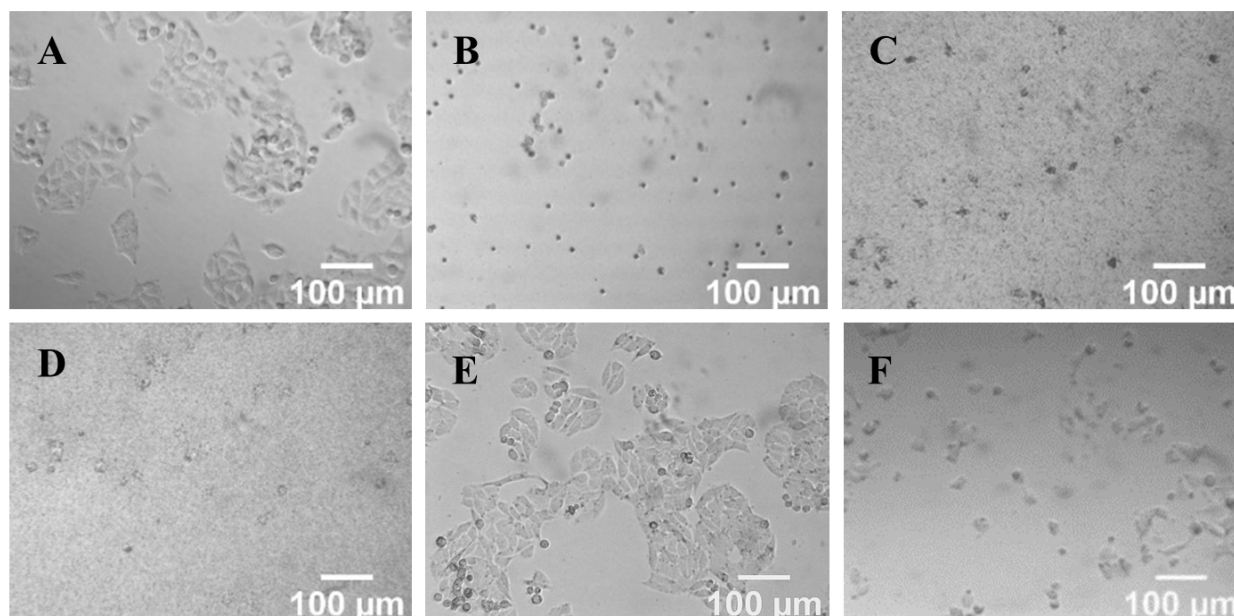


Fig. 2. A375 cells treated with different *F. betulina* extracts for 72 hours with a concentration equal to the IC_{50} value; light microscopy, magnified 10x. A – negative control cells (untreated), B – water extract, C – water-ethanol extract mixture, D – ethanol extract, E – control cells treated with a 1:1 water and ethanol mixture, F – control cells treated with ethanol.

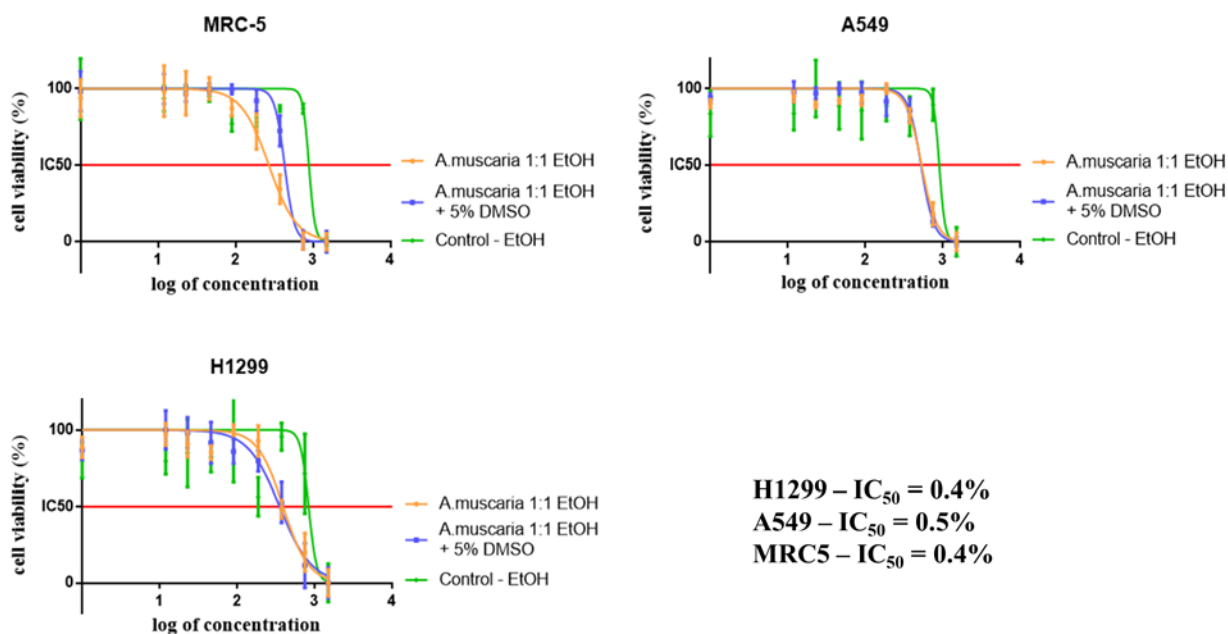


Fig. 3. Graphs representing the changes in cell viability for the cell line H1299 with increasing *A. muscaria* extract concentrations over the course of 72 hours. IC_{50} values of the *A. muscaria* ethanol extract on the different lung cell lines are shown here as a final ethanol percentage concentration per 100 μ L.

Upon evaluating the cytotoxic activity of the *A. muscaria* extract on the lung cells, we noticed that the presence of DMSO seemed to diminish the extract's cytotoxic activity. The ethanol *A. muscaria* extract yielded the highest direct cytotoxic effect out of all the examined fungal species; however, it remains to be seen whether this toxicity is due to the presence of amatoxins alone or in combination with other compounds. The ethanol control cells, treated with the same percentages of ethanol as present in the wells treated with extract, remained completely viable, indicating that none of the extract's activities are due to the ethanol in these low concentrations. Unlike with the other extracts, the cells treated with *A. muscaria* extract did not show a gradual decrease in cell viability with increase of concentration, but rather a sudden drop in live cell number, suggesting that very slight adjustments of the concentration can have a very profound effect on toxicity.

CONCLUSION

This work is a summary of the first general evaluation of native fungal cytotoxicity performed in our laboratory, and its main purpose was establishing primary species of interest. Our data has allowed us to identify the extracts with the most cytotoxic potential and narrow down the focus of our future research. The results we have obtained from our experiments with these crude extracts are promising, and the mushrooms that we have examined are common; the extraction procedures themselves can easily be performed outside of the laboratory (as has been done in East Asian traditional medicinal practice, where both alcohol and water extracts from medicinal wood fungi have been prepared and consumed as folk cures [16]). It is our hope that our results will help in leading the way towards therapies, both primary and adjuvant, that will have a beneficial effect on cancer patients' status.

Acknowledgements: *The author acknowledges the support of the National Scientific Program*

BioActivMed (D01-217) by the Bulgarian Ministry of Education. The author would like to thank mr. Vladimir Vazharov for his kind assistance and for generously providing the team with an ethanol extract from Amanita muscaria, prepared by him.

REFERENCES

1. V. P. Wasson, R. G. Wasson, *Mushrooms, Russia and history*, Pantheon Books, New York (1957).
2. S.-T. Chang, *Econ. Bot.*, **31**, 374 (1977).
3. P. M. Kidd, *Altern. Med. Rev.*, **5**, 4 (2000).
4. M. Fisher, L. X. Yang, *Anticancer Res.*, **22**, 1737 (2002).
5. E. Jiménez-Medina, E. Berruguilla, I. Romero, I. Algarra, A. Collado, F. Garrido, A. Garcia-Lora, *BMC Cancer*, **8**, 78 (2008).
6. T. Ikekawa, M. Nakanishi, N. Uehara, G. Chihara, F. Fukuoka, *GANN Japanese J Cancer Res*, **59**, 155 (1968).
7. G. Ren, X. Y. Liu, H. K. Zhu, S. Z. Yang, C. X. Fu, *Fitoterapia*, **77**, 408 (2006).
8. U. Peintner, R. Pöder, T. Pümpel, *Mycol. Res.*, **102**, 1153 (1998).
9. S. O. Lee, M. H. Lee, K. R. Lee, E. O. Lee, H. J. Lee, *Int. J. Mol. Sci.*, **20** (2019).
10. S. H. Kim, R. Jakhar, S. C. Kang, *Saudi J. Biol. Sci.*, **22**, 484 (2015).
11. Z. Alresly, U. Lindequist, M. Lalk, A. Porzel, N. Arnold, L. A. Wessjohann, *Rec. Nat. Prod.*, **10**, 103 (2015).
12. E. Pisha, H. Chai, I.-S. Lee, T. E. Chagwedera, N. R. Farnsworth, G. A. Cordell, C. W. W. Beecher, H. H. S. Fong, A. D. Kinghorn, D. M. Brown, M. C. Wani, M. E. Wall, T. J. Hieken, T. K. Das Gupta, J. M. Pezzuto, *Nat. Med. (N. Y., NY, U. S.)*, **1**, 1046 (1995).
13. I. Yoshida, T. Kiho, S. Usui, M. Sakushima, S. Ukai, *Biol. Pharm. Bull.*, **19**, 114 (1996).
14. J. M.-F. Wan, *Handbook of Biologically Active Peptides*, Academic Press (2013).
15. H. Faulstich, M. Cochet-Meilhac, *FEBS Lett.*, **64**, 73 (1976).
16. P. Dresch, M. N. D'Aguzzo, K. Rosam, U. Grienke, J. M. Rollinger, U. Peintner, *AMB Express*, **5**, 4 (2015).

Antifungal activity of separated fractions from the hemolymph of marine snail *Rapana venosa*

E. Krumova¹, P. Dolashka², R. Abrashev¹, L. Velkova², A. Dolashki², A. Daskalova², V. Dishliyska¹, V. Atanasov², D. Kaynarov², M. Angelova^{1*}

¹ The Stephan Angeloff Institute of Microbiology, Bulgarian Academy of Sciences, Sofia, Bulgaria

² Institute of Organic Chemistry with Centre of Phytochemistry, Bulgarian Academy of Sciences, Acad. G. Bonchev Str. Bl. 9, 1113 Sofia, Bulgaria

Received February 01, 2021; Revised March 19, 2021

For the first time the antifungal activities of the hemolymph isolated from mollusks marine snail *Rapana venosa* have been tested. Three protein fractions containing compounds with Mw<10 kDa (Rv/10), Mw between 10-50 kDa (Rv/10-50), and Mw between 30-100 kDa (Rv/30-100), were obtained by ultrafiltration of hemolymph with Mw below 100 kDa. Their effect against strains belonging to the species *Fusarium oxysporum*, *Penicillium griseofulvum*, *Alternaria solani*, *Mucor hiemalis*, *Aspergillus niger*, *Botrytis cinerea*, and *Candida albicans* was determined. Fungal growth inhibition and Minimum Inhibitory Concentration (MIC) were assayed by agar well diffusion (AWD) and broth micro-dilution (BMD) methods. The fraction Rv/30-100 was found to be the most effective against all tested strains. Other fractions, Rv/10-50 and Rv/10, displayed growth inhibitory activity against *F. oxysporum*, *P. griseofulvum*, *B. cinerea*, and *F. oxysporum*, respectively.

Key words: *Rapana venosa*; hemolymph; protein fraction; antifungal activity; fungi; MIC

INTRODUCTION

Fungal diseases are a major medical problem worldwide. These diseases are now more important and troublesome than ever before [1, 2]. Today almost a billion people suffer from skin, nail, and hair fungal infections. According to published data, many 10's of millions mucosal candidiasis and more than 150 million people have serious fungal diseases [3, 4]. The therapy for most invasive fungal diseases remains unsatisfactory given their high morbidity and mortality despite the available antifungal treatment. For example, fungal diseases such as aspergillosis have high mortality even when treated with appropriate therapy and are often incurable in hosts with impaired immunity [5]. In the near horizon, the prevalence of fungal diseases is likely to increase, as there will be more hosts with impaired immunity and drug resistance will inevitably increase after selection by antifungal drug use. Different species, belonging to genera *Aspergillus*, *Mucor*, *Penicillium*, *Cladosporium*, etc. have been reported as etiological agents of well-characterized respiratory disorders [6]. *Fusarium*, conventionally regarded as agents of onychomycosis, is now well known to cause fatal respiratory mycosis. *Aspergillus* spp. is the major

culprit of severe asthma with fungal sensitization (SAFS), although a range of other fungi, such as *Alternaria* and *Cladosporium* spp., are also involved [3]. In line with Fungal Infection Trust (7) in 2021, nearly 20 million people are living with aspergillosis, and over a million die each year. Moreover, new pathophysiological associations hitherto unknown, such as fungal sensitization and allergic bronchopulmonary mycosis in patients with chronic obstructive pulmonary disease, are unfolding [8].

The treatments with currently used antifungal agents require long term administration protocols capable of causing toxic. The standard antifungal therapies can be also limited because of low efficacy rates and drug resistance [9, 10]. Multidrug resistance (MDR) is a serious complication during treatment of the opportunistic fungal infections that frequently afflict immunosuppressed patients [2, 11]. These patients require antifungal therapy as part of their supportive care. Despite improvement of antifungal therapies over the last 30 years, the phenomenon of antifungal resistance is still of major concern in clinical practice [12, 13].

Antifungal activity of bioactive compounds is a new direction of scientific searching. Mollusks are a huge source to discover bioactive natural products [14]. In most cases these are substances with antibacterial effect. For example, methanol extracts of sea invertebrates demonstrated activity against

* To whom all correspondence should be sent:
E-mail: mariange_bg@yahoo.com

Pseudomonas aeruginosa [15]. The hemolymph of several molluscan species such as sea hares, sea slug, oysters, and mussels possess antibacterial and antiviral activities [16-18]. On the other hand, different snail proteins have been studied for their antimicrobial effect. But the compounds exhibiting antifungal effect are very rare found [10, 19, 20]. For instance, crude proteins extracted from the snail *Cryptozona bistrialis* demonstrated antifungal effect against *Candida albicans*, *Penicillium chrysogenum*, *Aspergillus fumigatus*, and *Mucor racemosus* [18]. The mucus secreted by *Achatina fulica* (Mollusca) has potential antifungal properties [21]. Suresh *et al.* [22] determined significant growth inhibition against *Babylonia zeylanica* and *Harpa conoidalis* (Molluscas) by *Candida albicans* and *Aspergillus niger*. Even less is known about the antifungal activity of peptide fractions (antifungal peptides, AFPs) isolated from mollusks and arthropods [20]. A cysteine-rich peptide, named mytimycin, isolated from mussels *Mytilus edulis* inhibited growth of *Neurospora crassa* and *Fusarium culmorum* [23]. Such strictly antifungal peptide from *M. edulis* was reported by Charlet *et al.* [24].

In our previous studies we investigated a broad range of peptide fractions isolated from marine and terrestrial molluscs for their antifungal properties. The present study was designed to determine the effect of fractions isolated from the hemolymph of marine snail *R. venosa* against several fungal strains belonging to the genera *Aspergillus*, *Penicillium*, *Fusarium*, *Alternaria*, *Mucor*, *Botrytis*, and *Candida*.

EXPERIMENTAL

Isolation of bioactive fractions from the hemolymph of marine snail R. venosa

The hemolymph was collected, which lives freely in the Black Sea. It is known that hemolymph of *R. venosa* contained above 90% hemocyanin as a major protein. After several purification steps, including filtration, centrifugation at 5000xg at 4 °C for 20 minutes to remove coarse particles and haemocytes and anew filtration, a crude hemolymph extract was obtained [25]. This extract was subjected to ultrafiltration under pressure (4 bar) on a 100 kDa membrane (Millipore Ultrafiltration Membrane Filters) of Amicon® Stirred Cell, which resulted in two fractions - one fraction with molecular masses

(Mw) above 100 kDa to obtain hemocyanin, and another fraction with Mw bellow 100 kDa. Hemolymph with Mw bellow 100 kDa was separated by ultrafiltration in three protein fractions containing compounds with Mw<10 kDa (Rv/10), Mw between 10-50 kDa (Rv/10-50), and Mw between 30-100 kDa (Rv/30-100).

Disc membranes from ultracel regenerated cellulose from 10 NMW, 30 NMW 50 NMW and 100 NMW (Millipore™ Corporation, Billerica, U.S.A) were used for processes of ultrafiltration.

SDS-PAGE Electrophoresis

Protein fractions were analyzed by sodium dodecyl sulphate-polyacrylamide gel electrophoresis (SDS-PAGE), according to Laemmli method with modifications [26]. Equal volumes containing approximately 20 µg/lane of the samples dissolved in Laemmli sample buffer and protein standard mixture (Precision Plus Protein., All Blue, Bio-Rad, Feldkirchen, Germany) were separated by 12.5% SDS-PAGE and visualized by staining with Coomassie Brilliant Blue G-250.

Microorganisms and culture conditions

Fungal strains *Fusarium oxysporum* NBIMCC 124, *Penicillium griseofulvum* P29, *Alternaria solani* CBS 106.21, *Mucor hiemalis* M2, *Aspergillus niger* 26, *Botrytis cinerea* NBIMCC 120, and *Candida albicans* 14 were used in this study. They were chosen as representatives of fungal infection. All of them belong to the Mycological collection of the Stephan Angeloff Institute of Microbiology, Sofia. Long-term preservation of these fungi was carried out in the Microbank system (Prolab Diagnostics, Richmond Hill, Canada) consists of sterile vials that contain 25 porous, colored beads and a cryopreservative fluid at -80°C. Before use, the conidiospores were grown on Beer agar medium [27] at 28 °C for 7 days.

Preparation of standardized spore suspension

Fungal strains were freshly subcultured on sterile on potato-dextrose agar (PDA) and incubated at 28 °C for 7 days. The resultant spores were washed into sterile solution of Triton X-100 and adjusted to a concentration of 2x10⁸ spores/mL.

Antifungal activity assay by agar well diffusion (AWD) method

The antifungal activity was assayed through a diffusion technique on PDA growth medium. Spore suspension of each fungal strain (200 μ L) was spread onto the surface of the Petri dishes. Then, 10-mm-diameter holes were punched and filled with 100 μ L of the previously prepared sampling fractions in decreasing dilutions (0.65, 0.32, and 0.17 μ g/mL). The used concentrations were selected based on our preliminary experiments. As control samples for each variant, Triton X-100 (negative control) and the fungicide nystatin (0.1%, positive control) were used. Subsequently, the plates were incubated at 28 °C. Each extract form was evaluated with 3 repetitions, and the assessment was conducted after 24, 48, 72, and 168 h by measuring the diameter of the inhibition of the fungi mycelial growth (clear zone of inhibition formed around were considered indicative of antifungal activity).

Antifungal activity assay by broth micro-dilution (BMD) method

Antifungal activity was tested by determining the minimum inhibitory concentration (MIC) using the microdilution method with resazurin, an indicator of microbial growth [23]. In general, the 96-well plates were prepared by dispensing into each well 50 μ L of potato dextrose broth amended with 50 μ L tested fraction at 0.32, 0.17, 0.08, and 0.04 μ g/mL. Then, 10 μ L spore suspension and 30 μ L of 0.02% resazurin were added and plates were incubated at 28 °C. Effect of tested fraction on fungal growth was evaluated after 24, 48, 72, and 168 h by visual inspection. Control samples contained 50 μ L nystatin in concentration 1 mg/mL instead of tested fraction.

The MIC was determined as the lowest concentrations that caused complete growth inhibition (100%) compared with control probes without antifungal compounds.

RESULTS AND DISCUSSION

The hemolymph of *R. venosa* is rich in different bioactive components. Up to now some extracellular proteins are identified, such as actin and several FUs of *R. venosa* hemocyanin, the remaining proteins are unknown. Therefore, the aim of our study was to evaluate the antifungal effect of three fractions isolated from *R. venosa* hemolymph with Mw <100, containing different

natural compounds. The main protein in the hemolymph of the sea snail (over 90%) is *R. venosa* hemocyanin (RvH) characterized previously [25, 29]. Moreover, antimicrobial proline-rich peptides with molecular masses below 10 kDa isolated from the hemolymph of marine snail *R. venosa* have been studied [30]. They have demonstrated antibacterial activity against Gram-positive (*S. aureus*) and Gram-negative (*K. pneumoniae*) bacteria [30].

The distribution of the proteins and peptides in three fractions of *R. venosa* hemolymph - Rv/10, Rv/10-50 and Rv/30-100 is represented in the 12.5% SDS-PAGE (Fig. 1). It was detected that the fraction below 10 kDa contained peptides with molecular masses between 3000 and 9500 Da, determined by mass spectrometric analysis in the study [25]. The presence of proteins in the region between 35-45 kDa was observed in both fractions. The proteins with Mw at ~ 16 kDa ~ 20 kDa and ~ 25 kDa are specific for fraction Rv/10-50. The protein band at ~26 kDa and ~30 kDa are more extensively expressed in fraction Rv/10-50 in comparison to the other fraction. The proteins with Mw at ~ 52 kDa, ~ 65 kDa and ~ 100 kDa are specific for fraction Rv/30-100. Moreover, on this lane, traces from protein bands with Mw above 100 kDa were observed (Fig. 1).

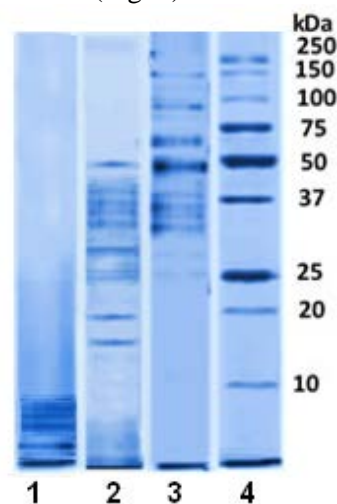


Fig. 1. 12.5% SDS-PAGE analysis, visualized by staining with Coomassie G-250, position: 1) peptide fraction with Mw <10 kDa; 2) Fraction from *R. venosa* hemolymph with Mw 10-50 kDa; 3) Fraction from *R. venosa* hemolymph with Mw 30-100 kDa; 4) Molecular weights of standard proteins from Bio-Rad.

In this study, three fractions (Rv/10, Rv/10-50 and Rv/30-100) of *R. venosa* were tested against seven potentially pathogenic fungal strains. Table 1 shows the antifungal activity determined by AWD method. Among these, the fraction Rv/30-100

Table 1. Antifungal inhibitory activity of the extracts using AWD method.

	Fractions	Antifungal effect						
		<i>F. ox.</i>	<i>P. gr.</i>	<i>A. sl.</i>	<i>M. mh.</i>	<i>A. ng.</i>	<i>B. cn.</i>	<i>C. al.</i>
1	Rv/10-50	FC/48***	N/I	N/I	N/I	N/I	FC/48***	N/I
2	Rv/10	N/I	N/I	N/I	N/I	N/I	N/I	N/I
3	Rv/30-100	FC/48** RG/72***	FC/48** RG/168***	FC/168*	FC/168*	FC/48**	FC/168*	FC/168*

Note: Fc – fungicidal activity; Fs – fungistatic activity; RG –retarded growth; N/I = no inhibition; 24-168 – number of hours; Minimal concentration dose * - 0.17; ** - 0.32; *** - 0.65 µg/mL. *F. ox* – *F. oxysporum*; *P. gr.* – *P. griseofulvum*; *A. sl.* – *A. solani*; *M. mh.* - *M. hiemalis*; *A. ng.* - *A. niger*; *B. cn.* - *B. cinerea*; *C. al.* - *C. albicans*

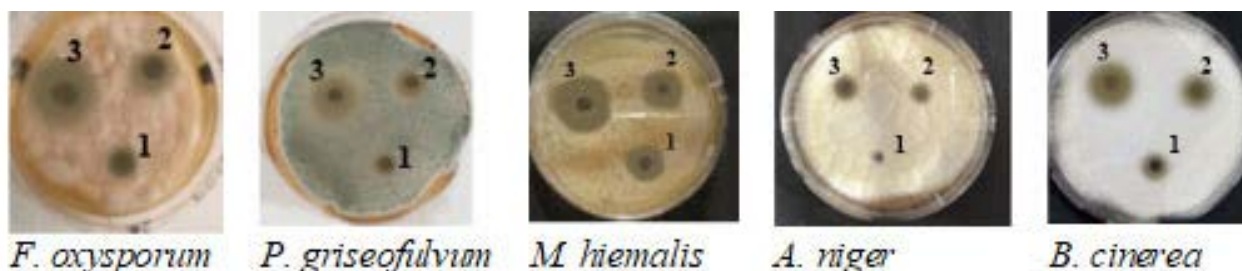


Fig. 2. Fungal growth inhibitory activity of the fraction Rv/30-100 in a concentration: 1 - 0.17 µg/mL; 2 - 0.32 µg/mL; 3 - 0.65 µg/mL.

Table 2. Antifungal inhibitory activity of the plant extracts using broth microdilution method.

№	Fractions	Antifungal effect						
		<i>F. ox.</i>	<i>P. gr.</i>	<i>A. sl.</i>	<i>M. mh.</i>	<i>A. ng.</i>	<i>B. cn.</i>	<i>C. al.</i>
1	Rv/10-50	IG/24****	FS/48****	N/I	N/I	N/I	FC/48***	N/I
2	Rv/10	IG/24****/	N/I	N/I	N/I	N/I	N/I	N/I
3	Rv/30-100	IG/48*** RG/72***	IG/24*** RG/72****	IG/168***	IG/168***	IG/48***	IG/168***	IG/72****

Note: IG – inhibition effect on mycelium growth; N/I = no inhibition effect; 24-168 – number of hours; Minimal concentration * - 0.04, ** 0.08, *** 0.17, **** 0.32 µg/mL; *F. ox* – *F. oxysporum*; *P. gr.* – *P. griseofulvum*; *A. sl.* – *A. solani*; *M. mh.* - *M. hiemalis*; *A. ng.* - *A. niger*; *B. cn.* - *B. cinerea*; *C. al.* - *C. albicans*

exhibited clear fungicidal effect towards all the seven tested fungi. These results are also demonstrated in Fig. 2.

At the same time, the fraction Rv/10-50 displayed growth inhibitory activity against *F. oxysporum* and *B. cinerea*. In contrast, fraction Rv/10 showed negative activity against all tested fungal strains. The most sensitive fungal strains were *F. oxysporum* and *B. cinerea* that demonstrated fungicidal effect towards two fractions (Rv/10-50 and Rv/30-100), followed by *P. griseofulvum*, *A. solani*, *M. hiemalis*, *A. niger*, and *C. albicans* whose growth was inhibited by Rv/30-100 only. It should be emphasized that the fraction Rv/30-100 revealed the most significant antifungal activity compared to other two fractions.

The antifungal activity of the *R. venosa* fractions was tested also using BMD method with resazurin (7-Hydroxy-3H-phenoxazin-3-one 10-oxide). The

resazurin is a blue dye which can be irreversibly reduced to a pink by oxidoreductase within viable cells. The results concerning growth inhibition effect on used fungal strains are shown in Table 2.

Visual inspection was sufficient to easily identify strains that are more sensitive to *R. venosa* fractions, i.e., their wells show more purple or less pink color than the control after a set time of incubation. The fraction Rv/30-100 showed significant activity against all strains tested (Fig. 3). This fraction completely inhibited the growth after 24 h of incubation for *P. griseofulvum*, 48 h for *F. oxysporum* and *A. niger*, 72 h for *C. albicans*, and 168 h for *A. solani*, *M. hiemalis*, and *B. cinerea*. The fraction Rv/10-50 proved less effective than Rv/30-100. Among the 7 tested species, 3 species (*F. oxysporum*, *P. griseofulvum*, and *B. cinerea*) showed positive results for antifungal activity for 24 or 48 h. Surprisingly, the fraction Rv/10

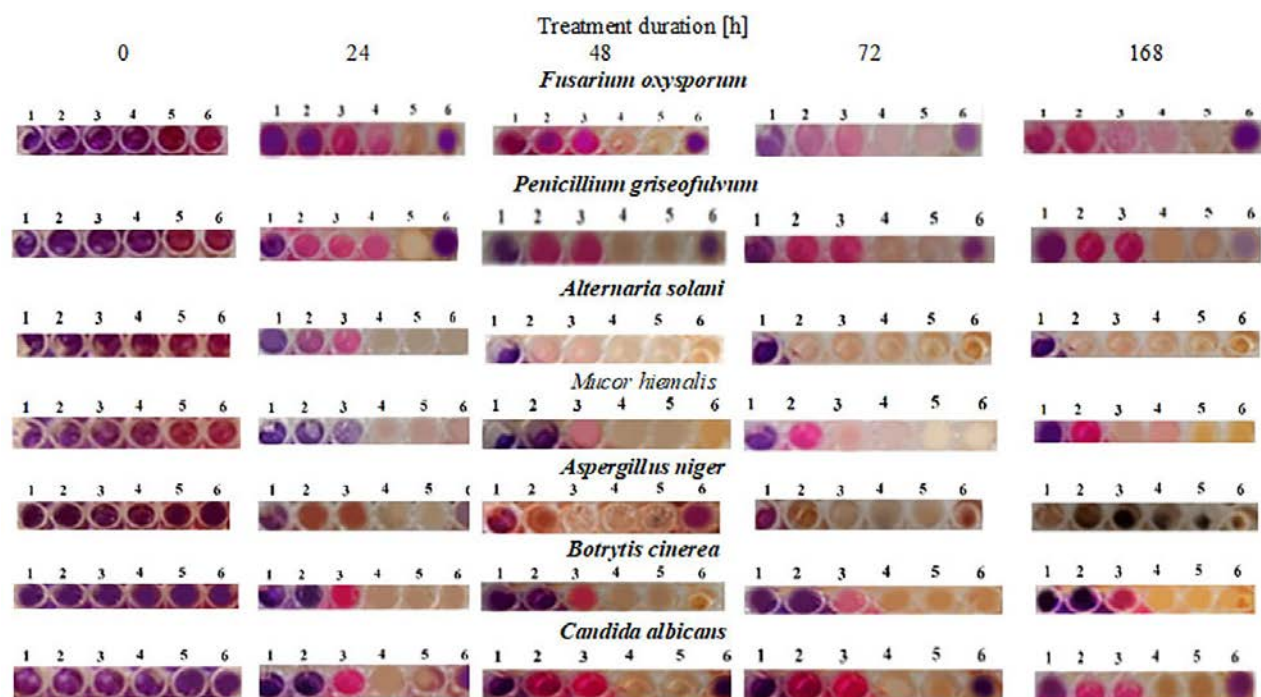


Fig. 3. Fungal growth inhibition by protein fraction Rv/30-100. Note: 24-168 – Number of hours; Minimal concentration: 1 - 0.32; 2- 0.17; 3- 0.08; 4 - 0.04 $\mu\text{g/mL}$; 5 – Negative control (non-treated culture); 7 – Positive control (culture treated with nystatin).

Table 3. The MIC values of *R. venosa* fractions against tested fungal strains assayed by AWD and BMD methods.

Strain	Fractions/MIC ($\mu\text{g/mL}$)					
	AWD method			BMD method		
	Rv/10-50	Rv/10	Rv/30-100	Rv/10-50	Rv/10	Rv/30-100
<i>F. oxysporum</i>	0.65	-	0.32	0.32	0.32	0.17
<i>P. griseofulvum</i>	-	-	0.32	0.32	-	0.17
<i>A. solani</i>	-	-	0.32	-	-	0.17
<i>M. hiemalis</i>	-	-	0.17	-	-	0.17
<i>A. niger</i>	-	-	0.32	-	-	0.17
<i>B. cinerea</i>	0.65	-	0.17	0.32	-	0.17
<i>C. albicans</i>	-	-	0.17	-	-	0.32

Note: Not detected (-)

exhibited antifungal activity against *F. oxysporum* (for 24 h). It should be noted that the fraction Rv/30-100 proved to be more suitable for growth inhibition of the strains *A. solani*, *M. hiemalis*, and *Botrytis cinerea* compared to the antifungal drug nystatin (Fig. 3).

The results shown in Table 3 give information about the MIC values determined by both the methods, AWD and BDM. The fraction Rv/30-100 was most effective having MIC value with widest spectrum of antifungal activity compared to the other tested fractions. Its MIC value according AWD method was 0.17 $\mu\text{g/mL}$ against *M. hiemalis*, *B. cinerea*, and *C. albicans* and 0.32 $\mu\text{g/mL}$ against *F. oxysporum*, *P. griseofulvum*, *A. solani* and *A. niger*. The MIC value for Rv/10-50 was 0.65 $\mu\text{g/mL}$ against *F. oxysporum* and *B. cinerea*. The

fraction Rv/10 showed non-detectable antifungal activity for the tested strains. As can be seen in Table 3, MIC values assayed by BDM method were 2-fold lower than those obtained by AWD method. Furthermore, the BDM method allowed to determine a MIC dose for Rv/10 against *F. oxysporum* (0.32 $\mu\text{g/mL}$). The two protein fractions have common proteins as well as specific proteins. Therefore, we hypothesized that differences in the observed antifungal activity against various tested pathogen strains is likely due to the specific proteins of each of both fractions. The similar antifungal activity against *F. oxysporum* and *B. cinerea* is probably due to the proteins common for both fractions, but present in different concentrations.

Taken together, our results revealed that the fraction containing proteins with Mw 30-100 is the most active against the growth of a wide range of fungal strains. This effect can be explained by clearly expressed antifungal activity of these proteins.

In the last three decades marine mollusks become a favorable object for searching biologically active molecules with health benefits, including antibacterial and antifungal activity. Potential antifungal activity of extracts of marine mollusks has been reported by Umayaparvathi *et al.* [31]. The authors suggested that this effect is due to the presence of antifungal peptide. The results of Ulagesan and Kim [22] also demonstrated that proteins extracted from seven different snails act as the bioactive compound against the pathogenic fungi belonging to the genera *Mucor*, *Aspergillus*, *Penicillium*, and *Candida*. Similar results have been described about plasma of the mussel *Mytilus galloprovincialis* [32] and *Perna viridis* [33], molluscs from the family *Muricidae* [34]. In contrast, the efforts of many authors to determine antifungal activity of mollusks and arthropods remain without a positive result [35]. It was proved that peptides from freshwater snail (*Pomacea insularium*) and crab (*Callinectes sapidus*) haemolymph ranged in molecular mass from 9 to 110 kDa and 40 to 100 kDa, respectively, possess high antimicrobial activity but not antifungal one [36]. Our main finding is that the fractions from *R. venosa* hemolymph have significant inhibition effect on the growth of potentially pathogenic fungi. It should be noted that the amount of MIC was lower compared to the reported results against strains belonging to the genera *Candida*, *Penicillium*, *Aspergillus*, *Mucor*, etc. [18, 19, 37].

CONCLUSION

In the present study, the bioactive fractions from the hemolymph of marine snail *R. venosa* were found to be promising source of highly potent antifungal agents. The used fractions exhibited remarkable activity against seven potentially pathogenic fungal strains. The results clearly demonstrated that the fraction containing proteins with Mw 30-100 used in a concentration 0.17 µg/mL, completely inhibited the fungal growth for a long period (168 h). Moreover, the fractions Rv/10-50 and Rv/10 in a concentration 0.32 µg/mL could be useful against *F. oxysporum*, *P. griseofulvum*, *B. cinerea*, and *F. oxysporum*, respectively.

Dedication: We dedicate this article to Prof. Wolfgang Voelter from the University of Tuebingen, Germany, who died on January 21, 2021.

Acknowledgements: This research was carried out with the support of DOI-217/30.11.2018 National scientific program "Innovative low-toxic biologically active precise medicine (BioActiveMed) and a project under contract No. DN 01/14 of 19.12.16, funded by the Scientific Research Fund of the Ministry of Education and Science in the Republic of Bulgaria.

REFERENCES

1. S. Arıkan, *Med. Mycol.*, **45**, 569 (2007).
2. X. Da, Y. Nishiyama, D. Tie, K. Z. Hein, O. Yamamoto, E. Morita, *Sci. Rep.*, **9**, 1683 (2019).
3. F. Bongomin, S. Gago, R. O. Oladele, D. W. Denning, *J. Fungi (Basel)*, **3**, 57 (2017).
4. C. Firacative, *Mem. Inst. Oswaldo Cruz*, **115**, e200430 (2020).
5. A. Casadevall, *Pathog. Immun.*, **3**, 183 (2018).
6. A. Chowdhary, K. Agarwal, J. F. Meis, *PLoS Pathog.*, **12**, e1005491 (2016).
7. Fungal Infection Trust (2021) <https://fungalinfectiontrust.org/fungal-infection-trust-honours-world-aspergillosis-day-with-the-launch-of-its-new-website/>
8. K. Agarwal, S. N. Gaur, A. Chowdhary, *Mycoses*, **58**, 531 (2015).
9. A. K. Gupta, E. Tomas, *Dermatol. Clin.*, **21**, 565 (2003).
10. A. Matejuk, Q. Leng, M. D. Begum, M. C. Woodle, P. Scaria, S. T. Chou, A. J. Mixson, *Drugs Future*, **35**, 197 (2010).
11. D. P. Kontoyiannis, *J. Infect. Dis.*, **216**, S431 (2017).
12. G. D. Brown, D. W. Denning, N. A. R. Gow, S. M. Levitz, M. G. Netea, T. C. White, *Sci. Transl. Med.*, **4**, 165rv13 (2012).
13. N. P. Wiederhold, *Infect. Drug Resist.*, **10**, 249 (2017).
14. N. Periyasamy, M. Srinivasan, S. Balakrishnan, *Asian Pac. J. Trop. Biomed.*, **2**, 36 (2012).
15. N. Kiran, G. Siddiqui, A. N. Khan, K. Ibrar, P. Tushar, *J. Clin. Cell. Immunol.*, **5**, 189 (2014).
16. C. Lopez-Abarrategui, A. Alba, L. Lima, S. Neto, I. Vasconcelos, J. Oliveira, S. Dias, A. Otero, O. Franco, *Curr. Microbiol.*, **64**, 501 (2012).
17. A. Kuppasamy, S. Ulagesan, *J. Appl. Pharm. Sci.*, **6**, 073 (2016).
18. S. Ulagesan, H. J. Kim, *Appl. Sci.*, **8**, 1362 (2018).
19. Y. Akkam, *Jordan J. Pharm. Sci.*, **9**, 51 (2016).
20. M. F. de Ullivarri, S. Arbulu, E. Garcia-Gutierrez, P. D. Cotter, *Front. Cell. Infect. Microbiol.*, **10**, 105 (2020).
21. W. Alcantara Santana, C. Melo, J. C. Cardoso, N. R. Pereira-Filho, A. Rabelo, F. P. Reis, de R. L. C. Albuquerque, *Int. J. Morphol.*, **30**, 365 (2012).

22. M. Suresh, S. Arularasan, N. Sri Kumaran, *Int. J. Pharm. Pharm. Sci.*, **4**, 552 (2012).
23. H. Li, M. G. Parisi, N. Parrinello, M. Cammarata, P. Roch, *ISJ*, **8**, 85 (2011).
24. M. Charlet, S. Chernysh, H. Philippe, C. Hetru, J. Hoffmann, P. Bulet, *J. Biol. Chem.*, **271**, 21808 (1996).
25. P. Dolashka-Angelova, H. Schwarz, A. Dolashki, S. Stevanovic, M. Fecker, M. Saeed, W. Voelter, *Biochim. Biophys. Acta*, **1646**, 77 (2003).
26. U. K. Laemmli, *Nature*, **227**, 680 (1970).
27. O. Fassatiová, In: *Moulds and Filamentous Fungi in Technical Microbiology*, Amsterdam Elsevier, pp. 233 (1986).
28. S. D. Sarker, L. Nahar, Y. Kumarasamy, *Methods*, **42**, 321 (2007).
29. P. Dolashka-Angelova, A. Beck, A. Dolashki, S. Stevanovic, M. Beltramini, B. Salvato, R. Hristova, L. Velkova, W. Voelter, *Micron*, **35**, 101 (2004).
30. P. Dolashka, V. Moshtanska, V. Borisova, A. Dolashki, S. Stevanovic, T. Dimanov, W. Voelter, *Peptides*, **32**, 1477 (2011).
31. S. Umayaparvathi, M. Arumugam, S. Meenakshi, T. Balasubramanian, *Asian J. Pharm. Biol. Res.*, **2**, 198 (2012).
32. G. Mitta, F. Hubert, T. Noel, P. Roch, *Eur. J. Biochem.*, **265**, 71 (2001).
33. B. Chandran, G. Rameshkumar, S. Ravichandran, *GJBB*, **4**, 88 (2009).
34. K. Benkendorff, D. Rudd, B. D. Nongmaithem, L. Liu, F. Young, V. Edwards, C. Avila, C. A. Abbott, *Mar. Drugs*, **13**, 5237 (2015).
35. A. Bano, A. A. Zarrien, *J. Zool.*, **44**, 1493 (2012).
36. N. C. J. Packia Lekshmi, S. Viveka, S. Anusha, S. Jeeva, J. Raja Brindha, M. Selva Bharath, *J. Pharm. Pharm. Sci.*, **7**, 109 (2015).
37. M. A. K Shakhathreh, M. L. Al-Smadi, O. F. Khabour, F. A. Shuaibu, E. I. Hussein, K. H. Alzoubi, *Drug Des. Devel. Ther.*, **10**, 3653 (2016).

A ¹H NMR based study of metabolites profiling of garden snail *Helix lucorum* hemolymph

N. Vassilev*, S. Simova, M. Dangelov, L. Velkova*, V. Atanassov, A. Dolashki, P. Dolashka

Institute of Organic Chemistry with Centre of Phytochemistry, Bulgarian Academy of Sciences, Acad. G. Bonchev Str. Bl. 9, 1113 Sofia, Bulgaria

Received January 19, 2021; Revised March 22, 2021

Nuclear Magnetic Resonance (NMR) was used to study the presence and functional role of the metabolites in hemolymph from land snail *Helix lucorum*. Fourteen metabolites were unambiguously identified by ¹H, 1D TOCSY, 2D J-resolved, 2D COSY, and 2D HSQC NMR spectra with water suppression. The type and concentration of metabolites in the two low molecular weight fractions (<1kD and <3kD) are very similar. Metabolites with known antioxidant, antibacterial, and antimicrobial activities have been detected by NMR metabolic analysis and tandem mass spectrometry of hemolymph samples from *H. lucorum*.

Key words: hemolymph; *Helix lucorum*; ¹H NMR; metabolites

INTRODUCTION

In recent years, the study of bioactive substances from invertebrates is extremely relevant, as it may lead to the discovery of new therapeutic agents. The mucus and hemolymph of mollusc contain an abundance of hemocytes and humoral factors which represent the first line of immune defense [1]. Various bioactive components, such as peptides and proteins with antimicrobial activity, dissolved in the hemolymph and mucus of garden snails can find application in medicine [2-9].

Molluscan hemolymph is a unique kind of body fluid which is a complex mixture that contains diverse biochemically and pharmacologically active components and in many respects is analogous to human blood, although there are several crucial differences [10]. The object of the present study is metabolites from the hemolymph of garden snails *H. lucorum*. The main protein in the hemolymph of *H. lucorum*, as well as other Mollusca organisms, is hemocyanin (over 90%) [11]. Molluscan hemocyanins are giant extracellular oxygen carriers in the hemolymph with different complex quaternary structure, usually with molecular weights between 4 and 9 MDa [12]. Hemocyanins from *H. lucorum* and *H. aspersa* have promising potential for the development of novel antitumor, antibacterial, and immunotherapeutic agents [11-15]. Moreover, several peptides with antimicrobial activity and molecular masses below 10 kDa have been identified and characterized from the

hemolymph of *H. lucorum* snail [16].

Recently, the antioxidant capacity of different fractions from the hemolymph of *H. lucorum* snail was evaluated [17]. The complex antioxidant effect of *H. lucorum* hemolymph with MW < 100 kDa is thought to be related to the presence of both antioxidant enzymes and peptides (with MW < 1 kDa) [17].

In the last years, the metabolic profiles of the hemolymph from *Mytilus galloprovincialis* and two mucus fractions of *H. aspersa*, as well as metabolic profiles of isolated organs in the snail *H. aspersa* maxima (kidney, heart, digestive gland, and pulmonary membrane) were determined using ¹H NMR spectroscopy [18-20]. However, the presence and functional role of serum metabolites have been insufficiently studied. The present study is the first report of low molecular weight metabolites identified in the hemolymph of garden snail by NMR spectroscopy. Knowledge of the active ingredients and their action in the hemolymph of *H. lucorum* is valuable for their potential application in food supplements and/or pharmacy.

EXPERIMENTAL

Hemolymph collection and preparation of different fractions

The hemolymph was extracted from the foot of garden snail *H. lucorum* in 50 mM Tris-HCl buffer, pH 7.5. After homogenization, filtration, and centrifugation at 10000 rpm at 4 °C for 30 min to remove rough particles and haemocytes, the crude

* To whom all correspondence should be sent:

E-mails: Nikolay.Vassilev@orgchm.bas.bg

Ljudmila.Velkova@orgchm.bas.bg

hemolymph extract was obtained. It was separated into two base fractions by ultrafiltration on membranes 10 kDa (Millipore™ Ultrafiltration Membrane Filters, Regenerated cellulose): below 10 kDa and above 10 kDa. The fraction below 10 kDa was subject to an additional separation in two fractions with low molecule masses – below 1 kDa and below 3 kDa, using the same method but using membranes with a different pore size (1 and 3 kDa Millipore™ Ultrafiltration Membrane Filters, Regenerated cellulose). Fractions from the hemolymph of *H. lucorum* containing compounds with molecule masses below 1 kDa and below 3 kDa were concentrated by lyophilized. The dried fractions were analyzed by NMR spectroscopy to determine the metabolic profile.

^1H NMR spectroscopy

The recently developed protocol for the determination and assignment of metabolites in mucus from *H. aspersa* by NMR spectroscopy [19] was adopted to study the low molecular weight fractions of hemolymph from *H. lucorum* (<1kD and <3kD). Details of the NMR spectroscopy experiments are presented in the Supp. info.

Assignment of metabolites and database search

After processing with Bruker TOPSPIN 3.5 program the 1D ^1H NMR spectra were analysed preliminary with Bayesil web system [21]. The assignment of the metabolite resonances was then manually checked and refined by comparison between experimental 1D NMR spectra and spectra of single metabolites downloaded from "BioMagResBank" [22]. In the case of overlapped multiples (Figure S2) JRES spectra with water suppression were very useful in the assignment of resonances. For identification of metabolites with close resonances or in cases of overlap of several multiplets 1D selective TOCSY experiments were used (Figure S3). For several samples, simultaneous suppression of the signals of water, Tris, and Acetic acid was utilized using the 3 channels of the spectrometer. In Figure S4 a typical ^1H 1D NOESY NMR spectrum of lyophilized hemolymph from *H. lucorum* (< 1kD) is presented.

RESULTS AND DISCUSSION

The crude hemolymph extract was collected from the foot of garden snail *H. lucorum* and three fractions were prepared: fraction containing compounds with molecular masses (Mw) below 10

kDa, a fraction containing compounds with Mw below 3 kDa, and a fraction containing compounds with Mw below 1 kDa. After lyophilization and concentration, the two low Mw fractions were analyzed by NMR spectroscopy to determine the metabolic profile.

*^1H NMR of hemolymph from *H. lucorum* and identification of the main metabolites*

Nuclear magnetic resonance (NMR) in combination with mass spectrometry was found to be an analytical approach suitable for metabolic profiling of garden snail mucus samples [19]. ^1H NMR spectra of hemolymph from *H. lucorum* (< 1kD or < 3kD) are presented in Fig. 1 and S1.

The spectra are dominated by the sharp resonances of low molecular weight metabolites in the aliphatic region between 4.5 and 0.5 ppm; while, the aromatic region is almost devoid of signals, or contains very low intensity ones. Overall, 1D-NMR spectra showed very good chemical shift reproducibility due to the addition of a concentrated phosphate buffer to the sample. The metabolic stability was assessed in preliminary experiments, where noesy1d NMR spectra of the freshly prepared sample of lyophilized hemolymph from *H. lucorum* (< 3kD) were analyzed immediately and after 24 h (sample kept at 298 K). It was found that there is not any visible change in the spectra and there are not any ongoing biochemical processes.

Five metabolites were unambiguously identified by signals in the HSQC (Table 1). The presence of these metabolites was confirmed by analysis of the COSY spectrum, as well. Nine additional metabolites were unambiguously identified during inspection and database-matching of the 1D-spectra. In addition, a number of resonances remain unassigned or ambiguously assigned, so they are not included in Table 1. The metabolites having the highest concentration in hemolymph were osmolytes (betaine and glycine) and nutrients (glucose and amino acids such as alanine). In addition to the resonances of assigned metabolites, several others could not be unambiguously assigned. In general, the resonances of unassigned species have low signal intensities.

Metabolic pathway and activity

The detected metabolites in hemolymph from *H. lucorum* are known to take part in various metabolic pathways in humans, mammals, and

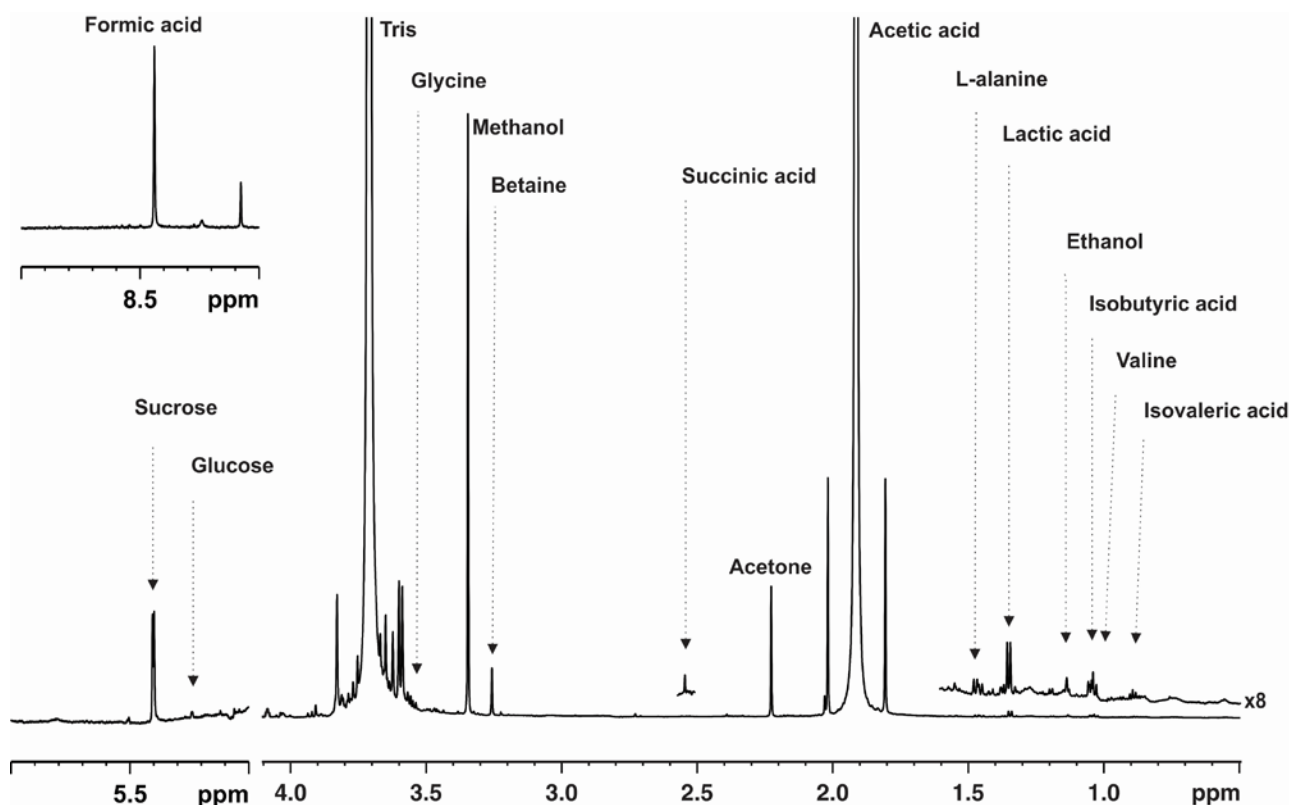


Fig. 1. ^1H -NMR spectrum of lyophilized hemolymph from *H. lucorum* (< 1 kD). 1D-noesy pulse sequence, with pre-irradiation of water, pH=7.35, 298.0 K), with resonance assignment. The spectral regions devoid of signals, that contain the residual water signal and that of reference TSP have been cut away.

Table 1. List of the metabolites identified by NMR in lyophilized hemolymph from *H. lucorum*, reported as the average from 5 controls.

Metabolite	Mass	^{13}C Chemical Shift ^{a,b}	^1H Chemical Shifts (Multiplicity, Coupling Constants) ^{a,c}	Concentrations (<1kD) Sample (mM)	Concentrations (< 3kD) Sample (mM)
Acetic acid	60.05	23.45	1.92(s)	374.74	311.80
L-alanine	89.09		1.49(d, J=7.2)	0.21	0.11
Betaine	117.15	53.31	3.27(s)	0.16	0.14
Ethanol	46.07	62.80	3.67(q, J=7.1), 1.19(t, J=7.1)	0.20	0.22
Formic acid/formate	46.03		8.46(s)	1.20	1.41
Glycerol	92.09		3.55(dd), 3.64(dd)	7.53	0.09
Glycine	75.07	62.73	3.56(s)	0.33	
Glucose	180.16		5.22(d)	0.67	
Isobutyric acid	88.11		1.05(d, J=7.2)	0.14	0.08
Isovaleric acid	102.13		0.90(d, J=6.5), 1.95(m), 2.04(d, J=7.4)	0.01	0.06
Lactic acid	90.08	20.23	4.12(q, J=7.0), 1.33(d, J=7.0)	0.59	0.45
Succinic Acid	118.09		2.40(s)	0.18	0.15
Sucrose	342.30		5.41(d, J=3.9), 4.22(d), 4.06(t), 3.48(t)	0.97	0.47
Valine	117.15		0.99(d, J=7.0), 1.02(d, J=7.0), 3.57(dt)	0.04	
TSP			-0.0159	0.186	0.186

^a ^1H chemical shifts (in ppm) are referenced to 0.186 mM TSP at -0.0159 ppm [23]. ^b Determined from HSQC (in ppm). ^c Only chemical shifts of easily distinguished signals in the ^1H -NMR spectra are reported. Chemical shifts that are not detectable and/or not distinguishable in either 1D or 2D NMR spectra are not provided.

plants. The available literature data will be discussed here in conjunction with the detected concentrations of these metabolites (Table 1).

Among the detected metabolites, the concentration of acetic acid was the highest one in the ^1H -NMR metabolic profile of hemolymph from

H. lucorum. This high concentration of acetic acid is not a surprise: it is produced by Gram-negative bacilli and Gram-positive cocci [24] and it is found in *Akkermansia*, *Bacteroidetes*, *Bifidobacterium*, *Prevotella*, and *Ruminococcus* [24, 25]. The concentration of other microbial metabolites, such as formic acid, lactic acid, and succinic acid, is moderate. In tissue extracts of many invertebrate species, including *A. subfuscus* and *H. aspersa*, the presence of lactate as a metabolite has been found [20, 26]. In mollusks, succinic acid is the major end product, while lactic acid is a minor product of anaerobic glycolysis. Lactate is an important end product in terrestrial and freshwater gastropods but not in marine species [27].

The concentration of betaine is also moderate. Betaine is known to function as a methyl donor and to facilitate the necessary chemical processes. Its origin is either from food or from oxidation of choline. Betaine insufficiency is associated with metabolic syndrome, lipid disorders and diabetes, and may have a role in vascular and other diseases [28]. Cytosine as a pyrimidine base is a major building block of nucleic acids. Cytosine is unstable and could be converted to uracil by spontaneous deamination. Not surprisingly, the nucleotide of cytosine is the prime mutagenic nucleotide in leukemia and cancer [29].

In the tested hemolymph fractions, only three amino acids (alanine, glycine, and valine) were found at relatively low concentrations. As a non-essential amino acid alanine is produced in the body from either the conversion of the carbohydrate pyruvate or the breakdown of DNA and the dipeptides carnosine and anserine. It is one of the most important amino acids released by muscle, functioning as a major energy source. It also participates in the metabolism of sugars and organic acids and improves the immune system through its contribution to the formation of antibodies. Glycine controls the release of oxygen during cell formation and strengthens the immune system. Glycine takes part in the production of DNA, phospholipids, and collagen, and in the release of energy in the body [30]. The detected valine along with leucine and isoleucine are essential amino acids. Therefore, valine must be ingested, usually as a component of proteins [29].

Recently, various amino acids (glycine, valine, lysine, threonine, asparagine, tyrosine, and histidine) were detected in hemolymph serum of *M. galloprovincialis* by ¹H NMR spectroscopy [18]. Contamination with Cu²⁺ leads to increased levels of glucose and amino acids, including lysine,

threonine, serine, glutamine, and alanine [18]. A number of free amino acids (for example, Ala, Arg, Glu, Gly, Leu, and Ile), including taurine, have been found previously in various marine mollusks and gastropods [31]. Free taurine, betaine, and glycine seem to be present as metabolites in all marine invertebrates. The concentrations of the following metabolites are also moderate: ethanol, glucose, and sucrose. Ethanol is also found as a metabolite in hemolymph serum from the marine mollusk *M. galloprovincialis* [18] as well as in other invertebrates *Lumbricus rubellus* (Hoffmeister) and *Eisenia andrei* (Savigny) [26]. Ethanol is metabolized in the body to acetyl CoA, an intermediate in glucose metabolism that can be used for energy in the citric acid cycle or biosynthesis [29]. The identified metabolite glucose is a major source of energy for living organisms. The carbohydrate metabolism of gastropods includes D-glucose as the most common monosaccharide, identified in the hemolymph and tissues of many gastropods. Renwranz et al. detected in hemolymph filtrates of the snail *Helix pomatia* the presence of glucose, galactose, fucose, and mannose [32, 33]. Glycogen and galactogen are the main storage polysaccharides. The presence of sucrose is detected in the hemolymph of snail *Littorina littorea* and *H. aspersa* mucus [19, 33].

In mollusc, classical vertebrate metabolic pathways such as glycolysis, Krebs cycle, and the respiratory chain have also been described [34]. In living organisms, succinic acid is known to be in the form of an anion, succinate, which has many biological roles as a metabolic intermediate. Succinate is known as an intermediate in the Krebs cycle, described in both vertebrates and molluscs [34]. The increase of this metabolite may be due to a decrease in Krebs cycle activity. Succinate is also the end product of the glucose-succinate and aspartate-succinate pathways, which assume anaerobic metabolism in invertebrates and may be associated with the lactate pathway described in molluscs, like the blue mussel *Mytilus edulis* [35].

The ¹H NMR detected concentration of glycerol in hemolymph from *H. lucorum* is relatively high in the lyophilized sample (<1 kDa). Glycerol and fatty acids are the basis of the structure of fats. Glycerol can be transformed into glucose, thus providing energy for cellular metabolism [29].

Metabolites with antibacterial activity

Metabolites with known antibacterial activity (acetic, citric, lactic, tartaric, isovaleric acids, and

glycerol) have been recently detected by NMR metabolic analysis of mucus samples from *H. aspersa* [19], which encouraged us to look for metabolites with the same effect in hemolymph from *H. lucorum*.

Some of the detected metabolites such as acetic acid, citric acid, lactic acid, and tartaric acid exhibit inhibitory effect against *Salmonella typhimurium* [36]. Moreover, it is found that 0.5% lactic acid could completely inhibit the growth of various bacteria as *Salmonella enteritidis*, *Escherichia coli*, and *Listeria monocytogenes* [37]. The results suggested that the antimicrobial effect is due to physiological and morphological changes in bacterial cells caused by treatment with lactic acid [37]. A study [38] has proved that low concentrations of acetic acid, act as a local antiseptic agent in problematic infections caused by organisms, such as *Proteus vulgaris*, *Acinetobacter baumannii*, or *Pseudomonas aeruginosa*. Additionally, it was found that pyruvic or succinic acid provides an effective reduction of Salmonella, after treatment of chicken meat [39]. Recently antimicrobial effects of glycerol monolaurate (monolaurin), ethanol, and lactic acid have been determined, either alone or in combination, against *L. monocytogenes* as well as their minimal inhibitory concentrations [40].

Antifungal metabolic activity of betaine derivatives

In a previous study [19], it was established the mucus fraction from *H. aspersa* below 1 kDa and below 3 kDa contained metabolites with known antifungal activity (alpha-ketoisocaproic acid, betaine derivatives, and choline) which encouraged us to look for metabolites with similar effect in hemolymph from *H. lucorum*. It is known that marine gastropods possess high levels of organic osmolytes (e.g. betaine, taurine, and trehalose), but data is scarce for terrestrial snails. Our results showed that betaine is present in fractions below 1 kDa and below 3 kDa from the hemolymph of *H. lucorum* as well as in the mucus from *H. aspersa*. Betaine is not only important for maintaining the osmotic balance in cells but its derivatives showed also antimicrobial potential. In a study [20], it was demonstrated the antifungal activity and mechanism of action of a betaine derivative. It established that lauryl betaine influences ergosterol synthesis in *Cryptococcus neoformans* and *Malassezia restricta* (considered an opportunistic pathogen associated with skin disorders such as seborrheic dermatitis and dandruff).

Antioxidant metabolic activity

The antioxidant capacity of *H. lucorum* hemolymph was recently assessed [17]. The complex antioxidant effect of hemolymph from *H. lucorum* is thought to be related to the presence of low molecular weight peptides in the MW<1 kDa fraction and mainly to the antioxidant enzymes in the MW<100 kDa fraction. The experimental results showed that the fraction with MW<1 kDa of *H. lucorum* hemolymph manifested $\text{O}_2^{\cdot-}$ -scavenger effect (about 42% inhibition of NBT reduction at the concentration 24.99 $\mu\text{g/mL}$) and chelating potential (about 33% inhibitory effect at concentration 90 $\mu\text{g/mL}$ and 130 $\mu\text{g/mL}$). The fraction, containing compounds with MW below 1 kDa, was analyzed using COMPACT UHPLC-QqTOF Systems (Bruker Daltonics, Germany) in positive ion mode detection, by MS- and MS/MS-experiments [17]. The results from MALDI-MS analysis showed that fraction with MW below 1 kDa from the hemolymph of *H. lucorum* contained a variety of peptides, present primarily as doubly charged ions $[\text{M}+2\text{H}]^{2+}$ [17]. The molecular structure characteristics (MW, amino acid composition, amino acid sequence and molecular conformation) and hydrophobicity of the peptides are considered to be closely related to their antioxidant activity [41]. Peptides with lower MW can interact with radicals more effectively, and it is easier to exert antioxidant capacity through the intestinal barrier in vivo [42]. Table 2 illustrates primary structures of peptides in fraction below 1 kDa identified by *de novo* sequencing (MALDI-MS/MS experiment) and some other characteristics from ExPASy ProtParam tool [17]. The obtained results showed that the identified peptide structures are characterized with short chains, containing from 7 to 10 amino acid residues, with molecular masses between 757.41 Da - 1079.44 Da, mostly with hydrophobic surface and amphipathic structures. It is known, that peptides with a high content of hydrophobic amino acids show a better radical scavenger effect than those with a higher content of hydrophilic amino acids [41]. This fact is recently experimentally confirmed with the results of Alexandrova et al. for the antioxidant activity of a fraction below 1kDa [17]. The peptides presented in Table 2 are associated with the demonstrated antioxidant activity of the fraction below 1 kDa unlike the peptides from *H. aspersa* mucus with antimicrobial activity [7, 19]. Amino acid residues such as Tyr, Met, His, Lys, Trp, and Cys are often present in polypeptides with strong antioxidant

Table 2. Peptides from the fraction with MW below 1 kDa of hemolymph from garden snail *H. lucorum*, identified by *de novo* sequencing on the COMPACT UHPLC-QqTOF Systems (Bruker Daltonics, GmbH), published in [17].

N ^o	Amino acid sequence of peptides	Measured mass (Da)	Calculated mass (monoisotopic) (Da)	pI	Grand average of hydrophobicity (GRAVY)
1	γ- ECG (glutathione)	308.05 [M+H] ⁺	307.08	4.00	
2	VVLKAKGK	319.22 [M+3H] ³⁺	954.66	10.30	0.711 (hydrophobic)
3	GIPLEMV	379.70 [M+2H] ²⁺	757.41	4.00	1.271 (hydrophobic)
4	SSPPFVM	382.68 [M+2H] ²⁺	763.36	5.24	0.586 (hydrophobic)
5	KVAPYPQ	401.72 [M+2H] ²⁺	801.44	8.59	-0.843 (hydrophilic)
6	VVMKELS	403.22 [M+2H] ²⁺	804.44	5.97	0.843 (hydrophobic)
7	GPLKIPLL	425.79 [M+2H] ²⁺	849.57	8.75	1.050 (hydrophobic)
8	AEPKIGKI	428.26 [M+2H] ²⁺	854.52	8.64	-0.312 (hydrophilic)
9	LAVSKLLY	453.78 [M+2H] ²⁺	905.56	8.59	1.425 (hydrophobic)
10	KWFKFGN	463.74 [M+2H] ²⁺	925.48	10.00	-1.000 (hydrophilic)
11	VSEGMIVSI	467.74 [M+2H] ²⁺	933.49	4.00	1.533 (hydrophobic)
12	GTLSSLLNF	476.26 [M+2H] ²⁺	950.51	5.52	0.889 (hydrophobic)
13	FLGDSTNLI	490.25 [M+2H] ²⁺	978.51	3.80	0.667 (hydrophobic)
14	AFQLm*KQV	490.76 [M+2H] ²⁺	979.52	8.80	0.450 (hydrophobic)
15	EIKLSDQY	498.25 [M+2H] ²⁺	994.50	4.37	-1.025 (hydrophilic)
16	ALSAWNAHE	499.73 [M+2H] ²⁺	997.46	5.24	-0.300 (hydrophilic)
17	HGMPLDLLD	505.75 [M+2H] ²⁺	1009.49	4.20	0.122 (hydrophobic)
18	STENDPSSML	540.72 [M+2H] ²⁺	1079.44	3.67	-0.950 (hydrophilic)

activity. The imidazole group of His is related to its metal chelation, hydrogen supply and lipid peroxidation capabilities [43]. Cysteine containing thiol can directly interact with radicals and has an important contribution to the antioxidant activity of peptides. Therefore, the presented peptide structures showed various amino acid residues, but mostly Val, Leu/Ile, Pro, Lys, Phe, Met, His, Trp, and Tyr (Table 2). We hypothesize that hydrophobic amino acids (Leu/Ile, Val, Met, Phe and Pro), aromatic amino acids (Trp, Phe and Tyr), as well as Lys and His contribute to the antioxidant activity established in the recent study of Alexandrova et al. [17]. Amino acid sequences of detected peptides in hemolymph fraction below 1 kDa from garden snail *H. lucorum* are rather different from the identified peptides in *H. aspersa* mucus [3, 7, 19]. In addition, the MALDI-MS analysis revealed tripeptide glutathione (GSH), detected as [M+H]⁺ at m/z 308.046 Da. Glutathione also is identified in mucus fraction below 1 kDa from *H. aspersa* snails [19] and in hemolymph serum of mussels *M. galloprovincialis* [18]. GSH is the major endogenous intracellular antioxidant that

is able to protect cell structures from oxidative damage by reacting directly with the reactive oxygen species and acts as a co-substrate of the antioxidant enzyme glutathione peroxidase [44].

Recently, *in vitro* tests established the antioxidant potential of lactate ions at different concentrations [45]. The results showed that lactate ion could prevent lipid peroxidation by neutralizing free radicals, such as O²⁻ and OH, but not lipid radicals. Therefore, lactate ion might be considered as a potential antioxidant agent.

Other compounds with antioxidant metabolic activity are some detected Krebs cycle intermediates, which act as energy substrates in mitochondria and manifest antioxidant neuroprotective effects on the brain, in neuronal cells, against oxidative stress [46]. It was found that pyruvate, oxaloacetate, and α-ketoglutarate, preserve HT22 cells from hydrogen peroxide-mediated toxicity. Because these intermediates did not have any toxic effects (at least up to 10 mM), they can be used in the treatment of chronic neurodegenerative diseases.

CONCLUSION

A protocol for the determination of metabolites in hemolymph from *H. lucorum* by NMR spectroscopy has been developed. The metabolic profiles of the two low molecular weight fractions (<1kD and <3kD) as well as the concentration of metabolites are very similar. A number of metabolites with known antioxidant, antibacterial, and antimicrobial activities have been detected by NMR metabolic analysis and tandem mass spectrometry of hemolymph samples from *H. lucorum*.

Acknowledgements: This research was funded by the Bulgarian Ministry of Education and Science through the National Scientific Program “Innovative Low-Toxic Biologically Active Means for Precision Medicine” BioActiveMed, grant number DOI-217/30.11.2018, by the Project VS.076.18N (FWO) and by the Bulgarian Science Fund (Grant KP-06-OPR 03-10/2018).

Electronic Supplementary Data available [here](#).

REFERENCES

1. B. Allam, D. Raftos, *J. Invertebr. Pathol.*, **131**, 121 (2015).
2. D. Bortolotti, C. Trapella, T. Bernardi, R. Rizzo, *Br. J. Biomed.*, **73**, 49 (2016).
3. P. Dolashka, A. Dolashki, L. Velkova, S. Stevanovic, L. Molin, P. Traldi, R. Velikova, W. Voelter, *J. BioSci. Biotechnol., SE/ONLINE*, 47 (2015).
4. L. Velkova, A. Nissimova, A. Dolashki, E. Daskalova, P. D. Y. Topalova, *Bulg. Chem. Commun.*, **50**, 169 (2018).
5. A. Dolashki, A. Nissimova, E. Daskalova, L. Velkova, Y. Topalova, P. Hristova, P. Traldi, W. Voelter, P. Dolashka, *Bulg. Chem. Commun.*, **50**, 195 (2018).
6. N. Kostadinova, Y. Voynikov, A. Dolashki, E. Krumova, R. Abrashev, D. Kowalewski, S. Stevanovic, L. Velkova, R. Velikova, P. Dolashka, *Bulg. Chem. Commun.*, **50**, 176 (2018).
7. A. Dolashki, L. Velkova, E. Daskalova, N. N. Zheleva, Y. Topalova, V. Atanasov, W. Voelter, P. Dolashka, *Biomedicines*, **8**, 315 (2020).
8. C. Trapella, R. Rizzo, S. Gallo, A. Alogna, D. Bortolotti, F. Casciano, G. Zauli, P. Secchiero, R. Voltan, *Sci. Rep.*, **8**, 17665 (2018).
9. V. Gentili, D. Bortolotti, M. Benedusi, A. Alogna, A. Fantinati, A. Guiotto, G. Turrin, C. Cervellati, C. Trapella, R. Rizzo, G. Valacchi, *PLOS ONE*, **15**, e0229613 (2020).
10. T. Machałowski, T. Jesionowski, *Appl. Phys. A*, **127**, 3 (2020).
11. A. Georgieva, K. Todorova, I. Iliev, V. Dilcheva, I. Vladov, S. Petkova, R. Toshkova, L. Velkova, A. Dolashki, P. Dolashka, *Biomedicines*, **8**, 194 (2020).
12. P. Dolashka-Angelova, T. Stefanova, E. Livaniou, L. Velkova, P. Klimentzou, S. Stevanovic, B. Salvato, H. Neychev, W. Voelter, *Immunol. Invest.*, **37**, 822 (2008).
13. A. Dolashki, P. Dolashka, A. Stenzl, S. Stevanovic, W. K. Aicher, L. Velkova, R. Velikova, W. Voelter, *Biotechnol. Biotechnol. Equip.*, **33**, 20 (2019).
14. A. Stenzl, A. Dolashki, S. Stevanovic, W. Voelter, W. Aicher, P. Dolashka, *Journal of US-China Medical Science*, **13**, 179 (2016).
15. P. Dolashka, A. Dolashki, J. Van Beeumen, M. Floetenmeyer, L. Velkova, S. Stevanovic, W. Voelter, *Curr. Pharm. Biotechnol.*, **17**, 263 (2016).
16. P. Dolashka, A. Dolashki, W. Voelter, J. Van Beeumen, S. Stevanovic, *Int. J. Curr. Microbiol. Appl. Sci.*, **4**, 1061 (2015).
17. A. Alexandrova, L. Petrov, L. Velkova, A. Dolashki, E. Tsvetanova, A. Georgieva, P. Dolashka, *J. Pharm. Pharmacogn. Res.*, **9**, 143 (2021).
18. G. Digilio, S. Sforzini, C. Cassino, E. Robotti, C. Oliveri, E. Marengo, D. Musso, D. Osella, A. Viarengo, *Comp. Biochem. Physiol. C Toxicol. Pharmacol.*, **183-184**, 61 (2016).
19. N. G. Vassilev, S. D. Simova, M. Dangelov, L. Velkova, V. Atanasov, A. Dolashki, P. Dolashka, *Metabolites*, **10**, 360 (2020).
20. D. Aude, B. Marion, C. Raphaël, J.-M. Colet, *Ecol. Indic.*, **105**, 177 (2019).
21. S. Ravanbakhsh, P. Liu, T. C. Bjordahl, R. Mandal, J. R. Grant, M. Wilson, R. Eisner, I. Sinelnikov, X. Hu, C. Luchinat, R. Greiner, D. S. Wishart, *PLOS ONE*, **10**, e0124219 (2015).
22. E. L. Ulrich, H. Akutsu, J. F. Doreleijers, Y. Harano, Y. E. Ioannidis, J. Lin, M. Livny, S. Mading, D. Maziuk, Z. Miller, E. Nakatani, C. F. Schulte, D. E. Tolmie, R. Kent Wenger, H. Yao, J. L. Markley, *Nucleic Acids Res.*, **36**, D402 (2008).
23. S. Kostidis, R. D. Addie, H. Morreau, O. A. Mayboroda, M. Giera, *Anal. Chim. Acta*, **980**, 1 (2017).
24. A. Gupta, M. Dwivedi, A. A. Mahdi, C. L. Khetrapal, M. Bhandari, *J. Proteome Res.*, **11**, 1844 (2012).
25. F. E. Rey, J. J. Faith, J. Bain, M. J. Muehlbauer, R. D. Stevens, C. B. Newgard, J. I. Gordon, *J. Biol. Chem.*, **285**, 22082 (2010).
26. J. O. T. Gibb, E. Holmes, J. K. Nicholson, J. M. Weeks, *Comp. Biochem. Physiol. B, Biochem. Mol. Biol.*, **118**, 587 (1997).
27. G. Cimino, G. Sodano, in: P.J. Scheuer (Ed.) *Marine Natural Products — Diversity and Biosynthesis*, Springer Berlin Heidelberg, Berlin, Heidelberg, 1993, pp. 77.
28. M. Lever, S. Slow, *Clin. Biochem.*, **43**, 732 (2010).
29. D. S. Wishart, Y. D. Feunang, A. Marcu, A. C. Guo, K. Liang, R. Vázquez-Fresno, T. Sajed, D. Johnson,

- C. Li, N. Karu, Z. Sayeeda, E. Lo, N. Assempour, M. Berjanskii, S. Singhal, D. Arndt, Y. Liang, H. Badran, J. Grant, A. Serra-Cayuela, Y. Liu, R. Mandal, V. Neveu, A. Pon, C. Knox, M. Wilson, C. Manach, A. Scalbert, *Nucleic Acids Res.*, **46**, D608 (2017).
30. W. Wang, Z. Wu, Z. Dai, Y. Yang, J. Wang, G. Wu, *Amino Acids*, **45**, 463 (2013).
31. R. S. Norton, *Comp. Biochem. Physiol. B, Comp. Biochem.*, **63**, 67 (1979).
32. L. Renwranz, W. Glöckner, K. E. Mitterer, G. Uhlenbruck, *J. Comp. Physiol.*, **105**, 185 (1976).
33. D. R. Livingstone, A. De Zwaan, 5 - Carbohydrate Metabolism of Gastropods, in: P.W. Hochachka (Ed.) *Metabolic Biochemistry and Molecular Biomechanics*, Academic Press, 1983, pp. 177.
34. H. Bacca, PhD Thesis, Université de Rennes, Rennes, France, 2007.
35. D. R. Livingstone, *J. Geolog. Soc. London*, **140**, 27 (1983).
36. A. El Baaboua, M. El Maadoudi, A. Bouyahya, O. Belmehdi, A. Kounoun, R. Zahli, J. Abrini, *Int. J. Microbiol.*, **2018**, 7352593 (2018).
37. C. Wang, T. Chang, H. Yang, M. Cui, *Food Control*, **47**, 231 (2015).
38. H. Ryssel, O. Kloeters, G. Germann, T. Schäfer, G. Wiedemann, M. Oehlbauer, *Burns*, **35**, 695 (2009).
39. A. Purohit, A. Mohan, *LWT*, **116**, 108596 (2019).
40. D.-H. Oh, D. L. Marshall, *Int. J. Food Microbiol.*, **20**, 239 (1993).
41. T.-B. Zou, T.-P. He, H.-B. Li, H.-W. Tang, E.-Q. Xia, *Molecules*, **21**, 72 (2016).
42. B. H. Sarmadi, A. Ismail, *Peptides*, **31**, 1949 (2010).
43. A. C. Freitas, J. C. Andrade, F. M. Silva, T. A. P. Rocha-Santos, A. C. Duarte, A. M. Gomes, *Curr. Med. Chem.*, **20**, 4575 (2013).
44. B. Halliwell, J. M. C. Gutteridge, *Free Radicals in Biology and Medicine*, 5 ed., Oxford University Press, Oxford, 2015.
45. C. Groussard, I. Morel, M. Chevanne, M. Monnier, J. Cillard, A. Delamarche, *J. Appl. Physiol.*, **89**, 169 (2000).
46. K. Sawa, T. Uematsu, Y. Korenaga, R. Hirasawa, M. Kikuchi, K. Murata, J. Zhang, X. Gai, K. Sakamoto, T. Koyama, T. Satoh, *Antioxidants*, **6**, 21 (2017).

Adaptation of activated sludge to treatment of landfill leachate during model process

A. Chobanova¹, M. Belouhova^{1,2}, I. Yotinov^{1,2*}, N. Dinova^{1,2}, E. Daskalova¹, Y. Todorova^{1,2}, S. Lincheva³, I. Schneider^{1,2}, Y. Topalova^{1,2}

¹ Sofia University “St. Kliment Ohridski”, Faculty of Biology, Sofia, Bulgaria

² Center of competence “Clean technologies for sustainable environment – water, waste, energy for circular economy”, Bulgaria

³ Municipal enterprise for waste treatment of Sofia City, Bulgaria

Received January 30, 2021; Revised March 19, 2021

Landfill leachate is generated from the waste degradation in landfill sites and rainwater infiltrates. Its treatment includes more often biological methods combined with physical and chemical methods. The availability of polycyclic aromatic carbohydrates, phenols, polychlorinated phenols, pesticides, heavy metals, and refractory organics in landfill leachate remains a critical technological problem during biological treatment. The effect of these toxic pollutants on activated sludge (AS) processes is related to deformations of AS structure /bulking or pin-point flocs/ and inhibition of biodegradation activity. One of the most economic and effective possibilities for problem solving is application of adaptation as a biological approach. The aim of the study is to assess the activated sludge from wastewater treatment plant to Municipal enterprise for waste treatment of Sofia City during model adaptation process with landfill leachate. The duration of adaptation process was 21 days. The results confirm that the leachate diluted 25X contains toxic xenobiotics, which concentration is close to the critical one for the development of adaptive potential of AS in the concrete experimental conditions. This dilution of the leachate and the ratio COD:BOD₅ are appropriate for accomplishment of wastewater treatment process.

Key words: landfill leachate; activated sludge; adaptation; biodegradation activity

INTRODUCTION

The enacted Directive 1999/31/EC aims a decrease in the consumption of natural resources and raw materials and a bigger decrease of the quantity of landfilled waste as in 2018 in Europe were generated 2317 million tons of waste [1]. It has been registered that for a year one landfill for non-hazardous waste in the early to the middle phase of its exploitation generates between 10000 and 20000 m³ of leachate [2]. Its quantitative and qualitative composition is defined also by the quantity of the rainfalls and the snowmelt as well as by the type of the landfilled waste. The leachate from the landfills for non-hazardous waste might contain high concentrations of xenobiotics such as aromatic hydrocarbons, pesticides and heavy metals such as cadmium, copper, chrome, lead, nickel, zinc [2, 3]. In Table 1 are represented some of the pollutants in the leachate as well as their concentrations.

In these cases, the leachate is characterized with a high toxicity. Different approaches for treatment of the leachate from non-hazardous waste landfills exist. Main significance for the choice of the approach to be implemented have the parameters

BOD₅, COD, nitrogen and halogen organic compounds. Often the equipment for the leachate treatment is designed in a combination to the conventional treatment systems [4]. For example, the landfill for non-hazardous waste of Sofia City, part of Municipal enterprise for waste treatment, on the “Sadinata” site works on the principle of a biological co-treatment of domestic wastewater and leachate.

The biological treatment of a leachate with xenobiotics has environmental risks that are related to the ineffective removal of the toxic compounds [5, 6]. They are related to a deformation of the structure of the activated sludge (AS) and an inhibition of the biodegrading and biotransforming processes [7]. The most common deformations in the AS structure are related to the formation of pin-point flocs or to a filamentous or non-filamentous bulking [8-10]. It is registered that the presence of xenobiotics leads to a restructuring of the communities of the microorganisms and the fauna in the AS [9, 10]. For example, in the bacterial complex start to dominate the representatives of the genera *Pseudomonas* and *Acinetobacter* [10-12], and in the complexes of the micro- and metafauna is registered a reduction of the attached and crawling ciliates and an increase of the part of the flagellates and the free-swimming ciliates [9, 10,

* To whom all correspondence should be sent:

E-mail: yotinov@yahoo.com

13]. On a functional level the AS reacts with an increase of the activities of key for the biodegradation enzymes such as the catechol-1,2-dioxygenase, catechol-2,3-dioxygenase, protocatechuate-3,4-dioxygenase and others [10].

Table 1. Concentrations of some pollutants in a landfill leachate [2,3].

Indicator	Concentration
BOD ₅ /biochemical oxygen demand/	2000-68000 mgO ₂ /L
COD /chemical oxygen demand/	2700-152000 mgO ₂ /L
TN /total nitrogen/	225 mg/L
TP /total phosphorus/	30 mg/L
Ca	270 6240 mg/L
Mg	1.4-164 mg/L
Na	474-2400 mg/L
K	350-3100 mg/L
Fe	48-2300 mg/L
Cl ⁻	659-4670 mg/L
SO ₄ ²⁻	5-1560 mg/L
Ni	0.03-1.87 mg/L
Cu	0.02-1.10 mg/L
Zn	0.09-140 mg/L
Cd	0.01-0.1 mg/L
Pb	0.04-0.65 mg/L
As	0.001-0.148 mg/L
Hg	0.0001-0.0015 mg/L
Polychlorinated biphenyls (PCB)	below 0.0007 mg/L
Dioxins	below 0.32 mg/L
Benzene	0.2-1630 µg/L
Toluene	1-12300 µg/L
Xylene	0.8-3500 µg/L
Ethylbenzene	0.2-2329 µg/L
Naphthalene	0.1-260 µg/L
Chlorobenzene	0.1-110 µg/L
1,1,1-trichloroethane	0.1-3810 µg/L
Trichloroethylene	0.5-750 µg/L
Phenol	0.6-1200 µg/L
Cresols	1-2100 µg/L

The activated sludge possesses a huge potential for biodegradation of pollutants based on a complex microbial consortium [14, 15]. The mechanism changing the structure and the function of the biological system is called an adaptation and the flexibility of the biological system depends on it [16]. That is why the adaptation of the AS is one of the possible solutions in the presence of biological treatment in the landfills for non-hazardous waste. One of the main factors for an effective adaptation of the microorganisms in the AS is the concentration of the xenobiotics in the leachate [17-

19]. These concentrations should be optimal for the sustainment of the enzyme activities of the bacterial consortium in the activated sludge [20, 21]. Reaching or exceeding the critical concentration for each xenobiotic and for the specific biological system would lead to a switching from a biodegradation to a resistance and inhibition [22-26]. To be established and be derived the rules how the AS to be adapted in an industrial scale it is necessary to be conducted model lab studies which have to be subsequently verified [27-29].

The aim of the article is to assess if the activated sludge from WWTP “Sadinata” could be adapted step-by-step to the pollutants in the leachate from the landfill for non-hazardous waste “Sadinata” in Yana village. The assessment of the activated sludge is made on the basis of the changes in its structure. The changes of the technological and microbiological parameters are analyzed in the simulated adaptation process with a step-by-step increase of the concentration of the pollutants in the leachate. The results are important regarding the solution of the real problems in the plants treating leachate from non-hazardous waste landfills through the implementation of adapting algorithms.

MATERIALS AND METHODS

Experimental design

The assessment of the AS adaption to a leachate has conducted in a model process. During the experiment it has been constructed a model bioreactor – type “aerobic biobasin”, presented on Fig. 1. The choice of an aerobic bioreactor has been made because the aerobic level is really important in the presence of highly toxic xenobiotics with an aromatic structure. The reactor was sequencing batch reactor (SBR) with five phases: 1/ fill phase, 2/ react phase, 3/ settle phase, 4/ decant phase and 5/ idle phase. The biological wastewater treatment was accomplished during the second phase, under aerobic conditions. The duration of the aerobic phase was between 46 and 70 hours. After aeration, the SBR enter the settle phase, where for a period from 2 hours under quiescent conditions (without aeration and mixing) activated sludge settles in the reactor. The biological system in the experiment has been the activated sludge from WWTP “Sadinata” to which periodically has been added a leachate from the non-hazardous waste landfill, part of Municipal enterprise for waste treatment of Sofia City. The activated sludge was taken from

sequencing batch reactor which operated under aerobic conditions. The quantity of the activated sludge was 3.39 g/L at the beginning of the experiment. The treatment process has started with a diluted quantity of leachate (50X) as the concentration of pollutants in the leachate has increased each week and at the same time has been added co-substrate glycerol with a concentration 0.79 g/L. The glycerol has been used as a source of easily assimilating organic compound. This compound was used in the real WWTP “Sadinata” for increase of concentration of biodegradable organic matter (measured as BOD₅). The ratio COD:BOD₅ in WWTP “Sadinata” and in our experiment was 3:1. The experiment has continued for three weeks or twenty one days.

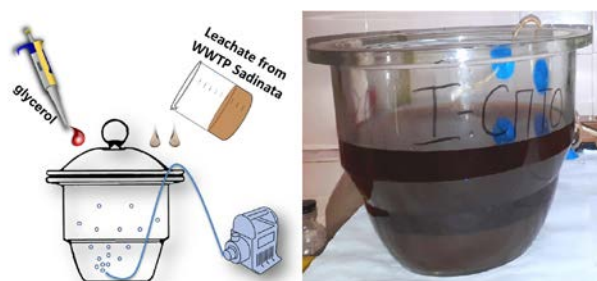


Fig. 1. Model aerobic bioreactor for simulation of adaptation processes with activated sludge to complex pollutants in landfill leachate.

The aim is to be achieved a step-by-step adaptation of the activated sludge towards toxic and hardly degradable pollutants through a step-by-step increase of the leachate concentration as on the 7th day of the start of the experiment has been added a 25X diluted leachate and on the 14th day – an undiluted leachate. In the adaptation of the biological systems, including the activated sludge, for wastewaters treatment of toxic and sustainable of biodegradation xenobiotics firstly, it is important to be defined what the critical concentration is according to the Haldane equation [30-32]. It depends mainly on the chemical structure of the compounds and on the adapting means of the biological system depending on their structure, enzyme potential and other their biological features [16]. The exceeding of the critical concentration would lead to a significant decrease of the growth speed of the microorganisms and their transition to a death phase and thus their biodegrading activity is inhibited. So the treatment process is strongly deformed and cannot be performed [33]. The challenge in the biological treatment of leachate is that in it is contained a complex of pollutants including inorganic and organic xenobiotics that

mutually modulate the biodegrading process. In a complex they define the adaptive potential of the activated sludge. In a different manner they influence its components – various types of microorganisms and representatives of the micro- and meta-fauna. Data for the choice of dilution and the definition of the critical concentration of the pollutants complex in the leachate till this moment miss in the scientific literature. It is well known that for the extraction of an algorithm for an adaptation of the activated sludge to the pollutants in the leachate in real conditions it is necessary to be switched consecutively over the modelling processes in lab conditions (lab scale). After the specification of all the elements of the adaptation algorithm in a small lab scale it could be proceeded to a step by step scaling of the processes so to be guaranteed that the extracted dependencies and rules will work effectively in a pilot scale and in a full scale [33]. That is why in the present experiment we started the modelling of the process in a lab scale with a 50X diluted leachate that does not manifest a toxicity for the activated sludge. The studied steps of dilution are comparatively large because in the first stage of the experiment the aim is to be found this dilution that is closest to the critical concentration but does not exceed it. In the log phase of the adaptive potential development this step could be comparatively large. In this phase the microbial adaptive potential is more plastic. In this stage at the same time are turning on the different microbial mechanisms of detoxification – a level of synthesis and activation of the constitutive and induced enzymes and a level of interactions of microorganisms and representatives of the micro- and meta-fauna.

The dilution from 50 to 25 times is comparatively large and it is applied regarding an approach to the critical concentration of the complex of toxic pollutants in the leachate. By the obtained results from the first and second week of the experiment it was registered that we still did not reached the critical concentration and in this composition of the pollutants the adaptive and biodegrading potential function. However, this composition is acceptable enough for the realization of the treatment process in the specific model equipment. In the third stage, it was also applied such a large step of dilution from 25X to an input of undiluted leachate. This concentration of the toxic pollutants exceeded the critical one and a treatment process occurred in unacceptable for the modelling process limits. Thus, the experiment is divided on three stages (Fig. 2) which differ on the

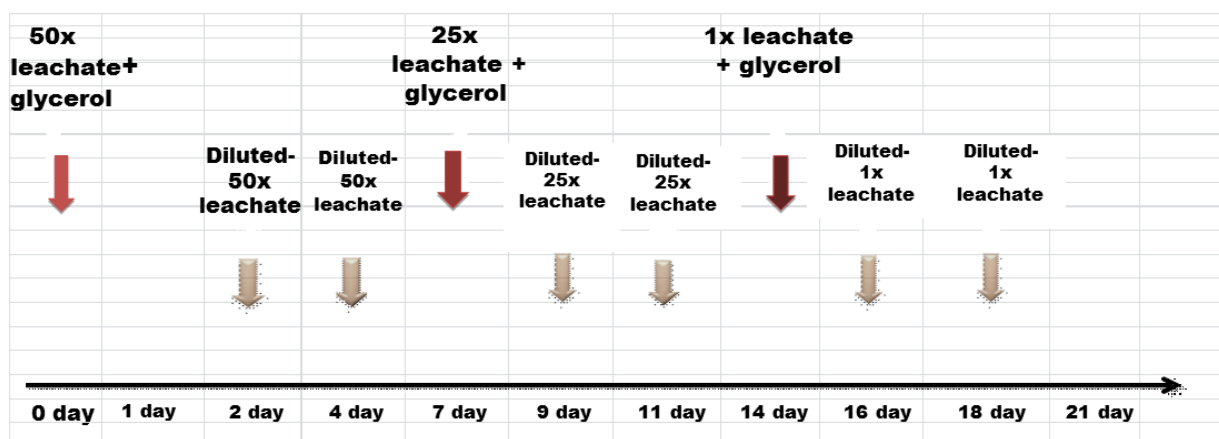


Fig. 2. Duration of process with addition of new leachate.

divided on three stages (Fig. 2) which differ on the incoming concentration of pollutants in leachate and it is expected to have a different effect on the biological system. It is important to note that in each stage of leachate addition the followed actions were accomplished in SBR: addition of influent and filling the reactor, aeration and biodegradation processes, stopping the aeration and settling the sludge, decanting the supernatant and filling the bioreactor with new leachate with the appropriate dilution for the next stage.

The first stage of the experiment occurs from the zero to the 7th day inclusive. At the beginning of the experiment to the activated sludge is added 50 times diluted leachate and a co-substrate glycerol. The first samples for analysis of technological, hydrochemical and microbiological parameters have been taken at the beginning of the experiment when the leachate has been added to the activated sludge. During the second and the fourth day the leachate has been changed with a fifty times diluted leachate but without the addition of a co-substrate glycerol.

The second stage of the experiment occurs from the seventh to the fourteenth day inclusive. On the 7th day has been added 25 times diluted leachate and a co-substrate glycerol. The samples from the activated sludge on the 7th day have been taken before the addition of the leachate and the glycerol as the analyzed parameters have been: technological, hydrochemical and microbiological. On the ninth and the eleventh day the leachate has been changed with a new one with a dilution of twenty five times without an addition of glycerol.

The third stage of the experiment is from the fourteenth to the twenty first day inclusive. On the fourteenth day have been added an undiluted leachate and a co-substrate glycerol. Samples from

the experiment have been taken at the same day before the addition of the leachate and the glycerol as analyzed have been: technological, hydrochemical and microbiological parameters. During the sixteenth and the eighteenth day the leachate has been changed with a new one but undiluted and without an addition of glycerol. Samples from these days have been taken for technological and hydrochemical parameters.

Analyzed parameters and methods

During the adaptation have been analyzed hydrochemical, technological and microbiological parameters. From the technological parameters have been analyzed dry matter and sludge volume index (SVI). The last one is important because it gives information about the presence or the absence of structural deformation of the AS. Sludge volume index (SVI) was analyzed according to BDS EN 14702-1:2006 [34]. SVI presents the volume in mL, which occupies 1 g of sludge after 30 minutes of precipitation. Mixed liquor suspended solids for calculation of SVI was determined by a standardized method [35].

From the hydrochemical parameters has been analyzed the chemical oxygen demand (COD) that indicates about the organic content in the leachate and its assimilation during the process. COD was determined by method with potassium dichromate and sample heating in presence of H₂SO₄ [35].

For a determination of the effectiveness (Eff) of the organic matter decrease (measured by COD) has been used the following formula (Eqn. 1):

$$\text{Eqn. 1) } \text{Eff} = \frac{Ct_1 - Ct_2}{Ct_1} \cdot 100, \%$$

where Ct_1 is the value of the chemical oxygen demand in the influent and Ct_2 is the value of the chemical oxygen demand in the effluent.

From the microbiological parameters has been analyzed the quantity of the bacteria from the genera *Pseudomonas* and *Acinetobacter*. They are important because they together eliminate carbon, nitrogen and phosphorus and degrade a wide circle of xenobiotics including such with an aromatic structure. The quantity of g. *Pseudomonas* and g. *Acinetobacter* were analyzed by classical cultivation method for determining the number of *Pseudomonas sp.* on Glutamate Starch *Pseudomonas* Agar and *Acinetobacter sp.* on Sellers Differential Agar. The bacterial quantity was presented as CFU/g and mixed liquor suspended solids was determined by a standardized method [35]. All of the analyses have been repeated at least three times.

RESULTS AND DISCUSSION

Organic biodegradation during the experiment

One of the key hydrochemical parameters for assessment of the water treatment processes regarding the organics are the chemical oxygen demand /COD/ and the biochemical oxygen demand /BOD₅/. Indirectly, by the decrease of these complex parameters, could be obtained information about the level of the organic pollutant's biodegradation. The data for COD during the experiment is presented on Fig. 3. It is registered that the COD values at the beginning of the experiment are high (2154.49 mgO₂/L) but at the end of the first stage (to the 7th day) the organic matter concentration decreases to 108.91 mgO₂/L.

At the end of the first week of the experiment with the 50 times diluted leachate and the added glycerol the activated sludge starts to adapt to the xenobiotics in the leachate. During the second stage also there is an organic biodegradation as the COD is on the average of 439.32 mgO₂/L. On the graph is registered a sharply increase of the COD values in the last days to 3403.305 mgO₂/L that indicates for a hard adaptation to the pollutants in undiluted leachate. The dynamic of the COD values at the end of the experiments indirectly indicates for an inhibition of the biodegrading activity of the AS in the last days of simulated process. As a whole, we could conclude that during the first and the second stage it is registered a high decrease of the organic matter measured as COD but during the third stage

of the experiment the adapting opportunities of the sludge are exceeded and the COD rests high.

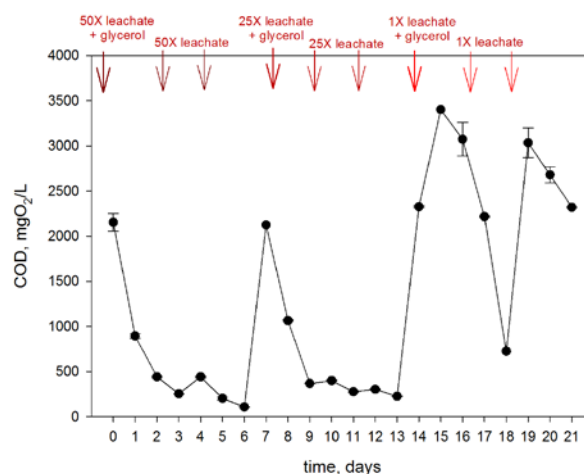


Fig. 3. Dynamics of organic matter concentration, measured as chemical oxygen demand (COD) during the experiment.

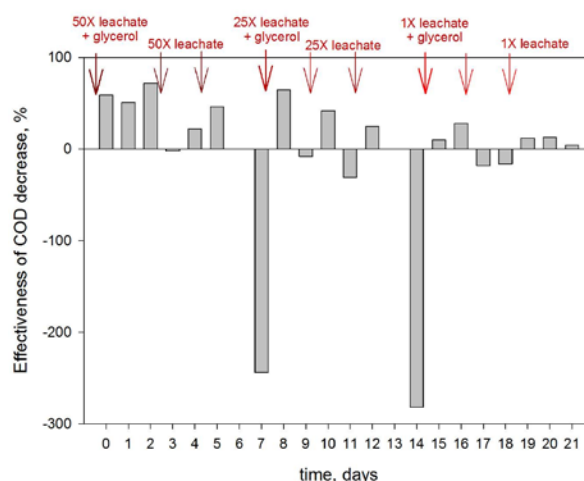


Fig. 4. Effectiveness of organic matter (measured as COD) removal during the process.

During the first stage of the experiment the effectiveness of the organic decrease measured as COD is highest (Fig. 4). The average value of the effectiveness for the first stage is 41% as the most probable reason is the low concentration of the pollutants in the 50X diluted leachate. In the second and the third stage the average values of the effectiveness are -25% and -36% namely more and more negative due to the leachate concentrating in these periods and the higher level of AS inhibition. In the 25 X dilution the adaptive potential of the activated sludge is sufficiently developed to be kept the treatment process in this concentration of the pollutants in the leachate. At the same time, the added quantity of glycerol is acceptable for the realization of the treatment of a

leachate containing a complex of toxic pollutants. In future experiments, it could be studied the state of the adaptive potential of the activated sludge in smaller steps of dilution regarding an additional approach to the critical concentration for the complex of toxic pollutants. It should be taken under consideration the fact that this complex is not constant in spite of the large level of average in the accumulation tanks in real conditions. This inconstant complex and concentrations are a sufficient argument to conduct a following treatment process in 25X without the risk to approach tightly to the values of the fluctuating critical concentration. In this dilution it is reached the necessary balance between the processes of intoxication/detoxification in the activated sludge and the relatively sustainable realization of the treatment process. This statement is confirmed by the below exhibited and commented parameters of the activated sludge.

Activated sludge assessment during the process

The activated sludge assessment during the adaptation has been made through an analysis of the changes in its structure as analyzed have been the sludge volume index, the macrostructure through a light microscope and the quantity of key taxonomic groups of microorganisms that participate in the xenobiotic biodegradation.

The indicator sludge volume index (SVI) is used for the determination of the settling capability of the sludge. The index, together with the macrostructure of the sludge, are convenient indicators for the assessment of the treating process and for the presence of a deformation in the structure of the activated sludge as well as for the eventual reasons. The high SVI (over 120-150 mL/g) is an indicator for a sludge bulking that could be filamentous or non-filamentous. The low SVI (under 70 mL/g) indicates for another sludge deformation in which predominate the so called pin-point (small) flocs. In this case the sludge is starving. The normally functioning activated sludge with a good settling capability is with an index between 100-120 mL/g [36]. The data about it is presented on Fig. 5. At the starting of the experiment it is registered that the activated sludge from WWTP "Sadinata", part of Municipal enterprise for waste treatment of Sofia City, is characterized with pin-point flocs as the sludge volume index has the value of 29.50 mL/g. In the first days the activated sludge starts to improve its settling capability from 29.50 mL/g on the 1st day to

67 mL/g on the 7th day. In the next two stages of the experiment when the pollutants concentration increases (from 25 times diluted to undiluted leachate) SVI bit by bit decreases its values. This data is an indicator for a deformation of the activated sludge and for a decrease of the biodegrading activity. The reason for this result is in the concentrated pollutants in the leachate and in the low concentration of the biodegradable organics.

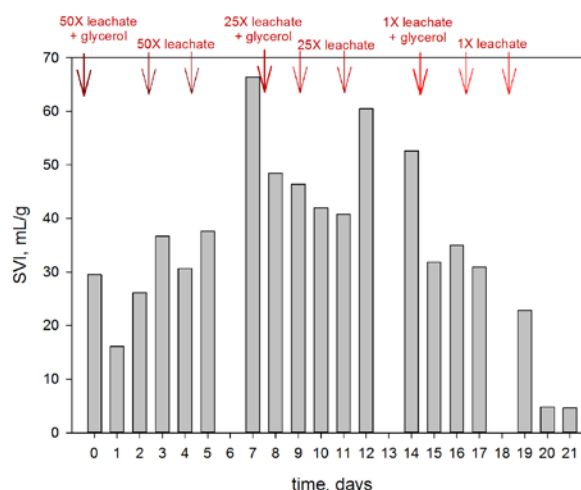


Fig. 5. Dynamics of sludge volume index (SVI) during the process.

By the obtained results we could conclude that the activated sludge is with a deformed structure by the type of the pin-point flocs (SVI under 70 mL/g). The deformation could be caused by the presence of toxic pollutants and/or hardly degrading compounds in the leachate. In the experiments conducted by the team of Center of competence "Clean technologies for sustainable environment – water, waste, energy for circular economy" the research group of prof. Djingova has registered the presence of aromatic amines, mono- and polyvalent alcohols, phenols, aldehydes and ketones.

The results obtained by the microscopic analysis of the samples from the 7th, 14th and 21st day (Fig. 6) completely approve the hypotheses expressed for the parameter SVI. On Fig. 6a during the 7th day of the conducted experiment the microscopic picture of the activated sludge shows formed pin-point flocs but also it could be seen a presence of a little part of filamentous microorganisms that indicates an attempt for restructuring to a normally functioning activated sludge. The following microscopic images presented on Fig. 6b and Fig. 6c from the 14th and 21st day show the presence of pin-point flocs with accumulated in them pollutants. In these two phases of the experiment

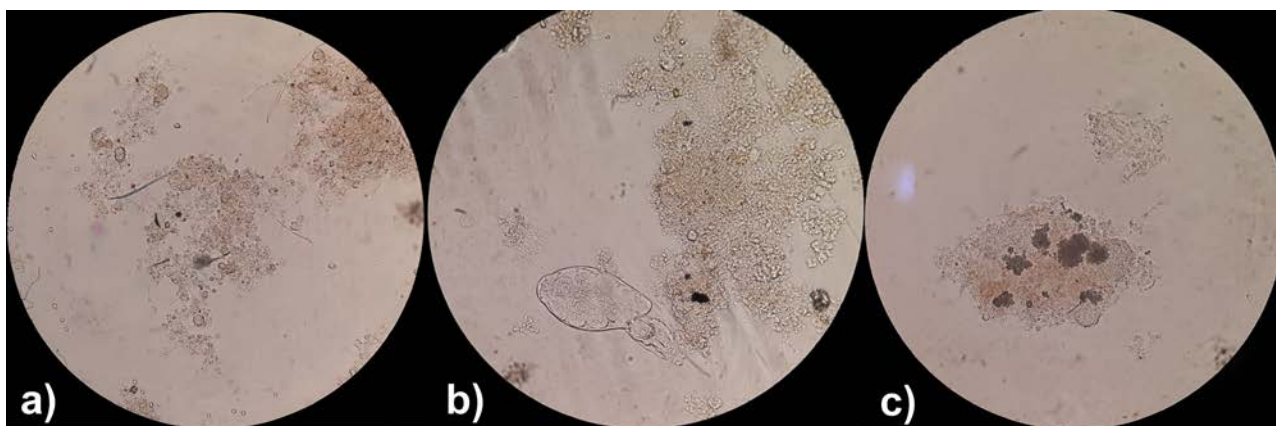


Fig. 6. Pictures of activated sludge on: a/ 7th day; b/ 14th day; c/ 21st day of experiment (Light Microscope – 100X).

the flocs represent a deformation of the activated sludge that is an indicator for a starving sludge.

The quantity of the bacteria from g. *Pseudomonas* and from g. *Acinetobacter* plays the role of an indicator for the flexibility of the biological system and its capability to adapt to degrade xenobiotics. These bacteria possess opportunities for alternative ways for energy provision and have more opportunities for a resistance development and unlocking of a xenobiotic degrading potential. The data for the bacteria from the g. *Pseudomonas* and from g. *Acinetobacter* is presented on Fig. 7.

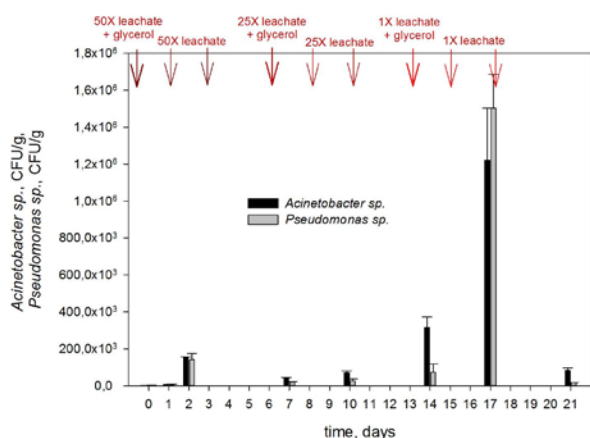


Fig. 7. Dynamics of quantity of *Pseudomonas* sp. and *Acinetobacter* sp.

The changes in the quantity of the bacteria from g. *Pseudomonas* and from g. *Acinetobacter* follow the same tendency in the simulated experiment (Fig. 7). In the first stage, the representatives of the both genera are in low quantities. After the transition in the second stage it is registered a quantitative increase to the 14th day. In the third stage, the microorganisms of the both genera sharply increase their quantities 4 times for g.

Acinetobacter and 20 times for g. *Pseudomonas*. This increase is a response to the addition of the highly concentrated leachate. According the previous results the first response of shock increase of toxic xenobiotic is the increase of the amount of homogenic bacteria of the genera from g. *Pseudomonas* and from g. *Acinetobacter*. The possible reason for that is the disruption and deformation of the flocs as well as the decrease the amount and inhibition of micro- and meta-fauna [9, 10]. These results as well as results for SVI and biodegradation activity of AS once again confirm that the adaptation process at these conditions enriches the critical concentration for the complex toxic pollutants in the leachate. After reaching the critical concentration the bacteria from g. *Pseudomonas* and from g. *Acinetobacter* decrease their quantities (from $1,5 \cdot 10^6$ CFU/g and $1,2 \cdot 10^6$ CFU/g to $1,7 \cdot 10^4$ CFU/g and $8,3 \cdot 10^4$ CFU/g).

In spite of the vast potential for xenobiotics biodegradation of the microorganisms of genera *Pseudomonas* and *Acinetobacter*, in the simulated experiment the shocking addition of undiluted leachate causes a negative impact on the xenobiotic degrading bacteria and on the biodegradation process. The results give the base to propose that 25X dilution of the leachate is close to the critical concentration for the development of adaptive potential of AS in the specific experimental conditions. Our proposal is that the real wastewater treatment process to be accomplished at dilution of leachate 25 times with water, containing easily degraded trivial substrates.

If the strategy of the technologists is to increase the concentration of leachate it is necessary to make that very slowly and carefully. This is risky technological process. So, recommendation is to test other mechanisms for the improving the wastewater treatment process, for example to rotate

aerobic and anoxic conditions. This rotation will stimulate purposely detoxification, denitrification and annamox process. Less risky, cost effective solution, will be replacement of glycerol with other cheaper and easily degradable substrate for acceleration of degradation of xenobiotic pollutants in leachate with high effectiveness. All these conclusions will be tested and verified in the next our research.

CONCLUSION

The obtained results clearly indicate that from the three stages of the conducted experiment the most favorable conditions for an adaptation of the activated sludge towards the pollutants in leachate are in the first stage. The improving of the settling capability and the macrostructure of the AS, as well as the higher biodegrading capability registered through the indicator effectiveness of organic matter decrease are the precondition for the adaptation of the activated sludge to a 50X diluted leachate. With the increase of the concentration in the second stage some of the parameters such as a presence of pin-point flocs with an absence of filamentous microorganisms and a negative effectiveness of organic matter decrease indicate a deterioration namely the functioning of the adaptive mechanisms of the activated sludge becomes difficult. In the third stage, by the results of the analyzed parameters, it is registered that the metabolic processes of the microorganisms of the activated sludge are inhibited by the high concentration of xenobiotics in the added undiluted leachate. The results confirm that the leachate diluted 25X contains toxic xenobiotics, which concentration is close to the critical one for the development of adaptive potential of AS in the concrete experimental conditions. This dilution of the leachate and the ratio COD:BOD₅ are appropriate for accomplishment of wastewater treatment process.

Acknowledgements: This research was supported by the Grant №BG05M2OP001-1.002-0019: "Clean Technologies for Sustainable Environment - Water, Waste, Energy for a Circular Economy", financed by the Science and Education for Smart Growth Operational Program (2014-2020) co-financed by the EU through the ESIF. The samples from activated sludge and landfill leachate were provided from the Municipal enterprise for waste treatment of Sofia City by project „Study of the impact of the toxic compounds in the landfill

leachate on the biological water treatment in WWTP "Sadinata".

REFERENCES

1. https://ec.europa.eu/eurostat/statistics-explained/index.php?title=Waste_statistics#Total_waste_generation
2. T. H. Christensen, Solid Waste Technology and Management, Blackwell Publishing Ltd., UK, 2011.
3. P. Kjeldsen, M. A. Barlaz, A. P. Rooker, A. Baun, A. Ledin, T. H. Christensen, *Crit. Rev. Environ. Sci. Technol.*, **32**, 297 (2002).
4. R. Stegman, U. K. Heyer, R. Cossu, in: *Proceedings Sardinia*, Vol. 10 (Proc. Sardinia 2005, 10th Int. Waste Manage. Landfill Symp.), 2005.
5. A. A. Abbas, G. Jingsong, L. Z. Ping, P. Y. Ya, W. S. Al-Rekabi, *J. Appl. Sci. Res.*, **5**, 534 (2009).
6. J. Wiszniewski, D. Robert, J. Surmacz-Gorska, K. Miksch, J. V. Weber, *Environ. Chem. Lett.*, **4**, 51 (2006).
7. Y. Ren, F. Ferraz, M. Lashkarizadeh, Q. Yuan, *J. Water Process. Eng.*, **17**, 161 (2017).
8. I. Schneider, M. Beluhova, Y. Topalova, *Ecol. Eng. Environ. Protect.*, **4**, 50 (2001).
9. I. Schneider, M. Ducheveva, I. Yotinov, Y. Todorova, E. Daskalova, Y. Topalova, V. Stefanova, *Ecol. Eng. Environ. Protect.*, **7**, 27 (2016).
10. Y. Topalova, Y. Todorova, I. Schneider, I. Yotinov, V. Stefanova, *Water Sci. Technol.*, **78**, 588 (2018).
11. A. B. Yahmed, N. Saidi, I. Trabelsi, F. Murano, T. Dhaifallah, L. Bousselemi, A. Ghrabi, *Desalination*, **246**, 378 (2009).
12. B. Xie, S. Xiong, S. Liang, C. Hu, X. Zhang, J. Lu, *Bioresource Technol.*, **103**, 71 (2012).
13. I. Yotinov, M. Belouhova, A. Kavazov, I. Hristova, N. Dinova, I. Schneider, E. Daskalova, S. Lincheva, Y. Topalova, in: Youth Scientific Conference Kliment's Days Abstracts 2019, p.67.
14. K. Wang, L. Li, F. Tan, D. Wu, *Archaea*, **2018**, 10 (2018).
15. A. M. Costa, R. G. D. S. M. Alfaia, J. C. Campos, *J. Environ. Manage.*, **232**, 110 (2019).
16. R. Dimkov, Y. Topalova, I. Schneider, Environmental biotechnology, Publish Sci-Set Eco, Sofia, 2017.
17. S. Kheradmand, A. Karimi-Jashni, M. Sartaj, *Waste Manage.*, **30**, 1025 (2010).
18. E. M. de Albuquerque, E. Pozzi, I. K. Sakamoto, P. Jurandy, *J. Water Process. Eng.*, **23**, 119 (2018).
19. S. F. Corsino, M. Capodici, D. Di Trapani, M. Torregrossa, G. Viviani, *New Biotechnol.*, **55**, 91 (2020).
20. A. I. Zouboulis, M. X. Loukidou, K. Christodoulou, *Chemosphere*, **44**, 1103 (2001).
21. F. Spina, V. Tigrini, A. Romagnolo, G. C. Varese, *Life*, **8**, 27 (2018).
22. S. Renou, J. G. Givaudan, S. Poulain, F. Dirassouyan, P. Moulin, *J. Hazard. Mater.*, **150**, 468 (2008).

23. Y. Liu, Z. Chen, L. Yang, Z. Liao, T. T. Sun, J. Wang, H. Wang, *Bulg. Chem. Commun.*, **47**, 193 (2015).
24. D. Bove, S. Merello, D. Frumento, S. A. Arni, B. Aliakbarian, A. Converti, *Chem. Eng. Technol.*, **38**, 2115 (2015).
25. P. Ghosh, I. S. Thakur, A. Kaushik, *Ecotox. Environ. Safe.*, **141**, 259 (2017).
26. H. Luo, Y. Zeng, Y. Cheng, D. He, X. Pan, *Sci. Total Environ.*, **703**, 135468 (2020).
27. M. Capodici, D. Di Trapani, G. Viviani, *Water Sci. Technol.*, **69**, 1267 (2014).
28. M. X. Loukidou, A. I. Zouboulis, *Environ. Pollut.*, **111**, 273 (2001).
29. M. S. Bilgili, A. Demir, B. Özkaya, *Environ. Manage.*, **38**, 189 (2006).
30. I. Ćosić, M. Vuković, Z. Gomzi, F. Briški, *Chem. Pap.*, **67**, 1138 (2013).
31. J. J. González-Cortés, F. Almenglo, M. Ramírez, D. Cantero, *J. Environ. Manage.*, **281**, 111902 (2021).
32. Z. Belhachmi, Z. Mghazli, S. Ouchtout, *Math. Comput. Simulat.*, **185**, 174 (2021).
33. Y. Topalova, *Biological Control and Management of Water Treatment*, Publish Sci-Set Eco, Sofia, 2009.
34. BDS EN 14702-1, (Characterization of sludges – settling properties. Part 1: Determination of settleability (Determination of the proportion of sludge volume and sludge volume index)), European Committee for Standardization, 2006, 16 p.
35. A. D. Eaton, L. S. Clesceri, E. W. Rice, A. E. Greenberg, *Standard Methods for the Examination of Water and Wastewater*, vol. 21, APHA-AWWA-WEF, Washington, D.C., 2005
36. D. Jenkins, M. G. Richard, G. Daigger, *Manual on the Causes and Control of Activated Sludge Bulking, Foaming and Other Solids Separations Problems*, Lewis Publishing, Boca Ration, FL, 2003.

Effect of extracts of some species from Phylum Mollusca against the replication of Human Alphaherpesviruses types

V. Tsvetkov¹, D. Todorov^{1*}, A. Hinkov¹, K. Shishkova¹, L. Velkova², A. Dolashki², P. Dolashka², S. Shishkov¹

¹ Laboratory of Virology, Sofia University “St. Kliment Ohridski”, Sofia, Bulgaria, Dragan Tsankov Blvd. 8, 1164 Sofia, Bulgaria

² Institute of Organic Chemistry with Centre of Phytochemistry, Bulgarian Academy of Sciences, Acad. G. Bonchev Str. Bl. 9, 1113 Sofia, Bulgaria

Received January 22, 2021; Revised April 09, 2021

In the present study, hemolymph from *Rapana venosa* (hRv), *Helix lucorum* (Hl) and *Eriphia verrucosa* (hEv), mucus from *Helix aspersa* (Ha) and structural subunit α -HaH from hemocyanin of *H. aspersa* (sHa) were tested against replication of antiviral drugs acyclovir (ACV) sensitive strain F and BA of human alphaherpesvirus type 1 and type 2 *in vitro*. All six extracts showed no anti-herpesvirus activity using an MTT-based colorimetric assay to detect inhibition of Human Alphaherpesviruses (HHV) replication. In a virus analysis, the six extracts tested reduced the infectivity of both viruses from the two strains used to varying degrees and applied at maximum non-toxic concentrations. Fractions from hemolymph from *R. venosa* (MW 30-100 kDa) and from *E. verrucosa* (MW 3-100 kDa) showed the highest activity (over 99% inhibition of extracellular virions infectivity by first and second type of viruses respectively), sufficient to be considered pharmacologically significant. Hemolymph from *R. venosa* and *E. verrucosa* and mucus from *H. aspersa* have little effect on the adsorption of BA strain of human alpha herpesvirus type 2, and strain F of the HHV 1. The effect on the first type being more pronounced.

Key words: hemolymph from *R. venosa*, *H. lucorum* and *E. verrucosa*; mucus from *H. aspersa*; human alphaherpesviruses

INTRODUCTION

“Herpes” is a medical condition caused by members of the genus Simplexvirus (Human Alphaherpesviruses (HHV) types 1 and 2). According to the WHO, worldwide 3.7 billion people under age 50 (67%) and 491 million people aged 15-49 (13%) are infected with HHV-1 and HHV-2, respectively [1]. Infection with both types of HHV may be asymptomatic (but the virus can still be transmitted to others). In the presence of symptoms, painful sores and blisters around the mouth and lips (when a person is infected with HHV-1) and on the genitals and anus (genital herpes) (when a person is infected with HHV-2) are observed. This causes in the infected individual psychological distress very often and forces him to adjust to live with the infection. The risk group is immunocompromised patients and neonates in whom the lack of an adequate immune response is the cause of encephalitis, meningitis, neonatal herpes and even death. All Herpesviridae family representatives establish a latent infection that

results in recurrence of symptoms. As the latent virus cannot be affected, modern therapy is aimed at controlling the symptoms of the primary and recurrent HHV infections [2].

Nucleoside analogues such as ACV and its derivatives are most commonly used for treatment. Although this group of substances are very effective selective inhibitors, their improper use leads to the development of resistant viral mutants [3]. An effective alternative is therefore needed. Such are, for example, substances of natural origin.

In invertebrates lack a highly specific adaptive immune system and they use their innate and non-adaptive immune system to resist pathogen invasions [4]. Many gastropods and arthropods are subject of scientific studies with aim discovery of novel antimicrobial and antiviral compounds. Cellular immunity of these species predominantly involves the phagocytic activity of hemocytes, whereas humoral immunity requires the release of antimicrobial factors [5, 6]. The structural subunit β c-HaH of hemocyanins of *Helix aspersa* and two peptides isolated from the hemolymph of the molluscan garden snail *Helix lucorum* shows antimicrobial activities against *Staphylococcus aureus*, *Streptococcus epidermidis* and also against

* To whom all correspondence should be sent:
E-mail: dani_todorov@biofac.uni-sofia.bg

Escherichia coli [7, 8]. The fraction with peptides (produced by the mucus of garden snail *Cornu aspersum*) with molecular masses below 3 kDa exhibited antibacterial activity against Gram-negative *Pseudomonas aeruginosa* AP9 and Gram-positive *Brevibacillus laterosporus* BT271 bacteria. The inhibition effects of the peptides can be explained with the amino acid residues [9].

Hemocyanins from *R. venosa*, *H. lucorum* and marine cancer *C. aestuarii* and their glycosylated derivatives have been shown a promising antiviral effect against a number of viruses from different groups, such as human respiratory syncytial virus (hRSV), influenza virus A (H3N2 type), herpes 1 and type 2 (HSV-1 and HSV-2), Epstein-Barr virus (EBV) It has been established a relationship between carbohydrate structures and the antiviral properties of hemocyanin derivatives, and a new mechanism has been proposed for explain the antiviral effect of hemocyanin by molluscs [10-12]. Haemolymph and lipophilic extract of the digestive gland (from abalone *Haliotis laevigata* (Haliotidae)) both showed antiviral activity against the human herpesvirus HSV-1 *in vitro*. The haemolymph inhibited viral infection at an early stage. In contrast, the antiviral effect of the lipophilic extract may act at an intracellular stage of infection [13]. A modified peptide derived from myticin C (an antimicrobial peptide from the Mediterranean mussel (*Mytilus galloprovincialis*)) or the nanoencapsulated normal peptide also showed antiviral activity against the human herpesviruses HSV-1 and HSV-2 *in vitro* [14]. One of the fractions of mucus of land slug *Phyllocaulis boraceiensis* with the main constituents hydroxy-tritriacontapentaenoic acid and hydroxy-pentatriacontapentaenoic acid, exhibited antiviral activity against measles virus *in vitro* [15].

And last but not the least. The human bladder cancer permanent cell line CAL-29 is sensitive to the action of the hemocyanins from the molluscs *Helix lucorum*, *Rapana venosa* and their functional units [16].

EXPERIMENTAL

Materials and Extracts

The hemolymph from garden snails *H. lucorum* and marine snail *R. venosa* were obtained as described previously [17, 18]. Two fractions were isolated from hemolymph of *R. venosa*, containing compounds with MW 1-10 kDa, and with MW 30-100 kDa.

Two protein fractions were also isolated from hemolymph of *H. lucorum* (with MW under 100 kDa) and from crab *E. verrucosa* (with MW 3-100 kDa). The hemolymph from *E. verrucosa* was extracted from 10 crabs (3-5 mL per crab) living in area near to Kamchia region of the Black Sea and homogenized in 0.01 mol/L Tris-buffer (Sigma-Aldrich, Steinheim, Germany) [19].

Two fractions we purified from snail *H. aspersa*, structural subunit α -HaH from the hemolymph [20] and a protein fraction with MW over 50 kDa from mucus [21].

All fractions were obtained from purified hemolymph from *R. venosa*, *H. lucorum* and *E. verrucosa* and *H. aspersa* mucus by ultrafiltration using membrane (Millipore™ Ultrafiltration Membrane Filters) with different size pores – MWCO from 100 kDa, 50 kDa, 30 kDa, 3 kDa and 1 kDa.

SDS-PAGE Electrophoresis

Protein fractions were analysed by sodium dodecyl sulfate-polyacrylamide gel electrophoresis (SDS-PAGE), according to Laemmli method with modifications [22]. Equal volumes containing approximately 15 μ g/lane of the samples dissolved in Laemmli sample buffer and protein standard mixture (Precision Plus Protein., All Blue, Bio-Rad, Feldkirchen, Germany) were separated by 12.0% SDS-PAGE and visualized by staining with Coomassie Brilliant Blue G-250.

Cells and Viruses

MDBK (Madine and Darby bovine kidney) cell line, grown in Dulbecco's Modified Eagle Medium (DMEM) supplemented with 8% (growth medium) and 4% (maintenance medium) fetal calf serum (FCS) (with Gentamycin 8 μ g/ml and 10 mM HEPES buffer), were used in the experiments. This study employed the F strain of Human alpha herpesvirus type 1 and Ba strain of Human alpha herpesvirus type 2. The virus was propagated in MDBK cells and stored at -70°C until used.

Determining the effect of extracts on cell culture

The cytotoxicity (cell viability) was determined by colorimetric MTT assay [23]. Confluent monolayers of MDBK cells in 96-well plates were overlaid with 0.1 ml/well maintenance medium, 0.1 ml/well of serial two-fold dilutions of the extracts (in maintenance medium) or 0.1 ml/well only maintenance medium (in cell controls) and were

incubated at 37 °C for 48 h. On the second day 0.020 ml of MTT (Sigma-Aldrich) – (5 mg/ml in PBS) was added to each well and the plates were incubated for 2 h at 37 °C. The optical densities (OD) were determined by plate reader at $\lambda = 540$ nm. The percentage of viable treated cells was calculated by the following formula $[(\text{OD}_{\text{exp.}})/(\text{OD}_{\text{cell control}})] \times 100$, where (OD_{exp.}) and (OD_{cell control}) indicate the absorbencies of the test sample and the cell control, respectively. The 50% cytotoxicity concentration (CC50) was calculated by regression analysis of the dose – response curves generated from the data. MTC was determined microscopically on the 48th hour.

Survival study of virus-infected and extract-treated cells. MTT-based colorimetric assay for detection of HHV replication inhibition

We used a modification of an MTT assay developed for screening of anti-HHV compounds by Takeuchi *et al.* [24]. Confluent monolayers in 96-well plates were overlaid with 0.1 ml/well of virus suspension – MOI = 100 CCID₅₀/well. The plates were incubated for 1 h at 37 °C and dilutions of the extracts or only maintenance medium (for virus control) were added after that. Uninoculated cells were used for cell control. On day 5, the plates were treated in the same way described in the method for measuring cell viability. The percentage of protection was calculated by the following formula $[(\text{OD}_{\text{exp.}}) - (\text{OD}_{\text{virus control}})/(\text{OD}_{\text{cell control}}) - (\text{OD}_{\text{virus control}})] \times 100$, where (OD_{exp.}), (OD_{virus control}), and (OD_{cell control}) indicate the absorbencies of the test sample, the virus control and the cell control, respectively. The 50% effective concentration (EC₅₀) was calculated by regression analysis of the dose – response curves generated from the data. Selectivity index (SI) was calculated as CC₅₀/EC₅₀.

Study of the effect of the extracts on the extracellular virions of HHV 1 and HHV 2

The direct virus inactivating effect of the plant extracts was tested by direct contact assay. Undiluted stock virus suspensions were treated with equal volumes of the compounds in MNC (maximal nontoxic concentration), prepared in maintenance medium and incubated at 37 °C for 5', 15', 30', 60', 120', 240' and 360'. Undiluted stock virus suspensions were treated with equal volumes of compound free maintenance medium for control. At the end of each time interval, the control and the

treated viruses were freezed, and the difference in the biological activities between them was determined on the base of infectivity. The surviving infectious virus titres were determined in CPE assay using the method of Reed and Muench [25].

Activity against viral adsorption

The effect of the extracts over viral adsorption was tested by direct contact assay. Undiluted stock virus suspensions were treated with equal volumes of the compounds in MTC, prepared in maintenance medium and incubated at 4 °C for 15', 30', 60', 120' over cell culture. Undiluted stock virus suspensions were treated with equal volumes of compound free maintenance medium for control. At the end of each time interval, the control and the treated cell layers were flushed twice with PBS and then fresh medium were put over the cells. After 24 hours both arrays were freezed, and the difference in the biological activities between them was determined on the base of infectivity. The surviving infectious virus titres were determined in CPE assay using the method of Reed and Muench [21].

RESULTS AND DISCUSSION

Protein fractions were characterized by 12.5% SDS-PAGE analysis. The analysis on Fig. 1 shows the difference in the performance of proteins in them.

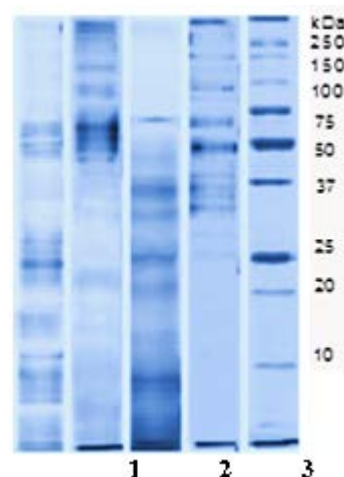


Fig. 1. 12.5% SDS-PAGE analysis, positions: 1) Fraction from *H. lucorum* hemolymph with Mw <100 kDa; 2) Fraction from *H. aspersa* mucus with MW >50 kDa, 3) Fraction from hemolymph of *E. verrucosa* with MW 3-100 kDa; 4) Fraction from hemolymph of *R. venosa* with Mw 30-100 kDa; 5) standard proteins from Bio-rad.

Analysis of the *H. lucorum* hemolymph fraction with Mw <100 kDa (Fig. 1, position 1) confirmed

the presence of various proteins and peptides with molecular weights between 2 and 6.8 kDa, recently determined by mass spectrometry [26]. Several proteins were identified in the protein fraction of *H. aspersa* mucus with MW above 50 kDa (Fig. 1, position 2) [27, 28]. As shown on Fig. 1 position 3, peptides with MW < 10 kDa and proteins in a wide range of ~ 20 kDa, ~ 25 kDa, between 30-40 kDa and ~ 75 kDa were found in the fraction of hemolymph from sea crabs *E. verrucosa*. Several proteins with MW 35-45 kDa, ~ 50 kDa, ~ 65 kDa and ~ 100 kDa were also found in hemolymph of *R. venosa* with Mw 30-100 kDa.

Determination of MTC and CC50 values and the effect of extracts on cell culture

We initially examined the cytotoxicity of each of the extracts we used. We applied the MTT test to determine live and early apoptotic cells [23].

In the used experimental setup, concentrations of the extracts in the range from 1 µg/ml to 20 µg/ml were tested. The values obtained for each extract are presented (Table 1).

Table 1. Data on the cytotoxicity of the studied extracts.

Extract	MTC [µg/ml]	CC ₅₀ [µg/ml]
Hemolymph from <i>Rapana venosa</i> with MW 1-10 kDa	10	>10
Hemolymph from <i>Rapana venosa</i> with MW 30-100 kDa	2	2.36
Hemolymph from <i>Helix lucorum</i> with MW under 100 kDa	>20	>20
Hemolymph from <i>Eriphia verrucosa</i> with MW 3-100 kDa	>20	>20
Mucus from <i>Helix aspersa</i> with MW over 50 kDa	>20	>20
Structural subunit α-HaH from hemocyanin of <i>Helix aspersa</i>	10	>10

After graphical expression of the obtained values, MTCs and CC₅₀ were determined. When comparing the experimental data (values for CC₅₀) it is seen that hemolymph from *R. venosa* 30-100 kDa have the highest cytotoxicity – 2.36 µg/ml. The fractions from hemolymph of *H. lucorum* with MW under 100 kDa, from hemolymph of *E. verrucosa* with MW 3-100 kDa and mucus from *H. aspersa* with MW over 50 kDa have the lowest respectively over 20 µg/ml.

The extract of hemolymph from *R. venosa* with MW 30-100 kDa was found to have the highest toxicity, followed by the extract with MW 1-10 kDa, which is equivalent to the toxicity of the α-

NaH structural subunit from hemocyanin of *Helix aspersa*. With the same toxicity are three extracts of hemolymph from *H. lucorum* with MW below 100 kDa, extract of hemolymph from *E. verrucosa* with MW 3-100 kDa and mucus from *H. aspersa* with MW over 50 kDa. However, they show lower toxicity than other extracts.

Survival study of virus-infected and extract-treated cells

All the extracts were tested for concentration depended activity over viral replication with maximal concentration tested – equal to the MTC concentration equal to the determined to one from the cell toxicity experiment. All six extracts were tested against both HHV-1 and HHV-2 viruses with no effect except the extract from hemolymph of *R. venosa* with MW 1-10kDa – with inhibition up to 20% when used in MTC. All other extracts showed no activity against the viral replication.

Study of the effect of the extracts on the extracellular virions of HHV 1 and HHV 2

For a more complete study of the antiherpes activity of the extracts, their effect on extracellular virions was studied by direct contact method. The extracts were administered at a concentration corresponding to their MTC. The change in the infectivity of the virus was observed at different duration of contact with the studied extract (5, 10, 15, 30, 60, 120, 240 and 360 minutes).

The results obtained for the virucidal action of the extracts are presented in Table 2. Data on the effect of the extracts on the extracellular virions of HHV 1 and HHV 2, after 360 min. of exposure

Table 2. Data on the Virucidal activity of the studied extracts.

Extract	MTC µg/ml	Virucidal effect [Δlog]	
		HHV-1	HHV-2
Hemolymph from <i>Rapana venosa</i> with MW 1-10 kDa	10	1.33	0.66
Hemolymph from <i>Rapana venosa</i> with MW 30-100 kDa	2	2.33	0.83
Hemolymph from <i>Helix lucorum</i> with MW under 100 kDa	>20	0.67	0.33
Hemolymph from <i>Eriphia verrucosa</i> with MW 3-100 kDa	>20	1.67	2.66
Mucus from <i>Helix aspersa</i> with MW over 50 kDa	>20	2	1.83
Subunit from hemocyanin of α-HaH from <i>Helix aspersa</i>	10	1.55	1.83

showed some virucidal activity against both types of viruses.

Virucidal action against HHV 1 strain F

The most pronounced effect on extracellular virions was shown by extract from hemolymph from *R. venosa* with MW 30-100 kDa and extract from mucus from *H. aspersa* with MW over 50 kDa. The present results in Table 2 show that the virus titer in the samples decreased by two or more logarithms (99.99 and more percent viral inhibition) compared to the virus titer in the control samples.

When examining hemolymph from *R. venosa* with MW 30-100 kDa, a reduction in viral infectivity was observed in the initial stages of exposure (at the fifth minute of treatment). At the thirtieth minute of treatment, the viral titer decreased by 1.33 log (95.32% inhibition). The effect is enhanced by increasing the treatment time of the samples. At the end of the study interval, a decrease in viral titer by more than 2 logs (99.53% inhibition of viral infectivity) was found (Table 2).

The study of *H. aspersa* mucus also showed a reduction in viral infectivity. The effect remains relatively constant with increasing sample treatment time. At the fifteenth minute of treatment, the viral titer decreased by 1.33 log (95.32% inhibition) At the end of the study interval (360 minutes), a decrease in viral titer by 2 logs (99%) was reported (Table 2).

The remaining extracts - hemolymph from *R. venosa* 1 with MW 1-10 kDa, from *H. lucorum* with MW under 100 kDa and hemolymph from *E. verrucosa* with MW 3-100 kDa, Structural subunit α -HaH from hemocyanin of *H. aspersa*, show some weak virucidal action in the initial stages of exposure. The decrease in viral infectivity at the end of the study interval and the decrease in viral titer in the samples was about 1 log (90%) compared to the virus titer in the control samples (Table 2).

Virucidal action against HHV 2 strain BA

In the study of the extracts provided to us against the extracellular virions of HHV 2, we found that Hemolymph from *Eriphia verrucosa* with MW 3-100 kDa has the strongest effect on the infectivity of the virus. The decrease in viral titer in the sample at the fifth minute was 0.66%, and at the 360th minute it reached 2.66 log or 99.78% viral inhibition (Table 2).

The virucidal effect is enhanced by increasing the treatment time, i. e. the virucidal activity of the extract against the HHV2 is 1 logarithm higher than that observed in the treatment of the HHV1. When studying the activity of the shown good effect against the first type of virus, Mucus from *H. aspersa* with MW over 50 kDa, we found a relatively good effect on HHV 2 (Table 2). The decrease in viral titer in the samples was 1.83 log compared to the viral control. A decrease in viral titer is reported as early as the 15th minute - 1 log. The tendency of decrease of the viral titer is preserved and at the end of the treatment the decrease is by 1.83 log. or 98.52% viral inhibition.

Hemolymph from *R. venosa* with MW 30-100 kDa, which has a significant effect on the first type of virus, has a significantly weaker effect on the HHV 2, at maximum exposure time Δ log is 0.83.

Activity against viral adsorption

Of all the extracts studied, hemolymph from *R. venosa* with MW 30-100 kDa, Hemolymph from *Eriphia verrucosa* with MW 3-100 kDa and mucus from *H. aspersa* with MW over 50 kDa showed the highest activity (Fig. 2 and Fig. 3). The remaining extracts showed no effect on the adsorption of the two types of viruses.

Activity of the extracts on the adsorption of the HHV-1 strain F

Already in the initial stages of treatment (15th minute) a decrease in the viral titer in the treated samples is reported in contrast to the virus titer in the untreated samples with extracts (Fig. 2). At the 120th minute from the beginning of the treatment, the hemolymph from *R. venosa* with MW 30-100 kDa showed the strongest effect on the adsorption.

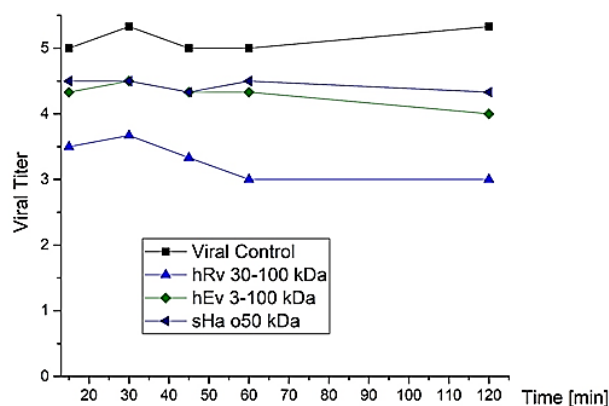


Fig. 2. Activity of the extracts on the adsorption of the HHV-1.

The decrease in viral titer compared to viral control was 2.33 log or 99.53% viral inhibition. When treated with other two extracts, hemolymph from *E. verrucosa* with MW 3-100 kDa and mucus from *H. aspersa* with MW over 50 kDa, a decrease in viral titer of about 1 log was also recorded. In hemolymph from *E. verrucosa* with MW 3-100 kDa - 1.33 log and in mucus from *H. aspersa* over 50 kDa 1 log. The percentage of viral inhibition was 95.32 and 90, respectively. These results were reported when treating the samples for 120 minutes. The remaining extracts had no effect on the adsorption of the HHV 1 strain F.

Activity of the extracts on the adsorption of the HHV-2 strain BA

Only three of the six extracts studied, hemolymph from *R. venosa* 30-100 kDa, hemolymph from *E. verrucosa* 3-100 kDa and mucus from *H. aspersa* over 50 kDa, had an effect on the adsorption of the two types of virus (Fig. 3).

Compared to the effect on the adsorption of the HHV 1, the three extracts showed a weaker effect. Again, the strongest effect of hemolymph from *R. venosa* with MW 30-100 kDa is reported. As early as the 15th minute of exposure, the viral titer decreased by 1.17 log, reaching 1-66 log or 97.81% viral inhibition at the end of the test period.

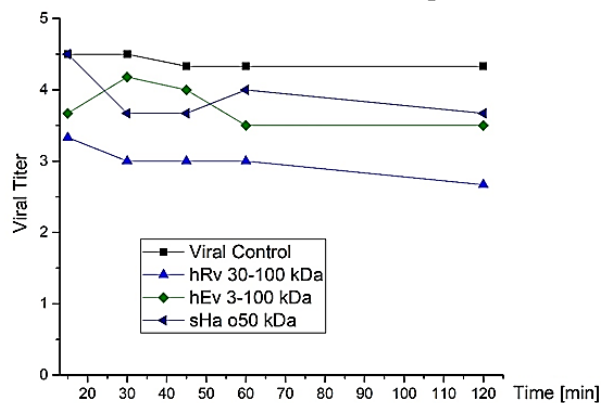


Fig. 3. Activity of the extracts on the adsorption of the HHV-2.

In the other two extracts, hemolymph from *E. verrucosa* with MW 3-100 kDa and mucus from *H. aspersa* with MW over 50 kDa, Δ log reached respectively 0.83 (85.21% viral inhibition) and 0.66 (78.12% viral inhibition).

CONCLUSION

Contrary to the reports of other author teams, the effect of various extracts of invertebrates on the intracellular stages of replication of some viruses

[13, 14, 29], our team did not find significant antiviral activity of the studied extracts. Only the extract of hemolymph of *R. venosa* with MW 1-10 kDa showed a weak effect - inhibition of up to 20%.

The antiviral activity of the studied extracts is manifested as activity against extracellular virions of HHV-1 and extracellular virions of HHV-2. The highest virucidal activity on the HHV 1 shows hemolymph from *R. venosa* with MW 30-100 kDa. Hemolymph from *E. verrucosa* with MW 3-100 kDa has the best virucidal effect in relation to the second type of virus and relatively good in relation to the first type. Mucus from *H. aspersa* with MW over 50 kDa also shows good virucidal activity against HHV type 1 and relatively good against the second type. Clarification of the mechanism of action of active extracts is the focus of future developments. Because the experiments involved an effect on extracellular virions, we assume that the extracts acted at the level of virus addressable proteins. The existence of some differences in the glycoproteins of the viral envelopes of the two types of viruses is the probable reason for the different activity of the extracts with respect to HHV-1 and HHV-2. Similar results for the virucidal action of biological mollusc material on a number of viruses, including HSV-1, have been reported by other scientific teams [15, 29].

Given the low cytotoxicity and the fact that virucidal activity of hemolymph from *E. verrucosa* with MW 3-100 kDa and mucus from *H. aspersa* with MW over 50 kDa against both types of viruses are strong and nearly 99%, that is sufficient to be considered pharmacologically significant.

It should be noted that the hemolymph of *R. venosa* with MW 30-100 kDa has a strong virucidal action against the first type of virus and a clear effect on the adsorption of both types of viruses. Similar activity against viruses with this type of pathophysiology can be considered a product for human use. The effect of some of the extracts on viral adsorption should not be underestimated, as the virus detects chronic infection in some of the infected tissues.

From the obtained results for the effect of the studied extracts on the adsorption of both types of viruses, as well as for the effect on the extracellular virions of both types of viruses, it can be concluded that the three extracts, hemolymph from *R. venosa* 30-100 kDa, hemolymph from *E. verrucosa* with MW 3-100 kDa and mucus from *H. aspersa* with MW over 50 kDa are suitable for pharmacological studies and use as products. for local application.

Acknowledgements: The work was done with the financial support by DOI-217/30.11.2018 National scientific program “Innovative low-toxic biologically active precise medicine (BioActiveMed).

REFERENCES

1. <https://www.who.int/news-room/fact-sheets/detail/herpes-simplex-virus>.
2. A. Hinkov, P. Angelova, A. Marchev, Y. Hodzhev, V. Tsvetkov, D. Dragolova, D. Todorov, K. Shishkova, V. Kapchina-Toteva, R. Blundell, S. Shishkov, M. Georgiev, *J. Herb. Med.*, **21**, 100334 (2020).
3. F. Morfin, D. Thouvenot, *J. Clin. Virol.*, **26**, 29 (2003).
4. A. F. Rowley, A. Powell, *J. Immunol.*, **179**, 7209 (2007).
5. R. P. Ellis, H. Parry, J. I. Spicer, T. H. Hutchinson, R. K. Pipe, S. Widdicombe, *Fish Shellfish Immunol.*, **30**:1209 (2011).
6. K. Söderhäll, L. Cerenius, *Annu Rev Fish Dis.*, **2**, 3 (1992).
7. P. Dolashka, A. Dolashki, J. Van Beeumen, M. Floetenmeyer, L. Velkova, S. Stevanovic, W. Voelter, *Curr. Pharm. Biotechnol.*, **17**, 263 (2016).
8. P. Dolashka, A. Dolashki, W. Voelter, J. Van Beeumen, S. Stevanovic, *Int. J. Curr. Microbiol. App. Sci.*, **4**, 1061 (2015).
9. A. Dolashki, A. Nissimova, E. Daskalova, L. Velkova, Y. Topalova, P. Hristova, P. Traldi, W. Voelter, P. Dolashka, *Bulg. Chem. Commun.*, **50** Sp.Iss. C, 195 (2018).
10. L. Velkova, D. Todorov, I. Dimitrov, S. Shishkov, J. Van Beeumen, P. Dolashka- Angelova, *Biotech. Biotech. Equip.*, **23**, 606 (2009).
11. P. Dolashka, L. Velkova, S. Shishkov, K. Kostova, A. Dolashki, I. Dimitrov, B. Atanasov, B. Devreese, W. Voelter, J. Van Beeumen, *Carbohydr. Res.*, **345**, 2361 (2010).
12. P. Dolashka, W. Voelter, *Invertebr. Surviv. J.*, **10**, 120 (2013).
13. V. T. Dang, K. Benkendorff, P. Speck, *J. Gen. Virol.*, **92**, 627 (2011).
14. B. Novoa, A. Romero, Á. L. Álvarez, R. Moreira, P. Pereiro, M. M. Costa, S. Dios, A. Estepa, F. Parra, A. Figueras, *J. Virol.*, **90**, 7692 (2016).
15. A. R. de Toledo-Piza, C. A. Figueiredo, M. I. de Oliveira, G. Negri, G. Namiyama, M. Tonelotto, K. Villar, H. K. de S., Rofatto, R. Z. Mendonca, *Antiv. Res.*, **134**, 172 (2016).
16. A. Dolashki, P. Dolashka, A. Stenzl, S. Stevanovic, W. K. Aicher, L. Velkova, R. Velikova, W. Voelter, *Biotech. Biotech. Equip.*, **33**, 20 (2019).
17. A. Alexandrova, L. Petrov, L. Velkova, A. Dolashki, E. Tsvetanova, A. Georgieva, P. Dolashka, *J. Pharm. Pharmacogn. Res.*, **9**, 143 (2021).
18. P. Dolashka-Angelova, H. Schwarz, A. Dolashki, S. Stevanovic, M. Fecker, M. Saeed, W. Voelter, *Biochim. Biophys. Acta*, **1646**, 77. (2003).
19. Y. K. Kizheva, I. K. Rasheva, M. N. Petrova, A. V. Milosheva-Ivanova, L. G. Velkova, P. Aleksandrova Dolashka, A. Dolashki, P. K. Hristova, *Biotechnol. Biotechnol. Equip.*, **33**, 873 (2019).
20. L. Velkova, I. Dimitrov, H. Schwarz, S. Stevanovic, W. Voelter, B. Salvato, P. Dolashka-Angelova, *Comp. Biochem. Physiol. B-Biochem. Mol. Biol.*, **157**, 16 (2010).
21. A. Dolashki, L. Velkova, E. Daskalova, N. Zheleva, Y. Topalova, V. Atanasov, W. Voelter, P. Dolashka, *Biomedicines*, **8**, 315 (2020).
22. U. K. Laemmli, *Nature*, **227**, 680 (1970).
23. T. Mosmann, *J. Immun. Methods*, **65**, 55 (1983).
24. H. Takeuchi, M. Baba, S. Shigeta, *J. Virol. Methods*, **33**, 61 (1991).
25. L. J. Reed, H. Muench, *Am. J. Hyg.*, **27**, 493 (1938).
26. P. Dolashka, A. Dolashki, W. Voelter, J. Van Beeumen, S. Stevanovic, *Int. J. Curr. Microbiol. App. Sci.*, **4**, 1061 (2015).
27. D. Bortolotti, C. Trapella, T. Bernardi, R. Rizzo, *Br. J. Biomed. Sci.*, **73**, 49 (2016).
28. S. J. Pitt, M. A. Graham, C. G. Dedi, P. M. Taylor-Harris, A. Gunn, *Br. J. Biomed. Sci.*, **72**, 174 (2015).
29. M. Salas-Rojas, G. Galvez-Romero, B. Anton-Palma, R. Acevedo, F. Blanco-Favela, A. Aguilar-Setien, *Fish Shellfish Immunol.*, **36**, 158 (2014).

Natural substances with therapeutic potential in wound healing

M. Kermedchiev^{1,3}, M. Lazarova², L. Tancheva^{2*}, D. Uzunova², K. Tasheva⁴, L. Velkova¹, A. Dolashki¹, A. Daskalova¹, V. Atanasov¹, D. Kaynarov¹, P. Dolashka^{1*}

¹ Institute of Organic Chemistry with Centre of Phytochemistry, Bulgarian Academy of Sciences, Acad. G. Bonchev Str., Block 9, Sofia, Bulgaria

² Institute of Neurobiology, Bulgarian Academy of Sciences, Acad. G. Bonchev Str., Block 23, Sofia, Bulgaria

³ UMBAL "Alexandrovska". Emergency Department and Surgery, Medical University of Sofia "Georgi Sofiyanski" Str, Sofia, Bulgaria

⁴ Institute of Plant Physiology and Genetics, Bulgarian Academy of Sciences, Acad. G. Bonchev Str., Block 21, Sofia, Bulgaria

Received January 28, 2021; Revised April 12, 2021

Untreated wounds are a significant health problem that affects the whole world. The healing wounds capacity of different plants and animals extracts is due to their wide variety of bioactive compounds with epithelial cell regenerative effects on wounds. The present study aims to investigate the efficacy of 3 combined preparations (extract 1, extract 2 and extract 3) as potential regenerative products used for healing of skin wounds. The gel compositions were prepared by mixing the extracts of garden snail mucus *H. aspersa* and plants (leaf extract of *Plantago major* and/or flower extract of *Calendula officinalis*) in 5:1:1 ratio. Their wound healing activity was evaluated using the excision wound model on female Wistar rats. The percentage of wound contraction area was calculated precisely on the 3rd, 6th, 10th, 14th and 19th day. Our results demonstrated that extract 3- treated group (containing extract from *P. major* and snail mucus extract) exerted the best rate of wound closer in the period between 6th and 10th day post injury. The reduction of wound area was by 55% on the 6th day and by 21% on the 10th day after injury versus the control untreated group, respectively. extract 1 was the best for wound closing in the period between 3rd and 6th day post injury. The wound area was reduced by extract 1 on the 3th post injury day by 133% and by 61% on the 6th day versus the control. In conclusion the best wound healing effect of Gel 1 suggests a synergic mechanism of action among the three ingredients: mucus from *H. aspersa*, *P. major* leaf extract and extract of *Calendula* flowers.

Key words: snail *Helix aspersa* mucus extract; *Calendula* flower extract; *Plantago major* leaf extract; healing effects

INTRODUCTION

Untreated wounds are one of the most significant health problems in the world and most often lead to complications and limb amputation [1]. Wound healing is a complex process that goes through four partially overlapping stages: hemostasis, inflammation, proliferation and maturation or tissue modelling [1, 2]. The efficiency of healing depends on the synchrony of the four phases, and it can be influenced by many internal (endogenous) and external (exogenous) factors.

Although there are good clinical practices in the world that prevent delayed or chronic wounds/ulcers healing, their effectiveness is still unsatisfactory. In this regard, numerous studies have been conducted on folk methods of treatment as an alternative to modern clinical practices [3, 4]. A number of herbal preparations including extracts and/or purified biologically active compounds with

plant origin have been used to treat skin lesions and are applied in the form of emulsions, creams and ointments [5-7].

Extracts of *Plantago major* (*Plantagiaceae*) and *Calendula officinalis* (*Asteraceae*) are ones of the most widely used natural products for the treatment of skin wounds. *Plantago major* leaves have been used as a wound healing herbal agent for many years in folk and traditional medicine [5]. Flowers of *Calendula officinalis* (*calendula*, marigold) is another medicinal plant which is also used in the modern world due to its pharmacological actions including wound healing and antioxidant. Some authors provide evidence that they increase the activity of white blood cells and accelerate tissue repair [8]. Stimulating angiogenesis, granulation, epithelialization and wound contraction effects were also proven [9, 10].

The combination of plant extracts with some animal products like a honey, propolis or snail extract significantly increases the effectiveness of treatment [7, 11, 12]. The positive wounds healing effects of different plants extracts is due to their

* To whom all correspondence should be sent:
E-mails: lyubkatancheva@gmail.com
pda54@abv.bg

bioactive compounds richness like polysaccharides, lipids, caffeic acid derivatives, flavonoids, iridoid glycosides, terpenoids, phytosterols, essential oils, fatty acids, vitamins, etc., which determines their anti-inflammatory, antibacterial, antifungal and antioxidant properties [11, 12].

The wound-healing effect of mucus from *Helix aspersa* has been related to its antioxidant capacity, possibility to stimulate fibroblast proliferation and also migration and survival of keratinocytes [13, 14]. These results shed light on the molecular mechanisms underlying the regenerative properties of mucus, based on its promoting effect on skin cell migration, proliferation and survival [14].

Recently, Gubitosa *et al.* (2020) used snail mucus from garden snails "Helix aspersa Müller" conjugated with gold nanoparticles (AuNPs-SS) to investigate its anti-inflammatory activity and wound healing potential [15]. The *in vitro* test for AuNPs-SS safety in human keratinocytes demonstrated that AuNPs-SS accelerates wound closure, being associated with increased expression of the urokinase receptor (uPAR), which converts plasminogen to plasmin, degrades the extracellular matrix and directly controls cell adhesion, differentiation and proliferation [15]. The authors explain the observed effect by the presence of functional groups in the proteins, peptides and amino acids (and/or polyphenols) of snail mucus present on the surface of the nanoparticles [15].

The aim of our team was to search alternative pathways for wound healing with bioactive compounds from natural sources. Hence, the present study aims to investigate the efficacy of combined preparations obtained from garden snail mucus (*Helix aspersa*), and extracts from medicinal plants *Calendula officinalis* (flower extract) and *Plantago major* (leaf extract), as potential regenerative products used for healing of skin wounds.

EXPERIMENTAL

Extract preparation

Extracts from medicinal plants *C. officinalis* and *P. major*, and from garden snail (*H. aspersa*) were prepared, as follows:

C. officinalis extract was prepared using dry flowers, extracted by maceration with aqueous ethanol solution (45% v/v ethanol), in a ratio of solvent to raw material 4:1. The maceration process takes place in a closed vessel in the dark for 12 hours, at a temperature of 45 °C, with continuous

shaking. The extraction process ends with ultrasonic extraction at room temperature for 5 minutes at temperature 25 °C (frequency: 40 kHz). After a series of operations, such as: decantation, pressing, centrifugation, vacuum filtration, concentration on a vacuum rotary evaporator, the resulting extract was lyophilized. An extract containing 15% ethanol and 35% glycerol was prepared, with concentration 100 mg/ml dry extract of calendula.

The extraction of the biologically active substances from *P. Major* was made from 300 g of deciduous plantain leaves purchased commercially. Maceration was performed in the dark with an aqueous-alcoholic solution containing 50% ethanol for 24 hours at room temperature (3: 1 solvent to raw material ratio). The extraction process was completed in an ultrasonic bath, in order to better extract the active substances. Ultrasonic extraction was performed for 5 minutes at 25 °C, using an ultrasonic cleaning bath (frequency: 40 kHz). After a series of operations, such as: decantation, pressing, centrifugation, vacuum filtration, concentration on a vacuum rotary evaporator, the resulting extract was lyophilized and finally 3.0 g of dry extract was obtained. Prepared aqueous extract contained 150 mg/ml dry extract of *P. major*.

Snail extract preparation. The mucus was collected from snails *H. aspersa*, grown in Bulgarian eco-farms using patented technology, so the snails survived without disturbing their biological functions [16]. The resulting crude mucus extract was homogenized and centrifuged to remove coarse impurities. After several steps of filtration (also object of patented technology), the native mucus extract was obtained. The protein concentration in the native mucus extract was determined by Bradford assay [17]. The three analysed compositions with potential regenerating effect (CERE) were prepared by mixing the extracts of garden snail, plantain and/or calendula in 5:1:1 ratio.

Mass spectrometric analysis of molecular mass of peptides

Peptides with MW below 10 kDa were analyzed by MALDI-TOF-TOF mass spectrometry on an Autoflex™ III. High Performance MALDI-TOF&TOF/TOF System (Bruker Daltonics). 1.0 µl of the mixture of 2.0 µl of matrix solution (7 mg/ml of α -cyano-4-hydroxycinnamic acid in 50% ACN containing 0.1% TFA) and 1.0 µl of the sample

were mixed and spotted on a stainless steel 192-well target plate. The mixture of angiotensin I, Glu-1-fibrinopeptide B, ACTH (1–17), and ACTH was used for calibration of mass spectrometer. The MS/MS spectra were carried out in reflector mode and the amino acid sequences of peptides were identified by precursor ion fragmentation using MALDI-MS/MS analysis.

SDS-PAGE electrophoresis

The native fresh extract from mucus was analyzed by sodium dodecyl sulfate-polyacrylamide gel electrophoresis (SDS-PAGE) using 5% stacking gel and 12% resolving gel according to Laemmli method with modifications [18]. 20 µg of the sample was loaded on the gel. Protein standard mixture ranging from 10 kDa to 250 kDa (Precision Plus Protein™ Standard All Blue, Bio-Rad Laboratories, Germany) was used as molecular marker. Coomassie Brilliant Blue G-250 staining was used for the visualization.

In vivo studies on the regenerating effect on wounds of the three combined extracts

Laboratory animals: Female adult Wistar rats (190–220 g) were adapted under standard conditions of the local vivarium for 7 days before the experiment. Rats were divided in 4 groups and received food and water ad libitum.

Experimental model of excision wounds: The rats were anaesthetized by Chloral hydrate (400 mg/kg intraperitoneally (i.p.)). All animals were depilated at dorsal thoracic region and full thickness of skin was cut off from a pre-determined area. The wound area was measured immediately by tracing it on transparent paper and calculated in square centimeters [19]. For measuring wound contraction, the same protocol was followed on the 3rd, 6th, 10th, 14th and 19th day and the percentage of wound contraction area was calculated.

The raw area at the time of wounding was considered as 100%, and the wounding day was considered as day zero.

Treatment: All wounds were initially disinfected with 3% of H₂O₂ and further daily treated with different CERE according to the groups. Control rats did not receive any treatment. Rats were divided in single cages to protect animals from additional hurts and infections. Each experimental group contained of 6 animals. The wound healing activity of the three snail gels (CERE 1, CERE 2 and CERE 3) was evaluated by monitoring wound's

contraction percentage in comparison to the controls using the excision wound model.

Statistical analysis

The statistical analysis of the experimental data was performed according to Student Fisher's *t*-test and the results were considered significant at $P < 0.05$.

RESULTS AND DISCUSSION

A number of natural extracts have been used in the care of skin wounds for many years due to their therapeutic activities, including anti-inflammatory, antimicrobial and cell stimulating properties. The native combined extracts of fresh mucus from garden snail (*H. aspersa*) as well as of some medicinal plants were known by folk medicine. Even though they were used for ages, new interest towards their skin regeneration properties had rapidly increased in the last few years [8, 14, 19]. Recent data discovered the variety of active components of the natural extracts, responsible for their biological activities. However, interdisciplinary studies are necessary for development of efficient standardized products for use in the medical practice.

Our team reported recently new data about antimicrobial activity of several peptide and protein fractions isolated from garden snail *H. aspersa* [16, 20, 21]. These data are in agreement with established antimicrobial properties of the mucus from *H. aspersa*, and *A. fulica* [22]. In the region above 100 kDa, proteins might correspond to glycoproteins and mucines, which have been detected in the mucus from *H. aspersa* and *H. pomatia* [23]. Additionally, the mucus from the garden snail has been found to contain allantoin (2,5-Dioxo-4-imidazolidinyl urea), glycolic acid, glutathione (GSH) and peptides with antibacterial and antioxidant properties [24, 25].

In fact, the proteins, peptides and amino acids (and/or polyphenols) in the mucus play a key role in cell regeneration and growth, preventing the effects of inflammatory disease [15, 26]. Recently, Gubitosa and co-workers explained the observed effect by the presence of functional groups in the proteins, peptides and amino acids (and/or polyphenols) of snail mucus present on the surface of AuNP [15]. Therefore, new studies revealed the regenerative properties of the secretion of *H. aspersa*. *In vitro* tests showed that the snail mucus promotes proliferation, migration and survival of keratinocytes and dermal fibroblasts [14]. On the

basis of this knowledge as well as having in mind the results from our previous studies, we prepared the combined extracts with potential regenerating effect (CERE) on open wounds. The complex - mixture of natural extracts, contains garden snail mucus, *C. officinalis* and *P. major*. We expect that their accelerating effects on wound healing processes will be due to stimulation of the regeneration process and prevention of the wound infection.

The content of the prepared snail extract was analyzed by 12% SDS-PAGE. Fig. 1 shows that the mucus is a complex mixture of substances with different molecular weight. Several protein bands in wide range 25 -35 kDa, 38 - 40 kDa, 45-50 kDa; 80-90 kDa and above 250 kDa were detected from SDS-PAGE (Fig. 1). Moreover, the mucus peptides with a MW below 3 kDa were determined by MALDI-MS analyzes (Fig. 2).

The amino acid sequence of different peptides from mucus of *C. aspersa* clearly demonstrates presence of many important amino acids such as glycine, proline and tryptophan [16], associated with established antibacterial activities in peptides.

The extracts of *C. officinalis* and *P. major* were prepared as it was described under Experimental section. Both extracts contain 15% ethanol and 35% glycerol, 100 mg dry *Calendula* extract and/or 150 mg dry *P. major* extract in 1 ml. The garden snail extract was obtained as it was described previously [16]. We combined the extracts after homogenization of aqueous mucus (with a

concentration of 0.3 mg/ml protein determined by Bradford analysis) [17] and/or an extract of *P. major* and/or an extract of calendula. The different CERE formulations tested in this study are shown in Table 1.

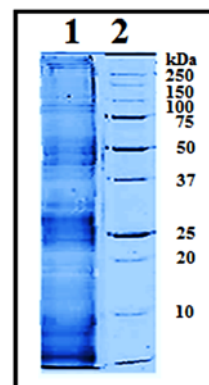


Fig. 1. SDS-PAGE of *H. aspersa* mucus (1), MW marker (2).

The wound healing potential of three tested combined extracts CERE 1, CERE 2 and CERE 3 was evaluated by using an excision wound model. Our results showed that local application of CERE 1 and CERE 3 accelerated the progression of wound healing as compared to control untreated animals. The positive effect on wound healing of CERE 1 and CERE 3 gels was different both in terms of strength and in terms of the stage of wound healing processes in which it occurs (Fig. 3). The healing effect of CERE 2 on wounds was not significant.

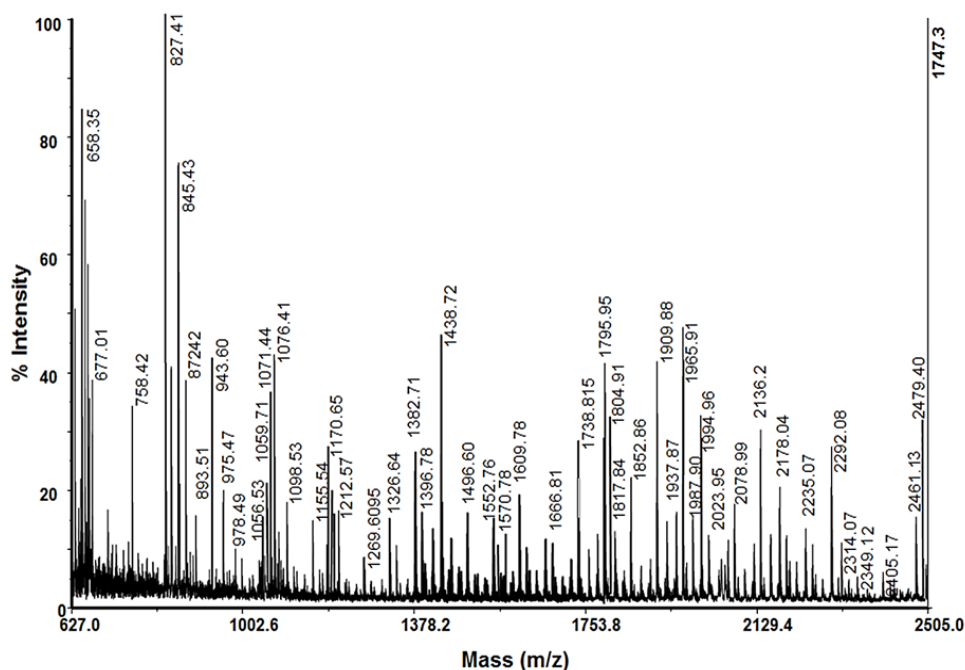


Fig. 2. Mass spectrometric spectrum of peptide fraction with Mw < 3 kDa by AutoflexTM III, High Performance MALDI-TOF&TOF/TOF Systems (Bruker Daltonics, Bremen, Germany).

Table 1. Composition of the studied Combined Extracts with potential Regenerating Effect (CERE).

Combined extract 1 (CERE 1)	
Native water mucus extract	25 ml
Extract from <i>Plantago major</i>	5 ml
Extract from <i>Calendula officinalis</i>	5 ml
Combined extract 2 (CERE 2)	
Native water mucus extract	25 ml
Extract from <i>Calendula officinalis</i>	5 ml
Distilled water	5 ml
Combined extract 3 (CERE 3)	
Native water mucus extract	25 ml
Extract from <i>Plantago major</i>	5 ml
Distilled water	5 ml

The complex process of wound-healing includes the following stages: coagulation, inflammation, collagenase, wound contraction and epithelialization [1, 2]. It is well known that approximately after 3 days from the initial wound, the proliferative phase centres around fibroblasts and the production of both collagen and ground substance forms the basis for the tissue scaffold of the wound area. This is a stage of enhanced macrophage secretion of growth factors and cytokines that promotes tissue proliferation and cell migration. Meanwhile, endothelial cells enter in a rapid growth phase and angiogenesis occurs within the granulation tissue, creating a rich vascular network supplying this very active area of healing [27], and the wound tissue matures and restores [8].

Our results demonstrated that wounds treated with CERE 1 (containing extract from *P. major*, *C.*

officinalis and mucus extract) exerted the best rate of wound closer in the period between 3th and 6th day post injury (Figs. 3, 4, 5 and 6). The wound area was reduced by CERE 1 on the 3th day post injury by 133% ($P < 0.01$) and by 61% ($P < 0.05$) on the 6th day versus the control. From the 10th days after injury until the end of our experiment the rate of wound healing in CERE 1 and control group was commensurable.

The best wound healing effect of CERE 1 suggests a synergic mechanism of action among the three ingredients, namely the native snail mucus, the extract of *P. major* and the extract of *Calendula*. The obtained results are in accordance with the known literature data, proving the effectiveness of the main components of the used extracts in the treatment of wounds of different origin. Wound-healing positive effect of mucus from *Helix aspersa* was already reported and it is due to the antioxidant capacity and possibility for stimulation of fibroblast proliferation [13]. Methanol and aqueous extracts from the leaves of *Plantago major* show regenerating and stimulating effect on wounds caused by burns [28], processes connected with enhanced cell proliferation and migration [29]. On the other hand, wound healing by enhancing fibroblast proliferation, collagen bundle synthesis and revascularization in skin injuries treated by combination of *Plantago major* with *Aloe vera* was also reported [30]. Ethanol extract of *Calendula blossom* significantly improves wound healing in experimentally induced thermal burns in rats due to the increase in collagen hydroxyproline and hexosamine content [31]. Antimicrobial, antioxidant properties, improved recovery from the inflammation phase and increased production of granulation tissue were also reported [32-34].

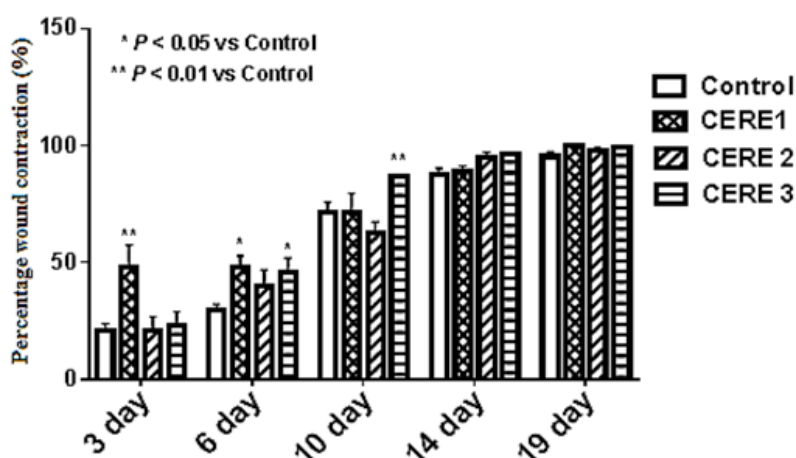


Fig. 3. Effect of combined extracts CERE 1, CERE 2 and CERE 3 on excision wound expressed as percentage of wound contraction.



Fig. 4. Control rats untreated with CERE. Measurement of the size of the wound on: (a) 3rd, (b) 6th, (c) 10th, (d) 14th and (e) 19th day.

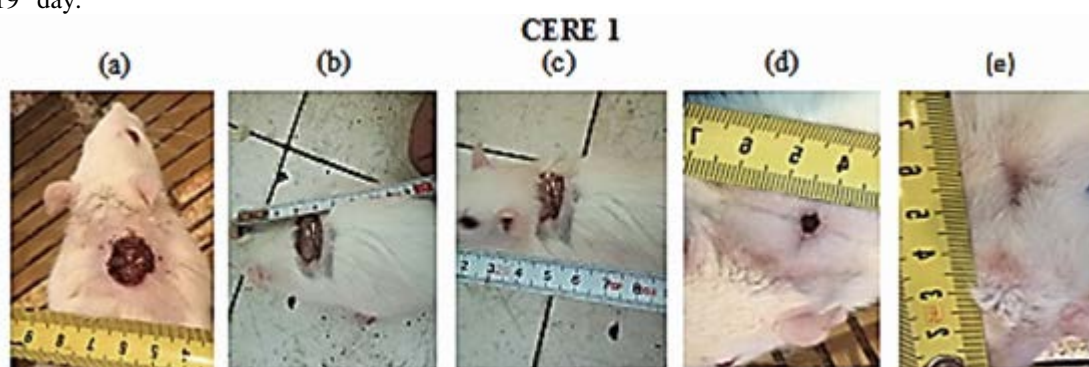


Fig. 5. Treated rats with CERE 1 and measurement of the size of the wound on: (a) 3rd, (b) 6th, (c) 10th, (d) 14th and (e) 19th day.

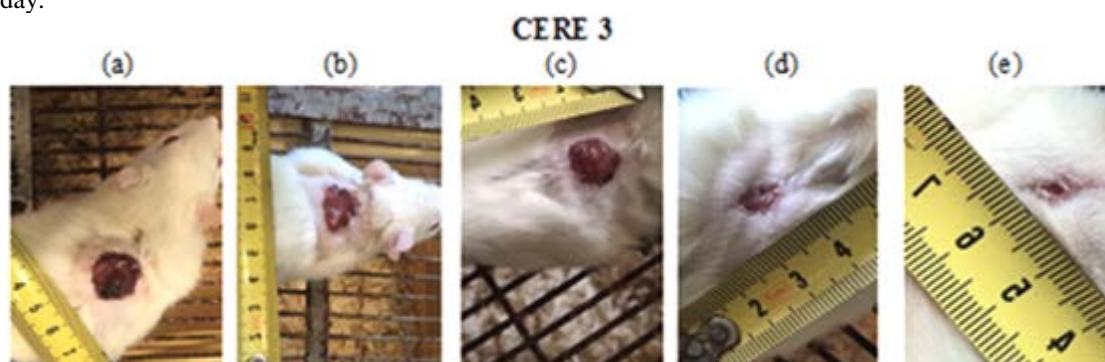


Fig. 6. Treated rats with CERE 3 and measurement of the size of the wound on: (a) 3rd, (b) 6th, (c) 10th, (d) 14th and (e) 19th day.

The herbal agents from leaves of *P. major* and *Calendula* extracts also have shown beneficial effects of the complex product in the treatment of wounds. Samuelsen *et al.* reported that the topical treatment with *P. major* extract eradicated the infections and healed the wounds [35]. However, our data showed that application of only the extract of *Calendula* with mucus extract (CERE 2) is the less efficient combination. The obtained experimental results clearly demonstrated positive effects of preparations CERE 1 and CERE 3 on wound healing process. Due to the richness of biologically active compounds in the three extracts, CERE 1 was found to be with the highest wound-

healing potential. It is known that plant extracts are rich in vitamins C, A and K, glycosides, allantoin, tannins terpenoids, flavonoids, saponins, coumarines, quinones, volatile oil, carotenoids and amino acids [11]. These phytoconstituents have wide applicability as antioxidant, antimicrobial, anti-inflammatory, anti-ulcer, anti-proliferative, antiparasitic, hypoglycemic, hypolipidemic and wound healing potential in experimental and clinical trials [7, 32].

CONCLUSION

On experimental rat's excised wound models we observed significant acceleration of healing process

of the wounds treated with CERE 1 and CERE 3 in comparison to untreated controls. The best wound healing effect showed mixture from mucus from *H. aspersa*, *P. major* leaf extract and extract of *Calendula* flowers (CERE 1). Further research shall clarify the individual role of biologically active ingredients as well as their interactions.

Acknowledgements: This research was supported by the Bulgarian Ministry of Education and Science (Grant D01-217/30.11.2018) under the National Research Programme “Innovative Low-Toxic Bioactive Systems for Precision Medicine (BioActiveMed)” approved by DCM#658 from 14.09.2018 and with the support of a project under contract No. KP-06-OPR 03-10/2018, funded by the Scientific Research Fund of the Ministry of Education and Science in the Republic of Bulgaria.

REFERENCES

- H. Brem, M. Tomic-Canic, *J. Clin. Invest.*, **117**, 1219 (2007).
- A. Gosain, L. A. Di Pietro, *World J. Surg.*, **28**, 32 (2004).
- D. Mathieu, J. C. Linke, F. Wattel, in: Handbook on Hyperbaric Medicine, D. E. Mathieu (ed.), Netherlands, Springer, 2006, p. 401.
- S. Das, B. Mishra, K. Gill, M. S. Ashraf, A. K. Singh, M. Sinha, S. Sharma, I. Xess, K. Dalal, T. P. Singh, S. Dey, *Int. J. Biol. Macromol.*, **48**, 38 (2011).
- I. Binić, A. Janković, D. Janković, I. Janković, Z. Vrucinić, *Phytother. Res.*, **24**, 277 (2010).
- M. Pellizzoni, G. Ruzickova, L. Kalhotka, L. Lucini, *J. Med. Plants Res.*, **6**, 1975 (2012).
- L. M. L. Parente, R. S. L. Júnior, L. M. F. Tresvenzol, M. C. Vinaud, J. R. de Paula, N. M. Paulo, *Evid. Based Complement. Alternat. Med.*, **2012**, 375671 (2012).
- G. Han, R. Ceilley, *Adv. Ther.*, **34**, 599 (2017).
- P. H. S. Kwakman, S.A.J. Zaat, *IUBMB Life*, **64**, 48 (2012).
- G. A. Burdock, *Food Chem. Toxicol.*, **36**, 347 (1998).
- B. P. Muley, S. S. Khadabadi, N. B. Banarase, *Tropic J. Pharmaceut. Res.*, **8**, 455 (2009).
- E. Reina, N. A.-Shibani, E. Allam, K. S. Gregson, M. Kowolik, L. J. Windsor, *J. Tradit. Complement. Med.*, **3**, 268 (2013).
- A. Brieva, N. Philips, R. Tejedor, A. Guerrero, J.P. Pivel, J.L. Alonso-Lebrero, S. Gonzalez, *Skin Pharmacol. Physiol.*, **21**, 15 (2008).
- M. C. Cruz, F. Sanz-Rodríguez, A. Zamarrón, E. Reyes, E. Carrasco, S. González, A. Juarranz, *Int. J. Cosmet. Sci.*, **34**, 1839 (2012).
- J. Gubitosa, V. Rizzi, P. Fini, A. Laurenzana, G. Fibbi, C. Veiga-Villauriz, F. Fanelli, F. Fracassi, A. Onzo, G. Bianco, C. Gaeta, A. Guerrieri, P. Cosma, *Soft Matter.*, **6**, 10876 (2020).
- A. Dolashki, L. Velkova, E. Daskalova, N. Zheleva, Y. Topalova, V. Atanasov, W. Voelter, P. Dolashka, *Biomedicines*, **8**, 315 (2020).
- M. M. Bradford, *Anal. Biochem.*, **72**, 2484 (1976).
- U. K. Laemmli, *Nature*, **227**, 680 (1970).
- J. J. Morton, M. H. Malone, *Arch. Int. Pharmacodyn. Ther.*, **196**, 117 (1972).
- P. Dolashka, A. Dolashki, L. Velkova, S. Stevanovic, L. Molin, P. Traldi, R. Velikova, W. Voelter, *J. BioSci. Biotechnol.*, SE/ONLINE, 147 (2015).
- L. Velkova, A. Nissimova, A. Dolashki, E. Daskalova, P. Dolashka, Y. Topalova, *Bulg. Chem. Commun.*, **50C**, 169 (2018).
- S. J. Pitt, J. A. Hawthorne, M. Garcia-Maya, A. Alexandrovich, R. C. Symonds, A. Gunn, *Br. J. Biomed. Sci.*, **76**, 129 (2019).
- U. I. Gabriel, S. Mirela, J. Ionel, J. Agroalim, *Processes Technol.*, **17**, 410 (2011).
- N. G. Vassilev, S. D. Simova, M. Dangelov, L. Velkova, V. Atanasov, A. Dolashki, P. Dolashka, *Metabolites*, **10**, 360 (2020).
- N. Kostadinova, Y. Voynikov, A. Dolashki, E. Krumova, R. Abrashev, D. Kowalewski, S. Stevanovic, L. Velkova, R. Velikova, P. Dolashka, *Bulg. Chem. Commun.*, **50C**, 176 (2018).
- A. S. Harti, S. D. Sulisetyawati, A. Murharyati, M. Oktariani, *Int. J. Pharma Med. Biol. Sci.*, **5**, 76 (2016).
- K. Haukipuro, J. Melkko, L. Risteli, M. Kairaluoma, J. Risteli, *Ann. Surg.*, **213**, 75 (1991).
- M. Amini, M. Kherad, D. Mehrabani, N. Azarpira, M. Panjehshahin, N. Tanideh, *J. Appl. Anim. Res.*, **37**, 53 (2010).
- R. Velasco-Lezama, R. Tapia-Aguilar, R. Roman-Ramos, E. Vega-Avila, M. S. Perez-Gutierrez, *J. Ethnopharmacol.*, **103**, 36 (2006).
- S. Ashkani-Esfahani, M. Khoshneviszadeh, A. Noorafshan, R. Miri, S. Rafiee, K. Hemyari, S. Kardeh, O. Koohi Hosseinabadi, D. Fani, E. Faridi, *World J. Plastic Surgery*, **8**, 51 (2019).
- P. K. Chandran, R. Kutton, *J. Clin. Biochem. Nutr.*, **43**, 58 (2008).
- M. J. Leach, *Wounds*, **20**, 236 (2008).
- O. Givol, R. Kornhaber, D. Vissentin, M. Cleary, J. Haik, M. Harats, *Wound Repair Regen.*, **27**, 548 (2019).
- C. Nicolaus, S. Junghanns, A. Hartmann, R. Murillo, M. Ganzera, I. Merfort, *J. Ethnopharmacol.*, **196**, 94 (2017).
- A. B. Samuelsen, *J. Ethnopharmacol.*, **71**, 1 (2000).

Silica supported iron and chromium oxide catalysts for methanol decomposition

G. Issa*¹, N. Velinov², D. Kovacheva², T. Tsoncheva¹

¹ Institute of Organic Chemistry with Centre of Phytochemistry, Bulgarian Academy of Sciences, Acad. G. Bonchev Str. Bl. 9, 1113 Sofia, Bulgaria

² Institute of General and Inorganic Chemistry, Bulgarian Academy of Sciences, Acad. G. Bonchev Str. Bl. 11, 1113 Sofia, Bulgaria

Received January 31, 2021; Revised March 25, 2021

In present study mesoporous iron–chromium oxide silica materials with different composition were prepared by wet impregnation method. The obtained composites were characterized by XRD, UV-Vis, FTIR, Mossbauer spectroscopy and temperature programmed reduction (TPR). The catalytic behaviour of the samples was tested in methanol decomposition to syngas. The effect of phase composition on the structure and redox properties was discussed in close relation with their catalytic activity and CO selectivity. It was found that the catalytic behavior of the samples in the methanol decomposition could be successfully controlled by the Fe/Cr ratio.

Key words: iron and chromium oxide catalysts; methanol decomposition

INTRODUCTION

Methanol is expected to become one of the new liquid energy carriers because it can be synthesized from biomass, coal and natural gas, all of them being more abundant resources than the crude oil. In the last two decades among the various procedures of methanol conversion (steam reforming, partial oxidation, etc.), methanol decomposition has received growing attention as a source of hydrogen and synthesis gas for chemical reactions or as an ecological fuel for gas turbines, vehicles and fuel cells [1-6]. The synthesis and characterization of novel multicomponent nanosized materials have been intensively investigated because of their wide application in various fields, in particular in the field of catalysis [7-10]. The requirements for them are high, both for their activity, selectivity and stability during operation, as well as from an economic point of view - low cost and ability to operate at relatively low temperatures. These issues are in the focus of many studies and patents in which innovative porous materials based on transition metals and nanosized metal oxides are used [11, 12]. They are one of the most important and widely used categories of solid catalysts that could be used both as active phases and supports. They have been widely used for various catalytic reactions, including oxidation, dehydration, dehydrogenation and isomerization [10-12]. The mixed metal oxides

are oxygen-containing combinations of two or more metal ions, which ratio can be varied or defined by strict stoichiometry. Furthermore, the nanosized materials consisting of more components in different proportions reveal unlimited possibilities to improve the catalytic properties of materials through structural, phase composition and textural changes, improved thermal stability, changes in the acid-basic and redox properties and the occurrence of synergistic effects between the individual components. Large scale application of iron oxide with small particles and tailoring of specific properties have prompted the development of widely used chemical methods, including sol–gel methods, microwave plasma, host template, coprecipitation, micro emission methods, citrate precursor techniques and mechanical alloying for the fabrication of stoichiometric and chemically pure spinel ferrite nanoparticles [13-15]. Iron–chromium oxides, both in crystalline and amorphous states, were obtained using ultrasonic radiation hydrothermal methods, and thermal decomposition of mixtures of salts as metal sources [16-20]. The Fe₂O₃–Cr₂O₃ mixed oxide system has been widely studied due to its potential application as catalysts in wide range of reactions especially in the high temperature water gas shift reaction, dehydration of ethyl benzene to styrene, oxidative dehydrogenation of butene to butadiene, etc [16-18]. The magnetite (Fe₃O₄) type of iron oxide was found to be the active phase of WGS reaction [21]. It was found the role of chromium is believed to increase the surface area of catalyst and prevent sintering, thus increasing catalyst life time. It is also

* To whom all correspondence should be sent:
E-mail: issa@abv.bg

reported by Instituto *et al.* [22], copper improves the performance of the iron and chromium based catalysts towards the high temperature shift reaction, by increasing the intrinsic activity. Nair and Kurian [23] tested chromium substituted zinc ferrite nanocatalysts for the degradation of 4-chlorophenol, 2,4-dichlorophenol and 2,4-dichlorophenoxy acetic acid by wet peroxide oxidation process. It is established that chromium substitution increased the activity of zinc ferrite catalyst and the unsubstituted chromium ferrite exhibited highest activity. Moreover, Gonzalez *et al.* [24] study the reduction properties of high temperature water gas shift catalysts (Cr_2O_3 added to Fe_2O_3) with various of reducing mixture. In their study, chromium is believed to act as a dispersing agent which makes Fe_2O_3 reduction process become easier. This study is focused on the preparation and characterization of series of supported on silica iron-chromium mixed oxides by wet impregnation techniques. Their application as catalysts for methanol decomposition was studied in details. The elucidation of the relation between the Fe/Cr ratio and the structure, texture, morphology, surface and catalytic properties of the obtained materials was the main challenge in the study. For the purpose, the obtained materials were characterized by a complex of different physicochemical techniques, such as XRD, FTIR, UV-Vis and Mossbauer spectroscopies and TPR with hydrogen.

EXPERIMENTAL

Iron and chromium supported on silica (Cabosil M5, 99.8%) materials with total metal content of 6 wt.% were prepared by wet impregnation method of silica with $\text{Fe}(\text{NO}_3)_3 \cdot 9\text{H}_2\text{O}$ ($\geq 98\%$) and/or $\text{Cr}(\text{NO}_3)_3 \cdot 9\text{H}_2\text{O}$ (99%) aqueous solution in appropriate ratio. The powder samples were calcined at 773 K for 2 h in nitrogen atmosphere and denoted as $m\text{Fe}n\text{Cr}/\text{SiO}_2$ where m/n corresponds to the ratio between the amount of different metals in wt.%

Powder X-ray diffraction study was performed on a Bruker D8 Advance diffractometer with $\text{Cu K}\alpha$ radiation ($\lambda=1.5406 \text{ \AA}$) and a LynxEye detector with constant step of $0.02^\circ 2\theta$ and counting time of 17.5 s per step. The FTIR and UV-Vis spectra were recorded on a Bruker Vector 22 FTIR spectrometer and Jasco V-650 apparatus, respectively. The Mossbauer spectra were obtained on a with a Wissel (Wissenschaftliche Elektronik GmbH, Germany) electromechanical spectrometer using

$^{57}\text{Co}/\text{Rh}$ source and $\alpha\text{-Fe}$ standard. The TPR/TG (temperature-programmed reduction/thermogravimetric) analyses were performed in a DSC/TGA NETZSCH instrument. Typically, 20 mg of the sample were placed in a microbalance crucible and heated in a flow of 50 vol.% H_2 in Ar ($100^\circ \text{cm}^3 \text{min}^{-1}$) up to 773 K at $5 \text{ K}\cdot\text{min}^{-1}$ and a final hold-up of 1 h. Methanol conversion was carried out in a fixed bed flow reactor (0.055 g of catalyst), argon being used as a carrier gas ($50 \text{ cm}^3 \cdot \text{min}^{-1}$). The methanol partial pressure was 1.57 kPa. The catalysts were tested under conditions of a temperature-programmed regime within the range of 350–770 K with heating rate of $1 \text{ K}\cdot\text{min}^{-1}$. On-line gas chromatographic analyses were performed on SCION INSTRUMENTS equipped with flame ionization and thermo-conductivity detectors, on a PLOT Q column, using an absolute calibration method and a carbon based material balance.

RESULTS AND DISCUSSION

Fig. 1 shows X-ray diffraction (XRD) patterns of the iron and chromium supported on silica materials. In case of the iron modification, the slight reflections at 35.4° , 42.8° , 56.7° and $62.6^\circ 2\theta$ are detected [19]. They could be indexed to (311), (400) (511) and (440) planes of cubic Fe_3O_4 with crystallite size of about 10 nm. The patterns of chromium modification exhibit reflections at 33.6° , 43.5° and $64.3^\circ 2\theta$ which are assigned as Cr_2O_3 with average crystallite size of about 9 nm [20].

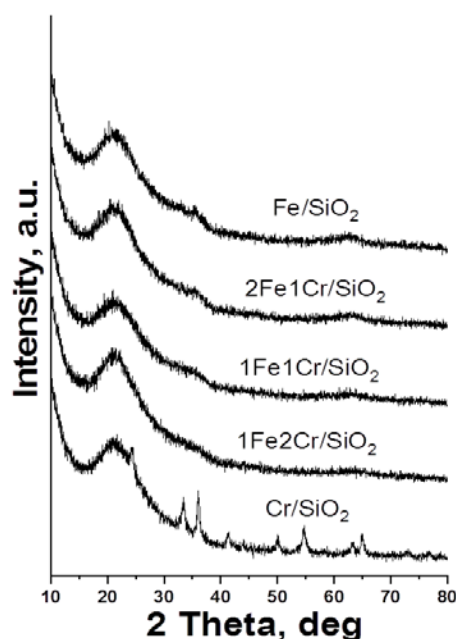


Fig. 1. XRD patterns of all iron and chromium oxide materials.

The XRD patterns of all mixed oxide (Fig. 1) represent very broad peaks and no reflections associated with the iron and chromium oxides are observed, probably due to their high dispersion. The formation of $\text{Cr}_{1.5}\text{Fe}_{1.5}\text{O}_4$ and CrFe_2O_4 mixed oxide with spinel structure has been reported [19, 22-25]. Similar tendency for homogeneous spreading of Cr^{3+} ions in the magnetite lattice by occupying of the octahedral sites and a simultaneous transfer of the displaced Fe^{2+} and Fe^{3+} ions to tetrahedral sites was reported in [25].

FTIR spectra of all silica materials consist of intense bands at around 1080, 800 and 450 cm^{-1} , which are typical of the characteristic symmetric and asymmetric vibrations of Si-O-Si bridges in silicas (Fig. 2a) [12]. The band around 1600 cm^{-1} is due to the adsorbed water molecules and the broad band in the interval 3100–3700 cm^{-1} is assigned to O-H stretching vibrations. The band at 538 cm^{-1} is assigned to Cr-O vibration, whereas a wider band centered at 640 cm^{-1} could be assigned to Fe-O vibrations [26-28]. The band around 960 cm^{-1} is more complicated and it is assigned generally to Si-O stretching vibrations in defect Si-O-M structures, where M is metal ion (Fig. 2a) [29]. The slight shift of the band as compared to pure silica support [29] indicates interaction between metal oxide species and surface silanol groups. This interaction seems to decrease for bi-component iron-chromium materials, probably due to the creation of new contact between both metal oxide nanoparticles.

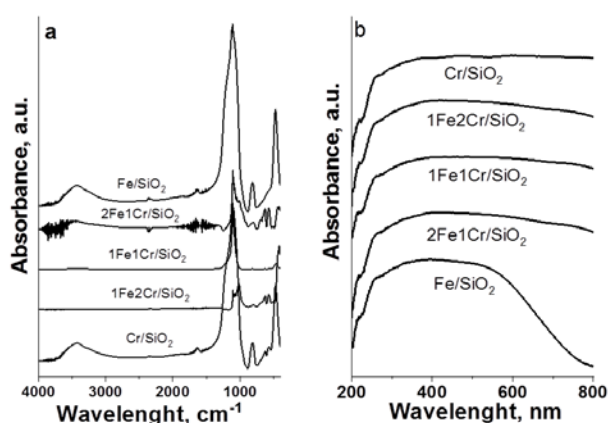


Fig. 2. FTIR spectra (a) and UV-Vis spectra (b) for all iron and chromium oxide materials.

The UV-Vis spectrum of pure iron oxide represents a broad absorption band in the 240-400 nm region which could be due to the superposition of various features assigned to mononuclear Fe^{3+} ions in octahedral coordination, small $(\text{FeO})_n$ clusters and/or Fe_2O_3 particles (Fig. 2b) [30-32]. The small absorption band observed below 250 nm

is possibly related to the presence of Fe^{3+} cations in tetrahedral coordination (Fig. 2b). The bands with maxima at about 250–300 and 300–400 nm can be connected with the presence of monomeric iron cations in octahedral coordination, while the band located above 400 nm is related to Fe_2O_3 particles [30]. The observed blue shift of these peaks for Fe/SiO₂ in comparison with bi-component oxides indicates the higher dispersion of iron nanoparticles in mixed materials or interaction between iron and chromium particles (Fig. 2b) and these results are consistent with XRD data. In the case of the chromium modified samples, the band at about 250, 350 and 450 nm are connected with the presence of tetrahedrally coordinated Cr^{6+} into small mono- or polychromate species [32]. The slight absorption above 600 nm is assigned to the presence of Cr^{3+} in ion-exchange positions ($\text{Cr}^{3+} \rightarrow \text{Cr}^{6+}$) or in Cr_2O_3 or Cr_xO_y clusters [32]. In accordance with XRD and FTIR data, the observed changes in absorption above 350 nm for all bi-component materials confirm the assumption done above for the existence of strong interaction between metal ions and/or to the improved metal oxides dispersion.

Mossbauer spectroscopy was applied to obtain more information about the phase composition, cationic occupations and/or different state distribution of iron ions in the studied oxide materials (Table 1). The characteristic parameter, isomer shift (IS), quadruple splitting (QS) and the relative part of each component (G) are listed in Table 1. The spectra of all oxide materials consist of doublet components. Their parameters indicate presence of paramagnetic or super paramagnetic phases, where iron is in trivalent state and octahedral coordination. The relatively high values of quadrupole splitting (QS), could be due to the spinel lattice distortion caused by the formation of oxygen vacancies. The QS parameters increase with the increase of chromium content in the samples (Table 1). This evidences that with the increase of chromium content in the samples the electric field around the iron cores becomes more asymmetric. This confirms the presence of chromium in the vicinity of the iron in proportion to the chromium content in the sample.

Table 1. Moessbauer parameters for all iron and chromium oxide materials.

Sample	Components	IS, mm/s	QS, mm/s	G_{exp} , mm/s
Fe/SiO ₂	Db - $\text{Fe}^{3+}_{\text{octa}}$	0.34	0.77	0.52
2Fe1Cr/SiO ₂	Db - $\text{Fe}^{3+}_{\text{octa}}$	0.33	0.87	0.52
1Fe1Cr/SiO ₂	Db - $\text{Fe}^{3+}_{\text{octa}}$	0.33	0.93	0.54
1Fe2Cr/SiO ₂	Db - $\text{Fe}^{3+}_{\text{octa}}$	0.31	1.03	0.68

To study changes in catalysts reducibility, iron and chromium materials were analyzed by TPR (Fig. 3). TPR profile of Fe/SiO₂ shows one reduction peak at about 630 K. According to the UV-Vis and Mossbauer data, this effect belongs to the reduction of Fe₂O₃ to Fe₃O₄ [32]. The second peak above 670 K originates with partial two step reduction of Fe₃O₄ to FeO and FeO to metallic Fe [19, 32-35]. The TPR effects for the binary oxide materials were broader and shifted to higher temperature as compared to the corresponding individual iron modification. This evidence change in the environment of iron ions, most probably due to the formation of ferrite phase (Table 1) [29, 36, 37]. The complexity of the TPR profile of 2Fe1Cr/SiO₂ can tentatively attributed to the existence of hematite and magnetite impurities in the spinel phase (Fig. 3).

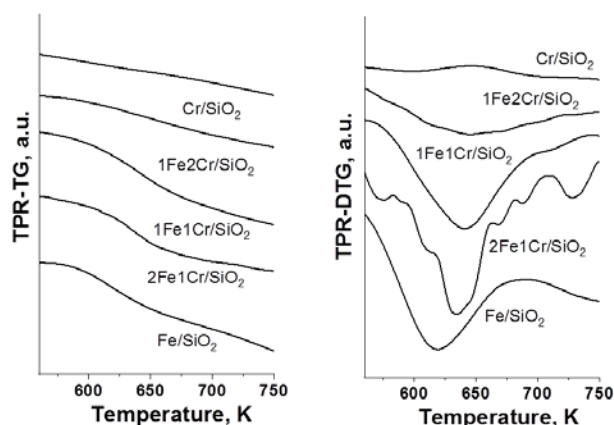


Fig. 3. TPR-TG and TPR-DTG profiles for all iron and chromium oxide materials.

In Fig. 4 are demonstrated the temperature dependencies of methanol decomposition on various iron and chromium modifications. The conversion is observed above 650 K and CO, methane, dimethyl ether (DME) and CO₂ in different proportions are detected.

Among the mono-component materials, the pure iron oxide demonstrates higher catalytic activity in methanol decomposition to syngas. The appearance of a plateau in its conversion curve above 680K is evidence for catalyst deactivation. In accordance with the TPR data (Fig. 3) this could be assigned to reduction transformations with the active magnetite phase. The observed high selectivity to methane (at 30% conversion, 98% for Fe/SiO₂, 67% for 2Fe1Cr/SiO₂, 43% for 1Fe1Cr/SiO₂ and 50% for 1Fe2Cr/SiO₂) could be related to facile C-O bond scission in the adsorbed methanol molecules due to the simultaneous activity of strong basic (oxygen ions) and acid (iron ions) sites in magnetite and/or

hematite species. The Cr/SiO₂ material exhibits extremely low catalytic activity during the whole temperature interval and maximum conversion of about 40% is detected just at 700 K. At this temperature a fast decrease in the conversion is observed (Fig. 4), most probably due to the aggregation of the active phase and/or formation of non-desorbable products.

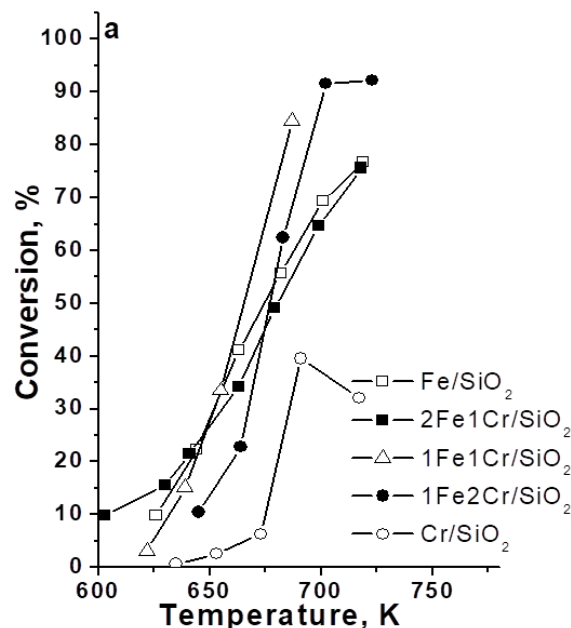


Fig. 4. Methanol conversion for all iron and chromium oxide materials.

All binary materials exhibit improved catalytic behavior as compared to the individual oxides (Fig. 4). The extremely high activity is observed for the sample with equimolar Fe/Cr ratio (1Fe1Cr/SiO₂) which could be due to the formation of finely dispersed spinel phase (Fig. 1, Table 1). The impact of the activity of Cr³⁺-Fe²⁺ redox pairs, situated in the highly exposed to the reactants octahedral positions in the spinel lattice could be proposed. In accordance with the TPR data, the lowest catalytic activity for the binary material with the highest Fe/Cr ratio could be attributed to the existence of FeO_x impurities in the spinel phase. The stability of all catalysts was examined after the catalytic test up to 773 K. All oxide materials retain their catalytic activity and selectivity, with the exception of mono-component chromium oxide, in which low stability is observed. A common feature of the binary catalysts is their improved stability to the influence of the reaction medium. This could be due to the fast release of the formed during the reaction carbon deposits *via* oxidation from the high mobile oxygen ions from the spinel lattice.

CONCLUSION

Supported on silica nanosized iron and chromium spinel oxides could be successfully synthesized using wet impregnation technique with aqueous solutions of metal salts in appropriate ratio. Their composition could be tuned with the Fe/Ce ratio. The equimolar Fe/Cr content facilitates formation of more homogeneous and finely dispersed materials. They demonstrate extremely high catalytic activity and improved stability in methanol decomposition in a wide temperature interval.

Acknowledgements: This work was supported by the Bulgarian Ministry of Education and Science under the National Research Programme “Young scientists and postdoctoral students” approved by DCM#577/17.08.2018 and the Bulgarian Science Fund Contract No KII-06-H29/2. Project BG05M2OP001-1.002-0019: „Clean technologies for sustainable environment – water, waste, energy for circular economy“(Clean&Circle), for development of a Centre of Competence is also acknowledged.

REFERENCES

1. T. Rauckyte, D. J. Hargreaves, Z. Pawlak, *Fuel*, **85**, 481 (2006).
2. A. Pohar, D. Belavi, G. Dolan, S. Hocevar, *J. Power Sources*, **256**, 80 (2014).
3. S. T. Yong, C. W. Ooi, S. P. Chai, X. S. Wu, *Inter. J. Hydrogen energy*, **38**, 9541 (2013).
4. A. Qi, B. Peppley, K. Karan, *Fuel Process. Technol.*, **88**, 3 (2007).
5. M. Luo, Y. Yi, S. Wang, Z. Wang, M. Du, J. Pan, Q. Wang, *Renew. Sustain. Energy Rev.*, **81**, 3186 (2018).
6. J. Rifkin, *The Hydrogen Economy*, Penguin Publishing Group, 2003.
7. L. Chmielarz, M. Jabłońska, *RSC Adv.*, **5**, 43408 (2015).
8. P. Li, R. Zhang, N. Liu, S. Royer, *Appl. Catal., B*, **203**, 174 (2017).
9. L. Chmielarz, A. Węgrzyn, M. Wojciechowska, S. Witkowski, M. Michalik, *Catal. Lett.*, **141**, 1345 (2011).
10. M. Jabłońska, A. Król, E. Kukulska-Zajac, K. Tarach, L. Chmielarz, K. Góra-Marek, *J. Catal.*, **316**, 36 (2014).
11. R. Prasad, G. Rattan, *Bull. Chem. React. Eng. Catal.*, **5**, 7 (2010).
12. L. Chmielarz, M. Jabłońska, A. Strumiński, Z. Piwowarska, A. Węgrzyn, S. Witkowski, M. Michalik, *Appl. Catal. B*, **130–131**, 152 (2013).
13. J. Pinkas, V. Reichlova, R. Zboril, Z. Moravec, P. Bezdicka, J. Matejkova, *Ultrason. Sonochem.*, **15**, 257 (2008).
14. X. Liao, J. Zhu, W. Zhong, H.-Y. Chen, *Mater. Lett.*, **50**, 341 (2001).
15. X. Liu, K. Shen, Y. Wang, Y. Wang, Y. Guo, Y. Guo, Z. Yong, G. Lu, *Catal. Commun.*, **9**, 2316 (2008).
16. J. Boon, E. van Dijk, Ö. Pirgon-Galin, W. Haije, R. van den Brink, *Catal. Lett.*, **131**, 406 (2009).
17. A. Sun, Z. Qin, S. Chen, J. Wang, *Catal. Today*, **93–95**, 273 (2014).
18. Y. K. Shin, H. Kwak, A. V. Vasenkov, D. Sengupta, A. C. T. van Duin, *ACS Catal.*, **5**, 7226 (2015).
19. M. García-Vázquez, K. Wang, J. M. González-Carballo, D. Brown, P. Landon, R. Tooze, F. R. García-García, *Appl. Catal. B: Environmental*, **277**, 119139 (2020).
20. V. S. Jaswal, A. K. Arora, M. Kinger, V. dev Gupta, J. Singh, *Oriental J. Chem*, **30**, 559 (2014).
21. C. Martos, J. Dufour, A. Ruiz, *Inter. J. Hydrogen Energy*, **34**, 4475 (2009).
22. M. Selvarej, A. Pandurangan, K.S. Seshadri, *Appl. Catal. A: Gen.*, **242**, 347 (2003).
23. D. S. Nair, Manju Kurian, *J. Hazardous Mater.*, **344**, 925 (2018).
24. J. C. Gonzalez, M. G Gonzalez, M. A Laborde, N. Moreno, *Appl. Catal.*, **20**, 3 (1986).
25. S. Musić, S. Popović, M. Ristić, *J. Mater. Sci.*, **28**, 632 (1993).
26. T. Ramachandran, F. Hamed, *Mater. Res. Bull.*, **95**, 104 (2017).
27. J. E. Amonette, D. Rai, *Clays Clay Miner.*, **38**, 129 (1990).
28. R. K. Sharma, R. Ghose, *Ceram. Inter*, **41**, 14684 (2015).
29. S. Zheng, L. Gao, J. Gao, *Mater. Chem. Phys.*, **71**, 174 (2001).
30. A. Wang, Y. Wang, E. D. Walter, R. K. Kukkadapu, Y. Guo, G. Lu, R. S. Weber, Y. Wang, C. H. F. Peden, F. Gao, *J. Catal.*, **358**, 199 (2018).
31. Y. Xia, W. Zhan, Y. Guo, Y. Guo, G. Lu, *Chin. J. Catal.*, **37**, 2069 (2016).
32. Y. Cheng, F. Zhang, Y. Zhang, C. Miao, W. Hua, Y. Yue, Z. Gao, *Chin. J. Catal.*, **36**, 1242 (2015).
33. F. Ayari, M. Mhamdi, T. Hammedi, J. Álvarez-Rodríguez, A. R. Guerrero-Ruiz, G. Delahay, A. Ghorbel, *Appl. Catal. A Gen.*, **439–440**, 88 (2012).
34. A. Pineau, N. Kanari, I. Gaballah, *Thermochim., Acta*, **447**, 89 (2006).
35. R. Köhn, D. Paneva, M. Dimitrov, T. Tsoncheva, I. Mitov, C. Minchev, M. Fröba, *Microporous Mesoporous Mater.*, **63**, 152 (2003).
36. S.S. Reddy Putluru, A. D. Jensen, A. Riisager, R. Fehrmann, *Top. Catal.*, **54**, 1286 (2011).
37. L. Li, Q. Shen, J. Li, Z. Hao, Z. Ping Xu, G.Q.M. Lu, *Appl. Catal. A Gen.*, **344**, 131 (2008).

Characterization of some carbon materials by Raman spectroscopy

A. Kosateva*, I. Stoycheva, B. Petrova, B. Tsyntsarski

Institute of Organic Chemistry with Centre of Phytochemistry, Bulgarian Academy of Sciences, Acad. G. Bonchev Str. Bl. 9, 1113 Sofia, Bulgaria

Received January 29, 2021; Revised March 31, 2021

Raman spectroscopy was used to analyze different type of carbon materials: activated carbon (AC), carbonized and green carbon foam (CF), and carbon adsorbents, produced from refuse derived organic fuel (RDF). The Raman spectroscopy allows assessment of surface chemistry, structure and difference in the degree of structure ordering of produced carbon materials. Degree of ordering of carbon structures is based on the identification of the intensity of spectral signals corresponding to the D band, characteristic for the amorphousness of carbon structures and the G band, indicating the ordering of carbon structures. Raman also contributes to identification of carbon structures. This allows studying the changes in the structure and the formation of the porous texture as a result of the physical activation of the carbon materials, which significantly determine their applicability in the purification industry. The results show that carbonized carbon foam possesses more regular structure than “green” carbon foam. The difference in the spectra of the carbonized and activated sample shows that the activation of the sample with water vapor at 700 °C leads to a significant increase of aromatic structures with CH₃ groups and alicyclic compounds.

Key words: Raman spectroscopy; carbon materials; activated carbons

INTRODUCTION

Carbon materials, particularly those classified into the graphite family, have a variety of structures and textures, nanotexture and microtexture. We will focus on several types of carbon materials in our study: activated carbon (AC), carbonized and green carbon foam (CF), and carbon adsorbents, produced from refuse derived organic fuel (RDF). Our choice was guided by their specific structural properties and their applications not only in the various industries but mainly as adsorbents for purifying drinking water.

Activated carbons (AC) are known as promising materials with wide application as adsorbents, catalysts or catalyst supports due to their tunable surface and textural characteristics, which could be easily controlled by the preparation procedure and the precursor used [1-9]. Due to the interest in low-cost activated carbons, it is given special attention to their preparation from various waste materials (biomass, waste polymeric materials, agricultural products, waste organic fuels (RDF), etc.) for applications related to drinking and wastewater treatment [10-14]. There are two fundamental methods for preparing activated carbons: physical and chemical activation. The physical activation method involves: carbonization of raw material and activation at high temperature in carbon dioxide or steam atmosphere [15-17]. Chemical activation is a

well-known method for the preparation of activated carbon, which has been the objective of numerous studies within the last few years, as it presents some advantages compared to the so-called physical activation. In a chemical activation process, the precursor is impregnated with a specific chemical agent and then it is pyrolyzed [18].

Carbon foam is a sponge-like carbon material, representing cellular ligament microstructure, and it is distinguished by certain features, such as light weight, high temperature tolerance in inert atmosphere, high mechanical strength, large external surface area and adjustable thermal and electrical conductivity. As new materials, carbon foams have essential advantages, enhanced structural properties, fire resistance, radar cross-section, corrosion susceptibility. These unique properties, which mainly depend on the precursor features and synthesis conditions, make carbon foams ultra-high performance engineering materials, and determine their many potential applications in numerous industries [19-21].

Raman spectroscopy is ideal for characterization of carbon materials, as it is extremely sensitive to geometric structure and bonding within molecules. It is a simple and non-invasive technique, and it is suitable method, because the carbon atoms are light, the sp² σ bonds are strong, and the π-electron-related optical transitions range from the infrared up to the visible range [22].

* To whom all correspondence should be sent:

E-mail: angelina.kosateva@orgchem.bas.bg

Raman spectroscopy, which is one of the best and most accurate methods for studying carbon materials, was used for physicochemical characterization of the samples. The Raman spectrum is characteristic and can serve for precise identification of the type (by comparison with literature data) and the amount (by the intensity of the bands) of the carbon material. The presence of glassy carbon, graphite, graphene and other carbon structures corresponds to a specific type (close band frequencies, close intensity ratio, etc.) of the Raman spectrum.

Raman spectra of carbon materials like graphene are classically defined by three major bands; these are G-band, D-band, and 2D-band (also known as the G'-band). The G-band appears around 1582cm^{-1} and represents the graphene in-plane sp^2 vibrational mode. This provides an idea for the crystallinity of the material. The peak ratio between the D-band and G-band of sp^2 carbon material is highly significant. Dispersion of the G-band is observed in disordered graphene materials, where the dispersion is proportional to the degree of disorder. The D-band at around 1350cm^{-1} is credited to the structural disorder near the edge of the microcrystalline structure that decreases the symmetry of the structure [23-27].

In this paper we will focus on the characterization of the Raman spectra of different type of carbon materials: activated carbon, carbonized and green carbon foam (CF), and carbon adsorbents, produced from refuse derived organic fuel (RDF) in order to obtain information about surface chemistry, structure and ordering of carbon samples before and after hydrolysis.

EXPERIMENTAL

The sample of carbon adsorbent, produced from RDF was obtained as a linoleum piece (obtain from industry) was heated to a molten state and then concentrated sulfuric acid is added by drops with continuous stirring until solidification. The resulting product is subjected to carbonization in an inert N_2 atmosphere up to $550\text{ }^\circ\text{C}$. The carbonizate is activated with water vapor at a temperature of $700\text{ }^\circ\text{C}$ and a retention time at the final temperature of 60 minutes [28].

Carbon foam (CF) was prepared using the following procedure: coal tar pitch was heated up to $120\text{ }^\circ\text{C}$ till melting conditions. Furfural was heated to the same temperature and added to the pitch with continuous stirring. The obtained mixture was treated at $120\text{--}200\text{ }^\circ\text{C}$ (during the reaction the

temperature rises up to $200\text{ }^\circ\text{C}$) with concentrated H_2SO_4 (98 wt%) or HNO_3 (68 wt%) - drops of acid were added to the mixtures with continuous stirring until solidification. Foaming was carried out in a stainless steel pressure vessel by heating the pitch precursor up to $500\text{ }^\circ\text{C}$ in a N_2 atmosphere at pressure up to 1 MPa. The resultant "green" foams were heated at $1000\text{ }^\circ\text{C}$ in N_2 atmosphere to increase the mechanical strength and to remove the volatiles [29].

The Raman spectroscopy gives spectra containing oscillatory bands corresponding to the normal vibrations of the molecules. The intensity of Raman bands is determined by the change in polarizability during normal vibration. Using this technique, it is possible to determine the crystal form, chemical composition, intermolecular interactions, the degree of ordering, and the spatial distribution of stresses in tested material [24, 25].

Raman spectra were recorded by using Raman Microscope Senterra II (Bruker). Samples were placed onto glass (approximately 10 mg) and analyzed using the vertical 20x objective in an 180° backscattering arrangement. The Raman spectrometer parameters used to analyze the carbon samples include: 532 nm laser wavelength and an exposure time of 100 seconds, resolution was 4 cm^{-1} for all samples, laser power was 6.5 mW.

RESULTS AND DISCUSSION

The analysis of the structure of the studied carbon materials, including the evaluation of the ordering of the crystal structure was possible thanks to research using the Raman spectroscopy. The spectra of the studied carbon materials contain bands directly related to the vibrations of carbon and hydrocarbon structures.

The comparison of the spectra of the carbonized raw material at $600\text{ }^\circ\text{C}$ and the activated carbonizate at $700\text{ }^\circ\text{C}$ is shown on Fig. 1. The analysis of the carbonizate samples shown in Fig. 1 demonstrates the changes occurring in the chemical composition of the different stages of RDF treatment. The difference in the spectra of the carbonized and activated sample (Fig. 1) shows that the activation of the sample with water vapor at $700\text{ }^\circ\text{C}$ leads to a significant increase of aromatic structures with CH_3 groups (1559 cm^{-1}) and the alicyclic compounds (1327 cm^{-1}) in the sample and they become completely predominant.

The chemistry and surface structure of reference and space samples were studied by Raman spectroscopy. In Fig. 1, a band at 1559 cm^{-1} , otherwise known as the G band, is observed. This

band corresponds to stretching vibrations with E_{2g} symmetry. The G band at $1580\text{--}1560\text{ cm}^{-1}$, comes from tensile vibrations of the sp^2 hybridization of the carbon bond pairs occurring in ring structures. An additional band located at the Raman shift at 1327 cm^{-1} characterizes the level of amorphousness of carbon structures and indicates a highly disordered carbon structure. This band is usually called the D (defect) band. D band is usually detected in carbon materials at $1380\text{--}1300\text{ cm}^{-1}$ corresponds to A_{1g} symmetry and is associated with plane imperfections, e.g., defects and heteroatoms [30]. Typical Raman spectrum of graphite contains high frequency line at about 1580 cm^{-1} and a small band around 1350 cm^{-1} (sometimes missing).

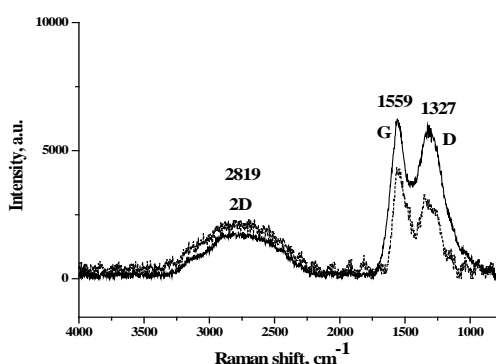


Fig. 1. Raman spectra of the activated carbonizate (black) and carbonizate (dashed) at $700\text{ }^{\circ}\text{C}$.

The analysis of the structure of the obtained carbonized and green carbon foam, including the evaluation of the ordering of the crystal structure, was possible due to research using Raman spectroscopy (Fig. 2 and Fig. 3).

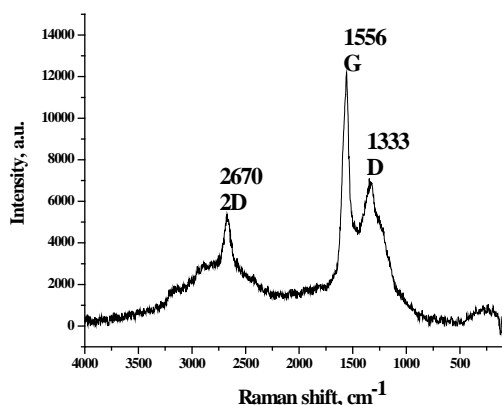


Fig. 2. Raman spectrum of carbonized carbon foam.

In the case of analysis of the Raman spectra obtained for carbon foams, a G bands is observed at 1556 (1574 (Fig. 3)) cm^{-1} . The bands located at the Raman shift at 1333 cm^{-1} (Fig. 2) and 1330 cm^{-1}

(Fig. 3) can be assigned as the so called D band. As we can see in Fig. 2 the intensity of the G band is much higher that one of the D band. The structure is much more ordered then the one of the green carbon foam (Fig. 3).

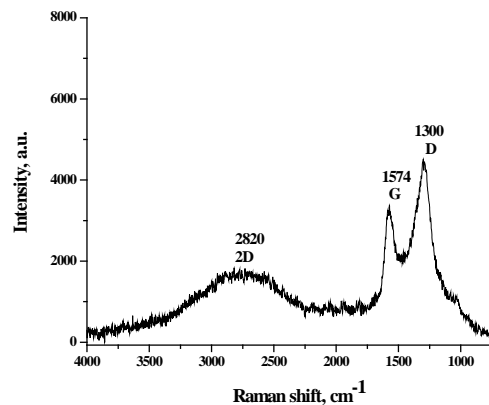


Fig. 3. Raman spectrum of green carbon foam.

In the Raman spectra of green carbon foam (Fig. 3) a great increase of the intensity of the D band can be seen. The increase in the D band can be produced by: (i) an increase in the amount of disordered carbon atoms in CF, corresponding to sp^3 domains; or (ii) a significant reduction in the size of sp^2 domains in the layer. This suggests the coexistence of sp^2 and sp^3 hybridization; i.e., CF contains crystalline and amorphous forms of carbon [31]. The 2D band is also present in the CF samples. The 2D band in the spectrum of the carbonized CF (Fig. 3) it is narrow and sharp. This fact and the very low intensity of the D band indicate a very regular structure compared with the one of the green CF.

CONCLUSION

Raman spectroscopy is suitable method for physicochemical characterization of carbon samples. The Raman spectrum is characteristic and can serve for precise identification of the type (by comparison with literature data) and the amount (by the intensity of the bands) of the carbon material. The presence of glassy carbon, graphite, graphene and other carbon structures corresponds to a specific type (close band frequencies, close intensity ratio, etc.) of the Raman spectrum. The Raman spectroscopy analysis also helps to obtain information about chemistry, surface structure, and difference in the degree of the produced carbon materials structure ordering.

For the obtained samples of carbon materials, two bands are most characteristic: the G band and

the D band. The G band comes from the stretching vibrations of carbon bond pairs of sp^2 hybridization occurring in ring structures and is closely related to the occurrence of ordered carbon structures. The D band characterizes the level of the amorphousness of carbon structures. The activation with water vapor at 700 °C leads to a significant increase of aromatic structures (1559 cm^{-1}) and alicyclic compounds (1327 cm^{-1}). It was determined that carbonized carbon foam possess more regular structure than green carbon foam.

The obtained results indicate the differences in the physicochemical properties of the synthesized carbon materials and help to identify the areas of their application in the electrochemistry, purification technique, etc.

Acknowledgements: This research was funded by the project BG05M2OP001-1.002-0019: „Clean technologies for sustainable environment – water, waste, energy for circular economy“, financed by the Operational program “Science and Education for Smart Growth” 2014-2020, co-financed by the European union through the European structural and investment funds. The authors also acknowledge financial support by Bulgarian National Science Fund, grant number KII-06-M37/3 from 06.12.2019 and by National Research Program “Young scientists and postdoctoral students” approved by DCM No 577 / 17.08.2018.

REFERENCES

1. F. Rodriguez-Reinoso, *Carbon*, **36**, 159 (1998).
2. H. Teng, T.-S. Yeh, L.-Y. Hsu, *Carbon*, **36**, 1387 (1998).
3. K. Fu, Q. Yue, B. Gao, Y. Sun, L. Zhu, *Chem. Eng. J.*, **228**, 1074 (2013).
4. Q. Miao, Y. Tang, J. Xu, X. Liu, L. Xiao, Q. Chen, *J. Taiwan Inst. Chem. Eng.*, **44**, 458 (2013).
5. Y.-R. Lin, H. Teng, *Micropor. Mesopor. Mater.* **54**, 167 (2002).
6. F. Bouhamed, Z. Elouear, J. Bouzid, *J. Taiwan Inst. Chem. Eng.* **43**, 741 (2012)
7. X. Ma, F. Ouyang, *Appl. Surf. Sci.* **268**, 566 (2013).
8. D. Kalderis, S. Bethanis, P. Paraskeva, E. Diamadopoulos, *Bioresour. Technol.*, **99**, 6809 (2008).
9. M. J. Ahmed, S. K. Theydan, *J. Anal. Appl. Pyrolysis*, **99**, 101 (2012).
10. N. Petrov, T. Budinova, M. Razvigorova, E. Ekinci, F. Yardim, V. Minkova, *Carbon*, **38**, 2069 (2002).
11. D. Savova, E. Apak, E. Ekinci, F. Yardim, N. Petrov, T. Budinova, M. Razvigorova, V. Minkova, *Biomass Bioenerg.*, **21**, 133 (2001).
12. J. Hayashi, T. Horikawa, I. Takeda, K. Muroyama, F. N. Ani, *Carbon*, **40**, 2381 (2002).
13. L. Helsen, E. Bulek, J.S. Hery, *W. Manag.*, **18**, 571 (1998).
14. V. Minkova, S. P. Marinov, R. Zanzi, E. Bjornbom, T. Budinova, M. Stefanova, L. Lakov, *Fuel Proc. Tech.*, **62**, 45 (2000).
15. K. Gergova, N. Petrov, S. Eser, *Carbon*, **32**, 693 (1994).
16. V. Minkova, T. Budinova, N. Petrov, M. Razvigorova, M. Goranova, *Acta Montana IRSM AS CR, Praha, Series BNO*, 1999, 112, p. 25.
17. D. Savova, E. Apak, E. Ekinci, F. Yardim, N. Petrov, T. Budinova, M. Razvigorova, V. Minkova, *Biomass Bioenerg.*, **21**, 133 (2001).
18. M. T. Gonzales, F. Rodriguez-Reinoso, A. N. Garcia, A. Marcilla, *Carbon*, **35**, 159 (1997).
19. B. Tsyntarski, B. Petrova, T. Budinova, N. Petrov, A. Popova, M. Krzesinska, S. Pusz, J. Majewska, *Bulg. Chem. Comm.*, **41**, 397 (2009).
20. M. Inagaki, *New Carbons: Control of Structure and Functions*, Elsevier, 2000.
21. Z. D. Rogers, J. Plucinski, P. Stansberry, A. Stiller, J. Zondlo, in: *Proc. Int. Symp. Soc. Adv. Mater. Proc. Eng.*, 2000; p. 293.
22. A. C. Ferrari, J. C. Meyer, V. Scardaci, C. Casiraghi, M. Lazzeri, F. Mauri, S. Piscanec, D. Jiang, K. S. Novoselov, S. Roth, A. K. Geim, *J. Phys. Review.*, **97**, 187401 (2006).
23. A. Merlen, J. G. Buijnsters, C. Pardanaud, *Coatings*, **7**, 2 (2017).
24. M. W. Smith, I. Dallmeyer, T. J. Johnson, C. S. Brauer, J. S. McEwen, J. F. Espinal, M. Garcia-Perez, *Carbon*, **100**, 678 (2016).
25. E. Groppo, F. Bonino, F. Cesano, A. Damin, M. Manzoli, Chapter 4, *Royal Society of Chemistry*, 2018, p. 103.
26. J.-B. Wu, M.-L. Lin, X. Cong, H.-N. Liua, P.-H. Tan, *Chem. Soc. Rev.*, **47**, 1822 (2018).
27. Z. Heidarinejad, M. H. Dehghani, M. Heidari, G. Javedan, I. Ali, M. Sillanpää, *Environ. Chem. Lett.*, **18**, 393 (2020).
28. G. Georgiev, B. Tsyntarski, I. Stoycheva, B. Petrova, K. Miteva, T. Budinova, N. Petrov, A. Sarbu, M. Dumitru, A. Ciurluca, A. Miron, *Bulg. Chem. Commun.*, **53** Sp. Iss. A (2021); doi: 10.34049/bcc.53.A.0012.
29. I. Stoycheva, B. Tsyntarski, M. Vasileva, B. Petrova, G. Georgiev, T. Budinova, U. Szeluga, S. Pusz, A. Kosateva, N. Petrov, *Diam. Relat. Mat.*, **109**, 108066 (2020).
30. H. Peng, G. Ma, K. Sun, J. Mu, Z. Zhang, Z. Lei, *ACS Appl. Mater. Interfaces*, **6**, 20795 (2014).
31. A. C. Ferrari, J. Robertson, *Phys. Rev.*, **B61**, 14096 (2000).

Refuse-derived fuel waste conversion to carbon adsorbent

G. Georgiev¹, B. Tsyntsarski^{1*}, I. Stoycheva¹, A. Kosateva¹, B. Petrova¹, K. Miteva¹, T. Budinova¹, N. Petrov¹, A. Sarbu², M. Dumitru², A. Ciurluca², A. Miron²

¹ Institute of Organic Chemistry with Centre of Phytochemistry, Bulgarian Academy of Sciences, Acad. G. Bonchev Str. Bl. 9, 1113 Sofia, Bulgaria

² National Research-Development Institute for Chemistry and Petrochemistry INCDCP-ICECHIM Bucharest, 202 Splaiul Independentei, 060021 Bucharest, Romania

Received February 01, 2021; Revised March 31, 2021

Refuse-derived fuel (RDF) fuel can be produced from various types of waste, consisting of combustible components, like paper, polypropylene, polystyrene, polyethylene, bitumen waterproofing, nylon and other waste materials. RDF can be also produced from used tyres and biomass waste. In this work nanoporous carbons are prepared from RDF from waste tarpaulin made of bitumen. First the precursor sample was subjected to oxidation at a temperature of 250-300 °C with constant stirring and feeding of oxidant. Second step is pyrolysis at 600 °C, followed by subsequent hydro-pyrolysis at 750 °C. The synthesized carbon was characterized by N₂ physisorption at -196 °C, elemental analysis, etc. The results show that nanoporous carbon from RDF is characterized by high surface area around 700m² and significant content of micro- and mesopores. The adsorption of dyes from water by obtained nanoporous carbon was studied, the change in the concentration of dye in the water was monitored by UV-VIS spectrophotometer. The results suggest that obtained nanoporous carbon is suitable for application as adsorbent of organic and inorganic pollutants. Liquid products and gases are also obtained.

Key words: RDF fuel; waste material; nanoporous carbon; adsorbent

INTRODUCTION

RDF can be produced from various types of waste, such as municipal waste and industrial waste, and its composition is a mixture of materials with higher flammability (paper, non-recyclable and not containing Cl, F plastics) compared to the components in the total waste stream. RDF fuel is used to produce electricity and heat in various types of equipment and cement industry. In some European countries there are strict standards, culture of recycling, collection system and better screening of well-combustible components for production of RDF [1, 2]. However, in most countries they are difficult to recycle due to limited technology and available facilities, which leads to severe pollution of the soil, air and water, due to the content of not so well combustible materials, pollutants such as carbon monoxide, sulfur and nitrogen oxides, heavy metals, polycyclic compounds, etc. [1, 2].

Carbon adsorbents are often synthesized from precursors based on expensive and exhaustible fossil fuels, but they can also be readily obtained from a variety of cheap and alternative precursors - coal, biomass, polymer waste [3-15].

Nowadays microplastics and nanoplastics have

become pollutants of global importance, due their slow biodegradation. They are small enough to be ingested by and accumulated in algae, plants and animals, and they could cross some biological barriers. In the last 60 years global plastic waste is around 6000 million tonnes, and 80% are accumulated in urban territories, beaches, landfills, aquatic environment, etc. [16].

In the last years, the scientific interest has focused on the development of carbon synthesis methods based on mixtures of organic substances - liquid products from thermal treatment of biomass, furfural, coal tar, polymer waste products, etc. [11-13].

Methods of synthesis used have additional contribution for waste utilization. Obtained materials found environmental application as adsorbents and catalysts. The experimental data obtained on the processes occurring during the thermo-catalytic treatment of some precursors show that the direction of this study is promising, with potential for further development and for promising results [11-13].

Various technologies for the production of polymers have led to the production of a large number of by-products, but most of these polymeric waste products have not found suitable application so far. Due to their affordability and low cost, polymers and polymer waste products are suitable

* To whom all correspondence should be sent:

E-mail: boyko.tsyntsarski@orgchm.bas.bg

precursors for the production of nanoporous carbon materials. Thermochemical conversion of polymer waste products is an appropriate way of producing energy as well as carbon with good adsorption properties and low content of mineral impurities. On the other hand, the current paper will be focused on the treatment of RDF fuel waste in order to obtain adsorbents for the treatment of industrial and waste water from various pollutants.

Wastewater can be classed as sanitary, commercial, industrial, agricultural or surface wastewater. The sources of industrial wastewater are cement, pharmaceutical, food, textile, pulp paper, rubber, leather, cosmetics, plastic industries, fertilizers, etc. 20% of industrial water pollution is result of textile dyeing and treatment. Dyes produced by the textile, printing and paper industries are a source of pollution of rivers and waterways. 700 000 tons of dyes used during the manufacturing of textile products is released into the environment worldwide annually [17, 18]. In high concentrations synthetic dyes have toxic, carcinogenic, mutagenic and teratogenic effects on humans, microorganisms, fish, etc. [17, 18].

The main aim is to utilize the RDF fuel obtained by processing it into liquid and gas products to be used as energy sources and a solid product /carbon adsorbent/ to be used for purification of water and air from industrial and domestic pollutants. An additional contribution is the utilization of waste products from the industry. The relationship between the physicochemical properties of the adsorbents obtained and their adsorption capacity against certain compounds hazardous to human health will be investigated. The most suitable raw materials, surface modification methods and processing conditions will be found to obtain effective carbon adsorbents to remove dyes (methyl orange and bromthymol blue) from water.

MATERIAL AND METHODS

Linoleum material is finely chopped to a fraction suitable for its processing, as the size of the pieces varies from 2 to 5 mm. The material is subjected to following procedures:

Thermal oxidation (Fig. 1) - the prepared fraction of bitumen waterproofing is poured into the reactor - 2, with constant stirring by a stirrer - 1, heating at temperature 250-300 °C for 30 min. and feeding oxidizer (in our case - conc. H₂SO₄, added by drops). The gases are captured by the drexel - 3. The oxidation and heat treatment of RDF with different oxidants affects the composition to a very

large extent, the resulting product has a very different composition from that of the starting product.

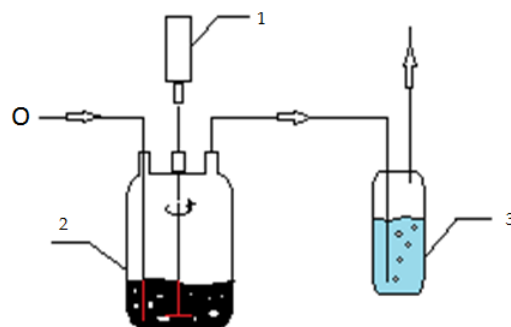


Fig. 1. Scheme of the thermal oxidation process.(1-mechanical stirrer, 2- stainless steel, 3- drexel).

The next stage is heat treatment in an atmosphere of its own volatiles (Fig. 2). The oxidized RDF is placed in the reactor - 2, after heating at 600 °C for 1h in the furnace - 1, the volatile substances are separated, the liquids are collected in a receiver - 5. The gases bubble in the drexel - 7, which contains a basic solution for capturing acid gases, the remaining amount flows through gas meter - 8, and could be used for fuel.

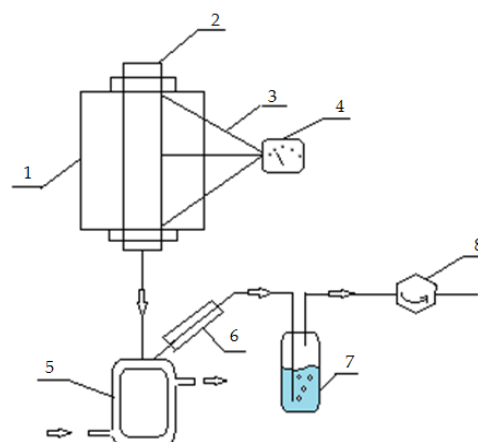


Fig. 2. Heat treatment (1 - furnace, 2 - reactor, 3 - thermocouples, 4 - thermal controller, 5-receiver, 6-condenser, 7-drexel, 8-gas meter).

The third stage is hydrolysis in a stainless steel reactor (Fig. 3). A steam generator -1, is added to the installation, as the atmosphere of water vapor for 1h at 750 °C forms new pores and expands the already formed ones.

Micro-meso-porous structure of the carbon adsorbent is formed.

The textural properties of adsorbents were measured on Quantachrome NOVA 1200e USA (model e-25, 2014) using N₂ adsorption-desorption

at $-196\text{ }^{\circ}\text{C}$. Prior to measurement, the samples were degassed at $300\text{ }^{\circ}\text{C}$ for 4 h to remove the presence of impurities and/or moisture.

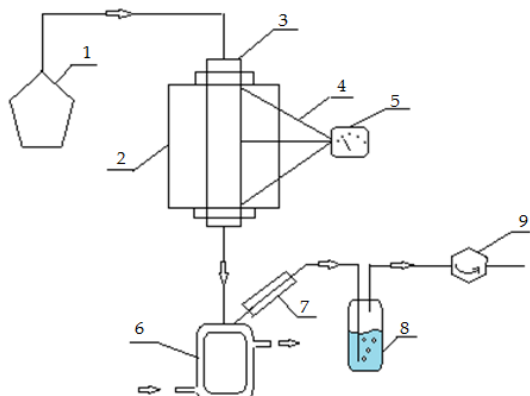


Fig. 3. Hydrolysis (1 – steam generator, 2 – furnace, 3 – reactor, 4 – thermocouples, 5 – thermal controller, 6 – receiver, 7 – condenser, 8 – drexel, 9 – gas meter).

The elemental analysis was performed on ELEMENTAR analyser, model VarioMacroCube (2018), to determine C, H, N, S. The dye concentration is determined on UV-VIS spectrophotometer Spectroquant Pharo 300 Merck (2008).

RESULTS AND DISCUSSION

Moisture was determined after drying in an oven at $120\text{ }^{\circ}\text{C}$ to constant weight, the ash content is the remainder after 10 min at $850\text{ }^{\circ}\text{C}$. Technical analyses, material balance and elemental analysis are presented in Tables 1-3, respectively.

Table 1. Technical analysis of activated carbon from RDF.

W, wt% (moisture content)	A, wt% (ash content)
0.5	30

Table 2. Material balance of the products of pyrolysis of activated carbon from RDF.

Solid product wt. %	Liquid products wt %	Gas + losses wt%
49.2	17.6	34.2

Table 3. Elemental analysis of activated carbon from RDF.

Sample	C, wt. %	C, at. %	H, wt. %	H, at. %	N, wt. %	N, at. %	S, wt. %	S, at. %
Activated carbon from RDF	47.1	3.93	2.25	2.25	4.2	0.3	2.3	0.07

The atomic ratio of carbon to hydrogen is 1.75. The result gives an idea of the degree of carbonization (predominant amount of carbon) and aromaticity. Data show the presence of significant amounts of polycyclic aromatic compounds, including condensed aromatic compounds. This proves the successful synthesis of the carbon adsorbent.

Nitrogen physisorption ($-196\text{ }^{\circ}\text{C}$) isotherm and textural parameters of the activated carbon from RDF are presented in Fig. 4 and Table 4. The results show that nanoporous carbon from RDF is characterized by high surface area and significant content of micro- and mesopores. The analysis clearly shows that the micropores predominate, which proves the nanoporous structure of the adsorbent. The results suggest that obtained nanoporous carbon is suitable for application as adsorbent of organic and inorganic pollutants.

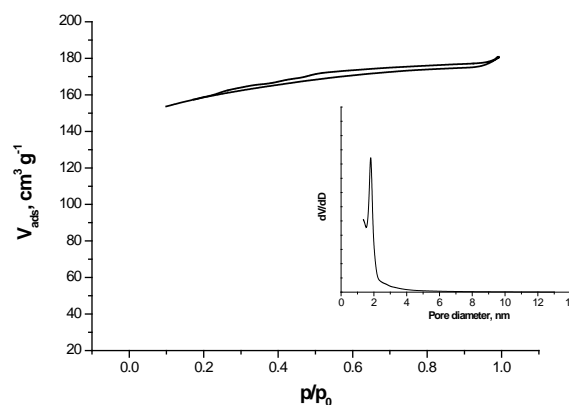


Fig. 4. Nitrogen physisorption ($-196\text{ }^{\circ}\text{C}$) isotherm of the activated carbon from RDF.

Determination of adsorption capacity is performed as follows. Solutions of methyl orange (MO) with a concentration of 0.5 to 10 mg / L and bromothymol blue (BTB) with concentrations of 10 to 30 mg / L were prepared, the adsorptions were carried out for periods of 10, 30 and 60 min.

The adsorption of methyl orange gave the best result (87 mg/g maximum adsorption capacity) at a concentration of 1 mg /L for a period of 10 minutes, whereas for bromothymol blue adsorption the best result (87 mg/g maximum adsorption capacity) was demonstrated at 10 mg /L for 60 minutes.

Table 4. Technical analysis of activated carbon from RDF.

Sample	BET specific surface S _{BET} , m ² /g	Total pore volume ^a V _{total} , cm ³ /g	Micropore volume ^b V _{micro} , cm ³ /g	Mesoporous volume ^c , cm ³ /g
Activated carbon from RDF	650	0.25	0.22	0.02

^a calculated at p/p⁰ = 0.99; ^{b, c} calculated by the Dubinin-Radushkevich method

CONCLUSION

Nanoporous carbons are successfully synthesized from RDF from waste tarpaulin made of bitumen. The synthesized carbon is characterized by N₂ physisorption at -196 °C, elemental analysis, etc. The results show that nanoporous carbon from RDF is characterized by high surface area and significant content of micro- and mesopores. The adsorption properties of obtained carbon material towards dyes in water was studied using UV-VIS spectrophotometry. The results suggest that obtained nanoporous carbon is suitable for application as adsorbent of organic and inorganic pollutants.

Acknowledgements: The authors acknowledge financial support for this work by Bulgarian National Science Fund, grant number KII-06-M37/3 from 06.12.2019. The authors acknowledge support for this work from the EU Project BG05M2OP001-1.002-0019: Clean Technologies for a Sustainable Environment - Water, Waste, Energy for a Circular Economy (Clean & Circle).

REFERENCES

1. A. Sever Akdag, A. Atımtay, F. D. Sanina, *Waste Manage.*, **47**, Part B, 217 (2016).
2. N. Srisaeng, N. Tippayawong, K. Y. Tippayawongm, *Energy Procedia*, **110**, 115 (2017).
3. K. Gergova, N. Petrov, S. Eser, *Carbon*, **32**, 693 (1994).
4. D. Savova, E. Apak, E. Ekinci, M. Ferhat Yardim, N. Petrov, T. Budinova, M. Razvigorova, V. Minkova, *Biomass Bioen.*, **21**, 133 (2001).
5. A. Bacaoui, A. Yaacoubi, A. Dahbi, C. Bennouna, R. Phan Tan Luu, F. J. Maldonado-Hodar, J. Rivera-Utrilla, C. Moreno-Castilla, *Carbon*, **39**, 425 (2001).
6. Z. Ryu, H. Rong, J. Zheng, M. Wang, B. Zhang, *Carbon*, **40**, 1144 (2002).
7. C. O. Ania, J.-B. Parra, A. Arenillas, F. Rubiera, T.J. Bandoz, J. J. Pis, *Appl. Surf. Sci.*, **253**, 5899 (2007).
8. N. Petrov, T. Budinova, M. Razvigorova, J.-B. Parra, P. Galiatsatou, *Biomass Bioen.*, **32**, 1303 (2008).
9. T. Budinova, D. Savova, B. Tsyntsarski, C. O. Ania, B. Cabal, J.-B. Parra, N. Petrov, *Appl. Surf. Sci.*, **255**, 4650 (2009).
10. N. Asasian, T. Kaghazchi, M. Soleimani, *J. Ind. Eng. Chem.*, **18**, 283 (2012).
11. N. Petrov, T. Budinova, M. Razvigorova, V. Minkova, *Carbon*, **38**, 2069 (2000).
12. B. Petrova, B. Tsyntsarski, T. Budinova, N. Petrov, C. Ania, J. Parra, M. Mladenov, P. Tzvetkov, *Fuel Proc. Technol.*, **91**, 1710 (2010).
13. B. Petrova, B. Tsyntsarski, T. Budinova, N. Petrov, L. Velasco, C. Ania, *Chem. Eng. J.*, **172**, 102 (2011).
14. K. Laszlo, A. Bota, L. G. Nagy, I. Cabasso, *Colloid. Surf.*, **A151**, 311 (1999).
15. J. B. Parra, C. O. Ania, A. Arenillas, F. Rubiera, J. J. Pis, *Appl. Surf. Sci.*, **238**, 304 (2004).
16. E.-L. Ng, E. H. Lwanga, S. M. Eldridge, P. Johnston, H.-W. Hu, V. Geissen, D. Chen, *Sci. Total Environ.*, **627**, 1377 (2018).
17. H. Li, Z. Sun, L. Zhang, Y. Tian, G. Cui, Sh. Yan, *Colloids Surf.* **2016**, A489, 191 (2016).
18. A. Z. M. Badruddoza, G. S. S. Hazel, K. Hidajat, M. S. Uddin, *Colloids Surf.*, **A367**, 85 (2010).
19. K. S. W. Sing, Assessment of Surface Area by Gas Adsorption, In: Adsorption by Powders and Porous Solids (F. Rouquerol, J. Rouquerol, K. S. W. Sing, P. Llewellyn, G. Maurin, eds.), Elsevier, 2014, pp. 237-268.

$M_{0.5}Zn_{0.5}Fe_2O_4$ (M = Cu, Co, Mn, Ni) ferrites supported on activated carbon as catalysts for methanol decomposition

R. Ivanova^{1*}, B. Tsyntsarski¹, G. Issa¹, I. Spassova², D. Kovacheva², N. Velinov³, T. Tsoncheva¹

¹ Institute of Organic Chemistry with Centre of Phytochemistry, Bulgarian Academy of Sciences, Acad. G. Bonchev Str. Bl. 9, 1113 Sofia, Bulgaria

² Institute of General and Inorganic Chemistry, Bulgarian Academy of Sciences, Acad. G. Bonchev Str. Bl. 11, 1113 Sofia, Bulgaria

³ Institute of Catalysis, Bulgarian Academy of Sciences, Acad. G. Bonchev Str. Bl. 11, 1113 Sofia, Bulgaria

Received January 29, 2021; Revised April 19, 2021

Activated carbon was prepared from cherry stones residues and used as a host matrix of nanosized $M_{0.5}Zn_{0.5}Fe_2O_4$ (M = Cu, Co, Mn, Ni) ferrites. The obtained composites were characterized by Low-temperature nitrogen physisorption, powder X-ray diffraction, Mossbauer and Infrared spectroscopies and temperature-programmed reduction with hydrogen. Their catalytic activity in methanol decomposition as a source of hydrogen was studied in details. The textural analysis demonstrated significant stability of the carbon support during the deposition of the ferrite phase. XRD and Mossbauer data revealed that the loaded metal oxide phase represented a complex mixture of finely dispersed ferrite and substituted magnetite particles. The catalysts based on Cu- and Co-containing ferrites demonstrated fast deactivation in methanol decomposition due to the agglomeration of the active particles and significant structural collapse of the activated carbon. The highly exposed to the reactants Mn^{2+} - Fe^{3+} redox pairs in $Mn_{0.5}Zn_{0.5}Fe_2O_4$ ferrite modification promoted the catalytic process at lower temperature. The observed extremely high catalytic activity for the $Ni_{0.5}Zn_{0.5}Fe_2O_4$ modification was related to the synergistic activity of Ni and ZnO nanoparticles, produced under the reaction medium. The obtained results demonstrated the potential of the activated carbon obtained from waste cherry stones for the preparation of cheap and effective catalysts for hydrogen production.

Key words: methanol decomposition; activated carbon; catalysts; zinc ferrites

INTRODUCTION

Recently, hydrogen was considered as the most effective and clean energy carrier. The only emission produced during the hydrogen burning is water vapor, which can significantly reduce the pollutants and the greenhouse gases in the atmosphere. The main drawback in hydrogen application is its safety storage and supply [1]. Methanol can be successfully used as a hydrogen carrier in gas turbines, fuel cells, vehicles, and industry, because it can easily release hydrogen in situ using different technologies, such as decomposition, steam reforming or partial oxidation [2]. However, the wide application of methanol as a hydrogen source, especially for the portable and mobile installations, requires development of cheap and active under the low operation temperature catalysts. Ferrites are important materials for many technological and industrial applications due to their electrical resistivity, high saturation magnetization, high permeability and tunable catalytic activity [3, 4]. The spinel-type ferrites are generally denoted as

MFe_2O_4 , where M is divalent metallic cations [5-12]. In Zn-containing ferrites, the Zn^{2+} ions preferentially occupy the tetrahedral sites. The presence of second metal ion in $ZnFe_2O_4$ can significantly affect its properties [13]. Boudjemaa *et al.* [14] reported that the Co substitution dramatically enhances the catalytic activity of $ZnFe_2O_4$ in hydrogen production by water photo-reduction. Murugesan *et al.* [13] demonstrated the superior properties of $Mn_{0.2}Zn_{0.8}Fe_2O_4$ in high-frequency electronic device applications. Velinov *et al.* [15] reported good catalytic activity in methanol decomposition of Ni-Zn ferrites obtained by spark ignition plasma sintering of nickel-zinc-iron hydroxide carbonate precursors. The significant impact of the reaction medium on the phase transformations in the ferrites was widely studied in [15, 16]. Over the past decades, the attention was focused on the synthesis of nanoferrites [17, 18]. The small size of the nanoparticles enhances the surface area per unit mass, which provides a more active area for the catalytic reactions [19]. However, the nanoferrites possess less cyclic stability due to the structural degradation through the redox process [20]. Improved electrochemical performance of the nanoferrites was reported when

* To whom all correspondence should be sent:
E-mail: Radostina.Ivanova@orgchm.bas.bg

they were incorporated within the carbon-based materials like CNT, porous carbon, and graphene [21, 22]. Among the carbon materials, activated carbon (AC) gains considerable attention due to its chemical inertness, high-temperature stability, and tunable texture and surface characteristics. Activated carbon can be synthesized from renewable and low-cost materials, such as agriculture and industrial residues, which makes it attractive both from the economic and environmental viewpoint [2]. Our previous investigation showed that $Ni_xZn_{1-x}Fe_2O_4$ modified activated carbons obtained from peach stones and coal treatment by-products possess a significant potential for sustainable environmental protection as cheap and effective catalysts for hydrogen production [23].

The present investigation is focused on the preparation of nanosized $M_{0.5}Zn_{0.5}Fe_2O_4$ ($M = Cu, Co, Mn, Ni$) ferrites, hosted in activated carbon obtained from waste biomass (cherry stones). The effect of the carbon support on the formation of the catalytic active phase was discussed in detail using various physicochemical techniques, such as Boehm method, low-temperature nitrogen physisorption, powder X-ray diffraction, Mossbauer spectroscopy, Infrared spectroscopy and temperature-programmed reduction with hydrogen. Their potential application as catalysts for methanol decomposition to hydrogen and carbon monoxide was also investigated.

EXPERIMENTAL

Synthesis of catalysts

Nanoporous carbon from cherry stones was prepared as follows: The precursor (30 g crushed cherry stones, size 1-3 mm) was subjected to carbonization at 973 K and subsequent physical activation with water vapor in a stainless-steel vertical reactor at 1173 K for 1 h. The obtained activated carbon was modified by incipient wetness impregnation with methanol solutions of $Fe(NO_3)_3 \cdot 9H_2O$, $Zn(NO_3)_2 \cdot 6H_2O$ and/or $Ni(NO_3)_2 \cdot 6H_2O$, $Co(NO_3)_2 \cdot 6H_2O$, $Cu(NO_3)_2 \cdot 3H_2O$, $Mn(NO_3)_2 \cdot 4H_2O$ in appropriate ratio as described in [23]. After the impregnation step, the samples were dried at room temperature for 24 h and then, treated in vacuum at 323 K for 2 h. The metal precursor was decomposed in nitrogen at 773 K for 2 h. The metal content in the samples was 8 wt.%, the $Fe/(Zn+M)$ molar ratio was 2 and the Zn/M molar

ratio was 1. The modifications were denoted as $M_{0.5}Zn_{0.5}Fe_2O_4/AC$, where M was Cu, Co, Mn, Ni, and AC is the carbon support.

Methods of investigation

The textural characteristics of the materials were studied by low-temperature nitrogen adsorption in a Quantachrome Instruments NOVA 1200e (USA) apparatus. The specific surface area was determined from Brunauer Emmett Teller (BET) equation, the total pore volume was obtained at a relative pressure of 0.99, the micropores volume was elucidated by the t-plot method. The amount of surface oxygen-containing acidic functional groups was determined following Boehm method and the total number of basic sites was determined by titration with HCl [23]. Powder X-ray diffraction (XRD) study was performed on a Bruker D8 Advance diffractometer (Bruker AXS GmbH, Germany) with Cu $K\alpha$ radiation and a LynxEye detector with a constant step of $0.02^\circ 2\theta$ and counting time of 17.5 s per step. The mean crystallite sizes were determined by the Topas-4.2 software. The Fourier Transform Infrared Spectroscopic (FTIR) study was performed on a Bruker Vector 22 FTIR spectrometer (Bruker Optics, Germany) at a resolution of 1 cm^{-1} and accumulating scans of 64 using KBr technique in the range of $4000\text{--}400\text{ cm}^{-1}$. The Mössbauer measurements were performed with a Wissel (Wissenschaftliche Elektronik GmbH, Germany) electromechanical spectrometer working in a constant acceleration mode at room temperature (RT). A $^{57}Co/Rh$ source (Activity @ 20 mCi) and Fe standard were used. The experimentally obtained spectra were fitted with WinNormos. The parameters of hyperfine interaction such as isomer shift (IS) line, quadruple splitting (QS), hyperfine magnetic field (H_{eff}), width (FWHM), relative weight (G) of the partial components in the spectra were determined. The Temperature Programmed Reduction/Thermo-gravimetric (TPR/TG) study was performed on a Setaram TG 92 apparatus (SETARAM Instrumentation, France) in a mixture of hydrogen and argon ($100\text{ cm}^3\text{min}^{-1}$, volume ratio $H_2:Ar = 1$) and heating rate of 5 Kmin^{-1} .

Catalytic test

Methanol decomposition was carried out in a flow-type microreactor (55 mg of catalyst diluted with crash glass (weight ratio of 1:3) at 1.57 kPa partial pressure of methanol and WHSV of 100 h^{-1} .

Before the catalytic test, the samples were pre-treated in situ for 1 h at 373 K in argon. Methanol dosage was achieved by a saturator kept at 273 K using argon as a carrier gas. The experimental data were collected under a thermo-programmed regime of heating rate of 2 K/min within the temperature range of 423–770 K. On-line gas chromatographic analyses were performed on an HP 5890 apparatus equipped with flame ionization (FID) and thermo-conductivity (TCD) detectors, on a PLOT Q column (J&W HP-PLOT Q GC Column, 30 m, 0.53 mm, 40.00 μ m, 7 inch cage). The results were calculated using the method of absolute calibration on the base of carbon material balance. The methanol conversion was calculated as $X = ((C_{ini} - C_{cur})/C_{ini}) \times 100$, where C_{ini} and C_{cur} were the initial and current detected amounts of methanol, respectively. The selectivity to i product from methanol conversion was calculated as $Y_i/X \times 100$, where Y_i was its yield determined from $C_i/C_{ini} \times 100$ (C_i was the amount of i product).

RESULTS AND DISCUSSION

Nitrogen physisorption

Low-temperature nitrogen physisorption analyses of parent activated carbon and all modifications revealed presence of micro- and mesopores (Fig. 1, Table 1). The carbon support possessed relatively high specific surface area and pore volume. After the modification, no significant decrease in the BET surface area and pore volume were observed, which evidences absence pore-blocking due to the deposition of the active phase. No substantial structural changes of the support

during the modification procedure could be assumed. The increase in the V_{mic}/V_{mes} ratio for $Mn_{0.5}Zn_{0.5}Fe_2O_4/AC$ as compared to the parent AC evidences predominant location of the metal species into the mesopores. The preservation of V_{mic}/V_{mes} ratio for $Cu_{0.5}Zn_{0.5}Fe_2O_4/AC$ and $Ni_{0.5}Zn_{0.5}Fe_2O_4/AC$ indicates almost random distribution of the metal species into the micro/mesopores of the carbon support or their deposition on the external surface.

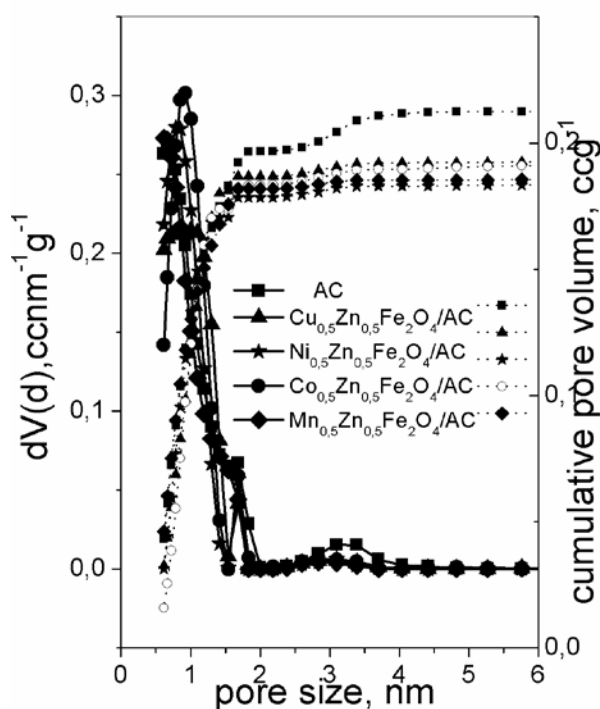


Fig. 1. Pore size distribution of the studied samples.

Table 1. Nitrogen physisorption data.*

Sample	$S_{BET}, m^2 g^{-1}$	$S_{mic}, m^2 g^{-1}$	$V_{mic}, cm^3 g^{-1}$	$V_t, cm^3 g^{-1}$	V_{mic}/V_{mes}
AC	488	430	0.18	0.23	3.6
$Cu_{0.5}Zn_{0.5}Fe_2O_4/AC$	465	417	0.17	0.22	3.4
$Ni_{0.5}Zn_{0.5}Fe_2O_4/AC$	454	407	0.16	0.21	3.2
$Mn_{0.5}Zn_{0.5}Fe_2O_4/AC$	453	411	0.17	0.21	4.3
$Co_{0.5}Zn_{0.5}Fe_2O_4/AC$	459	403	0.16	0.23	2.3

* BET surface area (S_{BET}), surface area of micropores (S_{mi}), micropores pore volume (V_{mi}), total pore volume (V_t)

Table 2. Phase composition, unit cell parameters and average crystallite size for the modifications.

Sample	Phase composition	Cell parameters, Å	Crystallite size, nm
$Cu_{0.5}Zn_{0.5}Fe_2O_4/AC$	Spinel, Fd-3m (97%)	8.425	21
	Cu_2O , Pn-3m (3%)	4.284	16
$Ni_{0.5}Zn_{0.5}Fe_2O_4/AC$	Spinel	8.404	34
$Mn_{0.5}Zn_{0.5}Fe_2O_4/AC$	Spinel	8.465	21
$Co_{0.5}Zn_{0.5}Fe_2O_4/AC$	Spinel	8.420	20
	Traces ZnO (<1%)		

Powder X-ray diffraction (XRD)

The structure and phase composition of the samples was studied by powder X-ray diffraction (XRD) (Fig. 2, Table 2). The main diffraction peaks at 30° , 35° , 43° , 56° , 62° 2θ were attributed to (220), (311), (222), (400), (422), (511) and (440) planes of a single-phase cubic spinel structure of Fd3m space group (JCPDS card no. 22-1012.). The average size of the spinel crystallites, calculated by Scherrer equation, was in the range of 16-34 nm. The diffraction peaks of the Ni-containing sample were narrower and highly intensive suggesting presence of larger crystallites. This is in accordance with [24] where the facile effect of Ni^{2+} ions on spinel grain growth was reported. The obtained unit cell parameters were lower than the reported in the literature for $ZnFe_2O_4$ [14] (Table 2). This effect could be attributed to the substitution of bigger Zn^{2+} ions by smaller Ni^{2+} , Cu^{2+} Co^{2+} ones in the spinel structure [14]. Boudjemaa *et al.* [14] reported that the lattice parameter of the spinel was not directly correlated with the ionic radius of the cation in the ternary ferrites since it depends not only on the radius of cation but also vary with the distribution of the cations over the octahedral and tetrahedral sites. Thus, changes in cation distribution could be assumed in the case of manganese modification.

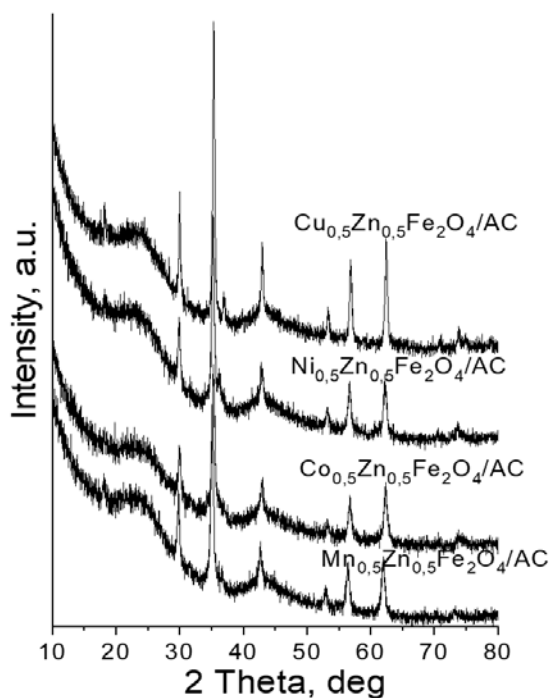


Fig. 2. XRD patterns of the studied samples.

Fourier transform infrared spectroscopy

FTIR analysis (Fig. 3 a, b) was performed to elucidate the chemical structure and functional groups of the materials. The broad band at about $3600-3000\text{ cm}^{-1}$ in the spectra of the carbon support (not shown) was ascribed to residual water or hydrogen-bonded O-H stretching vibrations [25]. The band at 1731 cm^{-1} and the broad absorption band at about 1600 cm^{-1} were assigned to the C=O stretching vibration in carbonyl groups (C=O), and C=C bonds in the aromatic structure, respectively (Fig. 3 a). The bands near 1420 cm^{-1} were due to the CH_2 asymmetric deformation and aromatic C-C stretching vibrations. The bands between 1373 and 1160 cm^{-1} were assigned to phenol O-H bending, C-O stretching in carboxylic acids, alcohols, esters, and phenol groups [25]. Table 3 shows information for the amount of carbon surface functional groups, obtained by Boehm method and by titration with HCl. The carbonyl groups dominate on the surface, which well correlated with the data from the FTIR analysis. FTIR spectra of all ferrite modifications (Fig. 3 b) consisted of two additional peaks at $\sim 580\text{ cm}^{-1}$ and below 400 cm^{-1} which could be assigned to M-O vibrations of metal ions in tetrahedral and octahedral positions in the ferrites, respectively [26]. The change in the position of the main FTIR bands after the modification of AC evidenced the interaction of metal species with the surface functional groups and carbon basal planes [27].

Mossbauer spectroscopy

The values of the line width (FWHM), isomer shift (IS), quadruple splitting (QS), hyperfine magnetic field (H_{eff}) and relative weight of each component (G) are listed in Table 4. The obtained Mössbauer spectra were fitted by considering two hyperfine magnetic sextets and a paramagnetic doublet. It is well-known fact that the magnetic parameters obtained for sextets and doublets are the characteristics of Fe ions occupying tetrahedral (A) as well as octahedral [B] sites, respectively. Note that, the observed values of quadrupole splitting except for doublet were very small. This could be attributed to the maintained cubic symmetry between Fe^{3+} and surrounding ions [28]. The sextets denoted as Sx1 and Sx2 with $IS=0.29\text{ mm/s}$ and $IS=0.66$ together with $QS\sim 0\text{ mm/s}$ corresponded to Fe^{3+} and $Fe^{2.5+}$ ions in tetrahedral and octahedral positions within the spinel lattice,

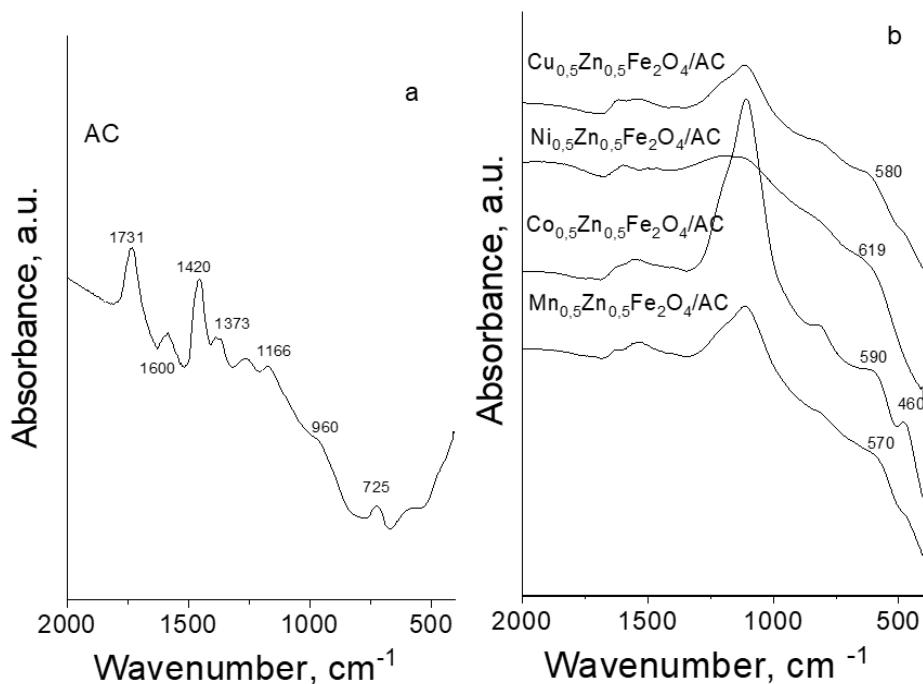


Fig. 3. FTIR spectra of carbon support (a) and all modifications (b).

Table 3. Surface functional groups, determined by the Boehm method.

Sample	Acidic groups (mmol g ⁻¹)				Total basic groups (mmol g ⁻¹)
	Carboxylic	Lactone	Phenolic	Carbonyl	
AC	BDL	BDL	0.10	2.5	1.08

Table 4. Moessbauer parameters of all modifications.^a

Sample	Components	IS, mm/s	QS, mm/s	Heff, T	FWHM, mm/s	G, %
Cu _{0.5} Zn _{0.5} Fe ₂ O ₄ /AC	Sx1-(Cu,Zn) _x Fe _{3-x} O ₄	0.29	0.00	39.5	1.82	39
	Sx2-(Cu,Zn) _x Fe _{3-x} O ₄	0.66	0.00	37.9	2.00	38
	Db-Fe ³⁺	0.34	0.50	-	0.54	22
Ni _{0.5} Zn _{0.5} Fe ₂ O ₄ /AC	Sx1-(Ni,Zn) _x Fe _{3-x} O ₄	0.29	0.00	44.5	0.98	35
	Sx2-(Ni,Zn) _x Fe _{3-x} O ₄	0.66	0.00	39.8	1.85	48
	Db-Fe ³⁺	0.34	1.23	-	1.03	17
Mn _{0.5} Zn _{0.5} Fe ₂ O ₄ /AC	Sx1-(Mn,Zn) _x Fe _{3-x} O ₄	0.29	0.00	37.3	1.45	36
	Sx2-(Mn,Zn) _x Fe _{3-x} O ₄	0.66	0.00	34.2	2.00	53
	Db-Fe ³⁺	0.36	1.14	-	1.03	11
Co _{0.5} Zn _{0.5} Fe ₂ O ₄ /AC	Sx1-(Co,Zn) _x Fe _{3-x} O ₄	0.29	0.00	44.9	1.60	36
	Sx2-(Co,Zn) _x Fe _{3-x} O ₄	0.66	0.00	40.9	1.88	43
	Db-Fe ³⁺	0.34	0.89	-	0.71	21
Cu _{0.5} Zn _{0.5} Fe ₂ O ₄ /AC *	Sx1- χ -Fe ₅ C ₂	0.22	0.07	18.7	0.58	58
	Sx2- χ -Fe ₅ C ₂	0.17	0.07	10.9	0.70	21
	Sx3 - χ -Fe ₅ C ₂	0.25	0.07	21.8	0.38	21

* after catalytic test; ^a isomer shift (IS) line, quadruple splitting (QS), hyperfine magnetic field (Heff), width (FWHM), relative weight (G).

respectively [23]. These results well correlate with the data obtained by powder X-ray diffraction (Fig. 2, Table 2) for the purity of the spinel phase. The doublets had characteristic parameters for Fe³⁺ in

octahedral coordination in paramagnetic or superparamagnetic phases. In the spectra of the studied samples, the doublets had higher values of quadrupole splitting. A possible reason for this

could be due to the presence of defects in the ferrite structure, due to the changes in the dispersion of the oxide particles [28].

Temperature programmed reduction-thermogravimetric analyses (TPR-DTG)

In Fig. 4 are shown TPR profiles for various modifications in the 400 - 850 K range. All modifications exhibited weight loss above 550 K and several reduction effects with different shape and position were detected up to 800 K. In accordance with the data from the XRD analyses, the significant differences in the TPR profiles could be assigned to the variations in the dispersion of the active phase (Fig. 2, Table 2). The reduction transformations occurred in the ranges around 650-700 K and 750-800 K and their intensity strongly depended on the type of the second metal component. According to the literature, the high-temperature effect could be related to the reduction of $Fe^{3+} \rightarrow Fe^{2.5+}$ to metallic iron [23]. The lack of well-distinguished reduction effects for $Mn_{0.5}Zn_{0.5}Fe_2O_4/AC$ and $Co_{0.5}Zn_{0.5}Fe_2O_4/AC$ modifications could be due to the presence of manganese and cobalt ions in a lower oxidation state [29, 30]. The reduction profile of

$Cu_{0.5}Zn_{0.5}Fe_2O_4/AC$ exhibited two well-distinguished peaks at about 674 K and 776 K indicated co-existence of Cu_2O and partially reduced mixed oxide phase, which formation was favored by the carbon support. For $Ni_{0.5}Zn_{0.5}Fe_2O_4/AC$ sample the reduction transformations were shifted to higher temperature. All these observations confirmed the crucial role of carbon support on the state and dispersion of the loaded ferrite phase [23].

Catalytic study

In Fig. 5 are presented the temperature dependencies of methanol decomposition on various ferrite-supported materials. Most of the samples initiate the catalytic process above 600 K. All materials possessed above 80% selectivity to CO. Methane (up to 15%) and CO_2 (up to 10%) were detected as by-products. Despite the catalytic process started at the lowest temperature for $Mn_{0.5}Zn_{0.5}Fe_2O_4/AC$, its catalytic activity increased extremely slowly with the temperature increase. The shift of the conversion curve of $Ni_{0.5}Zn_{0.5}Fe_2O_4/AC$ to lower temperature demonstrated its higher catalytic activity.

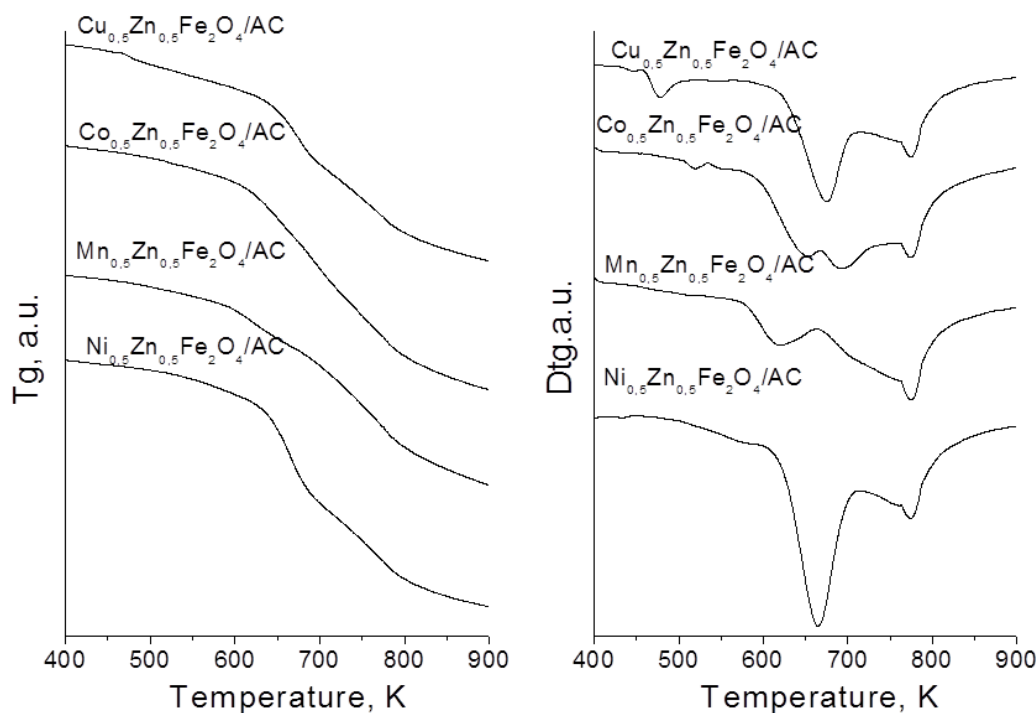


Fig. 4. TPR profiles for all samples.

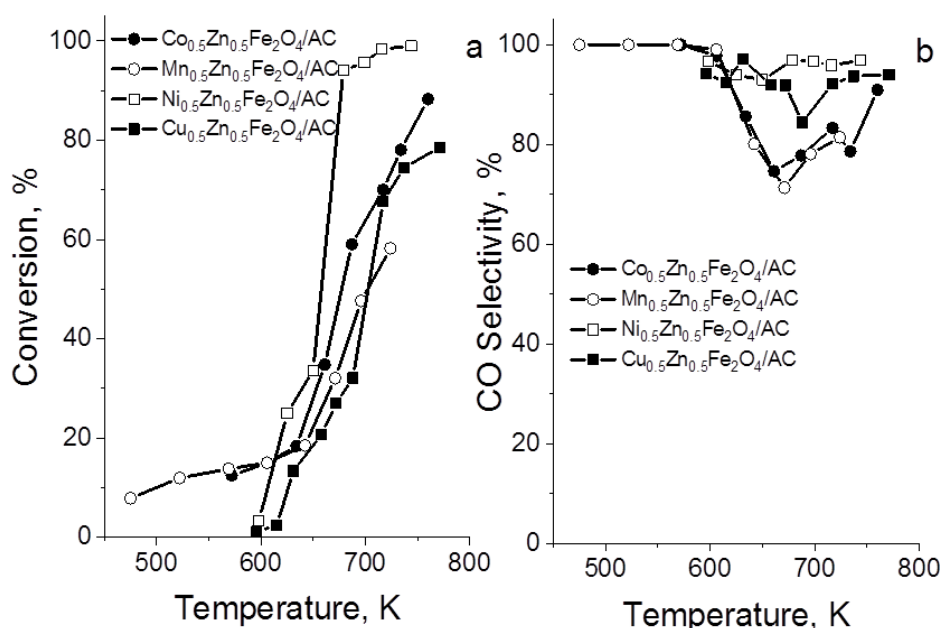


Fig. 5. Temperature dependencies of methanol decomposition (a) and selectivity to CO (b) on various modifications.

The changes in the slope of the conversion curves for the Cu- and Co-based modifications indicated fast deactivation of the catalysts due to irreversible changes with them. The TPR profiles (Fig. 4) and the Moessbauer spectra of the samples after the catalytic test (Table 4) indicated facile reduction decomposition of the loaded ferrite phases, which occurred both by carbon support and reduction reaction medium. These changes occurred not only during the preparation procedure but also during the catalytic test. As a result, a complex mixture of metals, metal oxides, and carbide phases was formed (Table 4). Thus, the catalytic behavior of the samples represented a superposition of the own catalytic activity of different phases. We can propose that the extremely high catalytic activity of $Ni_{0.5}Zn_{0.5}Fe_2O_4/AC$ was due to the synergistic action of metallic Ni and ZnO phases, where ZnO played a role of “reservoir” of the formation of methoxy intermediates and Ni promoted the C-H scission in them with the formation of H_2 and CO [23]. The fast reduction of Cu-based materials even during the preparation procedure rendered difficult the formation of ferrite-like structures and facilitated the formation of Cu_2O phase (Table 2). Further reduction and fast agglomeration of metallic Cu particles was most probably the main reason for its lowest catalytic

activity and well-defined tendency for rapid deactivation. Similar, but less pronounced changes were responsible for the behavior of the $Co_{0.5}Zn_{0.5}Fe_2O_4/AC$ modification. We suggest, that the highly exposed to the reactants $Mn^{2+}-Fe^{3+}$ redox pairs, situated at octahedral position in $Mn_{0.5}Zn_{0.5}Fe_2O_4$ initiated the reaction at significantly lower temperature, but the decomposition of the ferrite to MnO and ZnO phases under the reaction medium resulted in a decrease of the catalytic activity at higher temperatures.

CONCLUSION

Nanosized $M_{0.5}Zn_{0.5}Fe_2O_4$ ($M = Cu, Co, Mn, Ni$) ferrites supported on activated carbon from waste biomass were successfully prepared by incipient wetness impregnation and tested as catalysts in methanol decomposition. The results of the physicochemical analyzes show that the active phase on the carbon support is a complex mixture of finely dispersed metal oxide phases, which changes significantly by the influence of the reaction medium. The highest catalytic activity for $Ni_{0.5}Zn_{0.5}Fe_2O_4$ modification was related to the synergistic activity of metallic Ni and ZnO particles, which were produced during the reduction transformations of the ferrite phase.

Acknowledgements: This work was supported by Bulgarian National Science Fund (Grant Number KII-06-H27/9). Project BG05M2OP001-1.002-0019: „Clean technologies for sustainable environment – water, waste, energy for circular economy“(Clean&Circle), for development of a Centre of Competence is also acknowledged.

REFERENCES

1. M. Luo, Y. Yi, S. Wang, Z. Wang, M. Du, J. Pan, Q. Wang, *Renew. Sustain. Energy Rev.*, **81**, 3186 (2018).
2. T. S. Tsoncheva, A. B. Mileva, B. G. Tsyntsarski, D. G. Paneva, I. P. Spassova, D. G. Kovacheva, N. I. Velinov, D. B. Karashanova, B. N. Georgieva, N. V. Petrov, *Biomass Bioenergy*, **109**, 135 (2018).
3. N. M. Deraz, M. M. Hessien, *J. Alloy. Compd.*, **475**, 832 (2009).
4. M. Khodaei, S. A. Ebrahimi, Y. J. Park, J. M. Ok, J.S. Kim, J. Son, S. Baik, *J. Magn. Magn. Mater.*, **340**, 16 (2013).
5. A. V. Humbe, J. S. Kounsalye, S. B. Somvanshi, A. Kumar, K. M. Jadhav, *Mater. Adv.*, **1**, 880 (2020).
6. A. S. Albuquerque, M. V. Tolentino, J. D. Ardisson, F. C. Moura, R. de Mendonca, W. A. Macedo, *Ceramic Int.*, **38**, 2225 (2012).
7. S. Nair, M. Kurian, *J. Environ. Chem. Eng.*, **5**, 964 (2017).
8. S. A. Jadhav, S. B. Somvanshi, M. V. Khedkar, S. R. Patade, K. Jadhav, *J. Mater. Sci. Mater. Electron.*, **31**, 11352 (2020).
9. R. Sharma, P. Thakur, P. Sharma, V. Sharma, *J. Alloys Compd.*, **704**, 7 (2017).
10. S. Debnath, R. Das, *J. Mol. Struct.*, **1199**, 127044 (2020).
11. D. D. Andhare, S. R. Patade, J. S. Kounsalye, K. Jadhav, *Physica B*, **583**, 412051 (2020).
12. C. Murugesan, G. Chandrasekaran, *J. Supercond. Nov. Magnetism*, **29**, 2887 (2016).
13. C. Murugesan, K. Ugendar, L. Okrasa, J. Shen, G. Chandrasekaran, *Ceramic Int.*, **47**, 1672 (2021).
14. A. Boudjemaa, I. Popescu, T. Juzsakova, M. Kebir, N. Helaili, K. Bachari, I.-C. Marcu, *Int. J. Hydrog. Energy*, **41**, 11108 (2016).
15. N. I. Velinov, E. D. Manova, T. S. Tsoncheva, C. Estournès, D. G. Paneva, K. K. Tenchev, V. S. Petkova, K. V. Koleva, B. N. Kunev, I. G. Mitov, *Solid State Sci.*, **14**, 1092 (2012).
16. K. V. Koleva, N. I. Velinov, T. S. Tsoncheva, I. G. Mitov, B. N. Kunev, *Bulg. Chem. Commun.*, **45**, 434 (2013).
17. S. B. Somvanshi, S. A. Jadhav, M. V. Khedkar, P. B. Kharat, S. More, K. Jadhav, *Ceram. Int.*, **46**, 8640 (2020).
18. M. Ahmed, N. Okasha, S. El-Dek, *Nanotechnology*, **19**, 065603 (2008).
19. M. R. Chandra, T. S. Rao, H. S. Kim, S. V. Pammi, N. Prabhakarrrao, *J. Asian Ceram. Soc.*, **5**, 436 (2017).
20. A. Tabrizi, N. Arsalani, A. Mohammadi, H. Namazi, L. Saleh, *New J. Chem.*, **41**, 4974 (2017).
21. S. Chella, P. Kollu, E. Vara, P. Komarala, S. Doshi, M. Saranya, S. Felix, R. Ramachandran, P. Saravanan, V. L. Koneru, V. Venugopal, S. K. Jeong, A. N. Grace, *Appl. Surf. Sci.*, **327**, 27 (2015).
22. G. Wang, L. Zhang, J. Zhang, *Chem. Soc. Rev.*, **41**, 797 (2012).
23. T. S. Tsoncheva, B. G. Tsyntsarski, R. N. Ivanovaa, I. P. Spassova, D. G. Kovacheva, G. S. Issa, D. G. Paneva, D. B. Karashanova, M. D. Dimitrov, B. N. Georgieva, N. V. Petrov, I. G. Mitov, N. V. Petrov, *Micropor. Mesopor. Mater.*, **285**, 96 (2019).
24. A. Manohar, K. Chintagumpala, K. Kim, *Ceram. Int.*, **47**, 7052 (2021).
25. T. S. Tsoncheva, A. B. Mileva, S.P. Marinov, D. G. Paneva, N. V. Velinov, I. P. Spassova, A. D. Kosateva, D. G. Kovacheva, N. V. Petrov, *Micropor. Mesopor. Mater.*, **259**, 9 (2018).
26. H. He, Y. Yan, J. Huang, J. Lu, *Sep. Purif. Technol.*, **136**, 36 (2014).
27. M. Baysal, K. Bilge, B. Yilmaz, M. Papila, Y. Yürüm, *J. Environ. Chem. Eng.*, **6**, 1702 (2018).
28. S. S. Deshmukh, A. V. Humbe, A. Kumar, R. G. Dorik, K. M. Jadhav, *J. Alloys Compd.*, **704**, 227 (2017).
29. T. S. Tsoncheva, G. S. Issa, A. B. Mileva, R. N. Ivanova, M. D. Dimitrov, I. P. Spassova, D. G. Kovacheva, D. G. Paneva, N. I. Velinov, B. G. Tsyntsarski, N. V. Petrov, *Bulg. Chem. Commun.*, **49**, 167 (2017).
30. T. S. Tsoncheva, I. Genova, I. G. Stoycheva, I. P. Spassova, R. N. Ivanova, B. G. Tsyntsarski, G. S. Issa, D. G. Kovacheva, N. V. Petrov, *J. Porous Mater.*, **22**, 1127 (2015).

Antineoplastic immuno-modulating properties of hemocyanins

M. Nikolova^{1*}, S. Konstantinov¹, P. Dolashka²

¹ Medical University Sofia, Faculty of Pharmacy, Department of Pharmacology, Pharmacotherapy and Toxicology, Bulgaria, Dunav Str, 1000 Sofia, Bulgaria

² Institute of Organic Chemistry with Centre of Phytochemistry, Bulgarian Academy of Sciences, Acad. G. Bonchev Str. Bl. 9, 1113 Sofia, Bulgaria

Received January 22, 2021; Revised April 02, 2021

In this review, we summarize most of the available scientific information about the antineoplastic and immuno-modulating properties of hemocyanins. The key points here are the functional structure of hemocyanins, hemocyanins antitumor and immuno-modulating properties, and their possible application as anticancer vaccine carriers and adjuvants.

Key words: hemocyanins; hemocyanins structure; antitumor effect; immuno-modulating effect; vaccine carrier; vaccine adjuvant

INTRODUCTION

Nowadays, malignant diseases are one of the major public health problems. Cancer is characterized by abnormal cell growth with the potential to invade or spread to other parts of the body. Traditional types of cancer treatment (surgery, radiation therapy and chemotherapy) are still not effective enough against the potentially fatal illness. This is the reason why prevalent parts of the scientists are searching for new antineoplastic compounds and methods against different types of tumors, especially those with possible local controllability, e.g. skin cancers and non-invasive urinary bladder cancer.

New plant and animal bioactive compounds raise hopes for a successful fight against cancer. Hemocyanins are a good example of glycoproteins with a potential antitumor effect. They were described for the first time in 1878 by Leon Frederic, while he was studying the physiology of *Octopus vulgaris* [1]. The name of hemocyanins is coming from the Greek *haima* (blood) and *kyanos* (blue pigment) [2]. These huge glycoproteins were isolated from mollusc species and they have demonstrated significant antineoplastic activity. Moreover, there is plenty of information about hemocyanin antitumor effects based on its immuno-modulating properties. Recently, some structure-activity relationship details were found thus underlining the possibilities of these molecules to play different biological roles because of their very complex protein structure. On the one hand hemocyanins main function is to transport oxygen

to all molluscan tissues, but on the other hand, they could be beneficial for future innovative anticancer therapies.

Functional structure of HCS

Molluscan hemocyanins are cylindrical multimeric glycoproteins that are found freely dissolved in the hemolymphatic fluid. Their main function is to transport oxygen to all of the molluscan tissues. Hemocyanins are among the largest known proteins, with molecular masses varying approximately from 3.3 to 13.5 MDa. They are composed of subunits that form cylindrical decamers, didecamers or multidecamers [3]. Each subunit comprises several paralogous functional units (FUs) which are classified into eight groups (FU: a, b, c, d, e, f, g and h) and their homologous FUs (FU-d*, f1, -f2, -f3, -f4, -f5, and -f6). FUs (except FU-h) have a similar structure and composition. Two domains are responsible for their folding: the N-terminal core domain where the active site is located in a four-alpha-helix bundle and the C-terminal domain dominated by a six-stranded β -sandwich and shields the entrance to the active site [3]. The molecular mass of FU-h is larger than that of other FUs due to the presence of an extra cupredoxin-like domain at the C-terminus. All FUs possess a type-3 copper center at their respiratory active site located in the N-terminal core domain. Between two copper atoms are bound two oxygen atoms to form a Cu_2O_2 cluster and the geometry around the Cu_2O_2 - binding site is conserved in all known FUs [3].

Molluscan hemocyanins can be classified into four major groups according to the FU composition

* To whom all correspondence should be sent:
E-mail: maria.nikolova.sofia@abv.bg

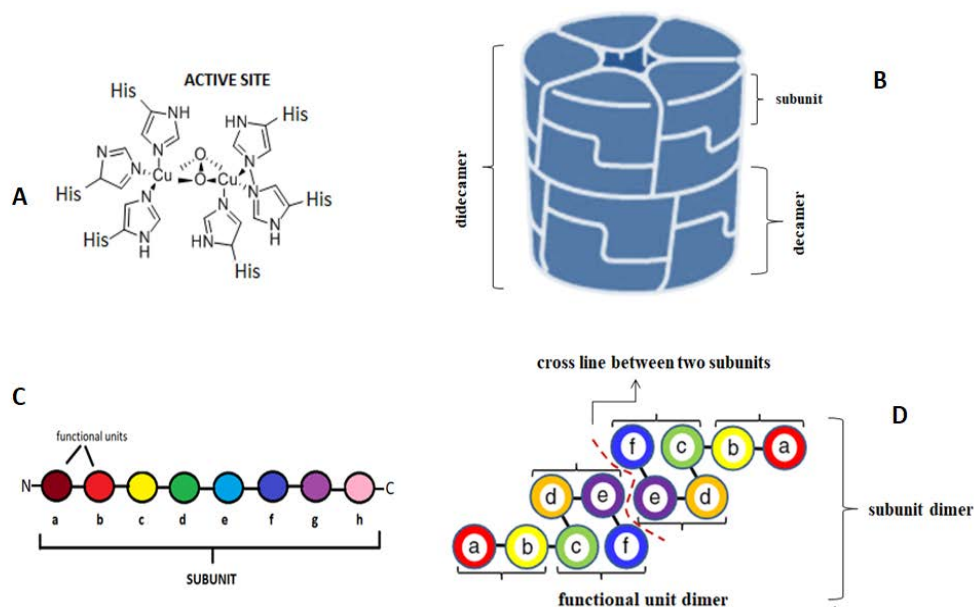


Fig. 1. Schematic illustration of molluscan hemocyanin structure. (A) Scheme of functional unit active site. At the active site, two oxygen atoms are bound between two copper atoms forming a Cu_2O_2 cluster. The copper ions are coordinated by six histidine residues. The active site is located at the N-terminal core domain and the C-terminal β -sandwich domain shields the entrance to the active site. (B) Schematic didecamer hemocyanin structure. Each decamer contains ten subunits and each subunit is composed of functional units. (C) Scheme of a molluscan hemocyanin subunit with eight different functional units (as in many gastropods). N, N-terminus; C, C-terminus; (D) Schematic illustration of subunit dimer. Five subunit dimers compose the hemocyanin wall region. One subunit dimer contains six functional unit dimers (2 a-b dimers, 2 c-f dimers, 2 d-e dimers).

of the subunit: (1) gastropods type, (2) mega-hemocyanin type, (3) nautilus and octopus – type and (4) squid-type [3].

Keyhole limpet belongs to gastropods, and their hemocyanins possess additional FU, namely h. The gastropod hemocyanin type has a hollow cylindrical didecameric structure and molecular size of 8 MDa. The molecule has a wall and inner collar regions. The wall region comprises of FUs: -a, -b, -c, -d, -e, and -f and the inner collar region contains FUs -g and -h. Additionally, it is confirmed by Swerdlow et al. [2], that Keyhole limpet hemocyanin (KLH) has two isoforms (KLH-A and KLH-B) which are composed of distinct subunits. Mega-hemocyanin type can be observed in cerithioid snails. Type -2 hemocyanin consists of two subunits: mega-subunit (550 kDa) and typical-subunit (400 kDa). They form tridecameric structure with a molecular size of 13.5 MDa. The mega subunit comprises of 12 FUs (FU-a, -b, -c, -d, -e, -f, -f1, -f2, -f3, -f4, -f5 and -f6) and the typical-subunit is similar to the Keyhole limpet subunit structure [3]. Nautilus and octopus hemocyanins (type 3) don't have a FU -h and they exist as decamers with a molecular size of 3.5 MDa (FU-a, -b, -c, -d, -e, -f and -g). Type 4 (squid type) is a decamer with a molecular size of 3.8 MDa. The

subunit contain following FUs: -a, -b, -c, -d, -d*, -e, -f and -g (FU-h is not observed in type 4) [3]. From the hemocyanin classification, it is obvious, that only glycoproteins with the FU -h can form didecamers and multi-decamers [3]. The wall region of hemocyanin molecules has a complex general architecture. The functional units -a, -b, -c, -d, -e and -f compose FU-dimers (a-b, c-f, d-e), which stack to form the plate-like subunit dimer. Five subunits dimers assemble to form the wall region with 5-fold symmetry resulting in a D_5 symmetrical cylinder [3].

It is known that hemocyanins have a high carbohydrate content. Hemocyanin N-glycosylation motifs are conserved near active sites and in between binding sites of their subunits. Glycosylation is a posttranslational process that increases protein solubility and prevents its denaturation or aggregation. Salazar et al. [4] demonstrated that N-glycans contribute to the quaternary structure of KLH, *Concholepa concholepa* hemocyanin (CCH) and *Fissurella latimarginata* hemocyanin (FLH). Furthermore, their study has proved that N-deglycosylation didn't change the secondary structure of hemocyanins but altered their refolding mechanisms. Hemocyanin glycans are highly

heterogeneous and primarily composed of mannose-rich N-glycans, N-mixed carbohydrates with fucose, galactose, N-acetylglucosamine and glycosylation branches that are not found in mammals [4]. Furthermore, hemocyanins contain highly immunogenic glycan patterns which were observed in the human parasite *Schistosoma mansoni* [5]. Also, galactose Gal(β 1–6) moieties have been found in some O-specific side chains of *Salmonella* lipopolysaccharides and capsular polysaccharides of *Klebsiella pneumoniae* [4]. Additionally, KLH contains Thomsen-Friedenreich antigen (or T-antigen) which is expressed on the cell surface of T-cell lymphomas and most human carcinomas [6]. There are evidences demonstrating how hemocyanin N-glycans promote proinflammatory cytokine secretion, humoral changes and antitumor effects.

Stimulation of the immune system by hemocyanins and mode of action

Cancer immunotherapy is an innovative treatment modality aiming to stop tumor growth, to eliminate tumor cells and prevent the metastatic process by activating the immune surveillance to detect and kill tumor cells. By multiple mechanisms of innate and adaptive immunity can be promote anticancer effect. For instance, T-cells produce cytokines such as tumor necrosis factor (TNF), which induce tumor cell lysis and enhance other antitumor cell effector responses. Macrophages contribute to anticancer defence by their antigen presenting properties and their ability to produce various cytokines. Also, natural killer cells (NK-cells) can lyse target cells, including tumor cells, unrestricted by the expression of antigen on the target cell [7]. There are two types of cancer immunotherapy: active and passive [8]. Passive therapy relies on the repeated application of large quantities of tumor antigen-specific antibodies e.g. Trastuzumab (Herceptin) - monoclonal antibody targeting HER-2/neu antigen presented in breast cancer cells. Passive immunotherapy is effective against cancer diseases with generalized immune dysfunction such as chronic lymphocytic leukemia (CLL), Hodgkin's disease (HD) and non-Hodgkin lymphoma(NHL). Alemtuzumab is a recombinant humanized monoclonal antibody of murine origin, which has been approved for CLL therapy. It targets the CD52 antigen expressed on malignant B and T lymphocytes. Rituximab, which is a chimeric murine/human monoclonal antibody, has a long story as registered and approved therapy for B cell NHLs. Rituximab targets the CD20 antigen

expressed in B lymphocytes and activates lysis of the respective malignant B-cells. Furthermore, some antibodies can interrupt the interaction between important growth factors and their receptors on the cancer cell surface. For instance, Cetuximab is specific for the epidermal growth factor receptor and it was approved for colorectal cancer treatment [8]. Active immunotherapy aims to generate tumor-specific immune responses by vaccination [8]. The immune response comprises of: presentation of tumor-associated antigens by the antigen presenting cells (APCs), antigen uptake by APCs, epitope presentation to CD4+T cells, cytokine release and B-cell activation. The immune response against cancer cells can be enhanced by unspecific immune stimulators, also called adjuvants. An ideal cancer vaccine should provoke a long-lasting effect by combining T-cell responses and humoral responses. Moreover, it is necessary to be safe without strong side effects [8]. Related to the above mentioned information about cancer immunotherapy, there are plenty of studies and evidences demonstrating the anticancer hemocyanin properties because of their immunomodulating and vaccine enhancing adjuvant functions.

In preliminary experiments, it was proved that hemocyanin glycans interact with several innate immune receptors on murine APCs (carbohydrate-recognizing C-type lectin receptors and Toll-like receptors). Also CCH, FLH and KLH bind *in vitro* to human mannose receptor (MR) and dendritic cell-specific intercellular adhesion molecule – 3-grabbing non-integrin (DC- SIGN) [4]. The main function of these receptors is to recognize pathogen glycosylated structures and to promote endocytosis, pro-inflammatory responses and antigen presentation to T-lymphocytes. APCs incorporate CCH, FLH and KLH by macro-pinocytosis and receptor-mediated endocytosis. Thus, hemocyanins undergo prolonged antigen presentation to T or B lymphocytes, promoting a Th1 immune response and antitumor effect [9]. According to Zhong *et al.* [9], hemocyanins are phagocytized by macrophage cells and slowly processed into smaller peptide fragments. Also, hemocyanins induce M1-polarization of macrophages and downregulate M2 cytokine genes. It is proved that M1 macrophages activate a tumor-killing mechanism and antagonize the suppressive activity of M2 macrophages, which promote tumor growth and metastasis [10].

Otherwise, KLH has been reported as causing a cross-reaction with the Thomsen-Friedenreich (or T-antigen) antigen by Wirguin *et al.* [11].

Antibodies that may recognize T-antigens were determined after rat immunization with KLH. The T-antigen is a simple mucin-type disaccharide presented on the outer cell surface of T-cell lymphomas and most human carcinomas (e.g. superficial non-invasive urinary bladder cancer, breast and prostate cancer). Thomsen-Friedenreich antigen has a significant role for tumor cell adhesion and metastasis formation. Moreover, the T-antigen is a specific tumor marker and a potential target for passive and active immunotherapy [12]. Immunotherapeutic effects of KLH in non-invasive urothelial cancer may be a consequence of a cross-reaction with the T-antigen and activation of the immune response against cancer cells [11].

Scientists are trying to find out more about hemocyanins' mechanism of action and how these glycoproteins stimulate the immune system. Accumulation of CD8+ T cells and activation of CD4+ T-cell response after mice immunization with KLH was demonstrated by Doyle *et al.* [13]. Moreover, mixed interleukin-4 (IL-4)/IFN- γ production profile was observed, too. Also, Salazar *et al.* [4] showed how N-glycosylation of mollusk hemocyanins contributes to their structural stability and immunomodulatory properties in mammals thus indicating their immunogenic potential.

Furthermore, there is research [14] showing how hemocyanins from *Helix lucorum* and *Rapana venosa* change gene expression profile of urothelial cancer cell lines. Significant upregulation of genes involved in the apoptosis and immune system activation were observed. Also, there is a downregulation of CCL2 (for monocyte chemotactic protein -1), CCL17 and CCL21 genes. The expression of chemokine ligands CCL17 and CCL21 is associated with the initiation of tumor metastasis and therefore it serves as a prognostic factor in gastric cancer patients [23].

It can be summarized, that hemocyanins activate immune responses because of their xenogenic structure and N-glycan chains. Plenty of trials demonstrated, that the use of hemocyanins as vaccine carriers and adjuvants could be of clinical relevance. Furthermore, they exert a strong anticancer effect and this could be used for future antineoplastic combination therapy.

Hemocyanin complex structures as vaccine carriers and vaccine adjuvants

Hemocyanins have a very complex structure, containing unique polypeptides with immunogenic properties thus enabling their use as vaccine carriers and adjuvants. Adjuvants (from the Latin

adjuvare – help or aid) are substances that increase the immunogenicity of a vaccine formulation by enhancing the strength of the antigen-specific immune responses [15,16]. Currently, KLH is used as a carrier protein and adjuvant to produce polyclonal and monoclonal antibodies, because of its structural stability and immuno-stimulating properties. An example of that is the clinical trial of the Sialyl-TN (STn) - KLH Vaccine [17]. Therapeutic cancer vaccines are being studied in the treatment of drug-resistant breast cancer because they induce humoral and cell-mediated immunity to tumor cells. Usually, these vaccines contain tumor lysates or defined tumor antigens. Sialyl-Tn-antigen (STn) is a carbohydrate epitope found on a variety of glycoproteins, including cancer-associated mucins. STn expression is associated with poor prognosis in metastatic colorectal, gastric, ovarian, and breast cancer diseases. Although the trial didn't show significant results against metastatic breast cancer, STn-KLH vaccine was well tolerated by the patients included. Additionally, KLH has been used as a carrier for N-propionylated polysialic acid (NP-polySA) [18]. Polysialic acid is a polymer weakly expressed on the cell surface of embryonal and adult brain tissues. Interestingly, it is frequently detectable in significant amounts in small cell lung cancer. The main function of polysialic acid is to inhibit cell adhesion and to promote metastasis formation. Patients vaccinated with NP-polySA-KLH vaccine were found to produce IgM antibodies against NP-polySA.

Musseli *et al.* [19], estimated the combination "antigen – KLH carrier –adjuvant" as a successful method for boosting the immune response against cancer cells. QS-21 (a purified saponin fraction separated from the bark of *Quillaja saponaria*) was used as an adjuvant. This substance activates APCs, B-cells and T-cells response. KLH was used as a carrier for the following tumor antigens:

- GM2 – sphingolipid monosialoganglioside and tumor-associated antigen.
- GD3 – acidic glycosphingolipid.
- Fucosyl GM1 – sphingolipid monosialoganglioside and tumor-associated antigen.
- Globo H – globohexaosylceramide, glycol-sphingolipid antigen.
- Lewis Y – difucosylated oligosaccharide with two fucoses carried by glycoconjugates (glycolproteins and glycolipids) on the cell surface.

- Tn – monosaccharide structure N-acetyl-galactosamine (GalNAc) linked to serine or threonine by a glycosidic bond.
- sTn – sialyl Tn antigen.
- Thomsen–Friedenreich antigen – disaccharide formed by additional galactose monosaccharid to Tn – antigen: (Gal(b1-3)GalNAc).
- MUC1 – mucin-1 glycoprotein; inhibits access of chemotherapeutic drugs to the cancer cell.
- KSA – glycoprotein, a marker for tumors with epithelial origin.
- Polysialic acid – an inhibitor of neural cell and tumor cell adhesion.

The summary of serological results in vaccinated patients showed significant immunoglobulin response to sTn, GM2 and Fucosyl GM1 antigens. Furthermore, Musselli *et al.* [19], confirmed that KLH in these conjugate vaccines (antigen – KLH carrier – QS-21 carrier) induces Th1 – cell response.

As a continuation, in a pilot trial, 11 patients with ovarian cancer were treated with heptavalent antigen-keyhole limpet hemocyanin vaccine plus QS21 [20]. The vaccine included carbohydrate epitopes, such as GM2, Globo-H, Lewis Y, sTn, Tn, Thomsen-Friedenreich antigen and Tn-MUC-1. As a result, the vaccine safely induced antibody responses against five of seven antigens (there was no significant response to GM2 and Lewis Y antigens). In addition, the heptavalent vaccine administration was well tolerated without any strong side effects. The most frequent unwanted reactions were fatigue, fever, myalgia and local injection site reactions.

Hemocyanins have been used not only for an antigen carrier but also as a vaccine carrier. Tumor antigen-presenting cell vaccine was co-injected with the CCH as an adjuvant in castration-resistant prostate cancer patients. In this study, CCH was able to induce an immune memory response followed by a delayed-type hypersensitivity skin test [21].

Furthermore, CCH and FLH have showed immunological properties based on their glycoprotein structure and ability to be recognized by immune cells. It was demonstrated that CCH and FLH are useful carriers of carbohydrate mimotopes such as P10, a mimetic peptide of GD2 (the major ganglioside constituent of neuroectodermal tumors). This trial indicates possibilities for future cancer vaccine research [22].

According to Dolashka *et al.* [23] hemocyanins, isolated from *Helix lucorum* and *Rapana venosa* could be a serious alternative of KLH as single

inductors of nonspecific, cell-mediated immune response and to propose it as a component of non-specific non-conjugated anti-tumor vaccines. It was demonstrated the resistance of the experimental animals against the progressive development of Guerin ascites tumor after treatment with *Rapana venosa* hemocyanin (RvH), *Helix lucorum* hemocyanin (b-HIH) and KLH in correlation to their specific carbohydrate constituents. b-HIH and its conjugate with tumor antigen exhibited stronger immunogenicity probably because of the specific carbohydrate structures (HIH has a heterogeneously glycosylated structure carrying mostly methylated high mannose-type moieties).

Antineoplastic activity of hemocyanins

There is a variety of evidences proving hemocyanins' antitumor activity based on their immune-modulating properties. Chilean gastropod *Concholepas concholepas* was shown to exert cytotoxic activity in murine bladder cancer model. This fact underlines, that not only KLH may have anticancer properties, but this could be a common feature of all hemocyanins regardless of their origin [24]. Moreover, FLH showed more potent anti-tumor activity and stronger humoral immune response in the B16F10 mouse melanoma model, rather than CCH and KLH. *In vitro* assays with FLH demonstrated stimulation of rapid pro-inflammatory cytokines which can explain stronger immunological activity [25].

Additionally, it was observed that *Helix aspersa* hemocyanin (HaH) has cytotoxic effects on a bladder cancer cells, human prostate and ovarian carcinoma, malignant glioma, Burkitt's lymphoma and acute monocytic leukemia tumor cells [26]. Noteworthy, an extract from *Helix aspersa* demonstrated antitumor activity against triple-negative breast cancer cells Hs578T and it was found to be a potent stimulator for TNF induced signal transduction changes, accompanied by beneficial NF- κ B inhibition as well [27]. Hemocyanins isolated from *Rapana thomasiana* and *Helix pomatia* showed strong *in vivo* anti-cancer effect in a murine model of colon carcinoma. Moreover, *Helix pomatia* hemocyanin (Hph) and *Rapana thomasiana* hemocyanin (RtH) were described to induce apoptosis in C-26 carcinoma cells *in vitro* [28]. Described experiments of Guncheva *et al.* [29] have shown that preparations of RtH-FO (*Rapana thomasiana* hemocyanins conjugated with folic acid), RtH-FE (ferulic acid), HIH-FO (*Helix lucorum* hemocyanins conjugated with folic acid) and HIH-

FE are not cytotoxic to human fibroblasts (BJ cells) and they exhibit an excellent cytotoxic effect to hormone-dependent MCF-7 and hormone-independent triple-negative MDA-MB-231 breast cancer cells.

CONCLUSION

There is a rising amount of published information linked to the immune-modulating properties of hemocyanins. These molluscan biomolecules are giant glycoproteins acting not only as oxygen-transporting proteins in invertebrates, but they could play a significant role in future immune therapies. The hemocyanins' complex structure is the basis of their multifunctionality. These molecules might be used as anti-cancer vaccine carriers and adjuvants. Moreover, there are evidence data about triggering anticancer immunity. Therefore, we assume that future experiments with hemocyanins (regardless of their origin) could be beneficial for developing anticancer immune therapies and believe in the expectation, that hemocyanins may play a key role in innovative anti-tumor therapies.

Acknowledgements: This research was funded by the Bulgarian Ministry of Education and Science through the National Scientific Program "Innovative Low-Toxic Biologically Active Means for Precision Medicine" BioActiveMed, grant number DOI-217/30.11.2018.

REFERENCES

1. A. Ghiretti-Magaldi, F. Ghiretti, *Experientia*, **48**, 971 (1992).
2. R. D. Swerdlow, R. F. Ebert, P. Lee, C. Bonaventura, K. I. Miller, *Comp. Biochem. Physiol., Part B: Biochem. Mol. Biol.*, **113**, 537 (1996).
3. S. Kato, T. Matsui, Y. Tanaka, *Subcell. Biochem.*, **94**, 195 (2020).
4. M. L. Salazar, J. M. Jiménez, J. Villar, M. Rivera, M. Báez, A. Manubens, M. I. Becker, *J. Biol. Chem.*, **294**, 19546 (2019).
5. H. Geyer, M. Wuhler, A. Resemann, R. Geyer, *J. Biol. Chem.*, **280**, 40731 (2005).
6. V. V. Glinsky, G. V. Glinsky, K. Rittenhouse-Olson, M. E. Huflejt, O. V. Glinskii, S. L. Deutscher, T. P. Quinn, *Cancer Res.*, **61**, 4851 (2001).
7. O. Martinez-Maza, J. S. Berek, *Glob. Libr. Women's Med.*, (2009).
8. M. Schuster, A. Nechansky, R. Kircheis, *Biotechnol. J.*, **1**, 138 (2006).
9. T. Zhong, S. Arancibia, R. Born, R. Tampe, J. Villar, M. D. Campo, A. Manubens, M. I. Becker, *J. Immunol.*, **196**, 4650 (2016).
10. P. J. Murray, T. A. Wynn., *Nat. Rev. Immunol.*, **11**, 723 (2011).
11. I. Wirguin, L. Suturkova-Milosević, C. Briani, N. Latov, *Cancer Immunol. Immunother.*, **40**, 307 (1995).
12. S. Goletz, Y. Cao, A. Danielczyk, P. Ravn, U. Schoeber, U. Karsten, *Adv. Exp. Med. Biol.*, **535**, 147 (2003).
13. A. G. Doyle, L. Ramm, A. Kelso, *Immunology*, **93**, 341 (1998).
14. O. Antonova, L. Yossifova, R. Staneva, S. Stevanovic, P. Dolashka, D. Toncheva, *JBUON*, **20**, 180 (2015).
15. T. W. Dubensky, S. G. Reed, Adjuvants for cancer vaccines, *Semin. Immunol.*, **22**, 155 (2010).
16. J. S. Apostólico, V. A. S. Lunardelli, F. C. Coirada, S. B. Boscardin, D. S. Rosa, *J. Immunol. Res.*, **2016**, ID 1459394 (2016).
17. D. Miles, H. Roché, M. Martin, T. J. Perren, *Oncologist*, **16**, 1092 (2011).
18. L. M. Krug, G. Ragupathi, K. Kenneth, C. Hood, H. J. Jennings, Z. Guo, M. G. Kris, V. Miller, B. Pizzo, L. Tyson, V. Baez, and P. O. Livingston, *Clin. Cancer Res.*, **10**, 916 (2004).
19. C. Musselli, P. O. Livingston, G. Ragupathi, *J. Cancer Res. Clin. Oncol.*, **127**, R20 (2001).
20. P. J. Sabbatini, G. Ragupathi, C. Hood, C. A. Aghajanian, M. Juretzka, A. Iasonos, *Clin. Cancer Res.*, **13**, 4170 (2007).
21. D. Reyes, L. Salazar, E. Espinoza, C. Pereda, E. Castellón, R. Valdevenito, C. Huidobro, M. I. Becker, A. Lladser, M. N. López, F. Salazar-Onfray, *Br. J. Cancer*, **109**, 1488 (2013).
22. M. Palacios, R. Tampe, M. Campo, T. Zhong, M. López, F. Salazar-Onfray, M. I. Becker., *Eur. J. Med. Chem.*, **150**, 74 (2018).
23. P. Dolashka, L. Velkova, I. Iliev, A. Beck, A. Dolashki, L. Yossifova, *Immunol. Invest.*, **40**, 130 (2010).
24. B. Moltedo, F. Faunes, D. Haussmann, P. Ioannes, A. Ioannes, J. Puente, M. I. Becker, *J. Urol.*, **176**, 2690 (2006).
25. S. Arancibia, C. Espinoza, F. Salazar, M. Campo, R. Tampe, T. Zhong, P. Ioannes, B. Moltedo, J. Ferreira, E. C. Lavelle, A. Manubens, A. Ioannes, M. I. Becker, *PLoS One*, **9**, e87240 (2014).
26. O. Antonova, P. Dolashka, D. Toncheva, H. Rammensee, M. Floetenmeyer, S. Stevanovic, *Z. Naturforsch.*, **69**, 325 (2014).
27. I. Ouar, C. Braicu, D. Naimi, A. Irimie, I. Berindan-Neagoe, *Phcog Mag*, **13**, 281 (2017).
28. V. Gesheva, S. Chausheva, N. Mihaylova, I. Manoylov, L. Doumanova, K. Idakieva, A. Tchorbanov, *BMC Immunol.*, **15**, 34 (2014).
29. M. Guncheva, E. Stoyanova, S. Todinova, K. Idakieva, *Proceedings*, **22**, 13 (2019).

In memoriam of our teacher Prof. Dr. Dr. h. c. Wolfgang Voelter



(1936 - 2021)

On January 22, 2021, we lost Wolfgang Voelter, professor at the University of Tübingen, Germany. With deep reverence, we bow our heads in the memory of the wonderful man and friend, erudite scholar and public figure! Gone is a person who was a model of innovation and reliability.

Prof. Dr. Dr. h. c. Voelter was a world-renowned scholar in the field of biochemistry of natural substances, internationally recognized with numerous awards for his contribution to science. His dedication, efficiency and principledness were exemplary, especially for young scientists. He was extremely modest and did his utmost best to the benefit of his colleagues and students, bringing academic spirit in scientific work, collegial relationships and public life!

Wolfgang Voelter (born in 1936 in Ludwigsburg) was professor of physics and biochemistry at the University of Tübingen. The positions he held were various: Director of the Central Institute of Chemistry and Deputy Dean of the Faculty of Chemistry and Pharmacy at the University of Tübingen, Head of the Board of the Institute for Scientific Cooperation, Tübingen, Permanent Member of the Board of Referees of the International Foundation for Science, Stockholm, Head of the Interdisciplinary Research Program of the Government of Baden-Württemberg "Isolation, Structure Elucidation and Synthesis of Biologically Relevant Peptides and Proteins", Coordinator of the EC/Jordan Cooperation Project in Science and Technology, Medicinal Plants; Catalysts; Natural

Products; Pollution Control, Member of about a dozen scientific organizations like the American Chemical Society, Royal Society of Chemistry, Gesellschaft Deutscher Chemiker, among others.

Prof. Voelter is the author of more than 1100 scientific publications in the field of natural products. For decades, he worked on the extraction of natural substances and their incorporation in medicinal products. Prof. Wolfgang Voelter and the team of Prof. Dolashka from Bulgaria collaborated in investigation of dosage forms based on mollusc and arthropod hemocyanins for cancer therapeutic applications.

Prof. Voelter initiated the Hussein Ebrahim Jamal Research Institute of Chemistry at the University of Karachi, Pakistan.

An exceptional merit of Prof. Voelter was his contributing to the academic growth of many Bulgarian scientists who specialized at the University of Tübingen for more than 25 years. He was also instrumental in providing a number of devices and apparatuses for the research laboratories in Bulgaria.

Prof. Voelter was awarded a multitude of honorary titles: Fellow of the Chemical Society London; Elected Member of the Art Foundation Baden-Württemberg; Elected Member of Bergmann-Kreis, Kneipp Award (for structure elucidation of natural products); Foreign Member of the Pakistan Academy of Sciences, Erich Krieg Award (for studies on drug metabolism); Member of the Japan Society for the Promotion of Science Award; Special Award and Gold Medal of the President of Pakistan, Doctor of Science (Honoris Causa), University of Karachi; Sitara Award; Elected Member of the Third World Academy of Sciences, Trieste; Bundesverdienstkreuz of the President of the Federal Republic of Germany; Doctor of Science honoris causa of Hamdard University; Member of the Board of Prof. Dr. Harald Grüber Foundation; Member of the International Advisory Board of Dr. Panjwani Center for Molecular Medicine and Drug Research, Karachi University; Gold Medal, University of Jordan (Amman); Honorary Badge of the Bulgarian Academy of Sciences, etc.

Prof. Voelter was founder and active member of various foundations. He and his wife, Dr. Heidi Voelter, set up their Voelter Foundation and for public use. They have given their houses a family

center with a café and German language courses for immigrants. He and his wife donated their private collection of prints to the Institute of Art History at the University of Tübingen.

We, his colleagues and students from the Bulgarian Academy of Sciences, had the exceptional opportunity privilege to work for years with this highly respected, universally recognized and prolific scientist, who was passionately devoted to science and its service to human health!

Goodbye, Dear Prof. Voelter!

We shall remember your human kindness and wisdom!

Pavlina Dolashka
Maria Angelova
Alexander Dolashki

*Institute of Organic Chemistry with Centre of
Phytochemistry, Bulgarian Academy of Sciences,
Acad. G. Bonchev Str. Bl. 9, 1113 Sofia, Bulgaria;
E-mail: pavlina.dolashka@orgchm.bas.bg*



Prof. W. Voelter with colleagues of the IOCCP-BAS.



Prof. W. Voelter with colleagues of the Institute of Microbiology – BAS.



Prof. Wolfgang Voelter among colleagues and students of the University of Tübingen.



Prof. Voelter and Dr. Alexander Dolashki and Prof. Pavlina Dolashka, on one of their visits to Tübingen.



Prof. Voelter with his Bulgarian PhD student Assoc. Prof. Alexander Dolashki in Tübingen.



Prof. Wolfgang Voelter on a visit to Bulgaria.



Research Institute of Chemistry "Prof. Dr. Dr. h.c. Wolfgang Voelter", Karachi, Pakistan.



Prof. Wolfgang Voelter 's 80th birthday.

Instructions about Preparation of Manuscripts

General remarks: Manuscripts are submitted in English by e-mail. The text must be typed on A4 format paper using Times New Roman font size 11, normal character spacing. The manuscript should not exceed 15 pages (about 3500 words), including photographs, tables, drawings, formulae, etc. Authors are requested to use margins of 2 cm on all sides.

Manuscripts should be subdivided into labelled sections, e.g. **Introduction, Experimental, Results and Discussion, etc.** The **title page** comprises headline, author's names and affiliations, abstract and key words. Attention is drawn to the following:

a) **The title** of the manuscript should reflect concisely the purpose and findings of the work. Abbreviations, symbols, chemical formulas, references and footnotes should be avoided. If indispensable, abbreviations and formulas should be given in parentheses immediately after the respective full form.

b) **The author's** first and middle name initials and family name in full should be given, followed by the address (or addresses) of the contributing laboratory (laboratories). **The affiliation** of the author(s) should be listed in detail by numbers (no abbreviations!). The author to whom correspondence and/or inquiries should be sent should be indicated by asterisk (*) with e-mail address.

The abstract should be self-explanatory and intelligible without any references to the text and containing not more than 250 words. It should be followed by key words (not more than six).

References should be numbered sequentially in the order, in which they are cited in the text. The numbers in the text should be enclosed in brackets [2], [5, 6], [9–12], etc., set on the text line. References are to be listed in numerical order on a separate sheet. All references are to be given in Latin letters. The names of the authors are given without inversion. Titles of journals must be abbreviated according to Chemical Abstracts and given in italics, the volume is typed in bold, the initial page is given and the year in parentheses. Attention is drawn to the following conventions: a) The names of all authors of a certain publication should be given. The use of "*et al.*" in the list of references is not acceptable. b) Only the initials of the first and middle names should be given. In the manuscripts, the reference to author(s) of cited works should be made without giving initials, e.g. "Bush and Smith [7] pioneered...". If the reference carries the names of three or more authors it should be quoted as "Bush *et al.* [7]", if Bush is the first author, or as "Bush and co-workers [7]", if Bush is the senior author.

Footnotes should be reduced to a minimum. Each footnote should be typed double-spaced at the bottom of the page, on which its subject is first mentioned. **Tables** are numbered with Arabic numerals on the left-hand top. Each table should be referred to in the text. Column headings should be as short as possible but they must define units unambiguously. The units are to be separated from the preceding symbols by a comma or brackets. Note: The following format should be used when figures, equations, etc. are referred to the text (followed by the respective numbers): Fig., Eqns., Table, Scheme.

Schemes and figures. Each manuscript should contain or be accompanied by the respective illustrative material as well as by the respective figure captions in a separate file (sheet). As far as presentation of units is concerned, SI units are to be used. However, some non-SI units are also acceptable, such as °C, ml, l, etc. The author(s) name(s), the title of the manuscript, the number of drawings, photographs, diagrams, etc., should be written in black pencil on the back of the illustrative material (hard copies) in accordance with the list enclosed. Avoid using more than 6 (12 for reviews, respectively) figures in the manuscript. Since most of the illustrative materials are to be presented as 8-cm wide pictures, attention should be paid that all axis titles, numerals, legend(s) and texts are legible.

The authors are required to submit the text with a list of three individuals and their e-mail addresses that can be considered by the Editors as potential reviewers. Please, note that the reviewers should be outside the authors' own institution or organization. The Editorial Board of the journal is not obliged to accept these proposals.

The authors are asked to submit **the final text** (after the manuscript has been accepted for publication) in electronic form by e-mail. The main text, list of references, tables and figure captions should be saved in separate files (as *.rtf or *.doc) with clearly identifiable file names. It is essential that the name and version of the word-processing program and the format of the text files is clearly indicated. It is recommended that the pictures are presented in *.tif, *.jpg, *.cdr or *.bmp format.

The equations are written using "Equation Editor" and chemical reaction schemes are written using ISIS Draw or ChemDraw programme.

EXAMPLES FOR PRESENTATION OF REFERENCES

REFERENCES

1. D. S. Newsome, *Catal. Rev.–Sci. Eng.*, **21**, 275 (1980).
2. C.-H. Lin, C.-Y. Hsu, *J. Chem. Soc. Chem. Commun.*, 1479 (1992).
3. R. G. Parr, W. Yang, *Density Functional Theory of Atoms and Molecules*, Oxford Univ. Press, New York, 1989.
4. V. Ponec, G. C. Bond, *Catalysis by Metals and Alloys (Stud. Surf. Sci. Catal., vol. 95)*, Elsevier, Amsterdam, 1995.
5. G. Kadinov, S. Todorova, A. Palazov, in: *New Frontiers in Catalysis (Proc. 10th Int. Congr. Catal., Budapest, (1992)*, L. Guczi, F. Solymosi, P. Tetenyi (eds.), Akademiai Kiado, Budapest, 1993, Part C, p. 2817.
6. G. L. C. Maire, F. Garin, in: *Catalysis. Science and Technology*, J. R. Anderson, M. Boudart (eds), vol. 6, SpringerVerlag, Berlin, 1984, p. 161.
7. D. Pocknell, *GB Patent 2 207 355* (1949).
8. G. Angelov, PhD Thesis, UCTM, Sofia, 2001, pp. 121-126.
9. JCPDS International Center for Diffraction Data, *Power Diffraction File*, Swarthmore, PA, 1991. 10. CA **127**, 184 762q (1998).
11. P. Hou, H. Wise, *J. Catal.*, in press.
12. M. Sinev, private communication.
13. <http://www.chemweb.com/alchem/articles/1051611477211.html>.

Texts with references which do not match these requirements will not be considered for publication!!!

CONTENTS

O. Stoilova, National Research Programme “Innovative Low-Toxic Bioactive Systems for Precision Medicine (BioActiveMed)”	5
Y. Topalova, Innovative and Applied Potential of Center of Competence “Clean technologies for Sustainable Environment – Water, Waste, Energy for Circle Economy”	8
I. Yankova, E. Ivanova, K. Todorova, A. Georgieva, V. Dilcheva, I. Vladov, S. Petkova, R. Toshkova, L. Velkova, P. Dolashka, I. Iliev, Assessment of the toxicity and antiproliferative activity of hemocyanins from <i>Helix lucorum</i> , <i>Helix aspersa</i> and <i>Rapana venosa</i>	15
M. R. Aleksova, L. G. Velkova, P. A. Dolashka, G. S. Radeva, Antibacterial activity of bioactive compounds isolated from crab and snail species	22
M. V. Belouhova, N. K. Dinova, I. D. Yotinov, S. K. Lincheva, I. D. Schneider, Y. I. Topalova, FISH analysis of ANAMMOX and <i>Azoarcus-Thauera</i> cluster – innovative indicative approach for management of the landfill leachate treatment	27
A. Dushkov, M. Petrova, J. Todorova, A. Gospodinov, I. Ugrinova, Natural medicine: an evaluation of the <i>in vitro</i> cytotoxic effect of several Bulgarian fungal species on two panels of cancer cell lines	35
E. Krumova, P. Dolashka, R. Abrashev, L. Velkova, A. Dolashki, A. Daskalova, V. Dishliyska, V. Atanasov, D. Kaynarov, M. Angelova, Antifungal activity of separated fractions from the hemolymph of marine snail <i>Rapana venosa</i>	42
M. N. Vassilev, S. Simova, M. Dangelov, L. Velkova, V. Atanassov, A. Dolashki, P. Dolashka, A ¹ H NMR based study of metabolites profiling of garden snail <i>Helix lucorum</i> hemolymph	49
T. A. Chobanova, M. Belouhova, I. Yotinov, N. Dinova, E. Daskalova, Y. Todorova, S. Lincheva, I. Schneider, Y. Topalova, Adaptation of activated sludge to treatment of landfill leachate during model process	57
V. Tsvetkov, D. Todorov, A. Hinkov, K. Shishkova, L. Velkova, A. Dolashki, P. Dolashka, S. Shishkov, Effect of extracts of some species from Phylum Mollusca against the replication of Human Alphaherpesviruses types	66
M. Lazarova, M. Kermedchiev, L. Tancheva, D. Uzunova, K. Tasheva, L. Velkova, A. Dolashki, A. Daskalova, V. Atanasov, D. Kaynarov, P. Dolashka, Natural substances with therapeutic potential in wound healing	73
G. Issa, N. Velinov, D. Kovacheva, T. Tsoncheva, Silica supported iron and chromium oxide catalysts for methanol decomposition	80
A. Kosateva, I. Stoycheva, B. Petrova, B. Tsyntsarski, Characterization of some carbon materials by Raman spectroscopy	85
G. Georgiev, B. Tsyntsarski, I. Stoycheva, A. Kosateva, B. Petrova, K. Miteva, T. Budinova, N. Petrov, A. Sarbu, M. Dumitru, A. Ciurluca, A. Miron, Refuse-derived fuel waste conversion to carbon adsorbent	89
R. Ivanova, B. Tsyntsarski, G. Issa, I. Spassova, D. Kovacheva, N. Velinov, T. Tsoncheva, M _{0.5} Zn _{0.5} Fe ₂ O ₄ (M = Cu, Co, Mn, Ni) ferrites supported on activated carbon as catalysts for methanol decomposition	93
M. Nikolova, S. Konstantinov, P. Dolashka, Antineoplastic immuno-modulating properties of hemocyanins	101
P. Dolashka, M. Angelova, A. Dolashki, In memoriam of our teacher Prof. Dr. Dr. h. c. Wolfgang Voelter	107
Instructions to authors	110